UNIVERSITÀ DEGLI STUDI DI TRIESTE

XXVIII CICLO DEL DOTTORATO DI RICERCA IN SCIENZE E TECNOLOGIE CHIMICHE E FARMACEUTICHE

THE IMPORTANCE OF LIGAND STRUCTURAL DIVERSITY IN PALLADIUM CATALYZED POLYMERIZATION

Settore scientifico-disciplinare: **CHIM/03**

DOTTORANDA
VERA ROSAR

COORDINATORE
PROF. MAURO STENER

SUPERVISORE DI TESI
PROF. BARBARA MILANI

ANNO ACCADEMICO 2014/2015

TABLE OF CONTENTS

ABSTRACT

One of the main challenges in the field of polymer chemistry is the incorporation of polar functional groups into polyolefin chains, with the aim to produce functionalized polyolefins that should show enhanced chemical, physical and mechanical properties with respect to polyolefins themselves. The most straightforward and thereof promising approach towards this goal is the direct, controlled, homogeneously catalyzed copolymerization of terminal alkenes with polar vinyl monomers. Indeed, in homogeneous catalysis the electronic and steric environment of the active metal center can be tuned by tailoring the ancillary ligand, and this should lead to a highly efficient catalyst that as the same time should be able to control the selectivity of the catalytic reaction, that, in the field of polymerization catalysis, means the fine control of the features of the final polymeric material.

This PhD thesis is aimed to demonstrate once more the validity of this general principle, with particular attention towards two copolymerization reactions: the CO/vinyl arene and the ethylene/methyl acrylate copolymerizations (methyl acrylate = MA). Both reactions are catalyzed by palladium(II) complexes with nitrogen-donor ancillary ligands (N-N). The research work carried out in the framework of this thesis comprises the typical steps of a project in homogeneous catalysis: i) synthesis and characterization of the molecules used as ancillary ligands; ii) synthesis and characterization of the related palladium(II) complexes; iii) study of the catalytic behavior of the synthesized precatalysts in the two copolymerization reactions, including the characterization of the catalytic products.

Chapter 1 consists in both a general introduction on the state of the art in polyolefin synthesis and an overview of the most relevant catalytic systems reported in literature for the copolymerization of ethylene with polar vinyl monomers.

Chapter 2 deals with the application of the same precatalysts, based on palladium complexes with naphthyl-substituted α-diimine ligands with either a BIAN or a DAB skeleton, to the CO/vinyl arene and the ethylene/methyl acrylate copolymerizations, in order to highlight the main analogies and differences between the two reactions. Particular attention was addressed to the synthesis and the study of the catalytic behavior of monocationic dimethyl sulfoxide derivatives of general formula $[Pd(CH_3)(dmso)(N\text{-}N)][PF_6]$, in comparison with the related acetonitrile derivatives $[Pd(CH_3)(NCCH_3)(N\text{-}N)][PF_6]$. The catalytic data highlighted that:

- For the CO/styrene copolymerization BIAN ligands led to more stable and more productive catalysts than the DAB counterparts;

- For ethylene/methyl acrylate copolymerization an opposite trend was found, DAB ligands generate more productive catalysts than the BIAN analogues;
- For both copolymerizations, complexes with the 2-naphthyl-substituted ligands, regardless of ligand skeleton, behaved as catalysts having aryl α-diimines with the aryl rings substituted in *meta* position. They exhibited similar productivities and led to atactic polymers in CO/styrene copolymerization, but they were inactive in ethylene/MA copolymerization;
- For both copolymerizations, complexes with the 1-naphthyl-substituted ligands, regardless of ligand skeleton, behaved as catalysts having aryl α-diimines with the aryl rings substituted in *ortho* position. They showed low productivities and led to isotactic/atactic stereoblock polymers in CO/styrene copolymerization, but they were catalytically active in ethylene/methyl acrylate copolymerization.

Moreover, with the aim of clarifying the reasons of the opposite trends observed, a very preliminary density functional theory analysis of the CO/styrene copolymerization was carried out using simplified precatalysts, confirming the mechanism reported in literature.

Chapters 3 and *4* deal with the development of catalysts for the ethylene/methyl acrylate copolymerization, that is considered the 'Holy Grail' of polymerization catalysis. In *Chapter* 3 the research has been addressed to the synthesis of two new nonsymmetric ligands, both characterized by the BIAN skeleton and by one aryl ring having a methoxy and a methyl group on the *ortho* positions and differing in the number and positions of the electron withdrawing groups (CF_3) on the other aryl ring. Their coordination chemistry to palladium was investigated, together with that of the symmetric analogue with a methyl and a methoxy group in the *ortho* positions of both aryl rings, and both acetonitrile and dimethyl sulfoxide derivatives $[Pd(CH_3)(L)(Ar,Ar'\text{-BIAN})][PF_6]$ ($L = CH_3CN$, dmso) were synthesized. The characterization of the Pd-dmso indicated that different species were present in solution depending on the nature of the ancillary ligand, but in all cases the S-bonded species was observed as the major isomer in solution. When tested in the copolymerization reaction, the monocationic complexes were found inactive, regardless to the nature of the ancillary ligand. Moreover, testing the effect of different solvents on the catalytic behavior highlighted the decomposition of the complex through the dissociation and breakdown of the ligand.

Considering that the DAB skeleton is best suited for the target copolymerization reaction with respect to the BIAN one, in *Chapter 4* a new nonsymmetric Ar,Ar'-DAB ligand having one aryl ring substituted in *meta* positions with electron withdrawing CF_3 groups and the other aryl ring substituted in *ortho* positions with electron donating methyl groups was studied. A new protocol for the synthesis of the relevant Pd(II)

complexes was developed using [Pd(cod)(CH_3)Cl] as templating agent. The neutral complex was used for the synthesis of the monocationic acetonitrile complexes [Pd(CH_3)(CH_3CN)(Ar,Ar'-BIAN)][X] (X = PF_6^-, SbF_6^-), and the ^{19}F-^{1}H HOESY spectrum of the hexafluorophosphate derivative indicated that in solution the counterion was preferentially located on top of the complexes and shifted towards the DAB skeleton, in contrast with the observation that in BIAN derivatives it was located mainly towards the Pd-$NCCH_3$ fragment. The series of monocationic complexes was extended to the dimethyl sulfoxide derivatives, and their NMR characterization highlighted that with this nonsymmetric Ar,Ar'-DAB ligand the dmso was always coordinated via the sulfur atom, in contrast with the observation of both S-bonded and O-bonded species reported for the Pd-dmso derivative with the analogous nonsymmetric BIAN ligand. The catalytic behavior of the monocationc complexes with the new nonsymmetric ligand and the two related symmetric ones was compared with that reported for the BIAN analogues: moving from the BIAN to the DAB skeleton an increase in productivity was observed, in agreement with literature, but for the catalysts with the nonsymmetric ligand the increase was not as pronounced as that found for the symmetric methyl-substituted derivative. No effect of the labile ligand nor of the counterion was observed on the catalytic behavior in 2,2,2-trifluoroethanol (TFE) of the tested complexes; on the other hand, moving to a less polar solvent such as dichloromethane, a general decrease in productivity was observed, and SbF_6^- derivatives were found to be roughly three times more productive than the corresponding PF_6^- derivatives, in agreement with the formation of the ion pair. Interestingly, acetonitrile derivatives were found to be more productive than the dmso analogues, leading to a product with a higher content of polar monomer.

In *Chapter 5* and *6* the catalytic behavior of palladium complexes with pyridylimines was investigated in two reactions, the CO/vinyl arene copolymerization and the alkoxycarbonylation of internal olefins, highlighting the versatility of this kind of nitrogen-donor ligands in palladium-catalyzed reaction. In *Chapter 5* pyridylimine ligands featured by an aryl ring on the imino nitrogen atom and differing for the presence of a hydrogen atom or a methyl group on the imino carbon atom and/or on the *ortho* positions of the aryl ring were synthesized and used for the synthesis of the corresponding neutral, [Pd(CH_3)Cl(N-N')], and monocationic, [Pd(CH_3)($NCCH_3$)(N-N')][PF_6], palladium(II) complexes. The monocationic complexes generated very efficient catalysts for the copolymerization of carbon monoxide with vinyl arenes such as styrene and 4-methyl-styrene, leading to the corresponding alternated polyketones, with productivities as high as 4.61 kg CP/g Pd, and molecular weights up to 1 775 000 g/mol, with polydispersity values in the range 1.67 – 8.08. The relatively high values of polydispersity suggested the presence of more than one active species. All synthesized polyketones were syndiotactic, with a *uu* triad

content depending on the ancillary ligand nature, and in contrast with the previously reported data, no effect of the vinyl arene on the stereoselectivity was observed. In *Chapter 6* a series of palladium(II) complexes of general formula [Pd(N-N')$(L)_2$], with N-N' being a pyridylimine ligand and L either acetate or trifluoroacetate, was tested in the alkoxycarbonylation of 1-octene and 4-octene. They were converted into the corresponding vicinal diester, respectively dimethyl 2-hexylsuccinate and dimethyl 2,3-dipropylsuccinate, indicating that no isomerization of the internal double bond to the terminal position occured before the carbonylation process took place.

As a general conclusion, the research activity carried out during this PhD project led to the synthesis and the characterization of several new ligands and of the relevant palladium complexes that were tested as precatalysts in the two target copolymerization reactions, leading to a remarkable enhancement of the state of the art in the field. It was shown that a subtle variation of both the ligand skeleton and the ligand substituents had a strong effect on the catalytic performances of the relevant palladium complexes highlighting the importance of ligand diversity in homogeneous catalysis.

RIASSUNTO

Una delle maggiori sfide nel campo della chimica dei polimeri è l'incorporazione di gruppi funzionali polari nelle catene poliolefiniche, allo scopo di produrre poliolefine funzionalizzate che dovrebbero mostrare migliori proprietà chimiche, fisiche e meccaniche rispetto alle semplici poliolefine. L'approccio più diretto e quindi più promettente per il raggiungimento di questo obiettivo è la copolimerizzazione diretta e controllata di alcheni terminali con monomeri vinilici polari catalizzata da catalizzatori omogenei. Infatti, nella catalisi omogenea, l'intorno elettronico e sterico del centro metallico cataliticamente attivo può essere controllato modificando il legante ancillare, e questo dovrebbe portare a catalizzatori altamente efficienti capaci di controllare la selettività della reazione catalizzata; questo, nel campo della catalisi di polimerizzazione, significa poter controllare le caratteristiche del prodotto finale.

Questa tesi di Dottorato ha come scopo l'ulteriore dimostrazione della validità di questo principio generale, con un'attenzione particolare verso due reazioni: la copolimerizzazione CO/vinil arene e quella etilene/metil acrilato (MA). Entrambe le reazioni sono catalizzate da complessi di palladio con leganti ancillari azotati (N-N). L'attività di ricerca svolta nel contesto di questa tesi comprende i passaggi tipici di un progetto sviluppato nell'ambito della catalisi omogenea: i) sintesi e caratterizzazione delle molecole da usare come leganti ancillari; ii) sintesi e caratterizzazione dei corrispondenti complessi di palladio(II); iii) studio dell'attività catalitica dei precatalizzatori sintetizzati nelle due reazioni di copolimerizzazione, inclusa la caratterizzazione dei prodotti catalitici.

Il *Capitolo 1* si compone di un'introduzione generale sullo stato dell'arte nella sintesi di poliolefine e di una panoramica dei principali sistemi catalitici finora riportati in letteratura per la copolimerizzazione dell'etilene con monomeri vinilici polari.

Il *Capitolo 2* riguarda l'uso di complessi di palladio con leganti α-diimminici sostituiti con gruppi naftilici e aventi uno scheletro BIAN o DAB, applicati come precatalizzatori nella copolimerizzazione CO/stirene e etilene/metil acrilato, al fine di identificare le principali analogie e differenze fra le due reazioni. Particolare attenzione è stata posta alla sintesi e allo studio dell'attività catalitica dei complessi monocationici contenenti il dimetilsolfossido come legante labile, di formula generale $[Pd(CH_3)(dmso)(N\text{-}N)][PF_6]$, in confronto ai corrispondenti derivati contenenti l'acetonitrile $[Pd(CH_3)(NCCH_3)(N\text{-}N)][PF_6]$.

I dati di catalisi hanno evidenziato che:

- Nella copolimerizzazione CO/stirene i leganti BIAN portano a catalizzatori più stabili e più produttivi rispetto agli corrispondenti DAB;
- Nella copolymerizzazione etilene/metil acrilato si è osservato l'andamento opposto, i leganti a scheletro DAB generano catalizzatori più produttivi rispetto agli analoghi BIAN;
- In entrambe le copolimerizzazioni, i catalizzatori con leganti contenenti il gruppo 2-naftile, indipendentemente dallo scheletro, funzionano come i catalizzatori basati su a-diimmine con gli anelli arilici sostituiti in posizione *meta*. Portano a produttività simili e a copolimeri CO/stirene atattici, mentre sono inattivi nella copolimerizzazione etilene/metil acrilato;
- In entrambe le copolimerizzazioni, i complessi contenenti leganti con il gruppo 1-naftile, indipendentemente dallo scheletro, si comportano come i catalizzatori con a-diimmine aventi gli anelli arilisi sostituiti in posizione *orto*. Nella copolimerizzazione CO/stirene portano a basse produttività e a polichetoni a stereoblocchi atattici/isotattici, mentre sono più attivi nella copolimerizzazione etilene/metil acrilato.

Inoltre, con l'obiettivo di spiegare le ragioni degli andamenti opposti osservati, è stata fatta un'analisi molto preliminare di teoria del funzionale della densità (Density Functional Theory, DFT) della copolimerizzazione CO/stirene, usando dei precatalizzatori semplificati, che ha confermato il meccanismo riportato in letteratura.

I *Capitoli 3* e *4* trattano lo sviluppo di catalizzatori per la copolimerizzazione etilene/metil acrilato, che è considerata il 'Sacro Graal' della catalisi di polimerizzazione. Nel *Capitolo 3* la ricerca è stata indirizzata verso la sintesi di due nuovi leganti non simmetrici, entrambi caratterizzati da uno scheletro BIAN e aventi un anello arilico sostituito in posizione *orto* da un gruppo metilico e uno metossilico, mentre differiscono per il numero e la posizione dei sostituenti elettron attrattori (CF_3) sull'altro anello arilico. Si è studiata la loro chimica di coordinazione al palladio, considerando anche l'analogo simmetrico avente entrambi gli anelli arilici sostituiti da un metile e un metosso in posizione *orto*. Sia i complessi cationici con l'acetonitrile che quelli con il dimetilsolfossido $[Pd(CH_3)(L)(Ar,Ar'\text{-BIAN})][PF_6]$ (L = CH_3CN, dmso), sono stati sintetizzati. La caratterizzazione dei complessi con il dmso ha evidenziato la presenza di diverse specie in soluzione, a seconda del legante ancillare coordinato al palladio, ma in ogni caso la specie principale era caratterizzata dal dmso coordinato via zolfo. Testati in catalisi, i complessi monocationici sono risultati inattivi, indipendentemente dalla natura del legante ancillare. Inoltre, considerando l'effetto del solvente, è stata osservata la decomposizione dei complessi attraverso la dissociazione e la rottura del legante.

Considerato che lo scheletro DAB è preferibile rispetto al BIAN nella reazione di copolimerizzazione di interesse, nel *Capitolo 4* è stato sintetizzato un nuovo legante non simmetrico Ar,Ar'-DAB avente un anello arilico sostituito in posizione *meta* con gruppi elettron attrattori (CF_3) e l'altro anello con sostituenti metilici elettron donatori in posizione *orto*. Per la sintesi del corrispondente complesso di Pd(II) è stata messa a punto una procedura basata sull'uso del [Pd(cod)(CH_3)Cl] come agente templante. Il complesso neutro è stato usato per la sintesi dei corrispondenti complessi monocationici con l'acetonitrile [Pd(CH_3)(CH_3CN)(Ar,Ar'-BIAN)][X] (X = PF_6^-, SbF_6^-), e dallo spettro ^{19}F-^1H HOESY del complesso con l'esafluorofosfato è stato possibile localizzare il controione, che in soluzione si trova preferenzialmente sopra il piano di coordinazione, spostato vero lo scheletro DAB del legante; al contrario, in letteratura è riportato che nei complessi con leganti a scheletro BIAN il controione è localizzato principalmente verso l'acetonitrile coordinato al palladio. La serie dei complessi monocationici è stata estesa ai derivati con il dimetilsolfossido, e la loro caratterizzazione NMR ha evidenziato, con il nuovo legante DAB non simmetrico, la presenza unicamente di specie con il dmso coordinato via zolfo, mentre con l'analogo legante BIAN si osserva la presenza, seppure in tracce, della specie avente il dmso coordinato via ossigeno. L'attività catalitica dei complessi monocationici con il nuovo legante non simmetrico e con i corrispondenti simmetrici è stata confrontata con quella riportata per gli analoghi complessi con leganti BIAN: passando dallo scheletro BIAN al DAB si è osservato un aumento di produttività, in accordo con la letteratura, ma l'aumento per il legante non simmetrico non era così pronunciato come quello osservato per il legante simmetrico con i metili su entrambi gli arili. Non si è osservato alcun effetto del legante labile né del controione in 2,2,2-trifluoroetanolo (TFE); al contrario, passando a un solvente meno polare come il diclorometano, si è vista una generale diminuzione della produttività, e i complessi con l'esafluoroantimoniato erano circa tre volte più produttivi dei corrispondenti catalizzatori con l'esafluorofosfato, in accordo con la formazione della coppia ionica. Inoltre, i complessi contenenti l'acetonitrile si sono rivelati più produttivi dei corrispondenti derivati con il dimetilsolfossido, portando alla formazione di un prodotto con un più alto contenuto di monomero polare.

Nei *Capitoli 5* e *6* si è studiata l'attività catalitica di complessi di palladio con leganti piridilimminici sia nella copolimerizzazione CO/vinil arene sia nell'alcossicarbonilazione di olefine interne, sottolineando la versatilità di tali molecole come leganti ancillari in reazioni catalizzate da complessi di palladio. Nel *Capitolo 5* sono state sintetizzate delle piridilimmine aventi un anello arilico sull'azoto imminico e caratterizzate dalla presenza di un idrogeno o un metile sul carbonio imminico e/o sulle posizioni *orto* dell'arile. Tali molecole sono state usate per la sintesi dei corrispondenti complessi di palladio neutri

[$Pd(CH_3)Cl(N\text{-}N')$] e monocationici [$Pd(CH_3)(CH_3CN)(N\text{-}N')][PF_6$]. I complessi monocationici hanno generato catalizzatori molto attivi nella copolimerizzazione CO/vinil arene (stirene, 4-metil-stirene), portando a produttività fino a 4.61 kg CP/g Pd (kg CP/g Pd = chilogrammi di copolimero per grammo di palladio) e pesi molecolari fino a 1 775 000 g/mol, con indici di polidispersità nel range 1.67 – 8.08. I valori di polidispersità relativamente alti indicano la presenza di più specie cataliticamente attive. Tutti i polichetoni sintetizzati erano sindiotattici, con un contenuto di triade *uu* che dipendeva dalla natura del legante ancillare, e, in contrasto con i nostri dati recentemente pubblicati, non si è osservato alcun effetto del vinil arene sulla stereochimica del prodotto. Nel *Capitolo 6* si è testata l'attività catalitica di una serie di complessi di Pd(II) con leganti piridilimminici [$Pd(N\text{-}N')(L)_2$], con L = acetato, trifluoroacetato, nell'alcossicarbonilazione di 1-ottene e 4-ottene. Gli alcheni sono stati convertiti nei corrispondenti diesteri vicinali, rispettivamente il dimetil 2-esilsuccinato e il dimetil 2,3-dipropilsuccinato, a indicare che l'isomerizzazione del doppio legame non avviene prima della carbonilazione.

In conclusione, l'attività di ricerca sviluppata durante questo dottorato ha portato alla sintesi e caratterizzazione di numerosi nuovi leganti e corrispondenti complessi di palladio, i quali sono stati testati quali precatalizzatori in catalisi di copolimerizzazione, portando a notevoli passi avanti nello stato dell'arte in questo campo. È stato dimostrato che una piccola variazione nello scheletro e nei sostituenti del legante ancillare risulta in una notevole variazione dell'attività catalitica dei corrispondenti complessi di palladio, confermando l'importanza della diversità dei leganti ancillari nella catalisi omogenea.

CHAPTER 1

General introduction

1.1. Polyolefins.

Polyolefins are the biggest class of plastics, and their market grows by 5 - 6 % every year thanks to their versatility with respect to physical and mechanical properties, their non-toxicity, their energy efficient and economically attractive production, their low cost and easily available raw materials.[1] Among these, the commodity polymers linear low density polyethylene (LLDPE) and polypropylene (PP), have shown the highest annual growth rates with more than 10 %, followed by high density polyethylene (HDPE) and low density polyethylene (LDPE).[2] This represents the main reason of the great progress in catalyst tailoring, in optimization of the polymerization process and in controlling the architecture of the structure and properties of these polymers, that still attract so much attention from academic and industrial research.

Metal-catalyzed olefin polymerization was a major breakthrough of the last century, and it means much more than transforming the light fraction of oil into plastics: thanks to precision syntheses, it represents an endless source of exactly defined chain architectures. Whole disciplines, like polymer crystallography and macromolecular chemistry, arose to investigate the structural properties of polyolefins, while at the same time the sophisticated methods for catalysts fingerprinting allows to identify general principles of selective coordination catalysis, in homogeneous as well in heterogeneous phase.[3]

Despite the widespread use of polyolefins as commodity plastics and the incredible advances recorded in the last half-century in characterizing and tuning polymer architecture, there is still space for improvement. On one hand, the polyolefin synthesis is not a perfect process: many molecular catalysts are too expensive for application in a market with very low margins, while the Ti-based Ziegler-Natta systems are not (yet) able to provide the fine control over the polymer properties that the use of molecular catalysts entails. Due to the production scale, even a very small increase in process efficiency would result in a huge profit, and, for this reason, research is crucial. On the other hand, specialties like the new olefin block copolymers, which broke long-standing paradigms in structure/properties relationships,[4] or the ever-green Ultra-High-Molecular-Weight PolyEthylene (UHMWPE), just to mention two, are commercialized at significantly higher market prices than standard polyethylenes or polypropylenes. This means that their production can be profitable at comparatively low scale already and allows the use of expensive catalysts.[3]

Up to now, most polymers are produced by Ziegler–Natta catalysis with heterogeneous catalysts generated from simple titanium compounds, such as $TiCl_4$, activators, donors, and a support such as $MgCl_2$, but there is also a growing market for single-site polyolefins, which exhibit more defined microstructures, controlled molecular weight distributions, and superior mechanical properties. A quarter of the worldwide LLDPE production (110 million tons per year) is based on single-site catalysts, mainly metallocenes, and during the last two decades an increasing number of polymerization processes employing post- or non-metallocene catalysts have been commercialized.[5] Although post-metallocene catalysts in itself consist of many different catalyst families, the activators are in fact the same as used for the metallocene ones (i.e. alluminoxanes like MAO and MMAO, tris(pentafluorophenyl)borane and tetrakis(pentafluorophenyl)borates based ion pairs);[6] this is why the development of new activators does not seem to target specific classes of (post-) metallocene catalysts.

While most industrial processes are in solution-phase, for gas- and slurry-phase application the single site catalyst has to be supported, usually on a metal oxide and in particular silica, through the co-catalyst itself, which is previously incorporated in the support.[5]

A class of post-metallocene catalysts used in LLDPE synthesis is based on *ansa*-cyclopentadienyl-amido ligands with a short $Si(CH_3)_2$ bridge (Figure 1.1a); constrained geometry catalysts are employed on large scale in high-temperature solution for the production of copolymers of ethylene and higher terminal alkenes, such as 1-hexene, 1-octene, and 1-decene, with up to 60 wt % of comonomer incorporated (marketed under Dow's ENGAGE and AFFINITY brands).[5]

The constrained geometry (Cp-M-N bite angle of 107.6°, Cp = cyclopentadienyl) is thought to be responsible for the high comonomer incorporation ratio and activity (complex (a) of Figure 1.1: $4.3 \cdot 10^7$ g P/mol Ti · h). Studies of structure–activity relationship by Dow showed that more electron deficient Cp ligands compared to tetramethylcyclopentadienyl (Cp*) resulted in lower activity and comonomer incorporation, and for the substituent on the nitrogen atom, a similar trend was observed. The nature of the bridging unit has a strong influence on the catalyst properties: an elongation of the bridge leads to a larger Cp-Ti-N bite angle and to lower activity and comonomer incorporation. Owing to their sterically open geometry, polymers obtained from cyclopentadienyl–amido catalysts are mainly atactic, especially when prepared at industrially relevant temperatures above 413 K.[5,7]

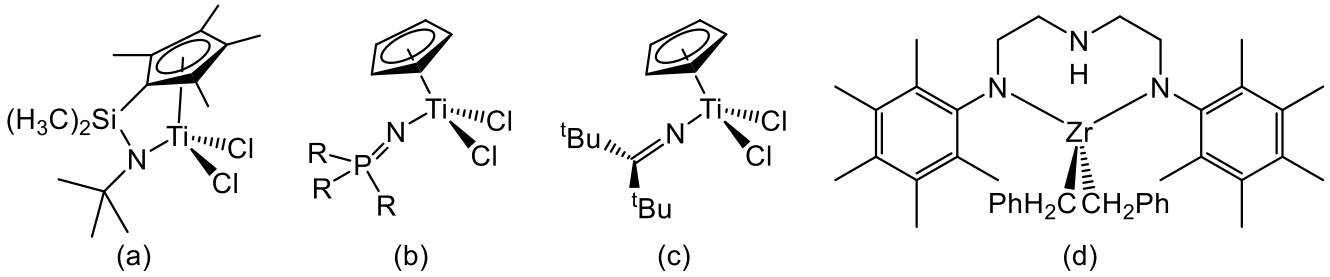

Figure 1.1. Examples of (a) Cp/amido; (b) Cp/phosphinimine; (c) Cp/ketimide; (d) diamido-amine complexes.[5]

The synthesis of the ligands necessary for such catalysts is not trivial, therefore much attention has been addressed in developing ancillary ligands with similar properties but easier to synthesize.

With the idea of mimicking the cyclopentadienyl ligand with synthetically readily accessible compounds, phosphinimide transition-metal olefin polymerization catalysts were developed (Figure 1.1b): the phosphinimide ligand has a similar cone angle as Cp but the steric hindrance is moved more far away from the metal center. This resulted in good activity in ethylene polymerization, with high molecular weight and narrow polydispersity (6.5 g P/mol Ti · h, Mw = 90000 g/mol (1.6)), and even better results were obtained with the dimethyl catalyst in place of the dichloride derivative.[8]

Similar complexes with ketimide ligands were claimed to be highly active olefin homo- and copolymerization catalysts both in gas phase, slurry, and high-temperature solution polymerization (Figure 1.1c).[5] Surprisingly, the activity increased dramatically in ethylene/1-hexene copolymerization to more than 10^9 g P/mol Ti · h,[9] and it was even able to copolymerize ethylene and styrene in a living manner, although both homopolymerization reactions are not living.[10]

Group 4 complexes bearing diamide ligands have been studied for olefin polymerization, owing to their high electrophilicity (Figure 1.1d); they are used in combination with metallocenes for the production of bimodal HDPE resins, which are well suited for example for long-lasting pressure pipe applications.[5]

Besides the optimization of the polyolefin synthesis, the interest of both academic and industrial research focused on new polymers displaying innovative chemical, physical and mechanical properties. For this reason, living olefin polymerization is a powerful tool for the synthesis of polyolefins with controlled molecular weight and very narrow molecular weight distribution, as well as with a wide array of architectures. The major drawback is the formation of a single polymer chain per catalyst, therefore the real value of living polymerization is the creation of new materials from a basic set of available monomers. In particular, one of the most attractive features of a living catalyst system lies in its ability

to produce well-defined block copolymers by sequential monomer addition. In addition, the vanadium catalysts have also been employed for the synthesis of block copolymers from polar monomers by transforming the living chain end to one capable of initiating a radical or cationic polymerization.[11]

A wide variety of catalyst for the living polymerization of olefins have been studied, ranging from early (Ti, Zr, Hf, V, Nb, Ta) to late transition metals (Co, Ni, Pd), including also rare-earth metals (La, Nd, Lu, Sm), often in combination with cyclopentadienyl ligands, but still the limited productivity makes these processes commercially unviable. This issue is overcome by a chain-shuttling polymerization process developed by Arriola and co-workers at Dow for the synthesis of olefin block copolymers: in this solution polymerization process, the growing polymer chain is transferred reversibly with a chain-transfer agent (i.e. $ZnEt_2$) between a catalyst that does not significantly incorporate comonomer (a phenoxyimine Zr complex, Figure 1.2a), and a catalyst with a high propensity for comonomer incorporation (a pyridylamido Hf complex, Figure 1.2b). This yields multiblock copolymers with highly crystalline polyethylene and amorphous poly(ethylene-co-1-olefin) blocks; as this polymerization system is not stoichiometric but catalytic in terms of polymer chains produced per metal center, commercially profitable polymer quantities are produced with relatively low catalyst loadings.[12] The process has been exploited at industrial level in a very short time and the copolymer is commercialized under the trademark of INFUSE®.[5]

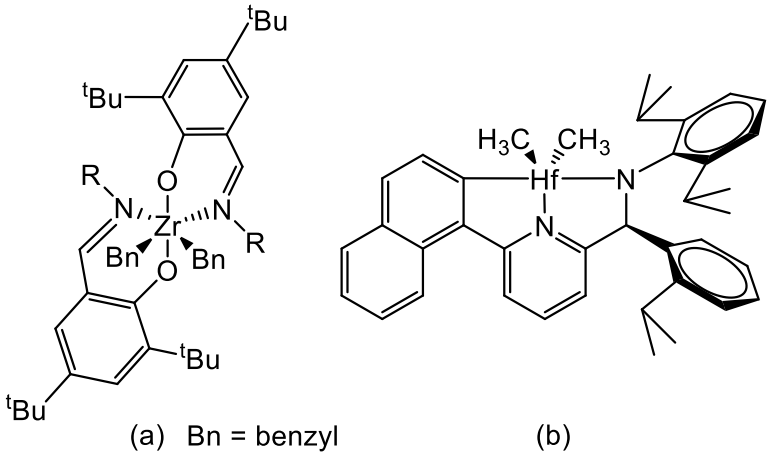

Figure 1.2. Chain-shuttling catalysts selective for (a) ethylene and (b) α-olefin incorporation.[12]

By using multifunctional chain-transfer agents, the chain shuttling concept was further expanded to the synthesis of telechelic polymers and block-copolymers, which can be employed as ingredients for coatings, sealants, adhesives, and rocket-fuel binder.[5]

Another approach towards large-scale production of precisely defined polyolefins with very narrow molecular weight distributions is the catalyzed chain growth or catalytic chain transfer polymerization. In this process, the polymer chain is reversibly transferred from the catalytically active metal center to a surrogate, typically a zinc or main-group metal-alkyl compound, with the chain transfer rate being faster than the chain growth rate. This leads to a simultaneous growth of all polymer chains and thus narrow molecular weight distributions. The number of polymer chains is not stoichiometric in the costly catalyst, but in the much cheaper chain transfer agent.[5]

A different route to novel materials based on polyolefins is the incorporation of inorganic nanomaterials such as metal oxides, carbon nanotubes or nanofibers, in the polyolefin matrix. The composite materials show, for example, improved stiffness with negligible loss of impact strength, high gas-barrier properties, significant flame retardancy, better clarity and gloss as well as high crystallization rates. Even low nanoparticle contents (2 - 4 wt %) are already sufficient to obtain new or modified material characteristics. The properties of the nanocomposites are not only influenced by the kind of fillers, but also by the microstructure of the polyolefins and the preparation process. Most composites are prepared up to now by mechanical blending of the particles or fibers above the melting temperature of the desired matrix, but this often leads to an insufficient filler dispersion. Such disadvantages can be overcome by *in situ* polymerization: the co-catalyst (MAO) is adsorbed or anchored on the filler and then the desired metallocene catalyst is added, generating active sites directly on the surface of the nanomaterials. The thickness of the polymer films, formed by addition of ethylene or propylene, depends on the polymerization conditions, especially the polymerization time, the kind of metallocene catalyst, and the pressure of the monomer. The *in situ* polymerization leads to composite materials where each particle or fiber is intensively covered with the polymer.[13]

All these examples highlight that the choice of the homogeneous catalyst deeply affects the properties of the produced polymer, and in particular that the catalytic behavior is deeply affected by subtle modifications of the ancillary ligand. This is the result of the application of the concept that by tailoring the coordination environment of the metal center, single-site catalysts are able to control the molecular weight, molecular weight distribution, comonomer incorporation, and the nature of the terminal groups of a polymer in a way that is often impossible using conventional heterogeneous catalysts (Scheme 1.1).[14]

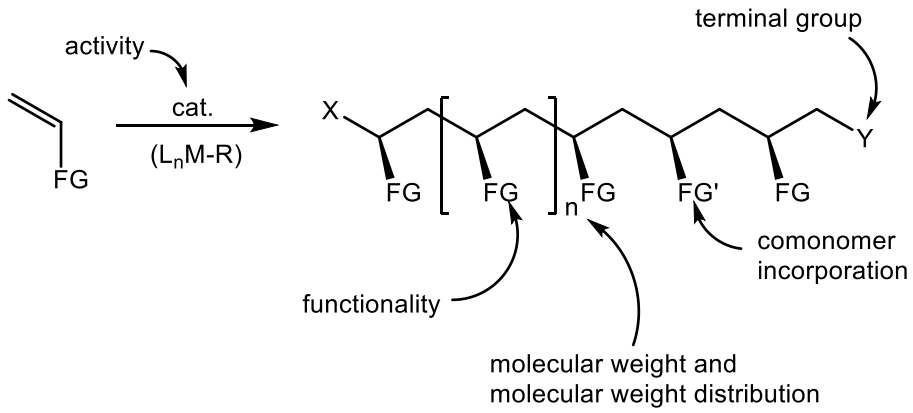

Scheme 1.1. Key factors affecting the polymer properties.

Another key feature of homogeneous catalysts is their ability to control the stereochemistry of the polymer, which deeply affects the physical and mechanical properties of the resulting material. The stereochemistry of the polymerization reaction can be controlled by either the enantiomorphic site or the polymer chain end, and in some cases both control mechanisms can be simultaneously operative.[15]

After examination of the results of many separate investigations in the stereocontrolled synthesis of polypropylene, the macromolecule of excellence when the control of stereochemistry is under debate, a relationship between complex symmetry and polymer tacticity is highlighted, although exceptions are not uncommon:

- catalysts exhibiting C_{2v} symmetry typically produce atactic polymers or moderately stereoregular polymers by chain-end control mechanisms;
- C_s-symmetric catalysts that have mirror planes containing the two diastereotopic coordination sites behave similarly, while C_s-symmetric catalysts that have a mirror plane reflecting two enantiotopic coordination sites frequently produce syndiotactic polymers;
- C_2-symmetric complexes, both racemic mixtures and enantiomerically pure ones, typically produce isotactic polymers via a site-control mechanism;
- stereoselectivities of asymmetric (C_1) complexes are unpredictable and have been reported to produce polymer architectures ranging from highly isotactic, to atactic, including isotactic-atactic stereoblock.[14]

A recent statistical analysis of the behavior of zirconocenes in olefin polymerization, quantifing factors that contribute to stereo- and regiocontrol highlighted the key role of the ligand, suggesting a series of guidelines for targeted ligand design. For example, it points out that an overcrowded catalyst is not necessarily able to act a better control on the stereochemistry of the product.[16]

Even though not belonging to the specific class of catalysts for polyolefin production, one of the most recent interesting examples of stereochemistry control is the gradient isotactic multiblock polylactide synthesized using well-defined single-diastereomeric aluminum complexes of enantiomerically pure salalen ligands that act as active catalysts in racemic lactide polymerization (Scheme 1.2). The catalytic activity is in the range of typical aluminium catalyst, with stereoselectivity depending on the specific substitution pattern of the ligand. Enantiomerically pure isoselective catalysts were found to act by a combination of enantiomorphic-site and chain-end control mechanisms, and led to polylactide of a proposed new microstructure, the gradient isotactic multiblock polylactide, consisting of D- and L-blocks of gradually exchanging lengths, the properties of which are still under investigation.[17]

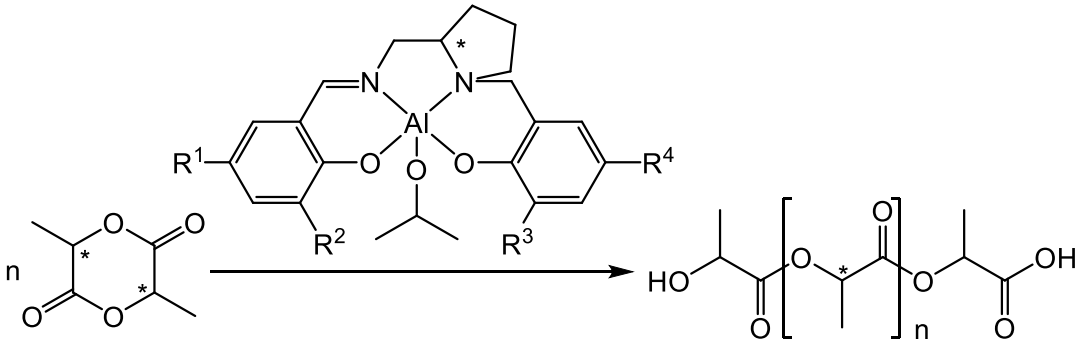

Scheme 1.2. Polymerization of lactide with salalen-type aluminium catalyst.[17]

1.2. Ethylene/methyl acrylate copolymerization reaction.

Despite their widespread use both as commodity plastics and specialty materials, polyolefins lack of surface properties such as adhesion, dyeability, printability, and compatibility with other materials.[18,19] The introduction of polar functional groups in the polyolefin backbone should overcome this lack, not only improving the surface properties of the final material, but also expanding the range of its applications.[18] Currently, commercial processes for functionalized polyolefins production are based on radical polymerization and post-polymerization functionalization, two technologies that suffer from high energy consumption, low cost-efficiency and poor control over the polymer microstructure, thus limiting the variety of available materials and holding back the synthesis of polymers with novel architectures and properties.[18]

The direct, homogeneously catalyzed copolymerization of an apolar monomer with a polar vinyl monomer represents one of the most powerful tool for the controlled incorporation of polar functionalities in the polyolefin backbone. Ethylene and methyl acrylate were chosen as model substrates for this reaction (Scheme 1.3). The polymerization of apolar and polar vinyl monomers has been

recognized as one of the major unsolved problems in the field of polymer synthesis, thus, in the last two decades, enormous efforts have been addressed to the discovery of homogeneous catalysts active in the target reaction under milder conditions and allowing a better control on polymer microstructure compared to radical polymerization.[18]

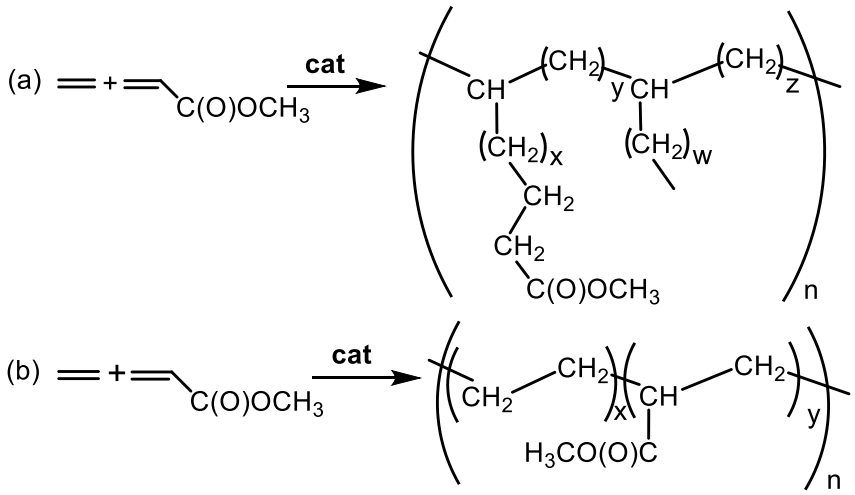

Scheme 1.3. Ethylene/methyl acrylate copolymerization: (a) branched functionalized polyolefin; (b) linear functionalized polyolefin.

As discussed in the previous part, the industrial catalysts applied for olefin polymerization are based on oxophilic, early d^0 transition metals such as Ti(IV) and Zr(IV), which are easily poisoned by compounds with polar functional groups.[20] Late transition metals are commonly known to be more functional group tolerant, and this has made them attractive targets on which to base new polymerization catalysts. However, till Brookhart's[20-22] and Gibson's discovery[23] in the middle of the Nineties, none complex based on late transition metals was known to be able to catalyze polyolefin synthesis. The discovered late transition metal catalysts are based on iron, cobalt, nickel and palladium and they are extremely efficient catalysts for ethylene polymerization.

In particular, Brookhart's system was based on a monocationic Pd(II) complex with a methyl fragment, diethyl ether as labile ligand, a neutral α-diimine as ancillary ligand and a non-coordinating counterion ($[BAr^F]^-$, Ar^F = 3,5-$(CF_3)_2C_6H_3$). The ancillary ligand is featured by a diimine backbone, mainly a 1,4-diaza-1,3-butadiene (DAB) or acenaphthene (BIAN) skeleton, bearing two aryl rings substituted in *ortho* positions with bulky groups. This ligand significantly affects the catalytic activity of the metal center; in particular, the aryl rings, nearly orthogonal to the coordination plane, create a large out-of-plane steric hindrance that encumbers the apical positions of the metal, thus disfavoring the chain transfer and β-hydride elimination that represent the chain termination process, leading to the formation of

polyolefin instead of butenese and hexenes. The highest value of productivity in ethylene polymerization was 253 g P/g Pd · h (grams of product per gram of palladium per hour) of amorphous, highly branched polyethylene.[21]

Brookhart's discovery opened the way to apply them in the ethylene/polar vinyl monomer copolymerization. In order to identify the best suited metal for the target copolymerization, the functional group tolerance, the ability to engage π back-bonding and the height of the ethylene insertion barrier have to be considered. Computational analyses of all the 30 d-block metals in many different oxidation states indicated that palladium(II) strikes the right balance among them, and no other suitable candidate was identified.[24] In fact, the two main catalytic systems reported in the literature for the ethylene/methyl acrylate copolymerization are based on palladium complexes and differ in the nature of the ancillary ligand present in the metal coordination sphere, which in one case is a neutral α-diimine (Figure 1.3a)[25,26] and in the other is an anionic phosphine sulfonate derivative (P-O) (Figure 1.3b).[27] Both catalytic systems lead to the formation of real copolymers and not to a mixture of the two homopolymers.

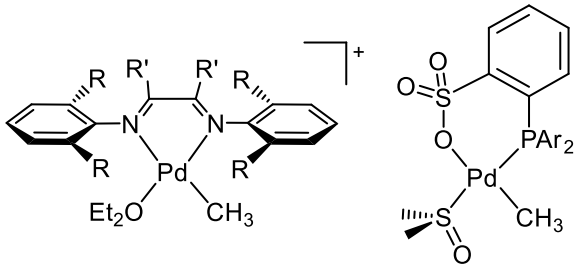

L1-3 **L4**

(a) **(b)**

N-N: see Figure 1.5

Figure 1.3. The classes of complexes reported in the literature: (a) α-diimino derivatives; (b) phosphine sulfonate derivative.

The first catalysts for ethylene/methyl acrylate copolymerization based on a phosphine sulfonate ligand was generated *in situ* from $Pd(AcO)_2$ with a ligand featured by anisol substituents on the P-atom. When applied in the copolymerization reaction (solvent: bis(2-methoxyethyl)ether), 10 h, 353 K, $P_{ethylene}$ = 30 bar), it showed an activity of 173 g CP/g Pd · h (g CP/g Pd · h = grams of copolymer per gram of palladium per hour). The product is a linear copolymer with a low branching degree, having 9 % of acrylate inserted in the main chain.[27]

A remarkable improvement derived by the replacement of the *in situ* system with a preformed catalyst having the same P-O ligand, and a methy group and a dimethyl sulfoxide in the palladium coordination sphere, [Pd(CH_3)(dmso)(P-O)] (**L4**, Figure 1.3b): this led to a very similar activity, 169 g CP/g Pd · h (in toluene, T = 368 K, $P_{ethylene}$ = 5 atm), and up to 52 % of incorporated polar monomer.[28]

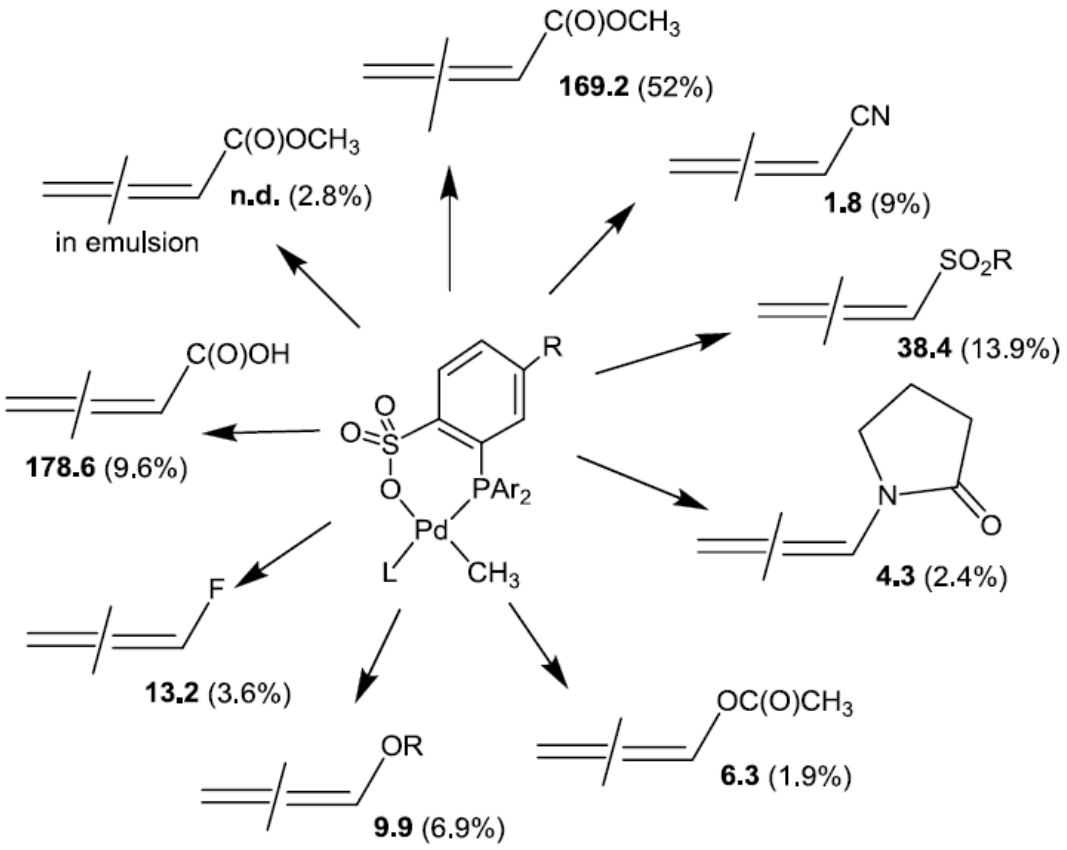

Figure 1.4. Ethylene/polar monomer copolymerization reactions catalyzed by the P-O systems.[28-36] Productivities (g P/g Pd · h) are reported in bold, polar monomer content in brackets.

Palladium complexes with P-O ligands were found to be rather versatile, being able to catalyze the copolymerization of ethylene with a variety of acrylates and polar monomers, such as acrylonitrile,[29] nitrogen-containing polar monomers,[30] vinyl acetate,[31] alkyl vinyl ethers,[32] vinyl fluoride,[33] acrylic acid,[34] vinyl sulfonate,[35] and were also applied in emulsion polymerization (Figure 1.4).[36]

The same P-O based complex (**L4**, Figure 1.3b) was applied as precatalyst for the copolymerization of ethylene with siloxane acrylate, leading to a copolymer with up to 12.9 % of inserted polar monomer, as well as the terpolymerization of ethylene with a fluorinated acrylate and siloxane acrylate. In both cases, the obtained polymer was rich in siloxane groups that can be hydrolyzed to form cross-links, yielding elastomers with good properties under mild conditions.[37]

A recent study highlighted that the activity of the catalysts depends on the electronic features of the polar monomer, and in particular, it increases on decreasing electron-density of the olefin; moreover, the insertion regiochemistry can be tuned by changing the steric and electronic properties of the functional group.[38]

A series of cationic palladium complexes having bis(phosphine) monoxide ligands was also tested in the copolymerization of ethylene with various polar monomers, like vinyl acetate, acrylonitrile, vinyl ethers and allyl monomers; they showed good activities, up to 74 g CP/g Pd · h, leading to linear copolymers with a random distribution of 1 - 4 % polar monomer. However, they were found to be totally inactive when methyl acrylate was employed as polar monomer (**L5**, Figure 1.5a).[39]

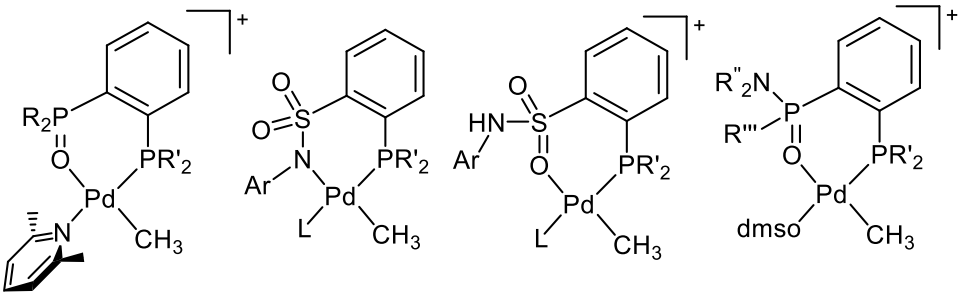

L5 **L6** **L7**

(a) (b) (c)

Figure 1.5. Examples of (a) bis(phosphine) monoxide derivatives; (c) phosphine sulfonamide derivatives; (c) phosphine phosphonic amide derivatives.

Phosphine-sulfonamide ligands were also taken into account (**L6**, Figure 1.5b); due to the presence of both nitrogen and oxygen atoms able to coordinate to palladium, either neutral (N-bonded) or monocationic (O-bonded) complexes can be obtained. The study of their reactivity with MA shows a remarkably different behavior: after the first MA insertion, which follows a 2,1-regiochemistry, with cationic O-bonded species the β-hydride elimination prevailed, while with neutral N-bonded complexes either a second MA insertion occurred or no reaction at all took place. This highlighted that N-coordination of the sulfonamide moiety promotes chain transfer versus chain growth, reasonably due to the steric bulk of the additional organic substituents on the coordinating nitrogen-donor, while for O-coordinated species, insertion barriers and barriers of chain transfer could be potentially favorable for insertion polymerization chain growth, providing that chain transfer can be suppressed.[40]

The latest reported class of palladium catalysts was based on phosphine phosphonic amides, in which substituents on three positions could be modulated independently, providing a great deal of flexibilities and opportunities to tune the catalytic properties (**L7**, Figure 1.5c). The related cationic complexes were

found very active in ethylene polymerization ($1.26 \cdot 10^5$ g P/g Pd · h), while in ethylene/MA copolymerization they led to lower activities with respect to the catalytic systems based on phosphine sulfonate ligands. Nevertheless, they are able to catalyze the copolymerization at room temperature, while higher temperatures are required for the P-O systems.[41]

As far as catalytic systems based on α-diimines are concerned (Figure 1.6), they are active in the ethylene/MA copolymerization under milder conditions with respect to the P-O systems (dichloromethane, T = 303 K, $P_{ethylene}$ = 2.0 - 2.5 bar), leading to 57 g CP/g Pd · h of amorphous, highly branched copolymers (ca 100 branches per 1000 C atoms), with the polar monomer content in the range 2 – 12 %, the acrylate units located at the end of the branches.[25,26]

The productivity of the catalytic system $[Pd(CH_3)(Et_2O)(N\text{-}N)][BAr^F]$ and the incorporation of the polar monomer can be tuned by modifying the ancillary ligand; in particular, the main systems are based on either a DAB or a BIAN skeleton with aryl rings bearing in *ortho* positions bulky isopropyl groups (Figure 1.5).[25,26]

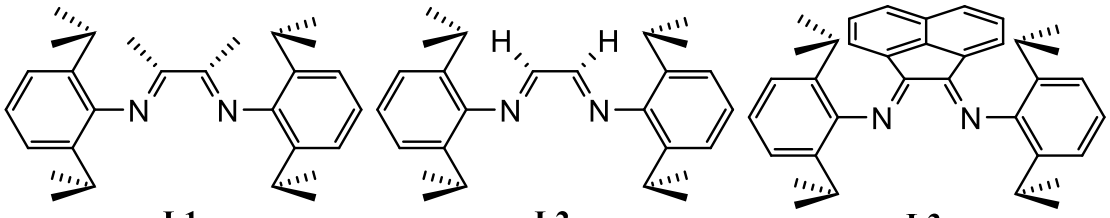

L1	**L2**	**L3**
57 g CP/g Pd · h	6.1 g CP/g Pd · h	6.1 g CP/g Pd · h
4.0 % MA	5.0 % MA	4.7 % MA
Mn = 42 000	Mn = 300	Mn = 10 000

Figure 1.6. Studied α-diimine ligands and productivities of the related catalysts. Reaction conditions: CH_2Cl_2, T = 308 K, t = 18.5 h, $P_{ethylene}$ = 6 atm, [MA] = 5.8 M.

Productivity is remarkably affected by the ligand skeleton: moving from **L3** and **L2** to **L1** resulted in an increase in the productivity of one order of magnitude, without significant variation of the inserted polar monomer content. The catalytic activity is also affected by the reaction conditions, in particular MA concentration: an increase in the polar monomer concentration led to a lower productivity together with a higher acrylate incorporation (Table 1.1).

Table 1.1. Ethylene/MA copolymerization reaction: effect of reaction conditions. Precatalyst: [Pd(**L1**)((CH_2)$_3$$COOCH_3$)][$BAr^F$][a]26

Run	[MA] (M)	T (K)	Yield (g)	g CP/g Pd · h[b]	% MA	M_w[c]
1	-	298	8.8	447.0	-	297000
2	0.6	308	22.2	112.7	1.0	88000
3	2.9	308	4.3	21.8	6.1	26000
4	5.8	308	1.8	9.1	12.1	11000

[a] Reaction conditions: 0.1 mmol Pd (run 1: 0.01 mmol), $P_{ethylene}$ = 2 atm, solvent: CH_2Cl_2 ($V_{tot.}$ = 100 mL), t = 18.5 h; [b] g CP/g Pd · h = grams of copolymer per gram of palladium per hour; [c] determined by GPC.

NMR investigation allowed to depict the mechanism of the copolymerization reaction: the insertions of acrylate can undergo either a primary or a secondary regiochemistry, although the 2,1-insertion is the predominant mechanism observed. This reaction step leads to a distorted four-membered metallacycle, with the oxygen atom of the carbonyl group of the inserted acrylate coordinating the fourth position of the metal. (Scheme 1.4). This chelate intermediate can be either opened by an incoming monomer, leading to chain growth, or it can follow a series of β-hydride elimination and reinsertion reactions, known as chain walking mechanism.

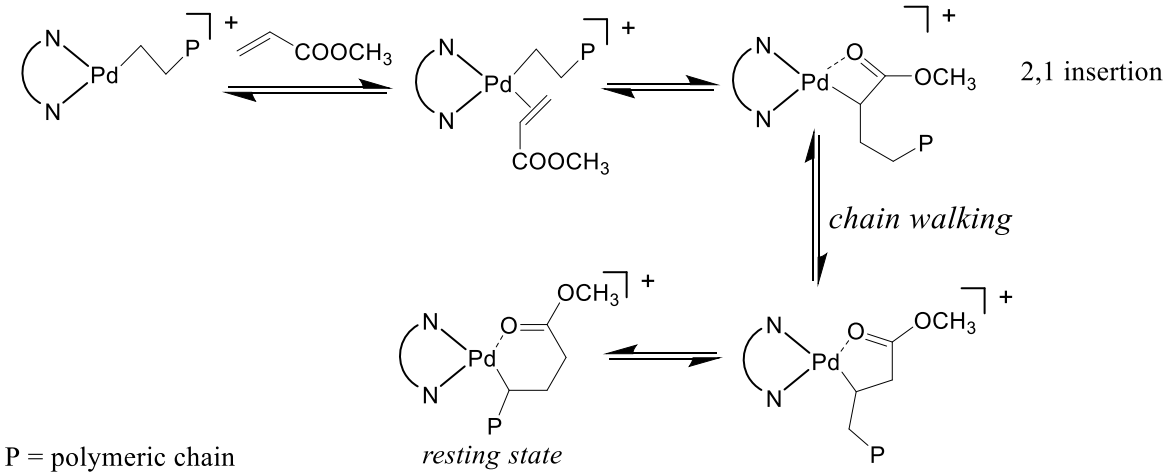

Scheme 1.4. Main reaction steps in the copolymerization of ethylene with MA for the α-diimine catalytic system.[26]

While for the P-O catalytic system the chain growth reaction rate is higher with respect to the chain walking one, thus leading to a linear product having the MA inserted in the main chain,[42] in the case of α-diimine catalytic systems the chain walking pathway is preferred.[26] In fact, the same mechanism is responsible for the formation of branched polymers with catalytic systems based on nickel and palladium with α-diimine ligands.[21] The chain walking mechanism leads to the expansion of the chelate ring, forming the more stable, and accordingly, more difficult to open, six-membered palladacycle, which represents the resting state of the copolymerization reaction.[21]

The study of the effect of the nature of the ancillary ligand on the catalytic behavior highlighted that an increase in MA incorporation can be achieved with a palladium complex having a DAB ligand with mesityl-groups on the N-donor atoms: this led to an activity of 1.3 g CP/g Pd · h, with the 25 % of inserted polar monomer.[26]

The use of a cyclophane-modified α-diimine (**L8**, Figure 1.7) generated a catalyst that is able to incorporate up to 21.8 mol % of MA, with an activity of 1.3 g CP/g Pd · h.[43] The effect of ligand backbone was investigated by using α-diimines with camphyl, phenyl, and substituted phenyl skeletons. For these ligands, the skeleton nature has a detrimental effect on the incorporation of MA, which is very low for all the catalysts, reaching the maximum value of 1.2 mol % and a TOF 11 h^{-1} for the camphyl α-diimine (**L9**, Figure 1.7).[44]

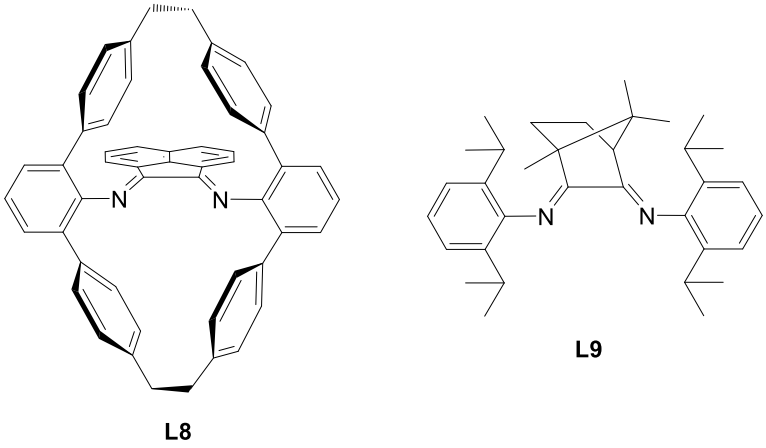

Figure 1.7. α-diimine ligands: the cyclophane substituted BIAN (**L8**)[43] and the camphyl derivative (**L9**).[44]

The palladium catalyst with ligand **L9** shows a higher thermal stability with respect to the Brookhart system, being active in the ethylene polymerization up to 343 K, and in ethylene/MA copolymerization

it leads to high molecular weight products (Mw = 19 100 g/mol) with 1.2 % of incorporated polar monomer.[44]

A cationic palladium(II) complex bearing a "sandwich" α-diimine ligand was reported to catalyze the living polymerization of ethylene at room temperature due to the axial steric hindrance provided by the capping aryl rings (**L10**, Figure 1.8): a branched polymer was obtained, with an average of 100 branches per 1000 carbon atoms, and molecular weight up to 63400 g/mol with very narrow polydispersity (1.09 – 1.18). This catalyst was also active in ethylene/MA copolymerization, leading to a living polymerization; the MA content linearly increased with the polar monomer concentration, while productivity and molecular weight decreased and no effect on the degree of branches was observed ([MA] = 5.0 M: 138 g CP/g Pd, Mw = 4700 (1.45), 13.8 % MA, 121 branches/1000 C atoms with *vs* [MA] = 0.6 M: 493 g CP/g Pd, Mw = 29600 (1.21), 1.7 % MA, 114 branches/1000 C atoms with).[45]

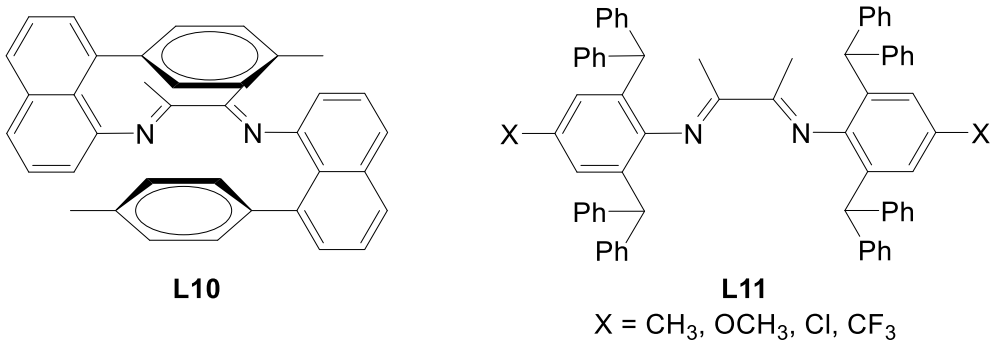

L10 **L11**

X = CH_3, OCH_3, Cl, CF_3

Figure 1.8. Hindered α-diimine ligands for Pd(II) catalysts.[45,46]

More recently, a series of palladium catalysts with sterically demanding α-diimine ligands bearing electron-donating and electron-withdrawing substituents were applied to both ethylene polymerization and copolymerization with MA (**L11**, Figure 1.8): they showed a higher thermal stability with respect to Brookhart's first system, being active for more than 20 min at 353 K in ethylene polymerization, while the latter decomposes at 333 K. Due to the high thermal stability and high activity, the obtained polyethylene is semicrystalline thanks to a low branching degree, and with high molecular weight (Table 1.2, runs 1 *vs* 2). As expected, in the ethylene/MA copolymerization the catalytic activity was much lower than in ethylene homopolymerization, but the new derivatives showed a better performance with respect to Brookhart's system: the activity is one order of magnitude higher, with a lower branching degree and a similar molecular weight, although the incorporated monomer is only 1.8 % (*vs* 5.8 % for **L1**) (Table 1.2, runs 3 *vs* 4).[46]

Table 1.2. Ethylene and ethylene/MA (co)polymerization: effect of the ligand. Precatalyst: $[Pd(CH_3)Cl(\mathbf{N\text{-}N})]$[a]46

Run	N-N	[MA] (M)	T (K)	kg CP/g Pd h	% MA	Mn (PDI)[b]	B[c]
1	**L11 (X = CH_3)**	-	353	17.4	-	72000 (2.10)	27
2	**L1**	-	313	2.4	-	5100 (1.64)	95
3	**L11 (X = CH_3)**[d]	2	313	1.2	1.8	3000 (1.81)	50
4	**L1**[d]	2	313	0.11	5.8	2500 (1.89)	105

[a] Reaction conditions: n_{Pd} = 5 μmol, $NaBAr^F$ (1.2 equiv), V_{CH2Cl2} = 2 mL, $V_{toluene}$ = 48 mL, t = 15 min, $P_{ethylene}$ = 9 atm; [b] molecular weight was determined by GPC in trichlorobenzene at 1508C with polystyrene standards; [c] number of branches per 1000 carbon atoms, as determined by ^1H NMR spectroscopy; [d] n_{Pd} = 10 μmol, V_{tot} of toluene and MA: 25 mL.

We recently reported the first nonsymmetrically substituted Ar,Ar'-BIAN ligand, featured by one aryl ring having electron-withdrawing groups in *meta* position and the other ring having electron-repulsing substituents in *ortho* position (**L12**, Figure 1.9). The related monocationic palladium complexes $[Pd(CH_3)(L)(Ar,Ar'\text{-BIAN})][PF_6]$ (L = CH_3CN, dmso) showed a productivity twice as high as that of the catalyst with the *ortho*-symmetrically substituted Ar-BIAN, and the catalytic behavior of these systems will be discussed more in detail in Chapter 3.[47]

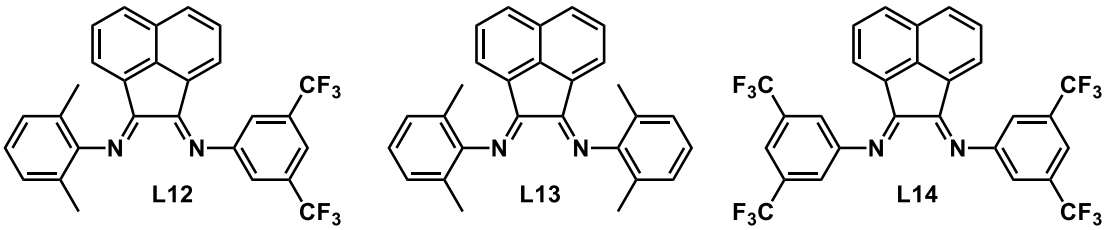

Figure 1.9. The reported nonsymmetric BIAN ligand **L12** and its symmetrical analogues.[47]

More recently, we reported a series of naphthyl-substituted α-diimine ligands having either a DAB or a BIAN skeleton (**1-4**, Figure 1.10). The related monocationic Pd(II) complexes $[Pd(CH_3)(L)(N\text{-}N)][PF_6]$ (L = CH_3CN, dmso) were applied not only in ethylene/MA but also in CO/styrene copolymerization; the collected data confirmed that DAB systems are better suited for the former reaction, with productivities nearly one order of magnitude higher with respect to catalysts having the BIAN ligands. The comparison in the catalytic behavior of these catalysts in both copolymerization reaction will be discussed more in detail in Chapter 2.[48]

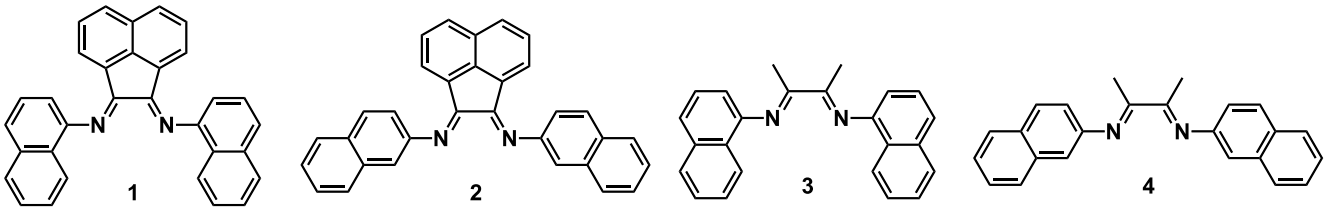

Figure 1.10. The naphthyl-substituted α-diimine ligands.[48]

Despite the efforts to find a catalyst able to incorporate a higher amount of polar monomer, it should be noted that, in order to maintain the properties of common polyolefins, lower incorporation ratio are preferable, while more than 20 % of inserted functional monomers would result in rather different mechanical and physical properties of the polymer. More importantly, the overview of the reported catalytic systems highlights that the productivity values achieved so far are too low for any industrial application, which requires an increase in the productivity of two or three orders of magnitude, thus the discovery of much better performing catalysts is a crucial challenge.[49]

1.3. Bibliography.

[1] Hilken, G. *Kunstsoffe* **2005**, *10*, 34.

[2] Kaminsky, W. *Macromol. Chem. Phys.* **2008**, *209*, 459.

[3] Busico, V. *Dalton Trans.* **2009**, 8784.

[4] Arriola, D.J.; Carnahan, E.M.; Hustad, P.D.; Kuhlman, R.L.; Wenzel, T.T. *Science* **2006**, *312*, 714.

[5] Baier, M.C.; Zuideveld, M.; Mecking, S. *Angew. Chem. Int. Ed.* **2014**, *53*, 9722.

[6] Chen, E.Y.-X.; Marks, T.J. *Chem. Rev.* **2000**, *100*, 1391.

[7] Stevens, J.C. *Stud. Surf. Sci. Catal.* **1994**, *89*, 277.

[8] (a) Stephan, D.W. *Organometallics* **2005**, *24*, 2548; Stephan, D.W.; Stewart, J.C.; Guerin, F.; Courtenay, S.; Kickham, J.; Hollink, E.; Beddie, C.; Hoskin, A.; Graham, T.; Wei, P.; Spence, R.E.v.H.; Xu, W.; Koch, L.; Gao, X.; Harrison, D.G. *Organometallics* **2003**, *22*, 1937.

[9] Nomura, K.; Fujita, K.; Fujiki, M. *J. Mol. Catal. A* **2004**, *220*, 133.

[10] Zhang, H.; Nomura, K. *J. Am. Chem. Soc.* **2005**, *127*, 9364.

[11] Coates, G.W.; Hustad, P.D.; Reinartz, S. *Angew. Chem. Int. Ed.* **2002**, *41*, 2236.

[12] Arriola, D.J.; Carnahan, E.M.; Hustad, P.D.; Kuhlman, R.L.; Wenzel, T.T. *Science* **2006**, *312*, 714.

[13] Kaminsky, W. *Materials* **2014**, *7*, 1995.

[14] Coates, G.W. *Dalton Trans.* **2002**, 467.

[15] Farina, M. *Top. Stereochem.* **1987**, *17*, 1.

[16] Talarico, G.; Budzelaar, P.H.M. *Organometallics* **2014**, *33*, 5974.

[17] Pilone, A.; Press, K.; Goldberg, I.; Kol, M.; Mazzeo, M.; Lamberti, M. *J. Am. Chem. Soc.* **2014**, *136* 2940.

[18] Nakamura, A.; Ito, S.; Nozaki, K. *Chem. Rev.* **2009**, *109*, 5215.

[19] (a) Berkefeld, A.; Mecking, S. *Angew. Chem.* **2008**, *120*, 2572; *Angew. Chem. Int. Ed.* **2008**, *47*, 2538; (b) Sen, A.; Borkar, S. *J. Organomet. Chem.* **2007**, *692*, 3291; (c) Dong, J.-Y.; Hu, Y. *Coord. Chem. Rev.* **2006**, *250*, 47; (d) Boffa, L.S.; Novak, B.M. *Chem. Rev.* **2000**, *100*, 1479; (e) Ito, S.; Nozaki, K. *Chem. Rec.* **2010**, *10*, 315.

[20] Ittel, S.D.; Johnson, L.K.; Brookhart, M. *Chem. Rev.* **2000**, *100*, 1169.

[21] Johnson, L.K.; Killian, C.M.; Brookhart, M. *J. Am. Chem. Soc.* **1995**, *117*, 6414.

[22] Small, B.L.; Brookhart, M.; Bennett, A.M.A. *J. Am. Chem. Soc.* **1998**, *120*, 4049.

[23] (a) Britovsek, G.J.P.; Gibson, V.C.; Kimberlye, B.S.; Maddox, P.J.; McTavish, S.J.; Solan, G.A.; White, A.J.P.; Williams, D.J. *Chem. Commun.* **1998**, 849; (b) Gibson, V.C.; Spitzmesser, S.K. *Chem. Rev.* **2003**, *103*, 283.

[24] Heyndrickx, W.; Occhipinti, G.; Bultinck, P.; Jensen, V.R. *Organometallics* **2012**, 31, 6022.

[25] Johnson, L.K.; Mecking, S.; Brookhart, M. *J. Am. Chem. Soc.* **1996**, *118*, 267.

[26] Mecking, S.; Johnson, L.K.; Wang, L.; Brookhart, M. *J. Am. Chem. Soc.* **1998**, *120*, 888.

[27] Drent, E.; van Dijk, R.; van Ginkel, R.; van Oort, B.; Pugh, R.I. *Chem. Commun.* **2002**, 744.

[28] Guironnet, D.; Roesle, P.; Rünzi, T.; Göttker-Schnetmann, I.; Mecking, S. *J. Am. Chem. Soc.* **2009**, *131*, 422.

[29] Kochi, T.; Noda, S.; Yoshimura, K.; Nozaki, K. *J. Am. Chem. Soc.* **2007**, *129*, 8948.

30 Skupov, K.M.; Piche, L.; Claverie, J.P. *Macromolecules* **2008**, *41*, 2309.

31 Ito, S.; Munakata, K.; Nakamura, A.; Nozaki, K. *J. Am. Chem. Soc.* **2009**, *131*, 14606.

32 Luo, S.; Vela, J.; Lief, G.R.; Jordan, R.F. *J. Am. Chem. Soc.* **2007**, *129*, 8946.

33 Shen, Z.; Jordan, R.J. *Macromolecules* **2010**, *43*, 8706.

34 Rünzi, T.; Fröhlich, D.; Mecking, S. *J. Am. Chem. Soc.* **2010**, *132*, 17690.

35 Bouilhac, C.; Rünzi, T.; Mecking, S. *Macromolecules* **2010**, *43*, 3589.

36 Skupov, K.M.; Hobbs, J.; Marella, P.; Conner, D.; Golisz, S.; Goodall, B.L.; Claverie, J.P. *Macromolecules* **2009**, *42*, 6953.

[37] Rünzi, T.; Mecking, S. *Adv. Funct. Mater.* **2014**, *24*, 387.

[38] Schuster, N.; Rünzi, T.; Mecking, S. *Macromolecules* **2016**, *49*, 1172.

[39] Carrow, B.P.; Nozaki, K. *J. Am. Chem. Soc.* **2012**, *134*, 8802.

[40] Jian, Z.; Falivene, L.; Wucher, P.; Roesle, P.; Caporaso, L.; Cavallo, L.; Göttker-Schnetmann, I.; Mecking, S. *Chem. Eur. J.* **2015**, *21*, 2062.

[41] Sui, X.; Dai, S.; Chen, C. *ACS Catal.* **2015**, *5*, 5932.

[42] Guironnet, D.; Caporaso, L.; Neuwald, B.; Gottker-Schnettmann, I.; Cavallo, L.; Mecking, S. *J. Am. Chem. Soc.* **2010**, *132*, 4418.

[43] Popeney, C.S.; Camacho, D.H.; Guan, Z. *J. Am. Chem. Soc.* **2007**, *129*, 10062.

[44] Guo, L.; Gao, H; Guan, Q.; Hu, H.; Deng, J.; Liu, J.; Liu, F.; Wu, Q. *Organometallics* **2012**, *31*, 6054.

[45] Allen, K.E.; Campos, J.; Daugulis, O.; Brookhart, M. *ACS Catal.* **2015**, *5*, 456.

[46] Dai, S.; Sui, X.; Chen, C. *Angew. Chem. Int. Ed.* **2015**, *54*, 1.

[47] Meduri, A.; Montini, T.; Ragaini, F.; Fornasiero, P.; Zangrando, E.; Milani, B. *ChemCatChem* **2013**, *5*, 1170.

[48] Rosar, V.; Meduri, A.; Montini, T.; Fini, F.; Carfagna, C.; Fornasiero, P.; Balducci, G.; Zangrando, E.; Milani, B. *ChemCatChem* **2014**, *6*, 2403-2418.]

[49] Gladysz, J.A.; Ball, Z.T.; Bertrand, G.; Blum, S.A.; Dong, V.M.; Dorta, R.; Hahn, F.E.; Humphrey, M.G.; Jones, W.D.; Klosin, J.; Manners, I.; Marks, T.J.; Mayer, J.M.; Rieger, B.; Ritter, J.C.; Sattelberger, A.P.; Schomaker, J.M.; Yam, V.W.-W. *Organometallics* **2012**, *31*, 1.

CHAPTER 2

Comparing BIAN and DAB Pd-catalysts in CO/styrene and ethylene/methyl acrylate copolymerization

Overview

The catalytic CO/styrene and ethylene/methyl acrylate copolymerizations were compared for the first time by applying the same precatalysts. With this aim, four α-diimines featuring 1- or 2-naphthyl substituents on the N-donor atom and having either an acenaphthene (BIAN) or a 1,4-diazabutadiene (DAB) skeleton were chosen. They were applied as ancillary ligands for the synthesis of Pd(II) neutral, [Pd(CH_3)Cl(N–N)], and monocationic, [Pd(CH_3)(L)(N–N)][PF_6] (L =CH_3CN, dmso), complexes. In the case of the complexes with the 1-naphthyl-substituted ligands, *syn* and *anti* isomers were found both in the solid state and in solution.

All the monocationic complexes generated active catalysts for the CO/styrene copolymerization leading to atactic or isotactic/atactic stereoblock polyketones depending on the ligand bonded to palladium. On the other hand, in the ethylene/methyl acrylate copolymerization only the complexes with the 1-naphthyl-substituted ligands led to active catalysts for this reaction.

Preliminary density functional theory (DFT) calculations were carried out with the aim of clarifying the reasons of the opposite trends observed in the catalytic behavior of the studied complexes in the two copolymerization reactions.

The work reported in this chapter related to the DFT calculation was carried out by V. Rosar in the group of Prof. Stuart Macgregor at the Heriot-Watt University of Edinburgh thanks to a STSM fellowship inside the framework of the COST Action CM1205-CARISMA.

Part of this chapter was published in:
Rosar, V.; Meduri, A.; Montini, T.; Fini, F.; Carfagna, C.; Fornasiero, P.; Balducci, G.; Zangrando, E.; Milani, B. *ChemCatChem* **2014**, *6*, 2403-2418.

2.1. Introduction.

During the last few decades, palladium(II) complexes with chelating nitrogen-donor ligands (N–N) have been widely investigated as homogeneous catalysts for (co)polymerization reactions.[1] Considerable attention was addressed to the copolymerization of carbon monoxide with vinyl arenes to yield perfectly alternating polyketones[2] and, more recently, to the copolymerization of ethylene with polar vinyl monomers, like acrylic esters, leading to functionalized polyolefins (Scheme 2.1).[3] These two reactions share the precatalysts, that are organometallic, monocationic monochelated palladium(II) complexes of general formula $[Pd(CH_3)(L)(N–N)][X]$ ($L = CH_3CN$, Et_2O; $X = PF_6^-$, $BArF = B(3,5\text{-}(CF_3)_2C_6H_3)_4^-$).

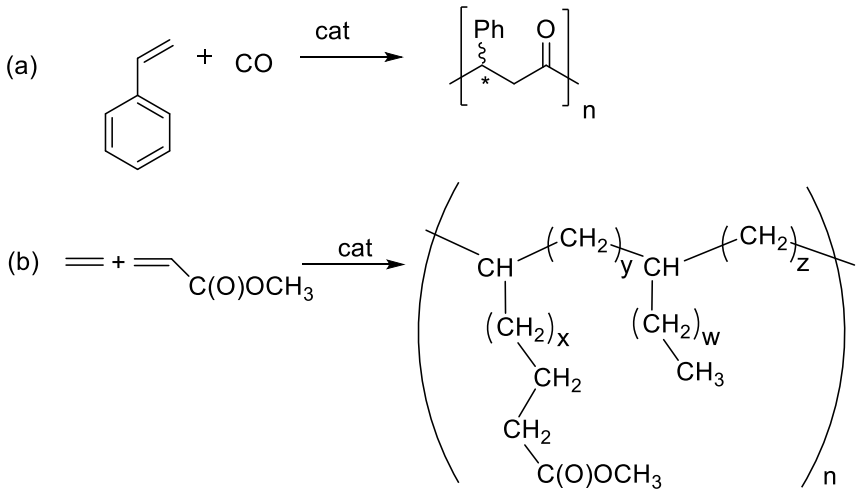

Scheme 2.1. (a) The CO/styrene and (b) the ethylene/methyl acrylate copolymerization reactions.

For the CO/vinyl arene copolymerization, a wide variety of N-donor ligands was studied, mainly with the aim of controlling catalyst stability and polymer stereochemistry. As an example, ligands belonging to the family of 1,10-phenanthrolines led to highly stable catalysts for the synthesis of polyketones of high molecular weight and high syndiotacticity.[4] As far as α-diimines are concerned, the highest productivity in terms of atactic polyketone (3.70 kg CP/g Pd) was reported for palladium complexes $[Pd(CH_3)(CH_3CN)(Ar_2BIAN)][PF_6]$ having an ancillary ligand with a BIAN skeleton bearing *meta*-substituted aryl rings.[4b]

On the other hand, for the ethylene/methyl acrylate (MA) copolymerization, the involved N-donor ligands are exclusively α-diimines with either a BIAN or a DAB skeleton. Changing the ligand skeleton from BIAN to DAB resulted in an increase in the productivity of one order of magnitude without affecting the content of the inserted polar monomer. The best results were reported for a palladium

complex with a DAB ligand in which both aryl rings were substituted in the *ortho* positions with sterically demanding isopropyl groups; this led to 1.05 kg CP/g Pd of productivity in a highly branched copolymer having 4.0 % of MA located at the end of the branches.[5]

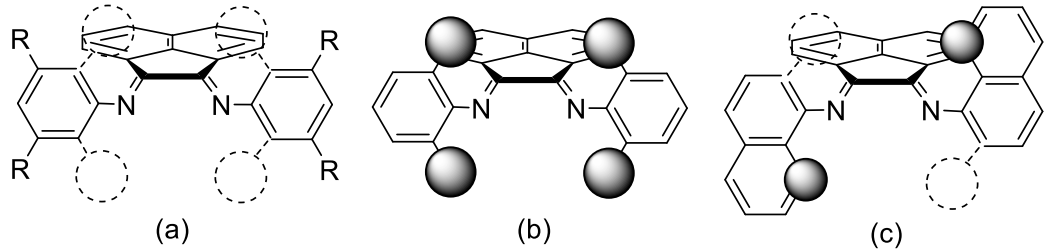

Figure 2.1. Schematic representation of the steric environment of (a) *meta*-substituted; (b) *ortho*-substituted; (c) 1-naphthyl-substituted BIAN.

Despite the extensive researches in both CO/vinyl arene and ethylene/MA copolymerizations, we were the first to report a direct comparison using the same palladium precatalysts. As the studied reactions require ligands with different steric features (Figure 2.1) and with the aim of identifying efficient catalysts for both copolymerizations, we studied α-diimines with either a BIAN or a DAB skeleton, substituted with 1- and 2-naphthyl groups (Figure 2.2).[6]

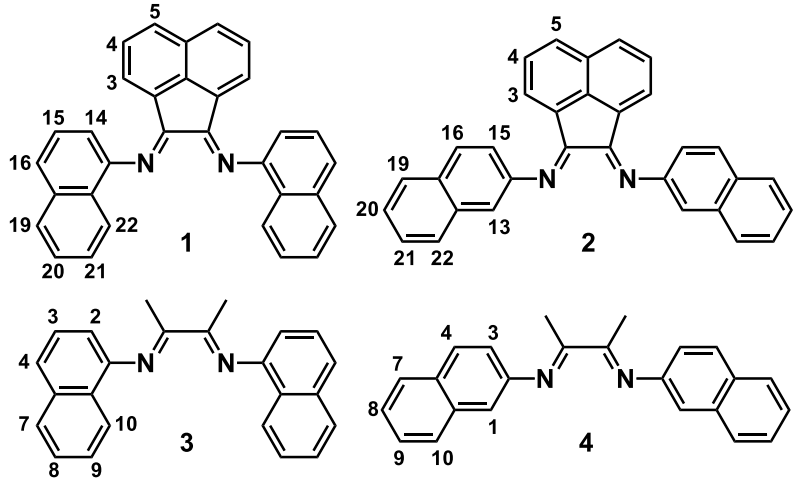

Figure 2.2. The ligands under investigation and related numbering scheme.

These ligands were used for the synthesis of the related neutral [Pd(CH_3)Cl(N–N)] (**1a**-**4a**), and monocationic, [Pd(CH_3)(CH_3CN)(N–N)][PF_6] (**1b**-**4b**) complexes following the literature methodology,[4a,7,8] and they were all fully characterized by NMR spectroscopy. In this context, the series of the monocationic complexes has been extended to Pd-dmso derivatives and all the monocationic

complexes were applied as precatalysts in the target reactions to compare their catalytic behavior in both copolymerizations.

Moreover, since this is the first study where a homogeneous comparison of the two copolymerizations is performed, we investigated via DFT calculations the reaction profiles for both CO/styrene and ethylene/MA copolymerizations with simplified analogues of the studied palladium catalysts.

2.2. Results and Discussion.

2.2.1. Synthesis and characterization of complexes 1c-3c.

Although Pd–dmso complexes are extensively studied in conjunction with phosphine sulfonate ligands,[9] the first example in combination with α-diimines was just recently reported by some of us.[8] Therefore, complexes **1c-3c** represent new examples of this class of compounds. They were obtained from the corresponding neutral derivatives **1a-3a** through a dehalogenation reaction with the proper silver salt in the presence of dimethyl sulfoxide, following the procedure introduced by us (Scheme 2.2).[8]

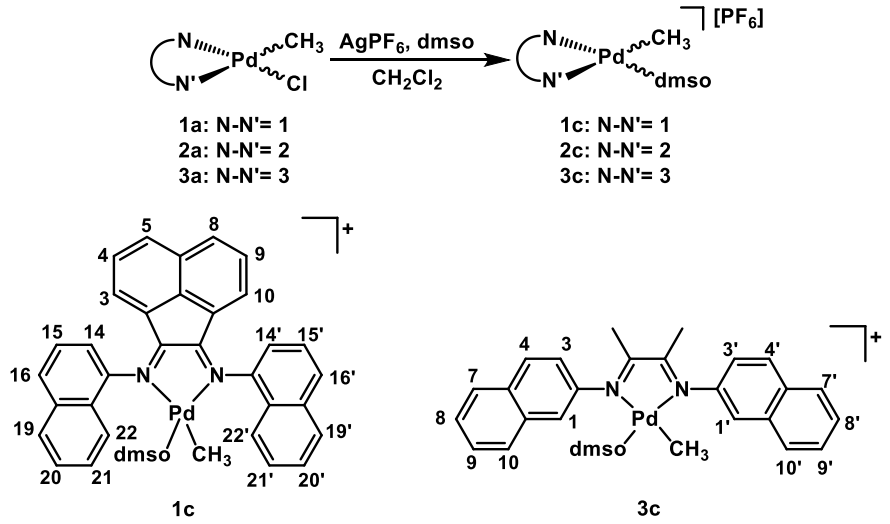

Scheme 2.2. Synthesis of monocationic dmso complexes **1c-3c**, with the related numbering scheme.

In the ^{1}H NMR spectra of these complexes, recorded in CD_2Cl_2, either sharp or broad signals were observed at room temperature, depending on the nature of the ancillary ligand. Focusing on the resonances of the Pd-dmso and Pd-CH_3 fragments, sharp signals were observed already at room temperature for **2c** and **3c**, while for **1c** decoalescence was reached at T = 253 K (Figure 2.3).

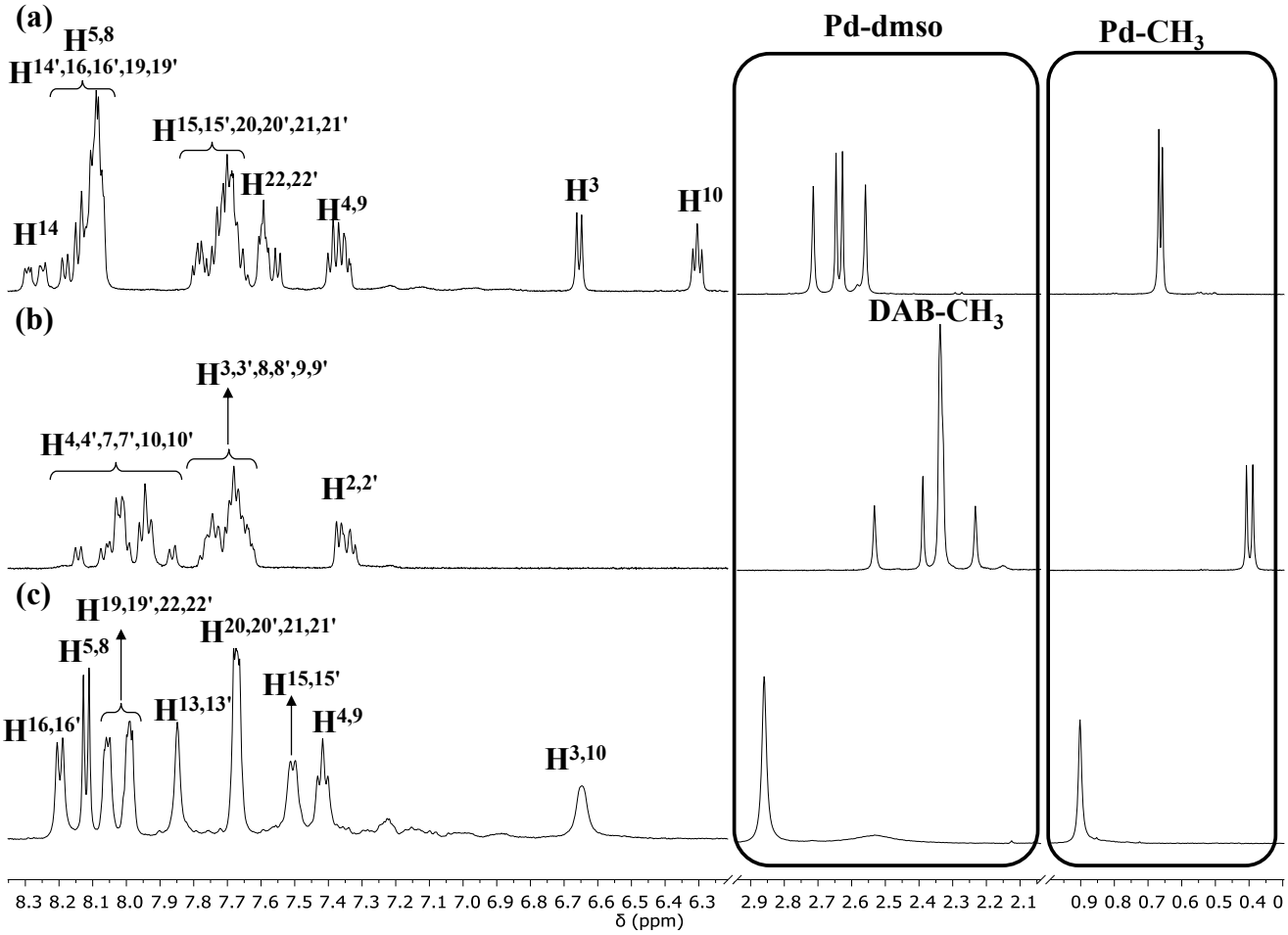

Figure 2.3. ^{1}H NMR spectra in CD_2Cl_2 of (a) **1c** at T = 253 K; (b) **2c** at T = 298 K; (c) **3c** at T = 298 K. Aliphatic and aromatic regions are not on scale.

In the ^{1}H NMR spectrum of **1c** the splitting of the Pd-CH_3 singlet and the presence of four signals for the coordinated dmso, together with the presence of two overlapped singlets for H^{10} provided evidence that both *syn* and *anti* isomers coexisted, as observed for the corresponding neutral complex,[6] and that in both isomers the palladium is chiral, thus the methyl groups of dmso are diastereotopic, generating one signal each. The presence in the NOESY spectrum recorded at T = 253 K of exchange peaks among all the signals generated by the dmso confirmed that these isomers are in exchange at a slow rate on the NMR timescale (Figure 2.4). In addition, the presence of exchange peaks between H^3 and H^{10} supported the hypothesis that the exchange mechanism involves the cleavage of one Pd-N bond.

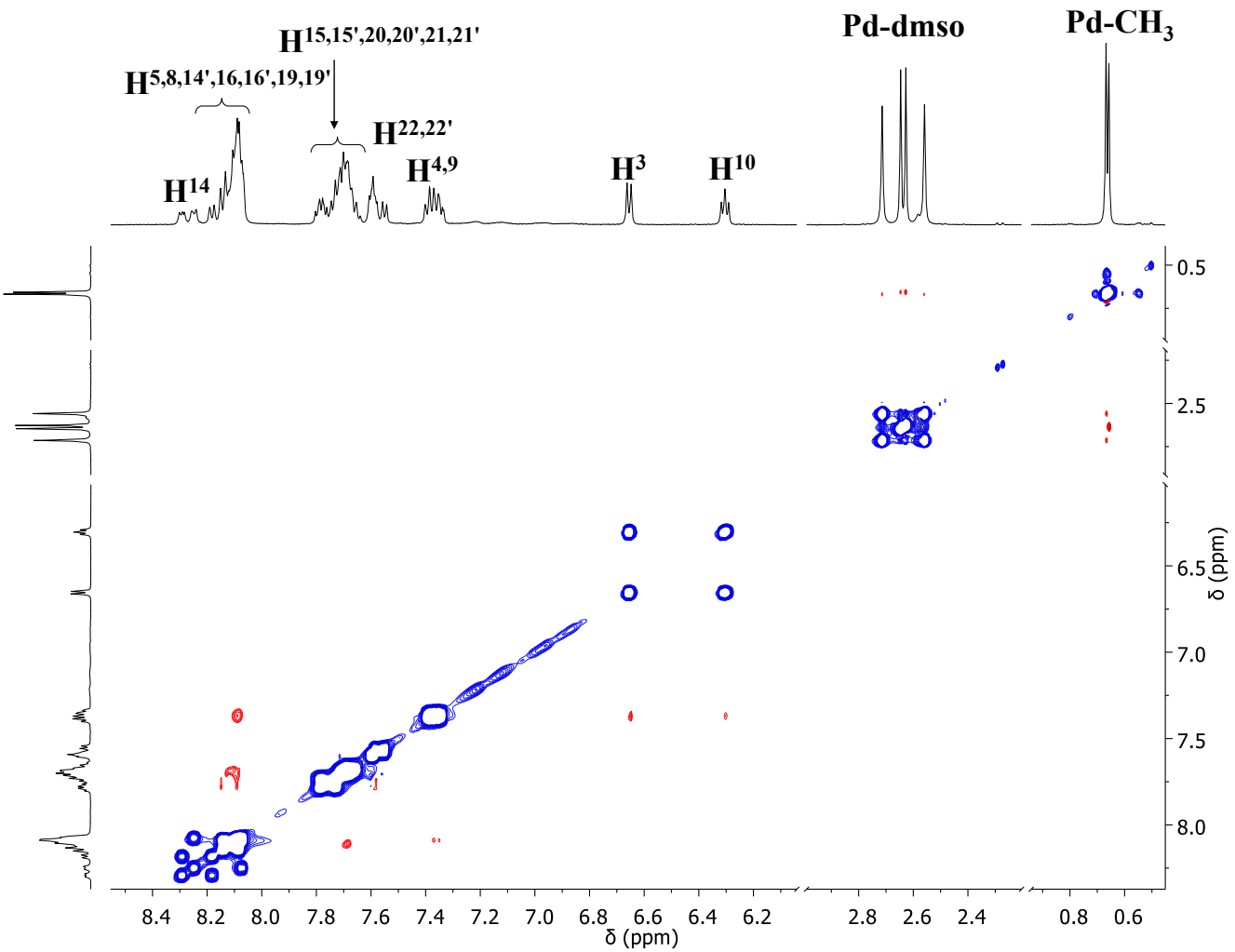

Figure 2.4. NOESY spectrum of **1c** in CD_2Cl_2 at 253 K.

Comparing the ^{13}C chemical shift of the methyl groups of the dmso observed in the ^{1}H-^{13}C HSQC spectrum with the signal of free dmso indicated that the dimethyl sulfoxide is coordinated to the palladium center via the sulfur atom (Figure 2.5): in fact, it is known from literature that the carbon atom of the methyl groups of dmso resonates at higher frequency if dmso is coordinated to a transition metal through sulfur, and at lower frequency if bonded via oxygen.[8,10]

This is in agreement with the presence of the S-bonded species as the major isomer in solution reported for the Pd-dmso complex with ligand **L1** (Figure 1.9), although it is interesting to note that no traces of the O-bonded species was detected, while it was reported for the dmso derivative with the nonsymmetric BIAN ligand.[8]

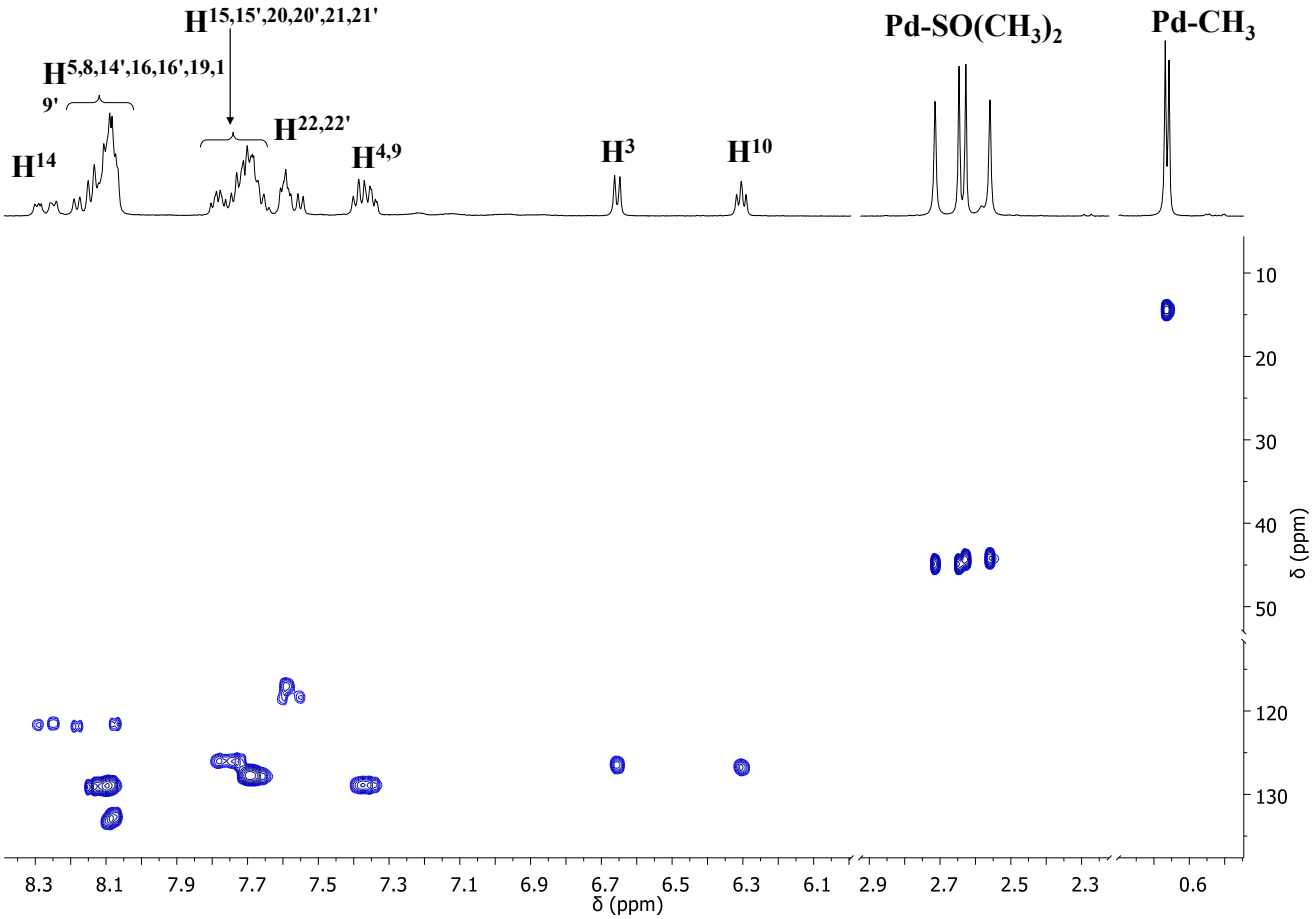

Figure 2.5. ^{1}H-^{13}C HSQC spectrum of **1c** in CD_2Cl_2 at 253 K.

As for **1c**, and in agreement with the characterization of the corresponding neutral derivative,[6] also in the ^{1}H NMR spectrum of **3c** the splitting of the Pd-CH_3 singlet and the presence of four signals for the methyl groups of the dmso indicated the presence of both *syn* and *anti* isomers, (Figure 2.3c). The palladium is a stereogenic center in both isomers, thus the methyl groups of the coordinated dmso are diastereotopic and they generate one singlet each.

As discussed for complex **1c**, the ^{1}H-^{13}C HSQC spectrum of **3c** allowed to unambiguously identify the dimethyl sulfoxide as coordinated to palladium via the sulfur atom (Figure 2.6).

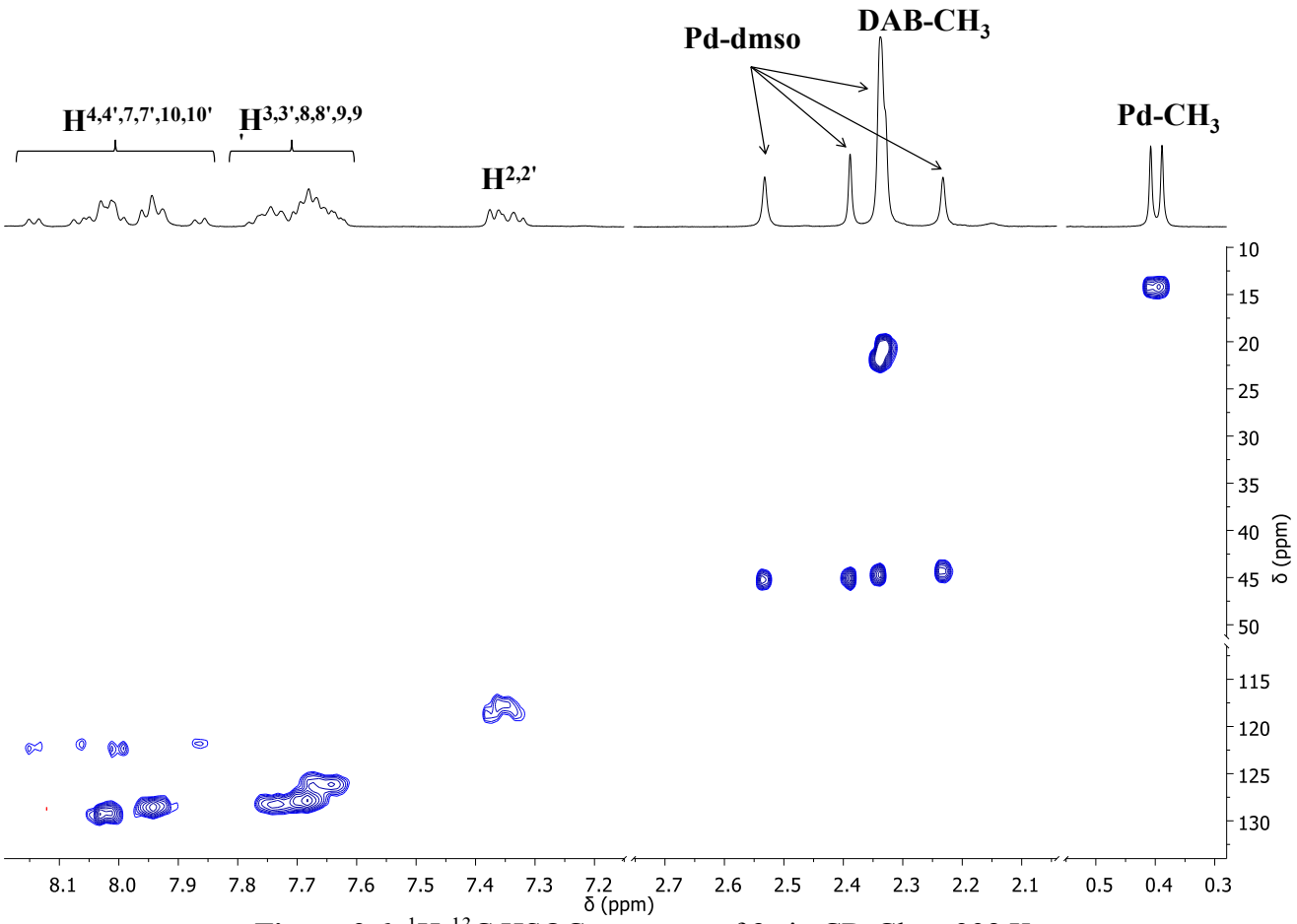

Figure 2.6. ^{1}H-^{13}C HSQC spectrum of **3c** in CD_2Cl_2 at 298 K.

The ^{1}H NMR spectrum of complex **2c** in CD_2Cl_2 at room temperature showed sharp peaks for both the Pd-CH_3 and Pd-dmso fragments, while broad signals were observed for the aromatic protons. Lowering the temperature up to T = 263 K did not result in any improvement in the peak resolution, and the number of signals corresponded to half of the protons of the ligand (Figure 2.3b), thus indicating the presence of a dynamic process that exchanged the two halves of the ligand. The same was observed in the spectrum of the complex recorded in dmso-d_6, thus confirming the presence of an exchange process.

The ^{13}C chemical shift of the Pd-dmso signal indicated that also in this case the dimethyl sulfoxide is coordinated to palladium via the sulfur atom (Figure 2.7).

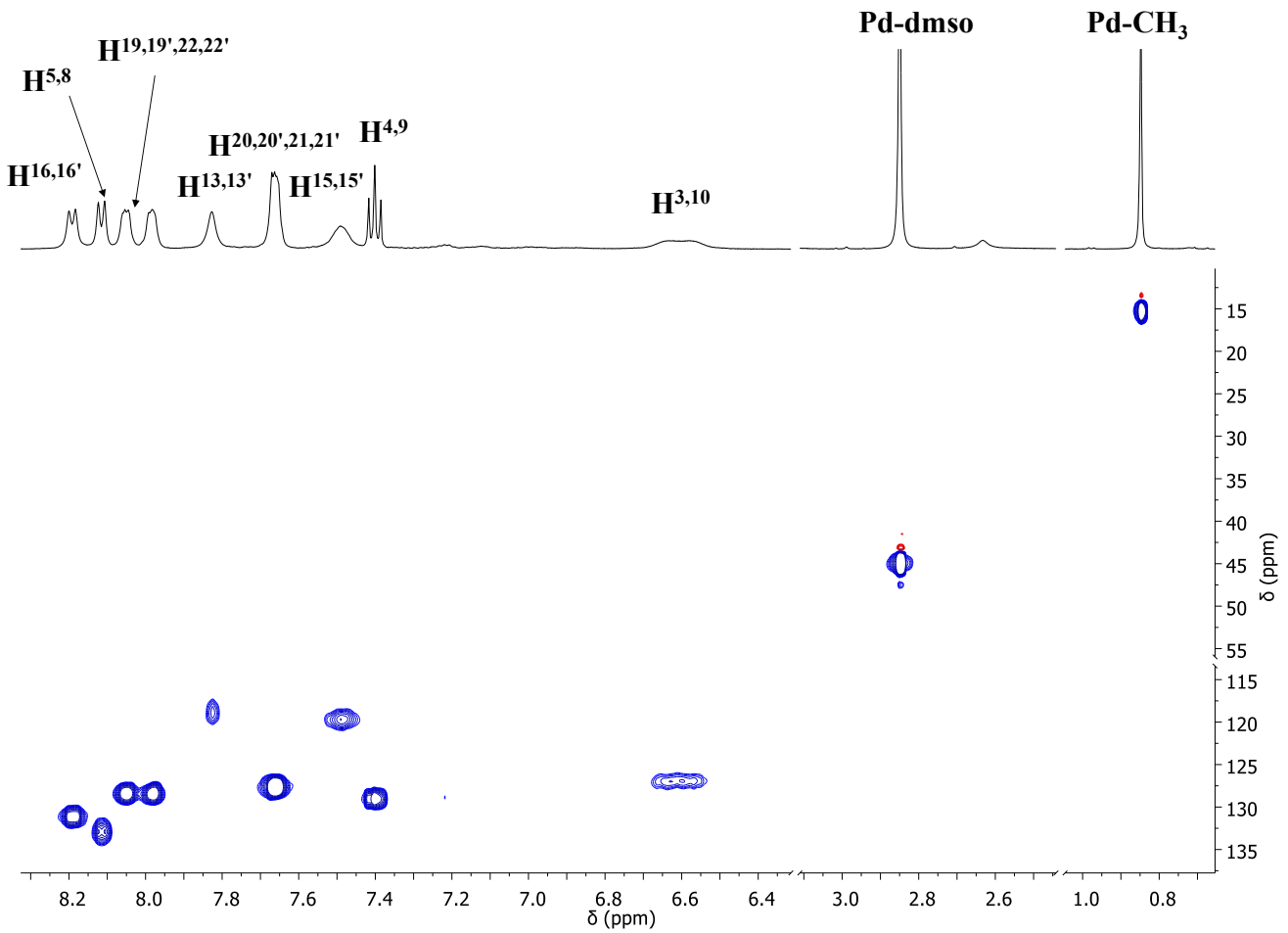

Figure 2.7. ^{1}H-^{13}C HSQC spectrum of **2c** in CD_2Cl_2 at 298 K.

For all the Pd-dmso derivatives, the S-bonded coordination of dmso was further confirmed by the IR spectra in solid state, that showed the presence of a single band in the region typical for this kind of coordination (1129 cm^{-1} for **1c**, 1111 cm^{-1} for **2c**, 1113 cm^{-1} for **3c**). This was in agreement with the hard/soft acids/bases theory, and was different from what was observed for the cationic complex with the nonsymmetrically substituted BIAN derivative **L1**, for which isomers with both S-bonded and O-bonded dmso were observed.[8]

2.2.2. CO/styrene copolymerization reaction.

The monocationic complexes **1c**, **3c** were tested as precatalysts for CO/styrene copolymerization under the same reaction conditions applied for the corresponding Pd-acetonitrile derivatives **1b-4b**,[6] that means performing the reaction in 2,2,2-trifluoroethanol (TFE) as solvent, at T = 303 K under a CO pressure of 1 bar, for 24 h and with a slight excess of 1,4-benzoquinone (BQ) with respect to palladium (Scheme

1.2a, Table 2.1). The produced polyketones were isolated as white solids and characterized by ^{13}C NMR spectroscopy.

All complexes generated active catalysts for the copolymerization reaction showing a remarkable effect of the nature of the nitrogen-donor ligand on the productivity: ligand **3** led to the least productive catalysts, while complex **2b** generated the most productive one (Table 2.1). The value of productivity of the latter was in the typical range for efficient catalysts with BIAN ligands,[4b] while the catalytic behavior of complexes with DAB ligands **3** and **4** was in line with literature data for analogous catalysts.[11]

Table 2.1. CO/styrene copolymerization reaction: effect of the N-N ligand and of the labile ligand L. Precatalyst: $[Pd(CH_3)(L)(\mathbf{N\text{-}N})][PF_6]$[a]

Run	N-N	L	yield (g)	productivity (kg CP/g Pd) [b]	Mw (Mw/Mn)	TON[c]
1	**1**	CH_3CN	1.66	1.23	23 000 (1.4)	5.68
2	**2**	CH_3CN	3.63	2.69	24 000 (1.8)	11.91
3	**3**	CH_3CN	0.60	0.44	21 000 (1.4)	2.24
4	**4**	CH_3CN	1.03	0.76	9 000 (1.6)	8.67
5	**1**	dmso	1.70	1.26	37 000 (1.5)	3.62
6	**3**	dmso	0.58	0.43	10 000 (1.4)	4.57

[a] Reaction conditions: $n_{Pd} = 1.27 \cdot 10^{-5}$ mol, $V_{TFE} = 20$ mL, $V_{styrene} = 10$ mL, [styrene]/[Pd] = 6800, [BQ]/[Pd] = 5, T = 303 K, P_{CO} =1 bar, t = 24 h. [b] kg CP/g Pd = kilograms of copolymer per gram of palladium. [c] TON = moles of copolymer per mole of Pd.

No difference in the productivity was found when the dmso precatalysts were used in place of the acetonitrile derivatives, suggesting that the active species should be the same and that dmso and acetonitrile play the role of leaving groups.

Catalysts with BIAN ligands were found to be 3 to 4 times as productive as those with DAB derivatives, this trend being related to catalyst stability: indeed, for BIAN catalysts the formation of inactive palladium metal within the first 24 h of reaction is negligible, in particular for precatalyst **1c**, whereas for the DAB derivatives, regardless of whether dmso or CH_3CN precatalysts were used, remarkable decomposition was observed.

Regardless of the ligand skeleton, catalysts with the 2-naphthyl-substituted ligands exhibited a productivity two times higher than that of catalysts with the corresponding 1-naphthyl-substituted ligands, and this trend is clearly related to the steric hindrance generated by the substituent on the N-donor atoms. These catalytic data suggest that catalyst stability is determined by the ligand skeleton, indicating that catalysts with the rigid BIAN are more stable than those with the more flexible DAB, a trend analogous to that found by comparing catalysts with the rigid phenanthrolines with those having the more flexible bipyridines.[12]

The effect of the ligand on the molecular weight of the produced polyketones was more peculiar, and a general trend was difficult to be rationalized. The copolymers obtained with the BIAN–acetonitrile precatalysts, **1b** and **2b**, have very similar Mw values (Table 2.1, runs 1 and 2), indicating that the improved productivity of catalyst **2b** was caused by an increase in the number rather than in the length of the polymeric chains. On the other hand, polyketones synthesized with the DAB–acetonitrile precatalysts, **3b** and **4b**, have different Mw values, and the Mw value of the macromolecules obtained with **4b** are lower than half the Mw value of the copolymer obtained with **3b** (Table 2.1, runs 3 and 4). Even though dmso and CH_3CN precatalysts exhibited the same productivity, the labile ligand affected the Mw values of the produced polyketones, but in a different way depending if BIAN or DAB catalysts were used. An increase in the Mw value was found from **1b** to **1c**, but a decrease was observed from **3b** to **3c** (Table 2.1, runs 1 *vs* 5 and 3 *vs* 6). For all the synthesized polyketones, the polydispersity values are lower than 2, indicating the single-site nature of the catalyst.

From the Mw, the TON values, expressed as moles of copolymer produced per mol of palladium, were calculated. Even though these were only approximated values, they indicated that, regardless of the ligand skeleton, catalysts with the 2-naphthyl-substituted ligands make more catalytic cycles than those with the 1-naphthyl-substituted molecules, thus suggesting their higher intrinsic activity (Table 2.1, runs 2 *vs* 1, 4 *vs* 3).

The stereochemistry of CO/styrene polyketones was analyzed by ^{13}C NMR spectroscopy recording the spectra in 1,1,1,3,3,3-hexafluoro-2-propanol (HFIP) at room temperature. The spectra of all the polyketones display the signals of all the four triads, but with different intensities depending on the substituent present on the ligand (Table 2.2). For the polyketones synthesized with the 2-naphthyl-substituted catalysts, an almost statistic distribution of the four triads was found, indicating the formation of an atactic copolymer. Instead, if the 1-naphthyl-substituted catalysts were applied, a preference for the *ll* triad was observed. This observation, together with the monomodal distribution of the Mw values, suggests the formation of isotactic/atactic stereoblock copolymers.

Neither the ligand skeleton, BIAN or DAB, nor the labile ligand, dmso or CH_3CN, affected the polyketone stereochemistry.

Table 2.2. Triads distribution in the CO/styrene polyketones. Precatalyst: $[Pd(CH_3)(L)(\mathbf{N\text{-}N})][PF_6]$[a]

Run	**N-N**	L	*ll* (%)	*lu* (%)	*ul* (%)	*uu* (%)
1	**1**	CH_3CN	40	25	25	10
2	**2**	CH_3CN	21	30	31	18
3	**3**	CH_3CN	44	22	24	10
4	**4**	CH_3CN	22	32	29	17
5	**1**	dmso	43	23	24	10
6	**3**	dmso	45	24	23	7

[a] Determined by ^{13}C NMR spectra recorded in HFIP/$CDCl_3$, T = 298 K, integration of C_{ipso} signals.

The formation of stereoblocks is in agreement with the presence in solution of the precatalyst as *syn* and *anti* isomers in equilibrium. The two conformers feature different symmetries. The mechanism, reported for the first time by Waymouth and Coates for the synthesis of atactic/isotactic stereoblock polypropylene,[13] applies well also in this case. Provided that the rate constant for the interconversion between *syn* and *anti* conformers is lower with respect to the propagation rate constant of the polymer chain, if the active catalyst is in the *anti* conformation (ligand of C_2 symmetry), an isotactic block grows, but when it switches to the *syn* conformer (ligand of C_s symmetry) the atactic block is obtained.

2.2.3. Ethylene/methyl acrylate cooligomerization reaction.

The monocationic complexes **1b-3b**, **1c-3c** were tested as precatalysts for ethylene/methyl acrylate (MA) cooligomerization by performing the reaction in TFE as solvent, at T = 308 K and ethylene pressure of 2.5 bar, for 24 h (Scheme 2.1b). The catalytic product was a red-brown oil that was characterized by ^1H and ^{13}C NMR spectroscopy as a mixture of ethylene/methyl acrylate cooligomers and ethylene oligomers. A small portion of the reaction mixture, before the workup, was analyzed by GC–MS to determine whether higher alkenes were also formed.

As recently reported,[8] a remarkable effect of the nitrogen-donor ligand on both productivity and amount of polar monomer inserted was observed also for the precatalysts under investigation (Table 2.3). Complexes with ligand **2** were found to be almost inactive, yielding palladium derivatives, traces of

ethylene/MA cooligomers and higher alkenes from butenes to hexenes. The most productive catalysts were originated from complexes with ligand **3**, achieving a productivity of 560 g P/g Pd and with a polar monomer content of approximately 20 %.

Table 2.3. Ethylene/MA cooligomerization reaction. Precatalyst: $[Pd(CH_3)(L)(\mathbf{N\text{-}N})][PF_6]$[a]

Run	**N-N**	L	yield (g)	productivity (g P/g Pd) [b]	mol % MA[c]	Alkenes[d]
1	**1**	CH_3CN	158	71.0	37	C^{4-8}
2	**2**	CH_3CN	18[e]			C^{4-6}
3	**3**	CH_3CN	945	423.8	20	C^{4-14}
4[f]	**3**	CH_3CN	1250	560.5	21	C^{4-14}
5	**1**	dmso	145	65.0	39	C^{4-8}
6	**2**	dmso	35[e]			C^{4-6}
7	**3**	dmso	939	421.3	22	C^{4-14}
8[f]	**3**	dmso	1230	551.6	21	C^{4-10}

[a] Reaction conditions: $n_{Pd} = 2.1 \cdot 10^{-5}$ mol, V_{TFE} = 21 mL, V_{MA} =1.130 mL, [MA]/[Pd] = 594, t = 24 h, T = 308 K, $P_{ethylene}$ = 2.5 bar; [b] g P/g Pd = grams of product per gram of Pd; [c] calculated by ^{1}H NMR spectroscopy on isolated product; [d] calculated by GC-MS; [e] mixture of palladium derivatives, ethylene/MA cooligomers and higher alkenes; [f] t = 48 h.

In agreement with the literature,[5] moving from the DAB to the BIAN derivatives a decrease of six times in the productivity was found. However, in contrast to what was found in the CO/styrene copolymerization, no differences in the catalyst stability were observed between the precatalysts containing ligand **1** or **3**. For both ligands, only traces of inactive palladium metal were found at the end of the catalytic runs if starting from the acetonitrile derivatives, and no formation at all was observed in the catalyses performed with the dimethyl sulfoxide complexes. This indicated that the remarkably different productivity is not caused by a different stability towards decomposition to inactive Pd metal, but it might be ascribed to both a higher intrinsic activity of catalysts with **3** with respect to those with **1** and to the possible presence for the latter of a deactivation pathway different from decomposition to Pd metal, such as the formation of the dicationic, bischelated $[Pd(Ar_2\text{-}DAB)_2]^{2+}$ as recently reported.[14]

In agreement with the behavior in the CO/styrene copolymerization (Table 2.1), also for the ethylene/MA cooligomerization within the first 24 h of reaction acetonitrile and dmso precatalysts exhibited very similar productivities. The same result was obtained if the reactions with the best performing catalysts, **3b** and **3c**, were prolonged up to 48 h, confirming that no significant effect of the labile ligand was present. Given that for all these reactions slight or negligible formation of palladium metal was observed, overall these data confirm our previous finding that for this copolymerization dmso plays a role in prolonging catalyst lifetime and that the difference between dmso and acetonitrile precatalysts becomes evident only if catalyst decomposition to palladium metal is relevant.[8]

In contrast to the literature,[5] with the catalysts under investigation the ligand skeleton also affected the content of inserted acrylate, which increased from 22 to 39 % going from **3b**,**c** to **1b**,**c**; the latter is the highest value of incorporated MA up to now with α-diimine catalysts.

With all precatalysts, the formation of higher alkenes was observed as a complex mixture of isomers, as a result of the chain walking mechanism;[15] the observed chain length distribution, expressed in terms of molar fraction of each alkene, can be reasonably fitted by the Poisson distribution. The highest amount of butenes and hexenes was observed for the catalysts containing the ligand **2**, and this, in combination with the negligible yield in cooligomer, suggested that the catalysts containing ligand **2** deactivated relatively soon, leading preferentially to higher alkenes instead of the desired cooligomers. Complex **2c** exhibited a higher activity in the production of higher alkenes than the corresponding acetonitrile analogue **2b**, in agreement with the relativly higher stability of dmso derivatives[8] and supporting the hypothesis that the effect of the labile ligand becomes evident if catalyst decomposition is significant. On the other hand, the complexes comprising ligands **1** and **3** produced lower amounts of higher alkenes: catalysts **1b-c** produced butenes to octenes, while **3b-c** led to longer alkenes, up to C^{14}, and in both cases no significant differences were observed moving from the Pd-$NCCH_3$ to the Pd-dmso derivatives nor increasing the reaction time.

Overall, the catalytic results presented in this study allow to point out the following analogies and differences between the two copolymerization:

- In the CO/styrene copolymerization, complexes with BIAN ligands led to more stable and more productive catalysts than the DAB derivatives;
- In the ethylene/methyl acrylate copolymerization an opposite trend was found, with DAB ligands generating more productive catalysts than BIAN derivatives;

- For both copolymerizations: complexes with the 2-naphthyl-substituted ligands, regardless to the ligand skeleton, behave as catalysts having aryl α-diimines with the *meta*-substituted aryl rings. They exhibit similar productivities and lead to atactic polymers in the CO/styrene copolymerization, but they are inactive in the ethylene/MA copolymerization;
- For both copolymerizations: complexes with the 1-naphthyl-substituted ligands, regardless to the ligand skeleton, behave as catalysts having aryl α-diimines with the *ortho*-substituted aryl rings. They show low productivities and lead to isotactic/atactic steroblock polymers in CO/styrene copolymerization, but they are catalytically active in the ethylene/methyl acrylate copolymerization.

Starting from the above reported considerations and taking into account the knowledge about the mechanism for both copolymerizations (see below), DFT calculations were performed with the aim to rationalize the different catalytic behavior of the two series of catalysts.

2.2.4. Mechanistic analysis.

The mechanism generally accepted for the two copolymerization reactions under investigation is known,[2b,5,11e,16] thus allowing a comparison of the relevant intermediates involved in the various steps of the catalytic cycles (Scheme 2.3). In both copolymerizations the precatalyst, which is the same Pd complex, is transformed into the active species through a substitution reaction of the coordinated acetonitrile with the incoming monomer, namely carbon monoxide for the CO/styrene and ethylene or MA for the ethylene/MA copolymerization, followed by the related migratory insertion. The product is a Pd-acyl species for the polyketones,[2b] and a Pd-alkyl or a Pd-metallacycle for the functionalized polyolefins,[5] respectively (Scheme 2.3a). On these species, the propagation step takes place according to two different pathways that characterize the two copolymerizations: alternated migratory insertions of CO into the Pd-alkyl bond and of styrene into the Pd-acyl bond constitute the growth of the polyketone chain; on the other hand, consecutive migratory insertions of ethylene and isolated migratory insertions of the polar monomer represent the formation process of functionalized polyolefins (Scheme 2.3b).

Finally, for both polymerizations the termination step occurs through a β-hydrogen elimination on the Pd-alkyl species, leading to the corresponding polymer with a vinylic termination and to the Pd-H intermediate (Scheme 2.3c). The latter is the key species for catalyst stability: it can either undergo the insertion of a monomer molecule starting a new catalytic cycle or decompose either to palladium metal or to a dicationic bischelated species.[14]

The resting state of the two catalytic processes is the Pd-carbonyl-acyl species for the polyketone synthesis and the six-membered palladacycle obtained after the acrylic monomer insertion for the functionalized polyolefins. However, even in the CO/alkene copolymerization five- and six-membered metallacycles are formed.

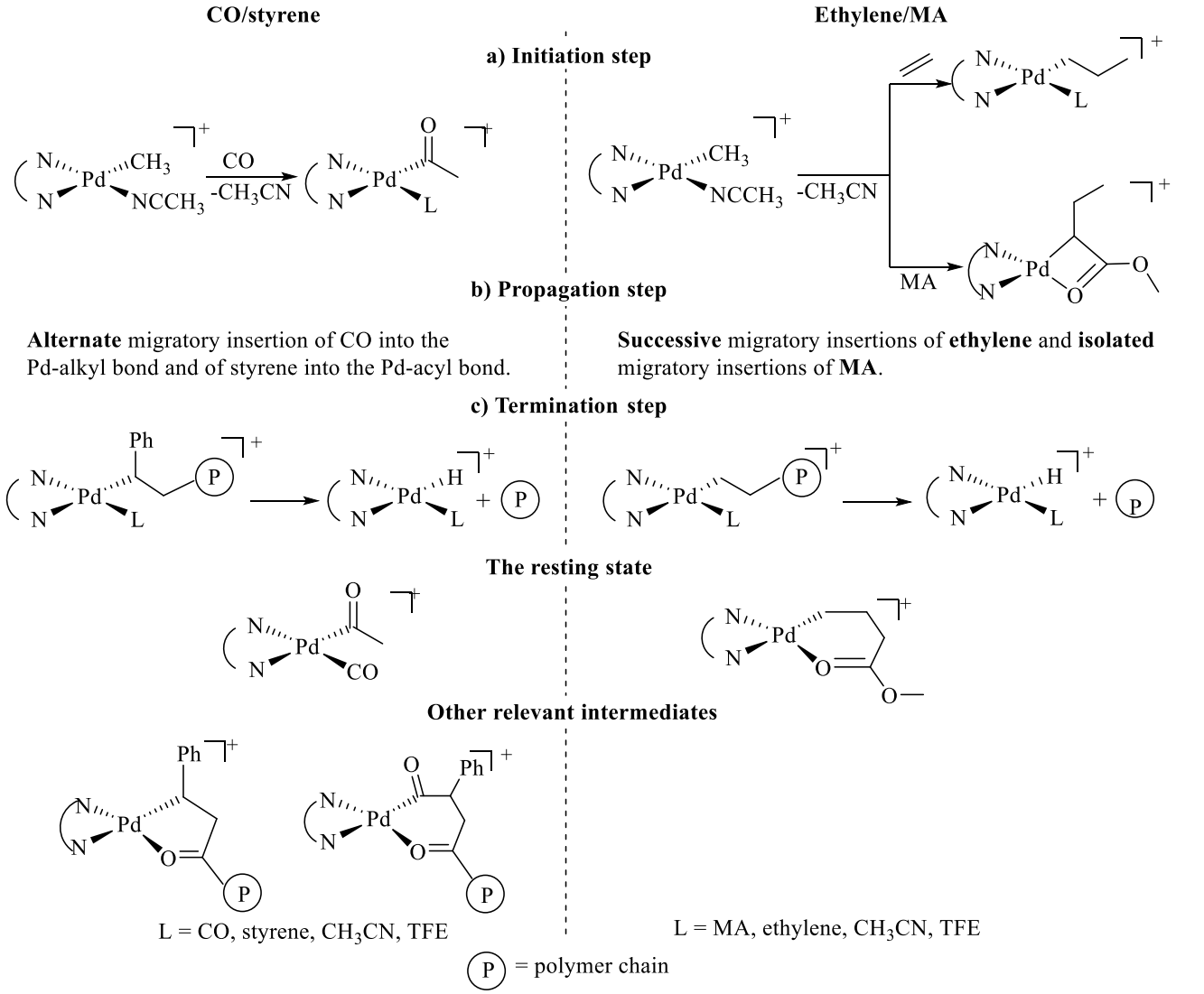

Scheme 2.3. Comparison of relevant steps and intermediates in CO/styrene and ethylene/MA copolymerizations.

In summary, this analysis highlighted that similar intermediates and reactions are involved in the two catalytic processes, thus allowing their direct comparison. The obtained catalytic data suggested that ligands with a rigid backbone (BIAN) are preferred for the CO/styrene copolymerization, whereas a higher flexibility in ligand skeleton (DAB) is desirable for catalysts applied to the synthesis of functionalized polyolefins. As far as the steric hindrance of the ligand itself is concerned, for the

polyketone synthesis a less encumbered situation around the palladium center is desired, likely to favor the coordination of the incoming vinyl arene (2-naphthyl is preferred over the 1-naphthyl group). On the other hand, for the functionalized polyethylene synthesis a highly hindered situation around the metal center is required for the catalysis to proceed (1-naphthyl is preferred over the 2-naphthyl substituent). Finally, the different interconversion rates of complexes bearing 2- or 1-naphthyl-substituted ligands (the result of the interconversion is the same as a rotation of the naphthyl-substituents) lead to different steric features around palladium. In the case of polyketone formation, the dynamic situation caused by the 2-naphthyl substituent does not allow the enantioface discrimination of the incoming styrene, which instead takes place if the more hindered 1-naphthyl group is present on the ligand. In the case of the ethylene/MA copolymerization, the rotation of the 1-naphthyl group might be responsible of the synthesis of cooligomers instead of copolymers. In addition, it is reasonable to assume that, by dividing the space around palladium in four quadrants, in each moment at least two of them are available for the approach of ethylene, thus favoring the displacement of the vinyl (co)oligomer by the associative mechanism discovered by Brookhart and coworkers over the growth of the polymer chain.[1]

With the aim of understanding the reasons beneath the opposite trend observed in the catalytic behavior in the two copolymerization reactions, a very preliminary DFT analysis on the reaction profile for CO/styrene copolymerization was carried out to identify the key intermediates and the role of the ligand skeleton on the catalytic behavior of the studied Pd(II) complexes.

Before considering the CO/styrene copolymerization, the energy profile for the CO/ethylene copolymerization was calculated using simplified precatalysts $[Pd(CH_3)(CO)(N\text{-}N)]^+$ with N-N ligands featuring methyl instead of naphthyl groups, and either DAB or BIAN skeleton, indicated as **DAB** and **BIAN**. The resulting data were then used to compute the energy profile for the CO/styrene copolymerization using the simplified derivatives (Schemes 2.4, 2.5).

The collected data for the **DAB** precatalyst showed that after the dissociation of the labile ligand, the first step is, as expected, the insertion of CO into the Pd-CH_3 bond, (**1-DAB** → **2-DAB**): the CO adduct is 9 kcal/mol more stable than the styrene one (**1-DAB** *vs* **1a-DAB**) and the activation barrier for the insertion of CO is 8.3 kcal/mol lower than that of the styrene insertion (11.7 *vs* 19.0 kcal/mol, respectively).

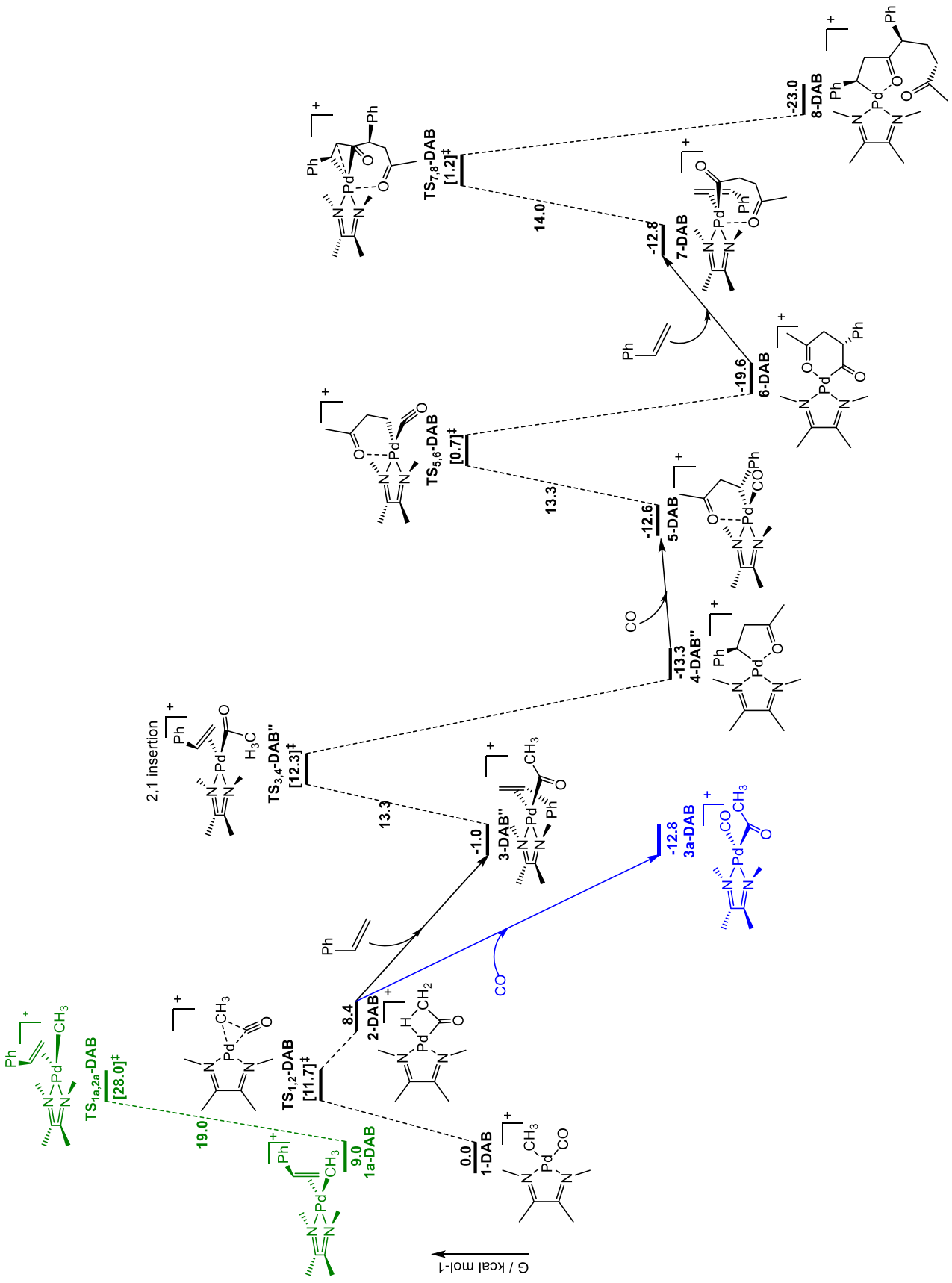

Scheme 2.5. Energy profile for the first steps of CO/styrene copolymerization with **DAB** precatalyst.

The following step is the styrene insertion into the Pd-acyl bond, leading to the five-membered metallacycle **4-DAB''** in which the oxygen atom of the carbonyl group coordinates to palladium, while for the double insertion of CO it was not possible to calculate the activation barrier, indicating that the reaction does not occur. The Pd-acyl-carbonyl species was found to be strongly stabilized with respect to the styrene analogues (e.g. **3a-DAB** *vs* **3-DAB**), confirming that it is the resting state of the catalytic cycle. The next step requires the substitution of the CO by a styrene molecule and subsequent insertion of styrene in the Pd-acyl bond (**3a-DAB → 3-DAB → 4-DAB''**); the overall barrier between the resting state and the next intermediate is 25.1 kcal/mol, which is rather high and is in agreement with the Pd-acyl-carbonyl being the resting state of the reaction, as experimentally observed. This leads to the stable five-membered metallacycle (**4-DAB''**) on which the coordination and insertion of CO occurs, generating a six-membered metallacycle, more stable than the previous one (**4-DAB'' → 6-DAB**, ΔG = 6.3 kcal/mol), as reported in literature.[2b]

In agreement with the reported theoretical studies[17] and the experimental results,[2b] the copolymerization reaction results from a sequence of alternated CO insertions into the Pd-alkyl species and styrene insertions into the Pd-acyl derivative.

The regiochemistry of the styrene insertion was investigated, showing a strong preference for the secondary regiochemistry over the primary one (**3-DAB → 4-DAB''** *vs* **3-DAB → 4-DAB'**), in agreement with the reported mechanism,[2b] while for this simple model catalyst the evaluation of the stereochemistry was not relevant (Scheme 2.5).

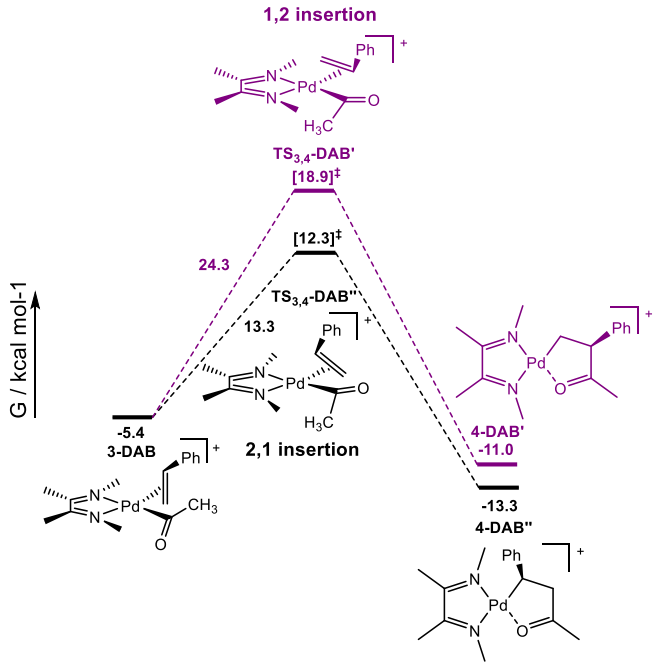

Scheme 2.5. Insertion of styrene into the Pd-acyl bond with **DAB**: 1,2- *vs* 2,1-insertion.

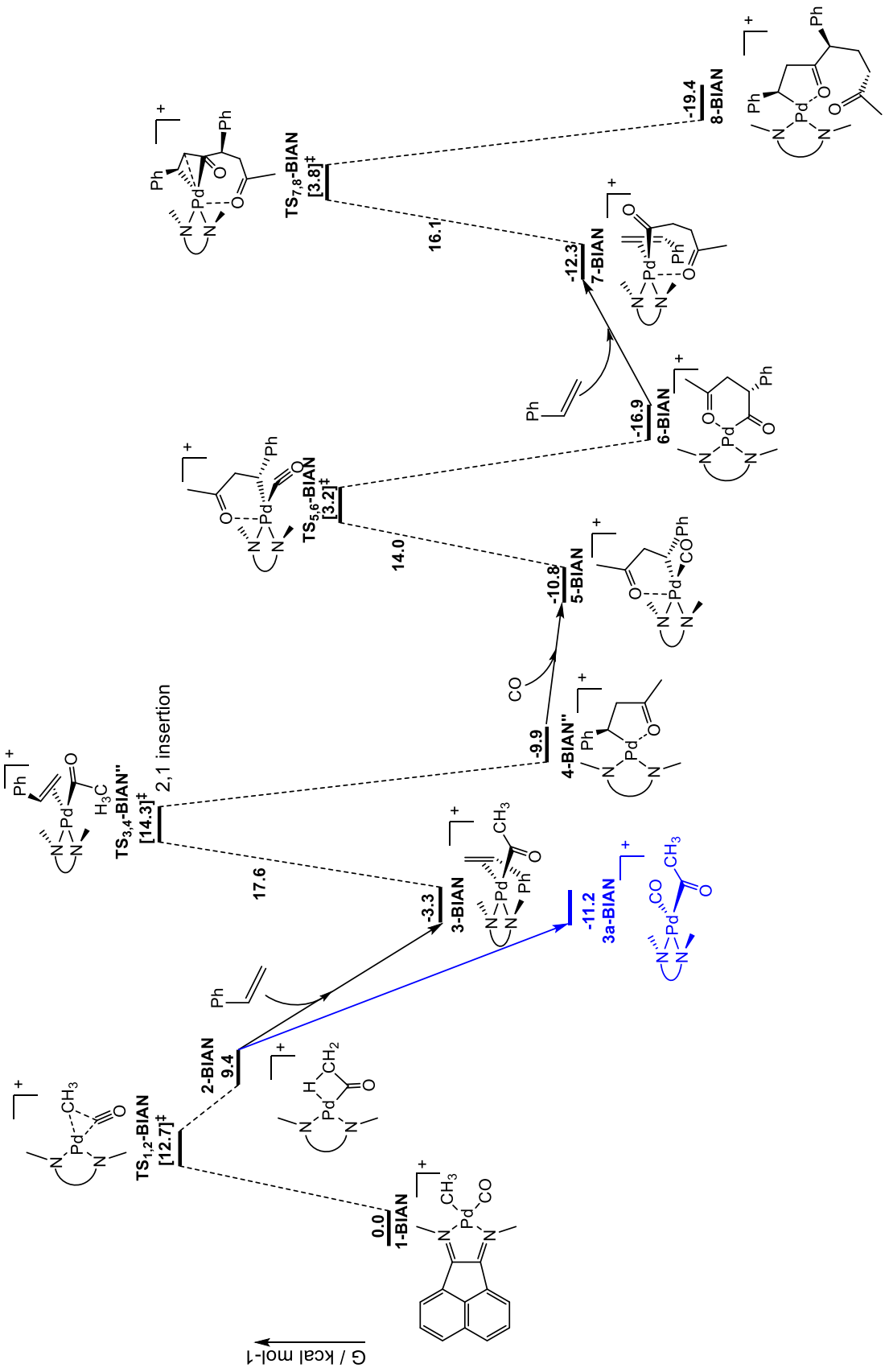

Scheme 2.6. Energy profile for the first steps of CO/styrene copolymerization with **BIAN** precatalyst.

When the reaction pathway was analyzed for the BIAN precatalyst, the same key steps were identified, once again confirming the mechanism reported (Scheme 2.6).[2b,16]

Comparing the two reaction profiles, it is possible to highlight that in both cases, the reaction is thermodynamically favored, with a higher gain in energy for the BIAN precatalyst than for the DAB one after the first four steps. On the other hand, considering the rate determining step, that is the insertion of styrene into the Pd-acyl (**3-DAB → 4-DAB''** *vs* **3-BIAN → 4-BIAN''**), the activation barrier is very close in both cases, 25.1 and 25.5 kcal/mol respectively, thus suggesting a similar catalytic activity.

It is important to say, however, that the collected data are not yet refined to consider the solvation effect and the dispersion correction; moreover, for the full system the behavior might be different from that calculated for the simplified complexes, thus further investigations will be required. Nevertheless, the obtained energy profile fits very well with the experimental mechanistic studies performed for the CO/styrene copolymerization

2.3. Conclusions.

As mentioned in the introduction, although Pd complexes with α-diimine ligands have been extensively applied as catalysts for both CO/vinyl arene and ethylene/acrylic ester copolymerizations, a direct comparison between these two reactions was lacking. Thus, these two reactions were compared by applying the same complexes as precatalysts. We investigated two series of Pd(II) complexes with α-diimines having either an acenaphthene (BIAN) or a 1,4-diazabutadiene (DAB) skeleton and substituted with 1- or 2-naphthyl groups. Monocationic palladium complexes with dimethyl sulfoxide and the studied ligands were synthesized, being only the second example of Pd(II) complexes with dmso in conjunction with α-diimines. The characterization pointed out that the dmso is always coordinated to palladium through the sulfur atom, in agreement with the hard/soft acids/bases theory and with the previous observation that this is the preferred species in solution.

Overall, the catalytic results pointed out the following analogies and differences:

- CO/styrene copolymerization: BIAN ligands lead to more stable and more productive catalysts than DAB ligands;
- Ethylene/MA copolymerization: an opposite trend was found, DAB ligands generate more productive catalysts than BIAN ligands;
- For both copolymerizations: complexes with the 2-naphthyl-substituted ligands, regardless of ligand skeleton, behave as catalysts having aryl α-diimines with the aryl rings substituted in *meta* position.

They exhibit similar productivities and lead to atactic polymers in CO/styrene copolymerization, but they are inactive in ethylene/MA copolymerization;

- For both copolymerizations: complexes with the 1-naphthyl-substituted ligands, regardless of ligand skeleton, behave as catalysts having aryl α-diimines with the aryl rings substituted in *ortho* position. They show low productivities and lead to isotactic/atactic stereoblock polymers in CO/styrene copolymerization, but they are catalytically active in ethylene/methyl acrylate copolymerization.

As these two catalytic reactions proceed via similar palladium intermediates, the current results suggested that in the energy profile these intermediates might be at remarkably different levels depending on the nature of the ancillary ligand and of the polymerization reaction considered.

A very preliminary DFT analysis of the CO/styrene copolymerization reaction was performed, using simplified precatalysts, confirming the mechanism reported in literature; the activation energy values were found very similar, slightly lower for the DAB derivative than for the BIAN one, in contrast with the experimental evidences of catalysts with BIAN ligands being more suited for the synthesis of polyketones. However, it has to be underlined that the calculations were performed on the simplified catalyst and for the full system the behavior might be significantly different.

2.4. Experimental.

2.4.1. Materials and methods. All complex manipulations were performed using standard Schlenk techniques under argon. Anhydrous dichloromethane was obtained by distilling it over CaH_2 and under argon; $ZnCl_2$ was stored in the oven at 110 °C overnight, prior to use. Ligands **1-4**, the neutral Pd complexes, the acetonitrile and the dmso derivatives were synthesized according to literature procedures.[6,8] $[Pd(OAc)_2]$ was a donation from Engelhard Italia and used as received. Carbon monoxide (CP grade 99.9%) and ethylene (purity ≥ 99.9 %) supplied by SIAD and methyl acrylate (99.9%, with 0.02% of hydroquinone monomethyl ether) and styrene (99 %, with 4-*tert*-butylcathecol) supplied by Aldrich were used as received. Deuterated solvents, Cambridge Isotope Laboratories, Inc., were stored as recommended by CIL. All the other reagents and solvents were purchased from Sigma-Aldrich and used without further purification for synthetic, spectroscopic and catalytic purposes.

NMR spectra of complexes and catalytic products were recorded on a Varian 500 spectrometer at the following frequencies: 500 MHz (^{1}H) and 125.68 MHz (^{13}C). The resonances are reported in ppm (δ) and referenced to the residual solvent peak versus $Si(CH_3)_4$: $CDCl_3$ at δ 7.26 (^{1}H) and δ 77.0 (^{13}C), CD_2Cl_2 at δ 5.32 (^{1}H) and δ 54.0 (^{13}C), dmso-d_6 δ 2.50 (^{1}H) and δ 39.51 (^{13}C). NMR experiments were

performed employing the automatic software parameters; in the case of NOESY experiments a mixing time of 500 ms was used. ^{13}C NMR spectra of polyketones were recorded in 1,1,1,3,3,3-hexafluoro-2-propanol (HFIP) with addition of $CDCl_3$ for locking purposes. Caution: HFIP is a very volatile and highly toxic solvent, so proper protection should be used when it is handled.

IR spectra were recorded in Nujol on a Perkin Elmer System 2000 FT-IR. Elemental analyses were performed in the analytical laboratories of Department of Chemistry of Universities of Udine and of Bologna. GC-MS analyses were performed with an Agilent GC 7890 instrument using a DB-225ms column (J&W, 60 m, 0.25 mm ID, 0.25 μm film) and He as carrier coupled with a 5975 MSD. Before analysis, samples were diluted with methanol and nonane was added as internal standard. Average molecular weight (Mw) and polydispersity (Mw/Mn) values of CO/styrene copolymers were measured in the laboratories of Dr. Carla Carfagna at the University of Urbino through gel permeation chromatography using polystyrene standards. Analyses were determined by a Knauer HPLC (K-501 pump, K-2501 UV detector) with a PLgel 5 mm 10^4 Å column. Chloroform was used as the eluent, with a flow rate of 0.6 mL min^{-1}. Samples were prepared by dissolving copolymer (2 mg) in chloroform (10 mL). Calculations were performed with the Bruker Chromstar software.

2.4.2. Synthesis of the dmso derivatives [Pd(CH_3)(dmso)(N-N)][PF_6] (1-3c). To a stirred solution of [Pd(CH_3)Cl(N-N)] (N-N = **1-3**) (0.24 mmol) in anhydrous CH_2Cl_2 (8 mL), anhydrous dimethyl sulfoxide (1.15 equiv.) and a solution of $AgPF_6$ (1.15 equiv.) in CH_2Cl_2 (1 mL) were added. The reaction mixture was protected from light and stirred at room temperature for 30 min. After this time, the reaction mixture was filtered over Celite®; the concentrated mother liquor was cooled to 273 K and cold diethyl ether was added dropwise until the complete precipitation of a powder. The precipitate was filtered, washed thoroughly with diethyl ether and dried under vacuum. Average yield: 75 %.

1c. IR: ν_{max} = 840 cm^{-1} (PF_6^-), 1129 cm^{-1} (S=O, S-bonded dmso). Found: C = 54.0, H = 3.8, N = 3.4. Calc. % for $C_{35}H_{29}N_2PdSOPF_6$: C = 54.10, H = 3.76, N = 3.61.

^1H NMR (500 MHz, CD_2Cl_2, 25°C) δ = 8.29 – 8.24 (m, 1H, H^{14}), 8.19-8.07 (m, 7H, $H^{5,8,16,16',19,19'}$), 7.81 – 7.64 (m, 6H, $H^{15,15',20,20',21,21'}$), 7.59-7.54 (m, 2H, $H^{22,22'}$), 7.40 – 7.33 (m, 2H, $H^{4,9}$), 6.66 (d, 1H, H^3), 6.30 (2d overlapping, 1H, H^{10}), 2.64 (2d overlapping, 6H, Pd-$SO(CH_3)_2$), 0.67 (2s, 3H, Pd-CH_3). ^{13}C NMR (125.68 MHz; CD_2Cl_2) δ =132.9 ($C^{5,8}$), 129.1- 129.0 ($C^{16,16',19,19'}$), 128.9 ($C^{4,9}$), 127.7 ($C^{20,20',21,21'}$), 126.76 (C^{10}), 126.48 (C^3), 126.05 – 126.0 ($C^{15,15'}$), 121.9 (C^{14}), 121.8 ($C^{14'}$), 118.4-117.1 ($C^{22,22'}$), 44.9 – 44.3 (Pd-$SO(CH_3)_2$), 14.4 (Pd-CH_3).

2c. IR: ν_{max} = 836 cm^{-1} (PF_6^-), 1111 cm^{-1} (S=O, S-bonded dmso). Found: C = 53.8, H = 3.5, N = 3.4. Calc. % for $C_{35}H_{29}N_2PdSOPF_6$: C = 54.10, H = 3.76, N = 3.61.
^{1}H NMR (500 MHz, CD_2Cl_2, 25°C) δ = 8.20 (d, 2H, $H^{16,16'}$), 8.12 (d, 2H, $H^{5,8}$), 8.06 – 7.89 (m, 4H, $H^{19,19',22,22'}$), 7.86 (s broad, 2H, $H^{13,13'}$), 7.68 – 7.66 (m, 4H, $H^{20,20',21,21'}$), 7.52 (d broad, 2H, $H^{15,15'}$), 7.41 (t, 2H, $H^{4,9}$), 6.64 (s broad, 2H, $H^{3,10}$), 2.85 (s broad, 6H, Pd-$SO(CH_3)_2$), 0.91 (s broad, 3H, Pd-CH_3).
^{13}C NMR (125.68 MHz; CD_2Cl_2) δ = 132.9 ($C^{5,8}$), 131.1 ($C^{16,16'}$), 129.0 ($C^{4,9}$), 128.4 – 128.4 ($C^{19,19',22,22'}$), 127.6 ($C^{20,20',21,21'}$), 126.9 ($C^{3,10}$), 119.7 ($C^{15,15'}$), 118.8 ($C^{13,13'}$), 44.9 (Pd-$SO(CH_3)_2$), 15.3 (Pd-CH_3).

3c. IR: ν_{max} = 846 cm^{-1} (PF_6^-), 1113 cm^{-1} (S=O, S-bonded dmso). Found: C = 47.8, H = 4.4, N = 4.11. Calc. % for $C_{27}H_{29}N_2PdSOPF_6$: C = 47.62, H = 4.29, N = 4.11.
^{1}H NMR (500 MHz, CD_2Cl_2, 25°C) δ = 8.15-7.86 (m, 6H, $H^{4,4',7,7',10,10'}$), 7.78 – 7.63 (m, 6H, $H^{3,3',8,8',9,9'}$), 7.38 – 7.32 (m, 2H, $H^{2,2'}$), 2.35, 2.39, 2.34, 2.23 (2d, 6H, Pd-$SO(CH_3)_2$), 2.34 (s, 6H, CH_3, CH_3'), 0.40 (2s, 3H, Pd-CH_3).
^{13}C NMR (125.68 MHz; CD_2Cl_2) δ =129.3 - 128.6 ($C^{4,4',10,10'}$), 128.3 – 126.2 ($C^{3,3',8,8',9,9'}$), 123.4 – 121.8 ($C^{7,7'}$), 118.7 – 117.7 ($C^{2,2'}$), 45.2, 45.0, 44.7, 44.3 (Pd-$SO(CH_3)_2$), 14.2 (Pd-CH_3).

2.4.3. CO/Styrene copolymerization reactions. All experiments were carried out at atmospheric CO pressure in a three-necked, thermostated, 75 mL glass reactor equipped with a magnetic stirrer. After establishment of the reaction temperature, the precatalyst ($1.27 \cdot 10^{-5}$ mol), 1,4-benzoquinone ([BQ]/[Pd] = 5), styrene (10 mL) and TFE (20 mL) were added. CO was bubbled through the solution for 10 min; afterwards two 4 L balloons previously filled with CO were connected to the reactor. After the desired time, the reaction mixture was poured into 100 mL of methanol and stirred for 1.5 h at room temperature. The solid was filtered and washed thoroughly with methanol, then dried under vacuum to constant weight.

2.4.4. CO/Styrene copolymers purification. Polyketones (100 mg) were dissolved in $CHCl_3$ (50 mL) and stirred at r.t. for 10 min; the solution was then filtered over Celite® and the solvent was removed from the mother liquor under vacuum. The solid was suspended in ethanol, filtered, washed with ethanol, and dried under vacuum.

2.4.5. Ethylene/methyl acrylate cooligomerization reactions. All catalytic experiments were carried out in a Büchi "tinyclave" reactor equipped with an interchangeable 50 mL glass vessel. The vessel was loaded with the desired complex (21 μmol), TFE (21 mL) and methyl acrylate (1.13 mL). The reactor was then placed in a preheated oil bath, connected to the ethylene tank and pressurized. The reaction mixture was stirred at constant temperature and pressure. After the proper time, the reactor was cooled to room temperature and vented. An aliquot (200 μL) of the reaction mixture was withdrawn and diluted in CH_3OH (1 mL) for GC-MS analyses. The reaction mixture was poured in a 50 mL round flask, together with the dichloromethane (3 x 2 mL) used to wash the glass vessel. No separation of Pd black was observed. Volatiles were removed under reduced pressure and the residual oil was dried at constant weight and analyzed by NMR spectroscopy.

2.4.6. Computational methods. All the calculation were run on Gaussian 03 (Revision D.01)[18] with the BP86 functional;[19] palladium centers were described using the Stuttgart relativistic effective core potentials (RECP) and associated basis sets,[20] with added f-polarization (ζ = 1.472),[21] while 6-31G** basis sets were employed for all other atoms. All stationary points were fully characterized via analytical frequency calculation as either minima (all positive eigenvalues) or transition states (one negative eigenvalue) and IRC calculations and subsequent geometry optimizations were used to confirm the minima linked by each transition state. Free energies were computed at 298 K and 1 atm.

2.5. Bibliography

[1] Ittel, S.D.; Johnson, L.K.; Brookhart, M. *Chem. Rev.* **2000**, *100*, 1169.

[2] (a) Lai, T.-W.; Sen, A. *Organometallics* **1984**, *3*, 866; (b) Drent, E.; Budzelaar, P.H.M. *Chem. Rev.* **1996**, *96*, 663; (c) Bianchini, C.; Meli, A. *Coord. Chem. Rev.* **2002**, *225*, 35; (d) Nakano, K.; Kosaka, N.; Hiyama, T.; Nozaki, K. *Dalton Trans.* **2003**, 4039; (e) Durand, J.; Milani, B. *Coord. Chem. Rev.* **2006**, *250*, 542; (f) Garcia Suarez, E. J.; Godard, C.; Ruiz, A.; Claver, C. *Eur. J. Inorg. Chem.* **2007**, 2582; (g) Anselment, T.M.J.; Vagin, S.I.; Rieger, B. *Dalton Trans.* **2008**, 4537.

[3] (a) Nakamura, A.; Ito, S.; Nozaki, K. *Chem. Rev.* **2009**, *109*, 5215; (b) Berkefeld, A.; Mecking, S. *Angew. Chem. Int. Ed.* **2008**, *47*, 2538; *Angew. Chem.* **2008**, *120*, 2572; (c) Sen, A.; Borkar, S. *J. Organomet. Chem.* **2007**, *692*, 3291; (d) Dong, J.-Y.; Hu, Y. *Coord. Chem. Rev.* **2006**, *250*, 47; (e) Boffa, L.S.; Novak, B.M. *Chem. Rev.* **2000**, *100*, 1479; (f) Ito, S.; Nozaki, K. *Chem. Rec.* **2010**, *10*, 315; (g) Franssen, N.M.G.; Reek, J.N.H.; de Bruin, B. *Chem. Soc. Rev.* **2013**, *42*, 5809; (h) Runzi, T.; Mecking, S. *Adv. Funct. Mater.* **2014**, *24*, 387; (i) Nakamura, A.; Anselment, T.M.J.; Claverie, J. Goodall, B.; Jordan, R.F.; Mecking, S.; Rieger, B.; Sen, A.; Van Leeuwen, P. W. N. M.; Nozaki, K. *Acc. Chem. Res.* **2013**, *46*, 1438.

[4] (a) Durand, J.; Zangrando, E.; Stener, M.; Fronzoni, G.; Carfagna, C.; Binotti, B.; Kamer, P.C.J.; Müller, C.; Caporali, M.; van Leeuwen, P.W.N.M.; Vogt, D.; Milani, B. *Chem. Eur. J.* **2006**, *12*, 7639; (b) Scarel, A.; Milani, B.; Zangrando, E.; Stener, M.; Furlan, S.; Fronzoni, G.; Mestroni, G.; Gladiali, S.; Carfagna, C.; Mosca, L. *Organometallics* **2004**, *23*, 5593.

[5] Johnson, L. K.; Mecking, S.; Brookhart, M. *J. Am. Chem. Soc.* **1996**, *118*, 267.

[6] Rosar, V.; Meduri, A.; Montini, T.; Fini, F.; Carfagna, C.; Fornasiero, P.; Balducci, G.; Zangrando, E.; Milani, B. *ChemCatChem* **2014**, *6*, 2403-2418.

[7] R. E. Rulke, J. M. Ernsting, A. L. Spek, C. J. Elsevier, P. W. N. M. Van Leeuwen, K. Vrieze, *Inorg. Chem.* **1993**, *32*, 5769.

[8] Meduri, A.; Montini, T.; Ragaini, F.; Fornasiero, P.; Zangrando, E.; Milani, B. *ChemCatChem* **2013**, *5*, 1170.

[9] (a) Guironnet, D.; Roesle, P.; Runzi, T.; Gottker-Schnetmann, I.; Mecking, S. *J. Am. Chem. Soc.* **2009**, *131*, 422; (b) Berkefeld, A.; Drexler, M.; Moller, H.M.; Mecking, S. *J. Am. Chem. Soc.* **2009**, *131*, 12613; (c) Bouilhac, C.; Runzi, T.; Mecking, S. *Macromolecules* **2010**, *43*, 3589; (d) Runzi, T.; Guironnet, D.; Gottker-Schnetmann, I.; Mecking, S. *J. Am. Chem. Soc.* **2010**, *132*, 16623; (e) Runzi, T.; Frohlich, D.; Mecking, S. *J. Am. Chem. Soc.* **2010**, *132*, 17690; (f) Guironnet, D.; Caporaso, L.; Neuwald, B.; Gottker-

Schnetmann, I.; Cavallo, L.; Mecking, S. *J. Am. Chem. Soc.* **2010**, *132*, 4418; (g) Neuwald, B.; Olscher, F.; Gottker-Schnetmann, I.; Mecking, S. *Organometallics* **2012**, *31*, 3128; (h) Friedberger, T. Wucher, P.; Mecking, S. *J. Am. Chem. Soc.* **2012**, *134*, 1010; (i) Wucher, P.; Roesle, P.; Falivene, L.; Cavallo, L.; Caporaso, L.; Gottker-Schnetmann, I.; Mecking, S. *Organometallics* **2012**, *31*, 8505; (j) Runzi, T.; Tritschler, U.; Roesle, P.; Gottker-Schnetmann, I.; Moller, H.M.; Caporaso, L.; Poater, A.; Cavallo, L.; Mecking, S. *Organometallics* **2012**, *31*, 8388; (k) Wucher, P.; Goldbach, V.; Mecking, S. *Organometallics* **2013**, *32*, 4516.

[10] Fotheringham, J.D.; Heath, A.G.; Lindsay, A.J.; Stephenson, T.A. *J. Chem. Res. (S)* **1986**, 82.

[11] (a) Bellachioma, G.; Binotti, B.; Cardaci, G.; Carfagna, C.; Macchioni, A.; Sabatini, S.; Zuccaccia, C. *Inorg. Chim. Acta* **2002**, *330*, 44; (b) Binotti, B.; Carfagna, C.; Zuccaccia, C.; Macchioni, A. *Chem. Commun.* **2005**, 92; (c) Binotti, B.; Bellachioma, G.; Cardaci, G.; Carfagna, C.; Zuccaccia, C.; Macchioni, A. *Chem. Eur. J.* **2007**, *13*, 1570; (d) Carfagna, C.; Gatti, G.; Mosca, L. Passeri, A.; Paoli, P.; Guerri, A. *Chem. Commun.* **2007**, 4540; (e) Carfagna, C.; Gatti, G.; Paoli, P.; Binotti, B.; Fini, F.; Passeri, A.; Rossi, P.; Gabriele, B. *Organometallics* **2014**, *33*, 129.

[12] Milani, B.; Anzilutti, A.; Vicentini, L.; Sessanta o Santi, A.; Zangrando, E.; Geremia, S.; Mestroni, G. *Organometallics* **1997**, *16*, 5064.

[13] Coates, G.W.; Waymouth, R.M. *Science* **1995**, *267*, 217.

[14] Guo, L.; Gao, H.; Guan, Q.; Hu, H.; Deng, J.; Liu, J.; Liu, F.; Wu, Q. *Organometallics* **2012**, *31*, 6054.

[15] Johnson, L.K.; Killian, C.M.; Brookhart, M. *J. Am. Chem. Soc.* **1995**, *117*, 6414.

[16] Carfagna, C.; Gatti, G.; Paoli, P.; Rossi, P. *Organometallics* **2009**, *28*, 3212.

[17] (a) Margl, P.; Ziegler, T. *J. Am. Chem. Soc* **1996**, *118*, 7337; (b) Rix, F.C.; Brookhart, M.; White, P.S. *J. Am. Chem. Soc.* **1996**, *118*, 4746.

[18] Frisch, M. J., et al. *Gaussian 03*, *Revision D.01*; Gaussian Inc., Wallingford, CT, 2004.

[19] (a) Becke, A. D. *Phys. Rev. A* **1988**, *38*, 3098; (b) Perdew, J. P. *Phys. Rev. B* **1986**, *33*, 8822.

[20] Andrae, D.; Häußermann, U.; Dolg, M.; Stoll, H.; Preuß, H. *Theor. Chim. Acta* **1990**, *77*, 123.

[21] Höllwarth, A.; Böhme, M.; Dapprich, S.; Ehlers, A. W.; Gobbi, A.; Jonas, V.; Köhler, K. F.; Stegmann, R.; Veldkamp, A.; Frenking, G. *Chem. Phys. Lett.* **1993**, *208*, 237.

CHAPTER 3

Pd-catalyzed ethylene/methyl acrylate copolymerization: effect of new nonsymmetric α-diimines with a BIAN skeleton

Overview

The series of Ar,Ar'-BIAN has been widened to two new nonsymmetric ligands, both characterized by one aryl ring having a methoxy and a methyl group on the *ortho* positions and differing in the number and positions of the electron withdrawing groups (CF_3) on the other aryl ring. To complete the series, also the symmetric ligand with a methyl and a methoxy group in the *ortho* positions of both aryl rings was studied. The NMR spectra of the free ligands highlighted in solution the presence of *E*,*E* and *E*,*Z* isomers, together with *syn* and *anti* conformers.

The new ligands were used to synthesize both the neutral, [Pd(CH_3)Cl(Ar,Ar'-BIAN)], and the monocationic, [Pd(CH_3)(L)(Ar,Ar'-BIAN)][PF_6], (L = CH_3CN, dmso) palladium(II) complexes.

The monocationic complexes were tested as precatalysts in the ethylene/methyl acrylate cooligomerization reaction under mild conditions of temperature and pressure, and in different solvents. In contrast to our previous results obtained with catalysts having other nonsymmetric Ar,Ar'-BIANs, these complexes were found to be inactive in the studied reaction.

Part of this chapter will be published in a feature work:

Rosar, V.; Meduri, A.; Zangrando, E.; Montini, T.; Milani, B.

3.1. Introduction.

The previous studies on the catalytic behavior of Pd(II) complexes with symmetric Ar_2-BIAN ligands applied as catalysts for the ethylene/methyl acrylate (MA) copolymerization reaction[1-3] pointed out the importance of the steric encumbrance on the *ortho* positions of the aryl rings of the ligand to address the catalyst selectivity towards the production of polymers rather than oligomers or higher alkenes. In our group, a positive effect in the mentioned copolymerization reaction was found when a subtle steric and electronic unbalance was introduced on the ligand; in fact, the palladium complexes $[Pd(CH_3)(L)(\mathbf{L12})][PF_6]$ with the nonsymmetric ligand **L12** and L = CH_3CN, dmso (Figure 3.1) generated more productive catalysts with respect to those with the symmetrical counterparts **L13**-**L14**, also leading to a product with a higher polar monomer content (Table 3.1).[4]

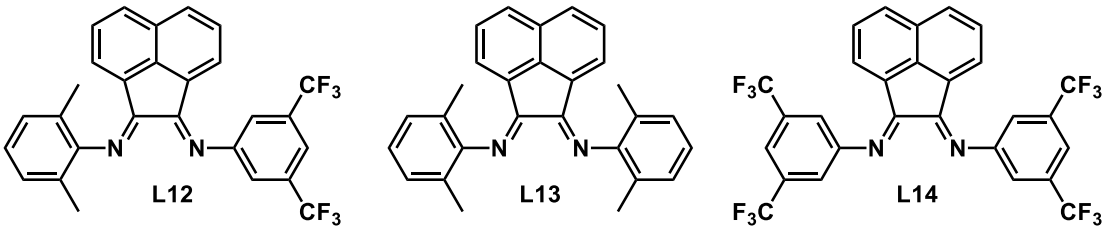

Figure 3.1. The reported nonsymmetric BIAN ligand **L12** and its symmetrical analogues.[4]

Table 3.1. Ethylene/MA cooligomerization reaction. Precatalyst: $[Pd(CH_3)(L)(Ar,Ar'\text{-BIAN})][PF_6]$[a][4]

Run	Ar,Ar'-BIAN	L	time (h)	yield (g)	productivity (g P/g Pd)[b]	mol % MA[c]	Alkenes/ Esters[d]
1	**L13**	CH_3CN	24	171.4	79.4	10.4	-
2	**L14**	CH_3CN	24	19.3	/	/	C^{4-6}
3	**L12**	CH_3CN	24	297.0	133.2	14.7	C^{4-16}
4	**L12**	CH_3CN	48	316.0	141.4	14.9	C^{4-16}
5	**L13**	dmso	24	221.8	99.5	6.6	-
6	**L14**	dmso	24	55.0	/	/	C^{4-6}
7	**L12**	dmso	24	520.8	233.5	12.5	C^{4-16}
8	**L12**	dmso	48	778.6	348.4	10.5	C^{4-16}

[a] Reaction conditions: $n_{Pd} = 2.1 \cdot 10^{-5}$ mol, V_{TFE} = 21 mL, V_{MA} =1.130 mL, [MA]/[Pd] = 594, T = 308 K, $P_{ethylene}$ = 2.5 bar; [b] g P/g Pd = grams of product per gram of Pd; [c] calculated by ^{1}H NMR spectroscopy on isolated product; [d] calculated by GC-MS.

Monocationic Pd-dmso complexes have been extensively studied in the case of P-O ligands,[5] whereas our study represented the first investigation of these derivatives in conjunction with α-diimine ligands With ligands **L12**, **L13**, the Pd-dmso precatalysts were found to be more productive than the corresponding Pd-$NCCH_3$ ones, leading to a larger production of both isolated cooligomers and higher alkenes. Moreover, with **L12** the Pd-dmso derivative showed a longer lifetime than the acetonitrile counterpart, since the latter was deactivated within the first 16 h of reaction, while the former resulted to be still active for at least 48 h (Table 3.1, Figure 3.2).[4] This behavior was ascribed to the possible favorable competition of dmso with the oxygen atom of the last inserted MA unit into the polymeric chain, that would disfavor the formation of the catalyst resting state (Scheme 1.4) favoring at the same time the insertion of the next incoming monomer.[4]

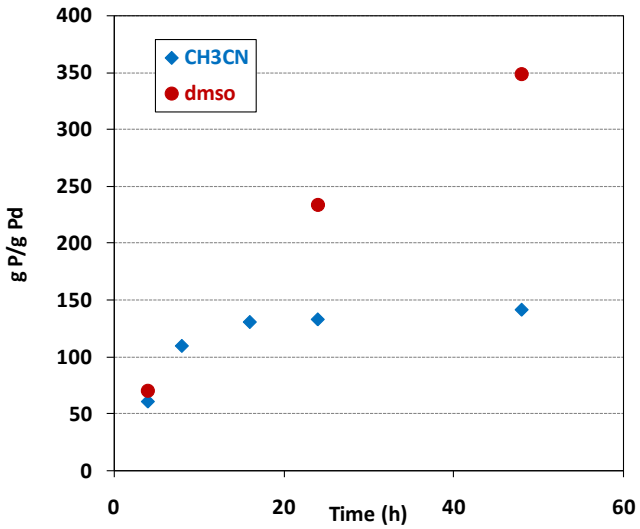

Figure 3.2. Ethylene/MA cooligomerization: effect of reaction time on productivity. Precatalyst: [Pd(CH_3)(L)(**L12**)][PF_6]. Reaction conditions: see Table 3.1.[4]

As far as the phosphine sulfonate palladium catalysts are concerned, it was reported that the presence of methoxy groups in the *ortho* position of the aryl rings led to an increase of nearly three times in productivity with respect to the non-substituted derivative (0.16 kg CP/g Pd *vs* 0.06 kg CP/g Pd), together with an increase in polar monomer content (13 % *vs* 7 %) and in molecular weight of the produced copolymer (Mw = 4100 *vs* 2700).[5a,6] These data suggested that the presence of methoxy groups on the ligand had a positive effect on the catalytic behavior of the corresponding palladium catalysts.

With the aim to obtain better performing catalysts for the target copolymerization reaction, we decided to merge the positive effect of the steric and electronic unbalance reported for the α-diimine ligands[4] with the positive role of methoxy groups observed for the P-O derivatives.[5,6] For this reason, we

synthesized two new nonsymmetric Ar,Ar'-BIAN ligands bearing a methyl and a methoxy group in the *ortho* positions of one aryl ring while the other ring is featured by electron withdrawing CF_3 groups either in *meta* or in *ortho* position (Figure 3.3).

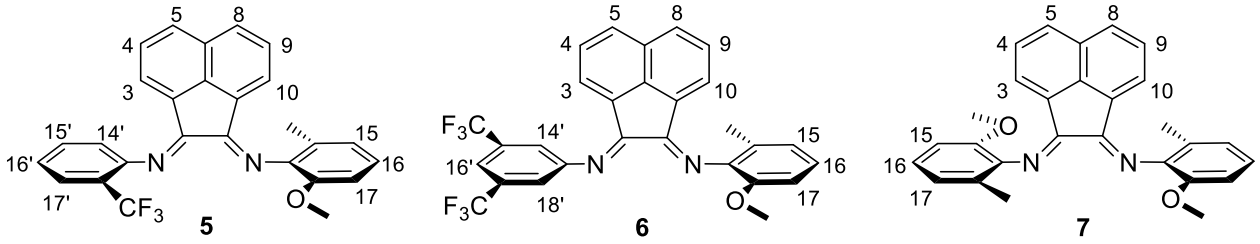

Figure 3.3. The synthesized nonsymmetric ligands **5**, **6** and the related symmetric ligand **7**.

Ligands **5-7** were synthesized by optimizing the protocol developed in our group for ligands **6**, **7**.[7] Their coordination to Pd(II) was investigated with the synthesis of both neutral [Pd(CH_3)Cl(Ar,Ar'-BIAN)] **5a-7a**, and monocationic complexes [Pd(CH_3)(L)(Ar,Ar'-BIAN)][PF_6] (L = CH_3CN, **5b-7b**; L = dmso, **5c-7c**). Special attention was paid to the dmso derivatives, since at that time these were only the third example for this class of complexes.[4,8]

The monocationic derivatives with ligands **5-7** were tested as precatalysts in the ethylene/MA copolymerization reaction, and their catalytic behavior was studied in detail.

3.2. Results and Discussion.

3.2.1. Synthesis and characterization of ligands 5-7.

The synthesis of ligands **6** and **7** was developed in our laboratories;[7] it was further optimized and applied with slight modifications to obtain ligand **5**. The protocol was based on the transimination reaction[8-10] of the zinc chlorido derivative of the symmetric Ar_2-BIAN ligand, containing the electron withdrawing CF_3 groups, with the 2-methoxy-6-methylaniline (Scheme 3.1). This led to the formation of the desired nonsymmetric derivative together with the symmetric **7**·$ZnCl_2$, which is thermodynamically favored and, in agreement with the literature,[10,11] was not obtainable through direct condensation of the 2-methoxy-6-methylaniline with acenaphthenequinone, as reported for other symmetric analogues.[12]

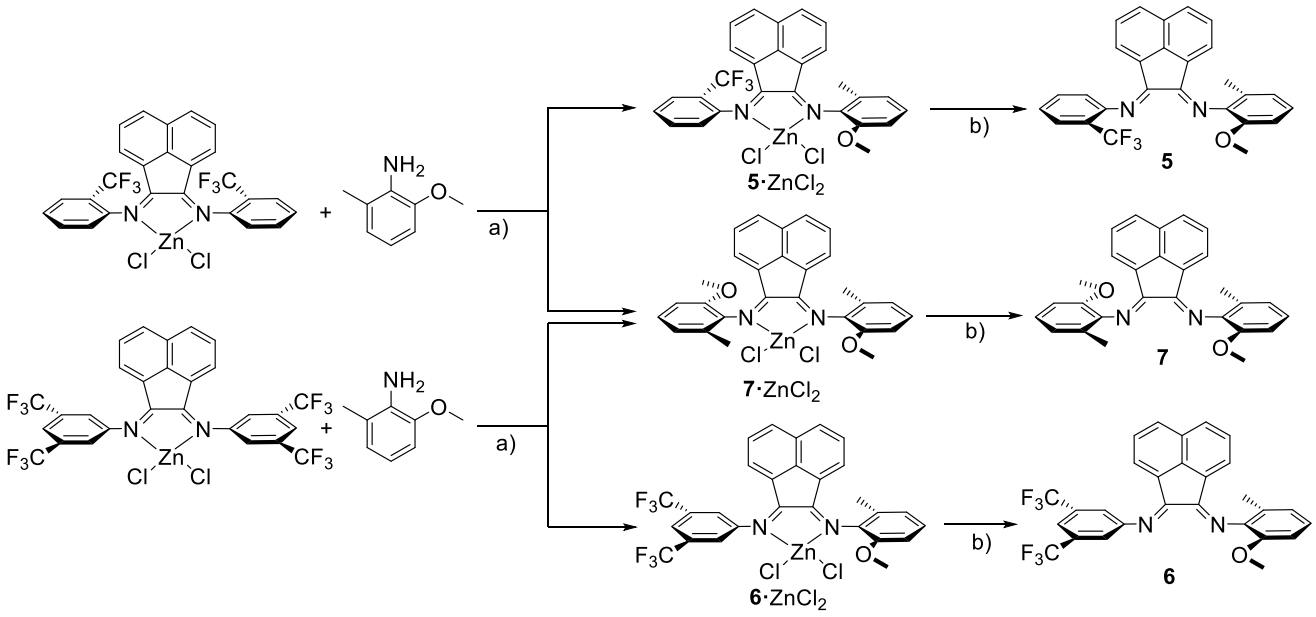

Scheme 3.1. Synthesis of ligands **5**-**7**. Reaction conditions: a) 2-methoxy-6-methylaniline (3 eq), zinc derivative (1 equiv.), methanol, room temperature; b) $Na_2C_2O_{4(aq)}/CH_2Cl_2$.

The reaction time was optimized to achieve the highest conversion together with the highest amount of nonsymmetric derivative; the best compromise for **6**·$ZnCl_2$ was found to be 24 h at 298 K, while for **5**·$ZnCl_2$ the proceeding of the reaction had to be monitored by TLC or ^{1}H NMR, and at least 5 days at 298 K were required. The crude reaction mixture was treated with an aqueous solution of sodium oxalate to remove the zinc moiety, and after the purification by column chromatography on basic alumina both the nonsymmetric ligands **5** or **6** and the symmetric **7** were recovered.

Ligands **5**-**7** were characterized in dichloromethane solution by ^{1}H and ^{13}C NMR spectroscopy, and the characterization of ligands **6** and **7** was in agreement with our previous results.[7] For **5** and **7** the NMR spectra highlighted the presence of unreacted anilines.[7]

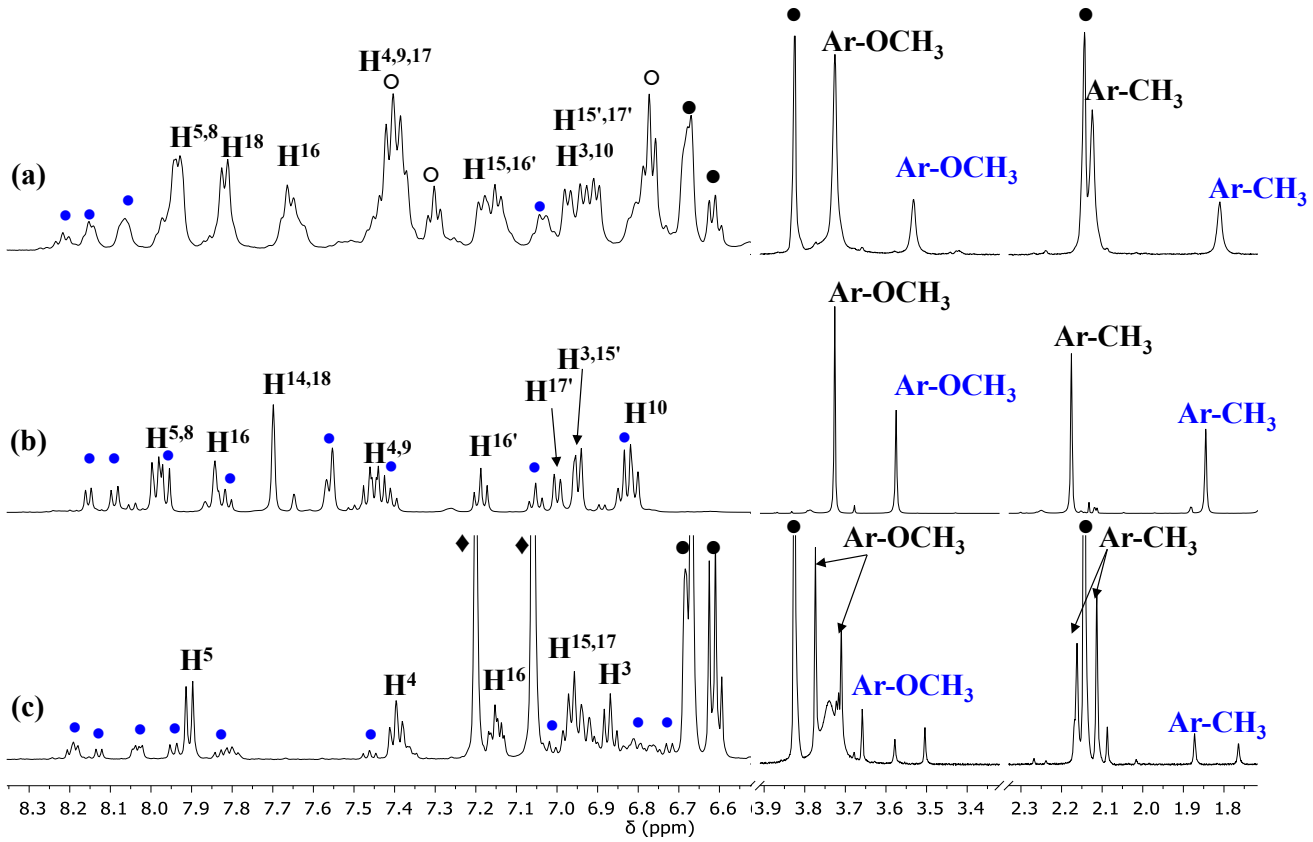

Figure 3.4. ^{1}H NMR spectra in CD_2Cl_2 at 298 K of (a) **5**, (b) **6**, (c) **7**: *E,E* (black) and *E,Z* (blue) isomers. Aliphatic and aromatic regions are not on scale.● 2-methoxy-6-methylaniline; ○ 2-trifluoromethylaniline; ♦ 3,5-bis(trifluoromethyl)aniline. For numbering scheme of the molecules see Scheme 3.3.

In the ^{1}H NMR spectra recorded at room temperature of all the synthesized ligands, two sets of signals were observed (Figure 3.4), and they were attributed to the (*E*,*E*) and (*E*,*Z*) isomers (Scheme 3.2a). In agreement with the literature,[4,8-12] the major species was always the (*E*,*E*) isomer, although the ratio between the two species depended on the substituents on the aryl ring: for **5** the ratio was 5 to 1, for **6** it was 2 to 1, while for **7** the ratio was 3 to 1. For **5** and **6**, two (*E*,*Z*) isomers were possible, depending on which aryl ring retained the *Z* geometry, and, in agreement with the behavior of similar Ar,Ar'-BIAN known in literature,[4,9,10] it was reasonable to assume that the fluorinated ring displayed the *Z* geometry. Moreover, in the case of ligands **5** and **7** also *syn* and *anti* conformers were possible, due to the presence of two different substituents on each aryl ring (Scheme 3.2b); in the ^{1}H NMR spectrum of **7** the presence of both conformers was demonstrated by the splitting of the methyl and the methoxy peaks; for ligand **5**

the singlets of these groups were slightly broad, suggesting the presence of the two conformers in exchange.

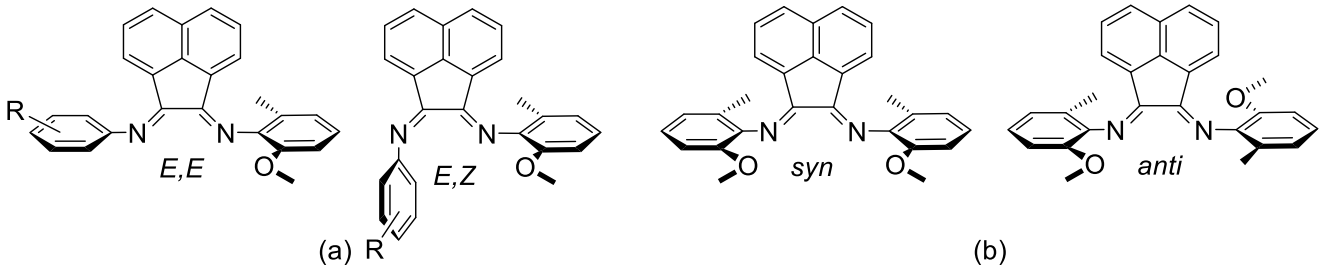

Scheme 3.2. The possible isomers of the studied ligands: (a) (*E*,*E*) and (*E*,*Z*) isomers; (b) *syn* and *anti* conformers for **7**.

3.2.2. Synthesis and characterization of Pd-complexes with ligands 5-7.

Ligands **5-7** were used for the synthesis of the relevant neutral palladium complexes **5a**-**7a** following the well-established procedure (Scheme 3.3).[13]

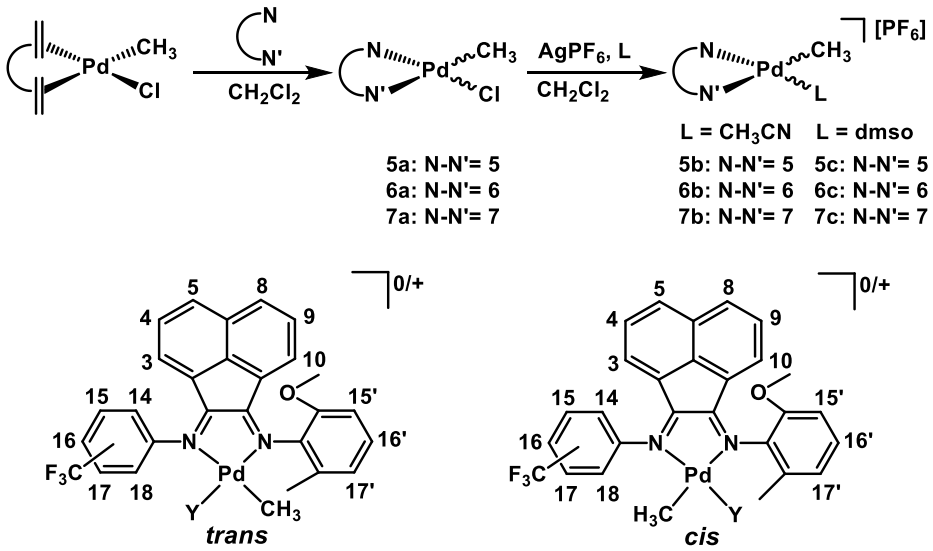

Scheme 3.3. Synthesis of neutral **5a**-**7a**, and monocationic complexes **5b**-**7b**, **5c**-**7c**, with the corresponding numbering scheme of the possible *trans* and *cis* isomers.

For **5a** and **6a** single crystals suitable for X-ray diffraction were obtained by slow diffusion of n-hexane in a dichloromethane solution of the complexes at 277 K (Figure 3.5). For **5a** two species, almost in a 1 : 1 ratio (55 : 45), were observed in the unit cell, differing for the relative position of the Pd-CH_3 and Pd-Cl groups with respect to the two nonequivalent moieties of the coordinated ligand; the main species was featured by the Pd-CH_3 fragment *cis* to the Pd-N bond bearing the fluorinated aryl ring on the nitrogen atom, that was defined as the *cis* isomer (Scheme 3.3). For **6a**, the solid state characterization

highlighted the presence in the unit cell of the *trans* isomer only (Scheme 3.3). In all cases, the palladium center had the expected square planar geometry with the nitrogen-donor ligand coordinated in a bidentate fashion with a relatively small bite angle, very similar in both structures (79.3(3)° for **5a** *vs* 78.9(3)° for **6a**) (Table 3.2).

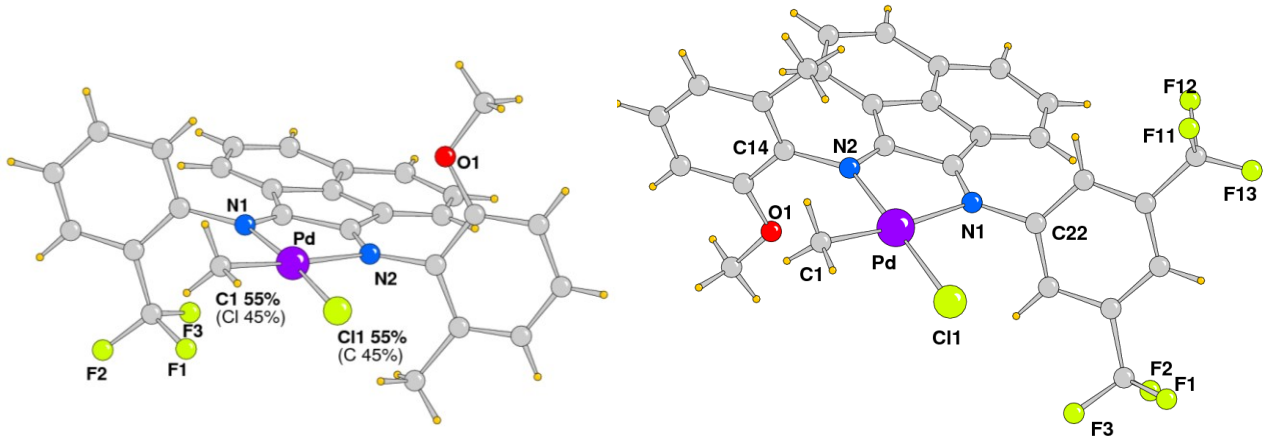

(a) (b)

Figure 3.5. ORTEP representation of (a) **5a**; (b) **6a**.

Table 3.2. Selected bond lengths and angles for complexes **5a** and **6a**.

5a		**6a**	
Bond lengths (Å)			
Pd(1)-N(1)	2.106(7)	Pd(1)-N(2)	2.046(7)
Pd(1)-N(2)	2.147(8)	Pd(1)-N(1)	2.176(7)
Pd(1)-C(1)	2.105(5)	Pd(1)-C(1)	2.009(11)
Pd(1)-Cl(1)	2.188(4)	Pd(1)-Cl(1)	2.283(3)
Bond angles (°)			
N(1)-Pd(1)-N(2)	79.3(3)	N(1)-Pd(1)-N(2)	78.9(3)
C(1)-Pd(1)-Cl(1)	76.1(2)	C(1)-Pd(1)-Cl(1)	88.7(3)
Dihedral angles (°)			
Ph(OCH_3,CH_3)/BIAN	79.0(4)	Ph(OCH_3,CH_3)/BIAN	78.9(1)
Ph(CF_3)/BIAN	86.7(3)	Ph(CF_3)/BIAN	67.7(1)

For both complexes, the Pd-N bond distance *trans* to the Pd-CH_3 fragment was longer than the other one (2.147(8) *vs* 2.106(7) Å in **5a**; 2.176(7) *vs* 2.046(7) Å in **6a**), in agreement with the stronger *trans* influence of the methyl group with respect to the chlorido.

In both structures, the acenaphthene moiety lies in the coordination plane, while the aryl rings are nearly orthogonal to it; the aryl ring bearing the methyl and the methoxy groups displays the same dihedral angle with the square plane both in **5a** (79.0(4)°) and in **6a** (78.9(1)°). On the other hand, the fluorinated phenyl is more bent towards the coordination plane in the latter (67.7(1)°) than in the former (86.7(3)°), and this is in agreement with an enhanced steric hindrance for the *ortho*-substituted aryl ring with respect to the *meta*-substituted one.

In the ^{1}H NMR spectra of the neutral complexes, recorded in CD_2Cl_2 at room temperature, sharp signals were observed, and the characterization of **6a** and **7a** was in agreement with our previous studies (Figure 3.6).[7]

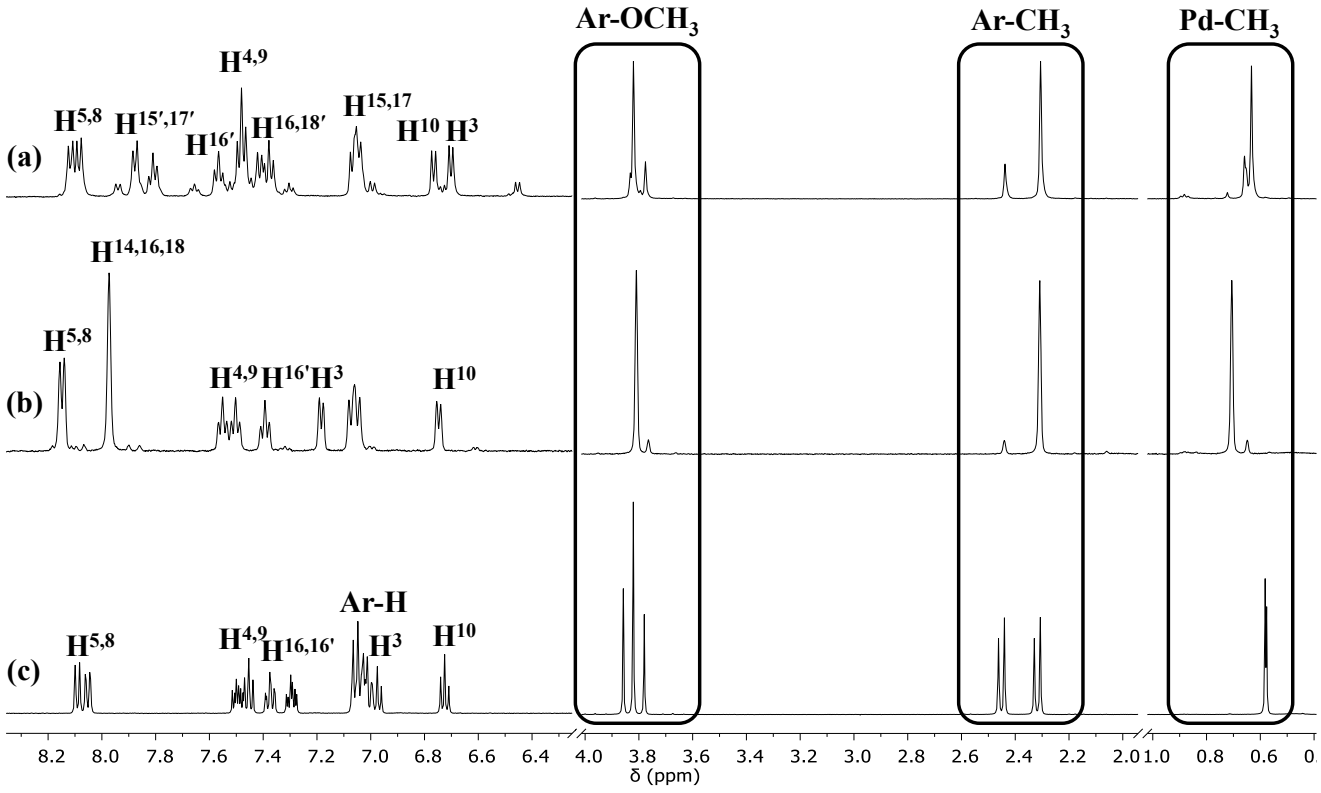

Figure 3.6. ^{1}H NMR spectra in CD_2Cl_2 at 298 K of (a) **5a**; (b) **6a**; (c) **7a**. Aliphatic and aromatic regions are not on scale. Assignments are reported only for the major isomer.

In particular, for complexes **5a** and **7a** the number of signals and their integration indicated the presence in solution of the *cis* and *trans* isomers, and from mono- or bi-dimensional NOE experiments (Figures

3.7, 3.8) the major species was identified as the *trans* isomer. For **6a** this was in agreement with the only species observed in the solid state, while it was the opposite for **5a**. For the two complexes, the ratio between the two isomers was very similar (*trans* : *cis* = 1 : 0.25 and 1 : 0.20 for **5a** and **6a**, respectively), thus suggesting that the discrimination between the two geometries was determined mainly by the electronic difference in the N-donor atoms of the ligand rather than the different steric encumbrance of the substituents on the aryl rings.

The presence in the NOESY spectrum of **5a** of exchange peaks, particularly evident for the methyl groups on the aryl ring, indicated that the two isomers were in exchange, at slow rate on the NMR timescale at room temperature (Figure 3.7). The same conclusion might be drawn from the NOE spectrum of **6a** recorded upon irradiation of the main singlet of the Pd-CH_3 fragment and observing the Pd-CH_3 peak of the minor isomer with same phase of the irradiated signal (Figure 3.8). However, this experiment was not a clear-cut, because due to the close proximity of the two signals a nonselective irradiation was performed.

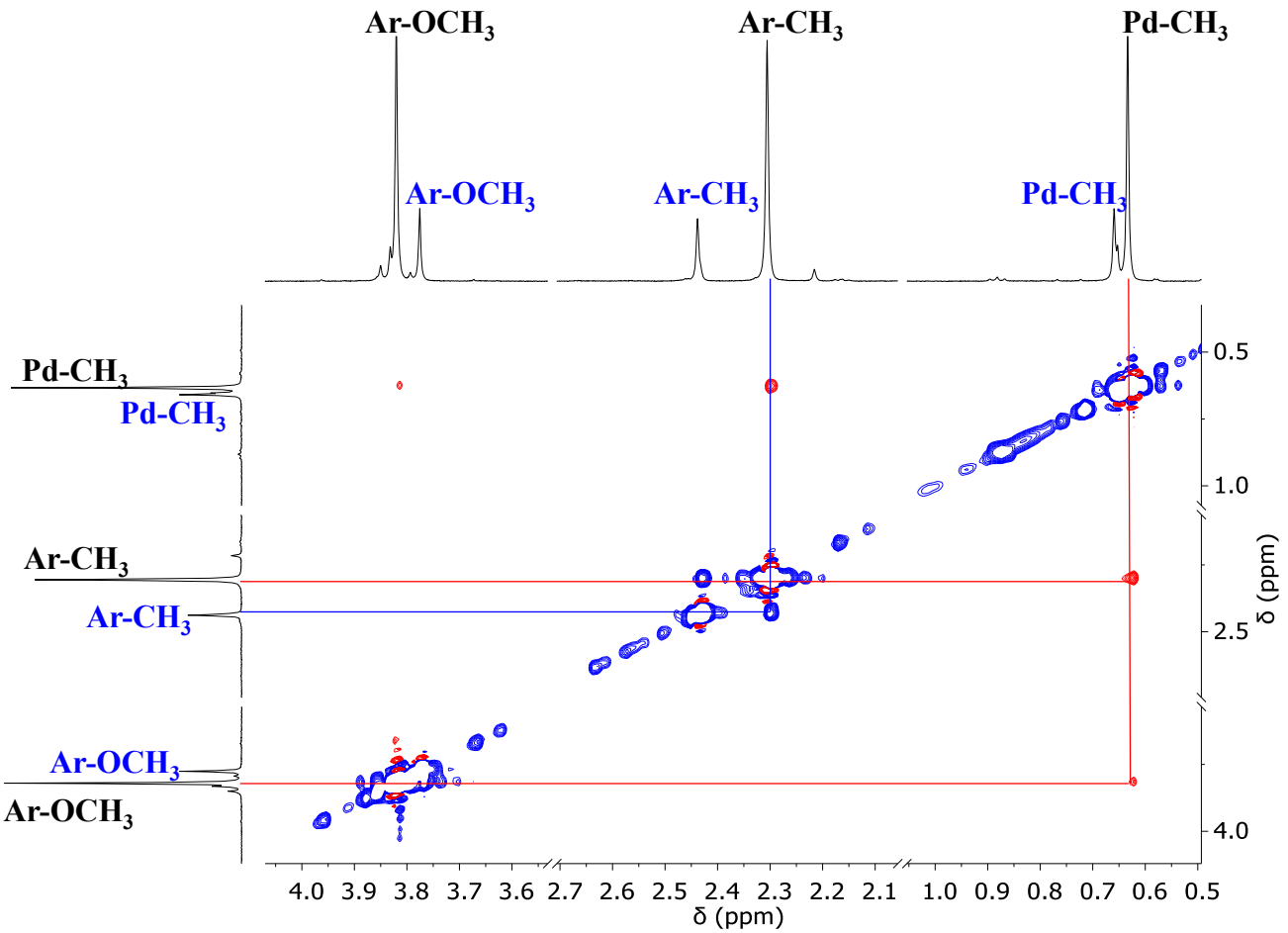

Figure 3.7. NOESY spectrum of **5a** in CD_2Cl_2 at 298 K. Aliphatic region. Red cross peaks are due to NOE; blue cross peaks are due to exchange.

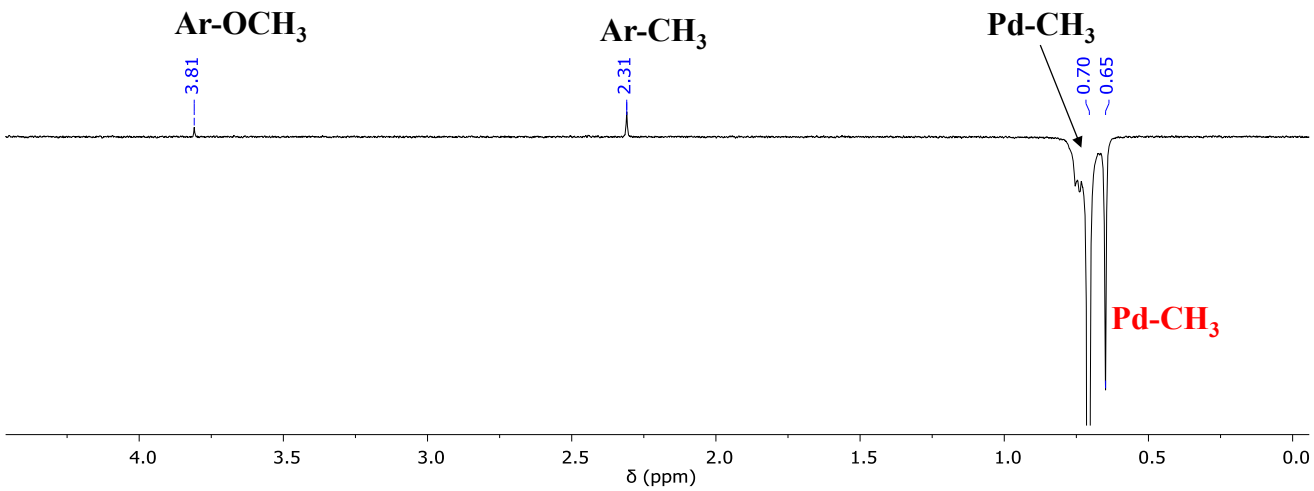

Figure 3.8. NOE spectrum in CD_2Cl_2 at 298 K of **6a** obtained by irradiating the most intense Pd-CH_3 signal. Aliphatic region.

In the ^{1}H NMR spectrum of **7a** (Figure 3.6c), the number of signals and their integration indicated the presence of a single species in solution. Upon coordination to palladium the two halves of the ligand are no longer equivalent, in agreement with the number of signals in the spectrum. When the Pd-CH_3 singlet was irradiated, positive NOE peaks were observed for the signals of one methyl and one methoxy group, allowing to identify that these are on the aryl ring *cis* to the Pd-CH_3 fragment (Figure 3.9). In both cases, the peaks were at lower frequencies with respect to the signals of the groups of the aryl ring *cis* to the Pd-Cl, in agreement with the literature.[4,8,10,13] On this basis, also the signals of the aromatic protons of the two non equivalent moieties of the ligand were assigned.

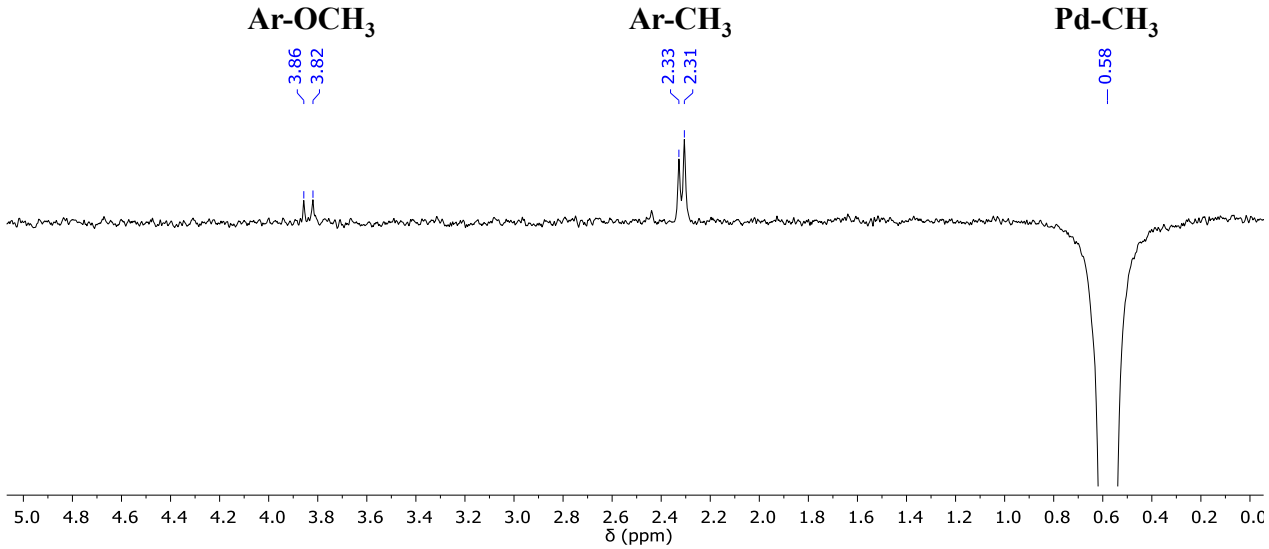

Figure 3.9. NOE spectrum in CD_2Cl_2 at 298 K of **7a** obtained by irradiating the Pd-CH_3 singlet. Aliphatic region.

The splitting of the singlets of Pd-CH_3, Ar-CH_3 and Ar-OCH_3 and the doublets of H^3, H^{10} and $H^{5,8}$ highlighted that both *syn* and *anti* conformers were present, with a slight preference for one of the two conformations, that was not possible to identify.

Moving from **7a** to **5a** to **6a**, the chemical shift of the Pd-CH_3 singlet was shifted to higher frequencies (0.58 ppm for **7a**, 0.63 ppm for **5a** and 0.71 ppm for **6a**), confirming that this is a sensitive probe for the electron density on the palladium center,[4] that, as predicted, decreased on going from ligand **7** to **5** to **6**.

Complexes **5a**-**7a** were reacted with $AgPF_6$ in the presence of the proper labile ligand, either acetonitrile or dimethyl sulfoxide, to yield the corresponding monocationic complexes, **5b**-**c**, **6b**-**c**, **7b**-**c** following the reported procedures (Scheme 3.3).[4,8]

As usually observed for the Pd-acetonitrile derivatives with α-diimine ligands,[4,8,10] the ^{1}H NMR spectra of **5b**-**7b** showed sharp signals already at room temperature (Figure 3.10).

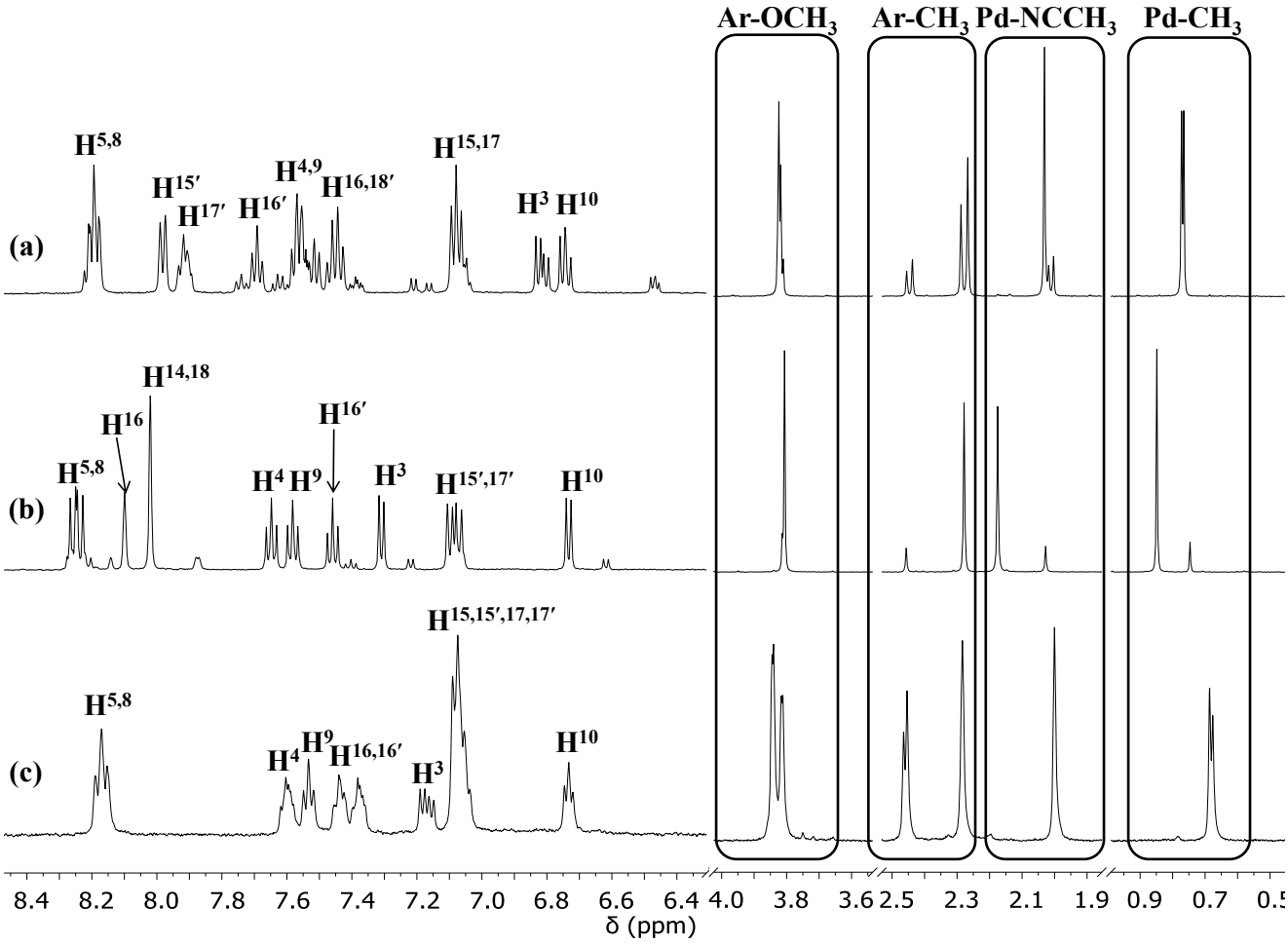

Figure 3.10. ^{1}H NMR spectra in CD_2Cl_2 at 298 K of (a) **5b**; (b) **6b**; (c) **7b**. Aliphatic and aromatic regions are not on scale. Assignments are reported only for the major isomer.

In the spectrum of **5b**, two signals were observed for the Ar-CH_3 group and for some of the aromatic protons, indicating the presence of *cis* and *trans* isomers, as observed for the neutral derivative (Figure 3.10). By chance the protons of the Pd-CH_3 fragment in the two isomers resonated at the same frequency, thus by NMR experiments it was not possible to distinguish between the major and the minor isomer. Therefore, the major species was identified as the *trans* isomer on the basis of what found for the neutral derivative and with other similar complexes.[4] The ratio between the *trans* and the *cis* isomers, calculated from the integrations of the signals of Ar-CH_3 groups, is 1 to 0.25. In the NOESY spectrum, recorded at room temperature, exchange peaks between the Ar-CH_3 groups of the two species were present, indicating that the two isomers are in equilibrium (Figure 3.11).

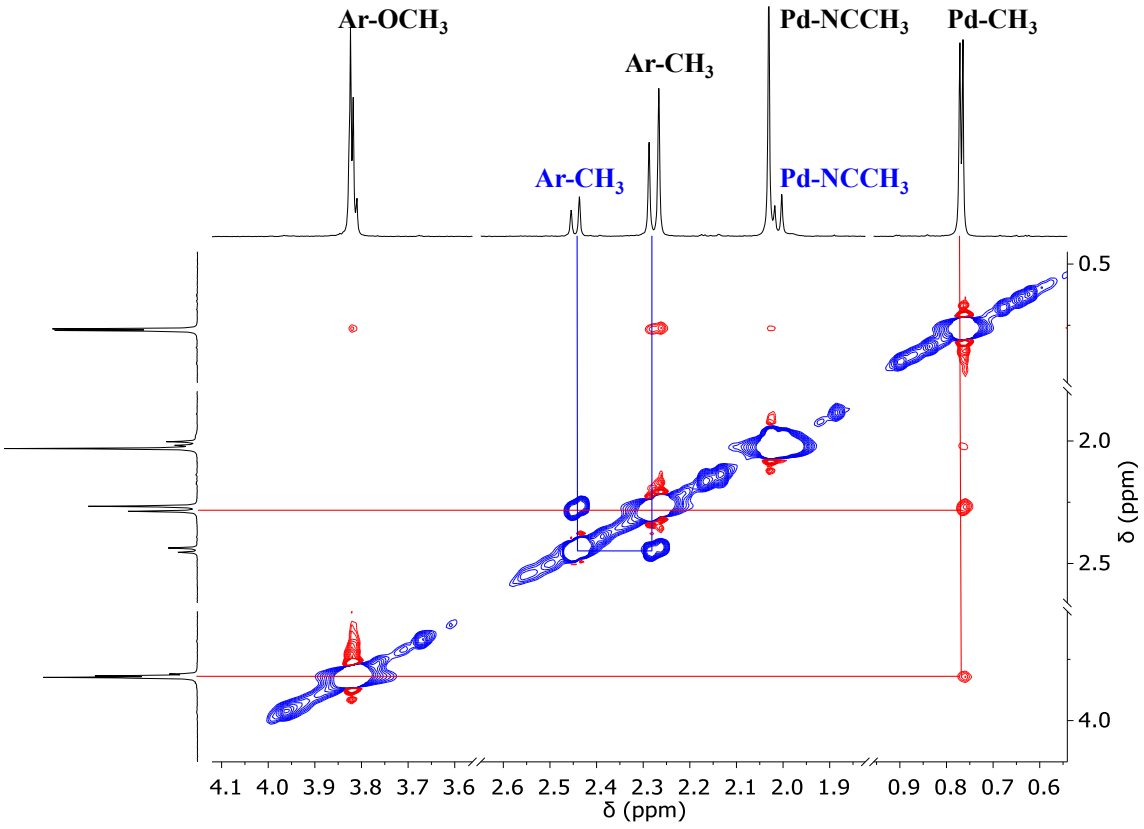

Figure 3.11. NOESY spectrum of **5b** in CD_2Cl_2 at 298 K. Aliphatic region. Red cross peaks are due to NOE; blue cross peaks are due to exchange.

The ^{1}H NMR spectrum of **6b** clearly showed the presence of two isomers as well, and on the basis of the ^{19}F-^{1}H HOESY spectrum (Figure 3.12) the major species was identified as the *trans* isomer, in a 1 : 0.15 ratio with the *cis* one.

As discussed in the characterization of the neutral complex **7a**, in **7b** the two halves of the ligand are not equivalent, and the signals of the two moieties were assigned on the basis of the comparison with the characterization of the corresponding neutral derivative.

The splitting of some signals, such as the singlets of Ar-CH_3 and the doublets of H^3 and H^{10} in the spectra of **5b** and **7b**, indicated that both *syn* and *anti* conformers were present in solution, and in the spectrum of **7b** slightly broad signals were observed, suggesting the presence of an exchange process in solution.

As for the neutral complexes, also in the Pd-$NCCH_3$ derivatives the Pd-CH_3 singlet moves towards higher frequency in the order **7b** > **5b** > **6b**, the same trend observed for the neutral complexes and thus confirming the role of this signal as a sensitive probe for the electron density on the metal center.

The interionic structure in solution of complex **6b** was investigated by the ^{19}F-^{1}H HOESY spectrum: the presence of the cross peaks due to NOE among the CF_3 groups of both isomers and protons $H^{14,18}$ confirmed that the parameter set for the experiment was correct (Figure 3.12). The correlation peaks between the CF_3 groups of the major species with the Pd-$NCCH_3$ fragment confirmed that this is the *trans* isomer. Thanks to the cross peaks of the PF_6^- anion with the Pd-$NCCH_3$, the Pd-CH_3, the methoxy group and protons $H^{14,18}$ it was possible to locate the counterion on top of the complex, shifted towards the Pd-$NCCH_3$ fragment. This is in contrast with the study reported for palladium complexes with DAB ligands [Pd(η_1,η_2-$C_8H_{12}OMe$)(Ar_2-DAB)][PF_6] (η^1,η^2-$C_8H_{12}OMe$ = methoxy-cyclooctenyl), that located the counterion always close to the N-donor atom and the ligand backbone,[14] suggesting that the ligand skeleton plays a key role in defining the preferred position of the counterion.

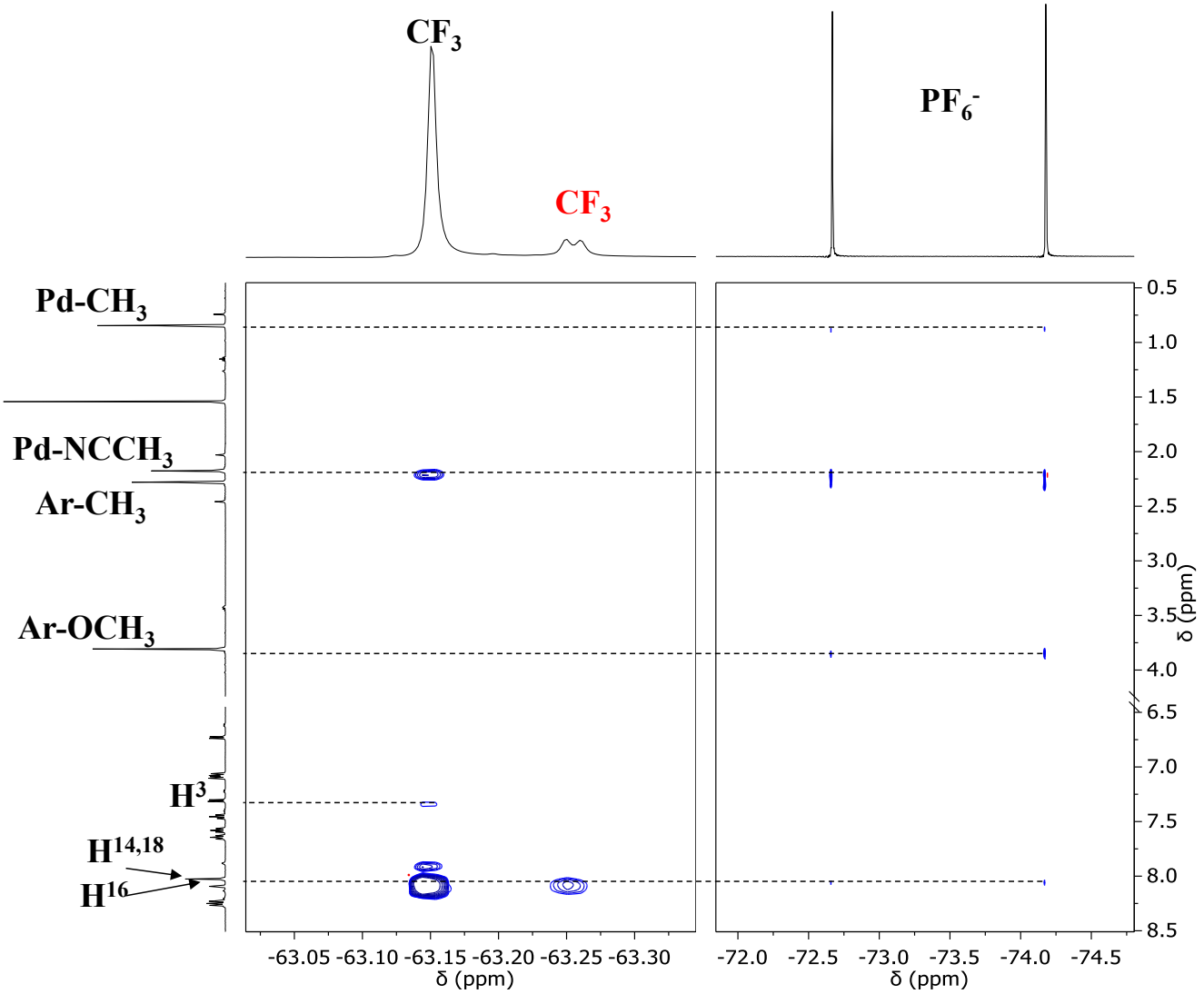

Figure 3.12. ^{19}F-^{1}H HOESY spectrum of **6b** in CD_2Cl_2 at 298 K.

In agreement with our previous studies (Chapter 2),[4,8] in the ^{1}H NMR spectra of the dimethyl sulfoxide derivatives, recorded in dichloromethane, broad signals were observed at room temperature. The signals became sharper by decreasing temperature, and the decoalescence of the peaks of the aliphatic protons was reached at 263 K for **5c** and 233 K for **6c**, **7c** (Figure 3.13).

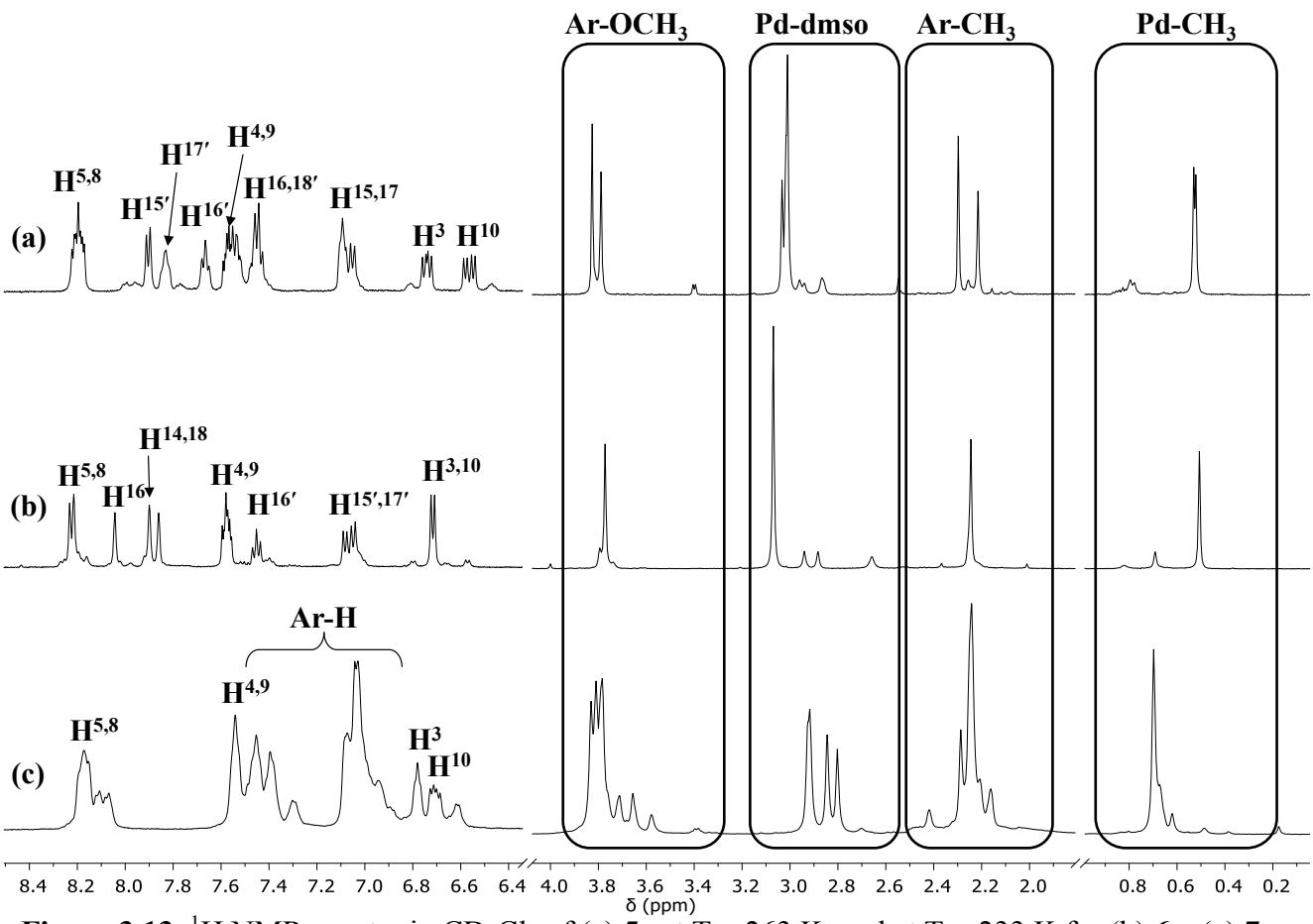

Figure 3.13. ^{1}H NMR spectra in CD_2Cl_2 of (a) **5c** at T = 263 K; and at T = 233 K for (b) **6c**; (c) **7c**. Aliphatic and aromatic regions are not on scale.

Due to its ambidentate nature, as previously discussed (Chapter 2), dimethyl sulfoxide can coordinate to palladium via the sulfur or the oxygen atom, and since for complexes **5c** and **6c** both *cis* and *trans* isomers are also possible, there are four possible combinations: the *trans* and *cis* isomers having S-bonded dmso (*i* and *ii* respectively), and *trans* and *cis* isomers with the O-bonded dmso (*iii* and *iv* respectively) (Scheme 3.4).

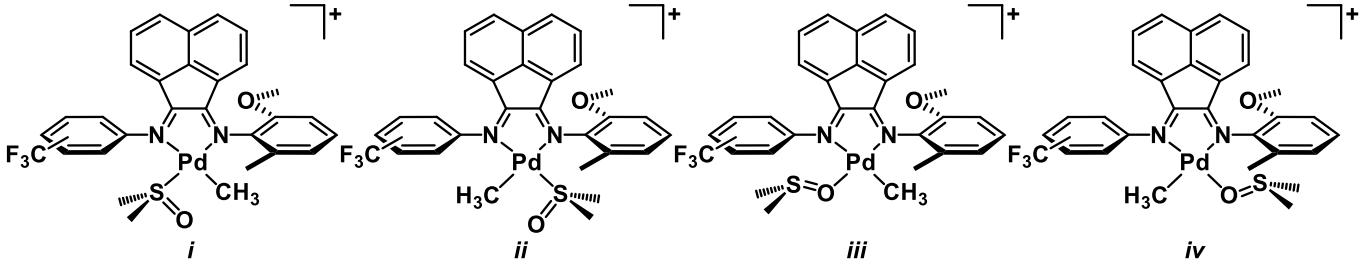

Scheme 3.4. Schematic representation of the possible isomers for complexes **5c**, **6c**.

For complex **5c** two species were observed, and, as discussed in Chapter 2, both of them were characterized by the dmso coordinated through the sulfur atom as evidenced by the ^{13}C chemical shift in the ^{1}H-^{13}C HSQC spectrum (Figure 3.14).[15] From the comparison with the related neutral and acetonitrile derivatives, and in agreement with our previous work,[4,8] the major species was identified as the *trans* isomer (*i*), while the other is the corresponding *cis* isomer (*ii*). For both isomers, the splitting of the Pd-CH_3 singlet and the presence of two peaks for Ar-CH_3 and Ar-OCH_3 highlighted that both *syn* and *anti* conformers were present (Figure 3.14).

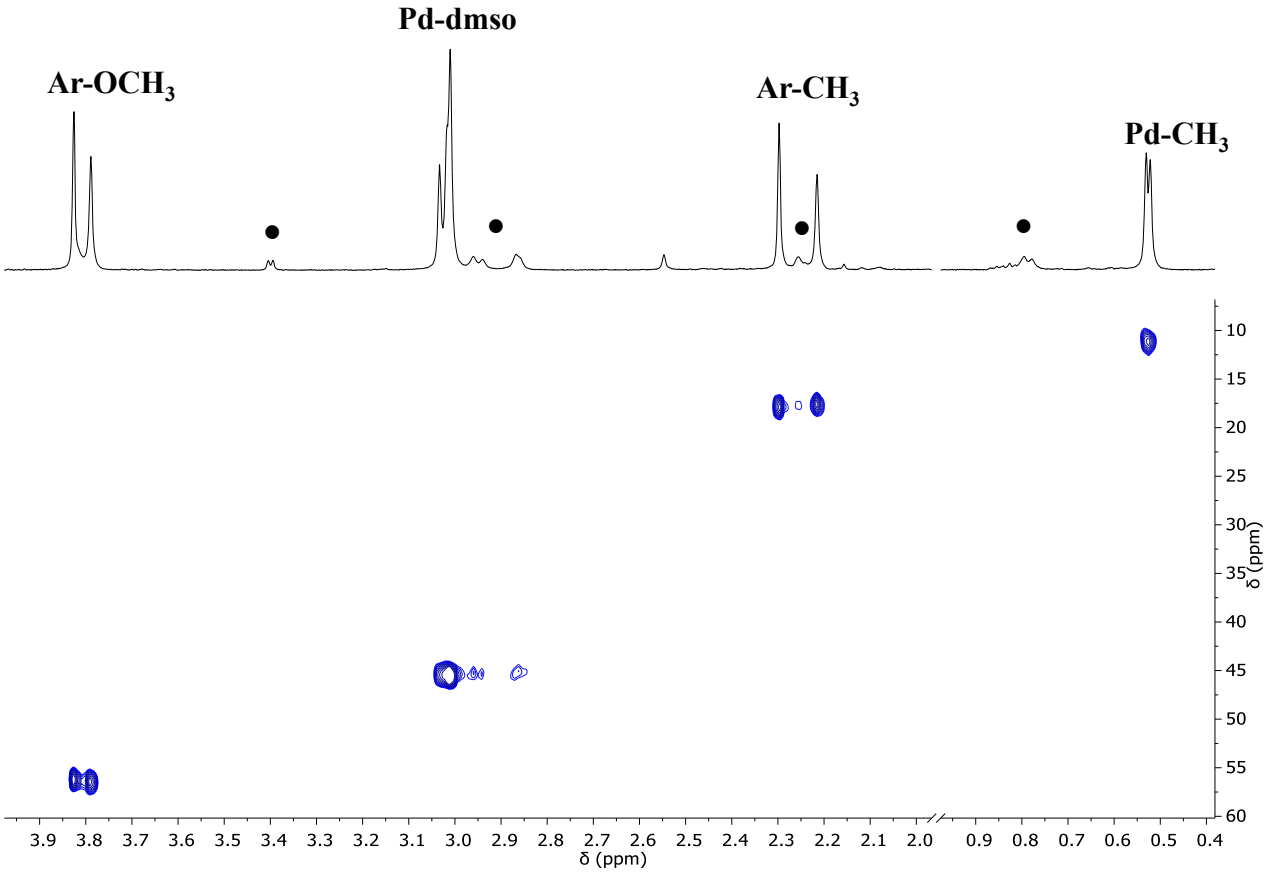

Figure 3.14. ^{1}H-^{13}C HSQC of **5c** in CD_2Cl_2 at 263 K. Aliphatic region. ● *cis*-(S-dmso).

In the ^{1}H NMR spectrum of **6c** at 233 K the number of signals and their integration indicated the presence of three species in solution, of which two were featured by S-bonded dmso, whereas the less abundant one was characterized by O-bonded dmso, as evident from the ^{13}C chemical shift of the dimethyl sulfoxide (Figure 3.15). When the Pd-CH_3 singlet of the major species was irradiated at the decoalescence temperature, positive NOE peaks were observed for both the Ar-CH_3 and Ar-OCH_3, allowing to identify the main species as the *trans* isomer (Figure 3.16).

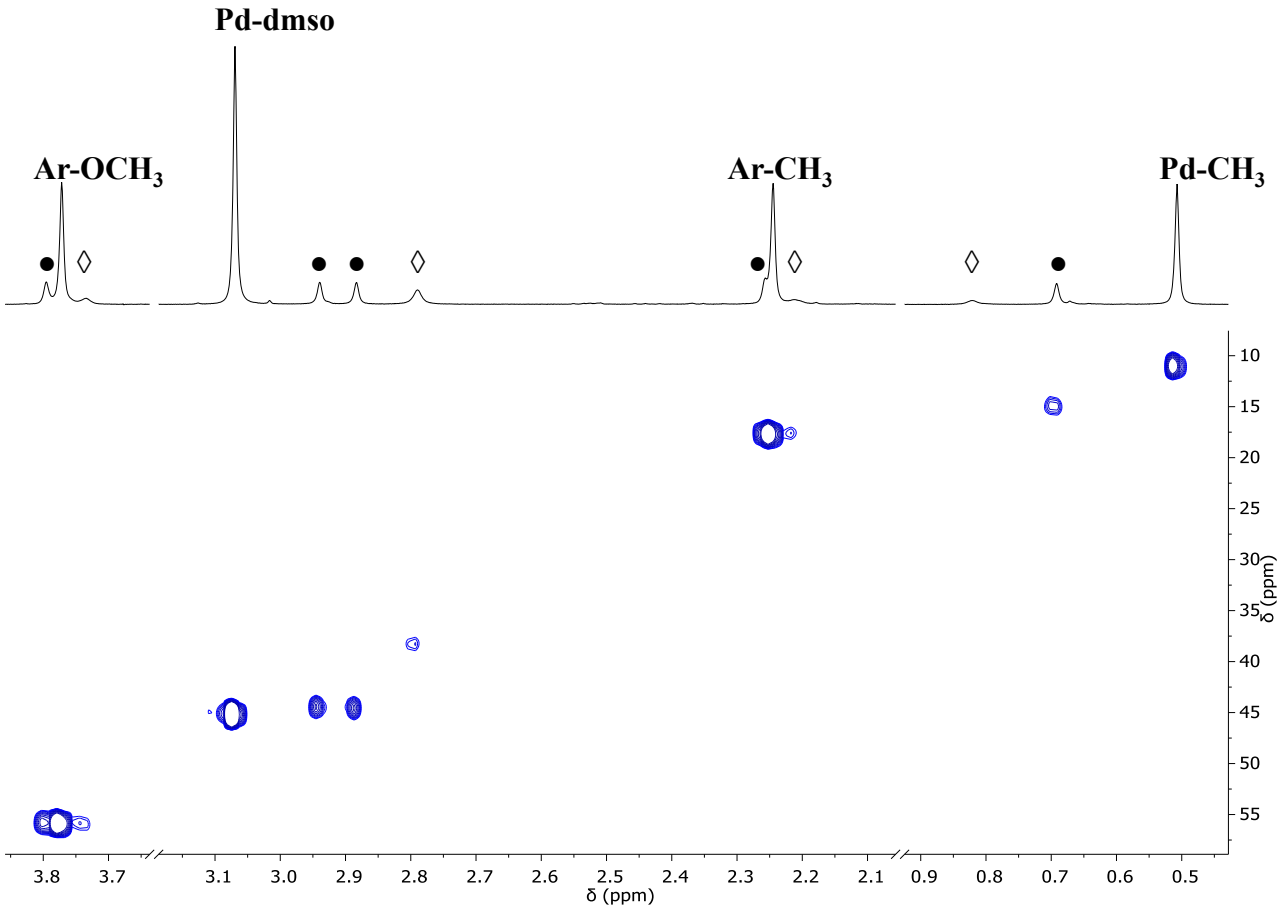

Figure 3.15. ^{1}H-^{13}C HSQC of **6c** in CD_2Cl_2 at 233 K. Aliphatic region. ● *cis*-(S-dmso); ◊ *trans*-(O-dmso).

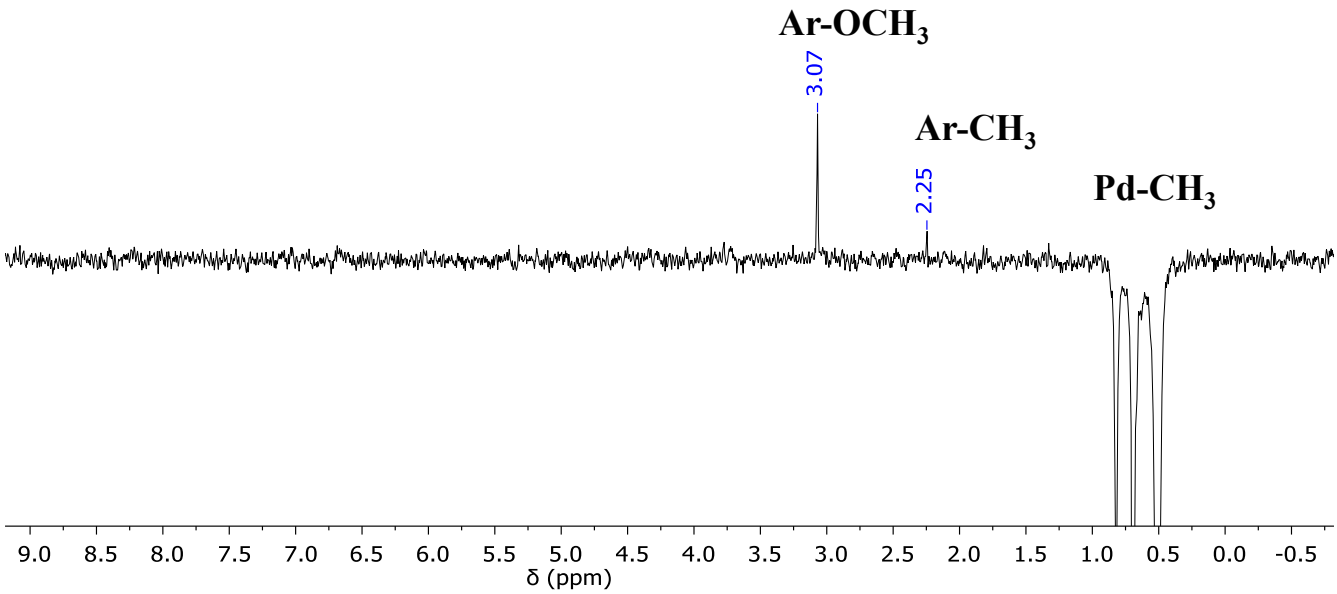

Figure 3.16. NOE spectrum of **6c** in CD_2Cl_2 at 233 K obtained by irradiating the most intense Pd-CH_3 signal.

In the *cis*-(S-dmso) species (*ii*) the methyl groups of the dimethyl sulfoxide originate two singlets, indicating that they are diastereotopic; this suggested that in the *cis* isomer the rotation of the *ortho*-substituted aryl ring is hindered, while it is free when the dmso is *cis* to the *meta*-substituted phenyl, as in the *trans* isomer (*i*).

For complex **7c** the possible isomers differ for the atom of dmso bonded to palladium and for the relative position of the aryl rings with respect the square plane (*syn* and *anti* isomers). In the ^{1}H NMR spectrum at 233 K several peaks were observed in the aliphatic region, indicating the presence of the different isomers in solution. From the ^{1}H-^{13}C HSQC spectrum it was clear that mainly S-bonded dmso species was present, with only traces of the O-bonded one. As discussed above for **6c**, also in this case the methyl groups of dmso generated two signals due to hindered rotation, each one being split into two singlets due to the presence of *syn* and *anti* conformers, as already observed for the neutral and acetonitrile derivatives with ligand **7** (Figure 3.17).

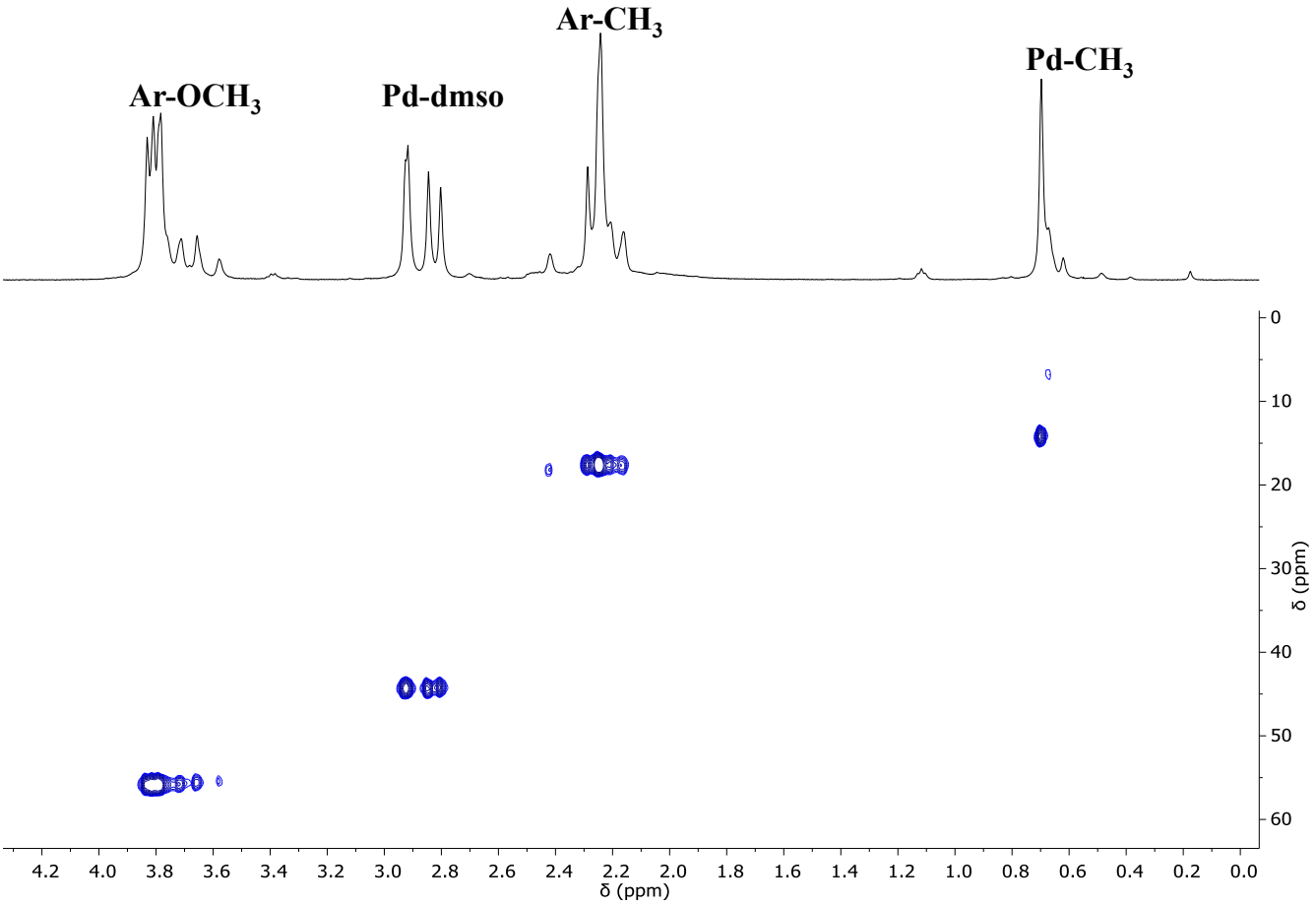

Figure 3.17. ^{1}H-^{13}C HSQC of **7c** in CD_2Cl_2 at 233 K. Aliphatic region.

By simple considerations about coordination chemistry, the major isomer (species *i* in Scheme 3.4) should be the most stable: in agreement with the hard/soft acids/bases theory, dmso is bonded through sulfur (soft base) to Pd^{2+} (soft acid); the Pd-CH_3 bond is *trans* to the Pd-N bond of the nitrogen atom bearing the fluorinated ring, thus characterized by a lower Lewis basicity. Contrarily, isomer *iv* (Scheme 3.4), with dmso bonded through oxygen (hard base) to Pd^{2+} (soft acid) and the Pd-CH_3 *trans* to the N-donor atom of higher Lewis basicity, should be the least stable and was never detected. The stability of the other two species, *ii* and *iii*, should lie in between that of *i* and *iv*.

For complexes **5c**, **6c**, the *trans*-(S-dmso) isomer was always found as the major species in solution, while the (O-dmso) isomer was only observed in traces for complexes **6c**, **7c**. The observation that the *trans* isomer was the prevailing species for both complexes was in agreement with the literature, in which a preferential coordination of the methyl group *trans* to the less basic nitrogen atom in Pd–CH_3 complexes with nonsymmetric N-donor ligands was reported.[4,13b,16]

3.2.3. Ethylene/methyl acrylate cooligomerization reaction.

Complexes **5b-c**, **6b-c** and **7b-c** were tested as precatalysts for the ethylene/methyl acrylate cooligomerization under mild reaction conditions of temperature and ethylene pressure (T = 308 K, P = 2.5 bar), in 2,2,2-trifluoroethanol (TFE) as solvent (Table 3.3). The isolated product was characterized by NMR spectroscopy and GC-MS, resulting in a mixture of ethylene/MA cooligomers and oligomers of ethylene.

All the complexes were found to be poorly active towards the target reaction, with the highest productivity of 93.4 g P/g Pd; in contrast with our previous studies,[4,8] the ancillary ligand did not affect the catalytic behavior of these complexes and no positive effect of the nonsymmetric ligand was observed.

Furthermore, in contrast with literature,[1-3,4,8] with all catalysts, including those with the ancillary ligand bearing sterically hindered substituents in the *ortho* position of both aryl rings (**7**), the formation of higher alkenes was observed. In all cases the produced alkenes are a complex mixture of isomers, as expected in consequence of the chain walking mechanism;[1] the GC-MS characterization of the volatile fraction highlighted that the chain length distribution can be reasonably fitted with a Poisson distribution.

Table 3.3. Ethylene/methyl acrylate cooligomerization reaction: effect of the Ar,Ar'-BIAN ligand and of the labile ligand L. Precatalyst: $[Pd(CH_3)(L)(Ar,Ar'\text{-BIAN})][PF_6]$[a]

Run	Precatalyst	L	yield (mg)	productivity (g P/g Pd) [b]	mol % MA[c]	Alkenes[d]
1	**5b**	CH_3CN	133.7	60.0	36	C^{4-6}
2	**5c**	dmso	28.2	12.6	46	C^{4-6}
3	**6b**	CH_3CN	157.1	70.4	25	C^{4-12}
4	**6c**	dmso	208.3	93.4	23	C^{4-16}
5	**7b**	CH_3CN	157.5	70.6	32	C^{4-8}
6	**7c**	dmso	178.4	80.0	31	C^{4-6} traces

[a] Reaction conditions: $n_{Pd} = 2.1 \cdot 10^{-5}$ mol, $V_{TFE} = 21$ mL, $V_{MA} = 1.130$ mL, [MA]/[Pd] = 594, T = 308 K, $P_{ethylene} = 2.5$ bar, t = 24 h; [b] isolated yield, productivity as g P/g Pd = grams of product per gram of Pd; [c] calculated by ^{1}H NMR spectroscopy on isolated product; [d] calculated by GC-MS.

From the ^{1}H NMR characterization of the isolated product, the polar monomer content was in the range 23 - 36 %, and, as generally observed,[4,8] the MA incorporation decreased with increasing productivity. Moving from the Pd-$NCCH_3$ to the Pd-dmso derivatives, no effect was observed on either productivity or polar monomer incorporation, in contrast with the positive effect reported by us (Table 3.1).[4] Another notable feature of these new catalytic systems is the nearly negligible decomposition to inactive palladium black after 24 h of reaction: with the acetonitrile derivatives only traces of palladium black were evident, and with the dmso precatalysts, no palladium black was formed at all at the end of the reaction time. This suggested that either the generated catalyst decomposed leading to inactive species other than palladium black or their inactivity was not related to catalyst decomposition. As already observed in the case of the CO/ethylene copolymerization catalyzed by palladium complexes with phosphorus donor ligands having *ortho*-anisol groups on the phosphorus atom,[17] one possible explanation is that the TFE strongly interacts with the methoxy groups of the ligand through hydrogen bonding, thus preventing the incoming monomer to coordinate on the palladium center and therefore hampering the catalytic activity. To validate this hypothesis the effect of the solvent on the catalytic behavior was explored by testing precatalyst **6b** in various solvents (Table 3.4).

Table 3.4. Ethylene/methyl acrylate cooligomerization reaction: effect of the solvent. Precatalyst: $[Pd(CH_3)(CH_3CN)(\mathbf{2})][PF_6]$[a]

Run	Solvent	yield (mg)	productivity (g P/g Pd)[b]	mol % MA[c]	Alkenes[d]
1	TFE[e]	157.1	70.4	25	$C^{4\text{-}12}$
2	CH_2Cl_2	16.5	-	-	$C^{4\text{-}8}$, $C^{5\text{-}7}$
3	toluene	24.3	-	-	-
4	methanol	10.6	-	-	-

[a] Reaction conditions: $n_{Pd} = 2.1 \cdot 10^{-5}$ mol, $V_{solvent}$ = 22 mL, V_{MA} =1.130 mL, [MA]/[Pd] = 594, T = 308 K, $P_{ethylene}$ = 2.5 bar, t = 24 h; [b] isolated yield, productivity as g P/g Pd = grams of product per gram of Pd; [c] calculated by ^{1}H NMR spectroscopy on isolated product; [d] calculated by GC-MS; [e] V_{TFE} = 21 mL.

In contrast to our expectations, moving from TFE to other solvents, such as dichloromethane, toluene and methanol, typically applied in the literature catalytic systems, no catalytic activity was observed, confirming the fluorinated solvent to be the best choice for the ethylene/MA copolymerization with the α-diimine catalysts under the reaction conditions we apply.[18]

The NMR characterization of the isolated products highlighted that when the reaction was carried out in TFE or CH_2Cl_2 or toluene, traces of the expected ethylene/MA cooligomers were formed. In all spectra, except that of the product obtained in TFE, in the aromatic region the signals of acenaphthenequinone were observed, indicating that not only the catalyst decomposition took place, but also that of the ligand itself, that was transformed into its reagents (Figure 3.18).

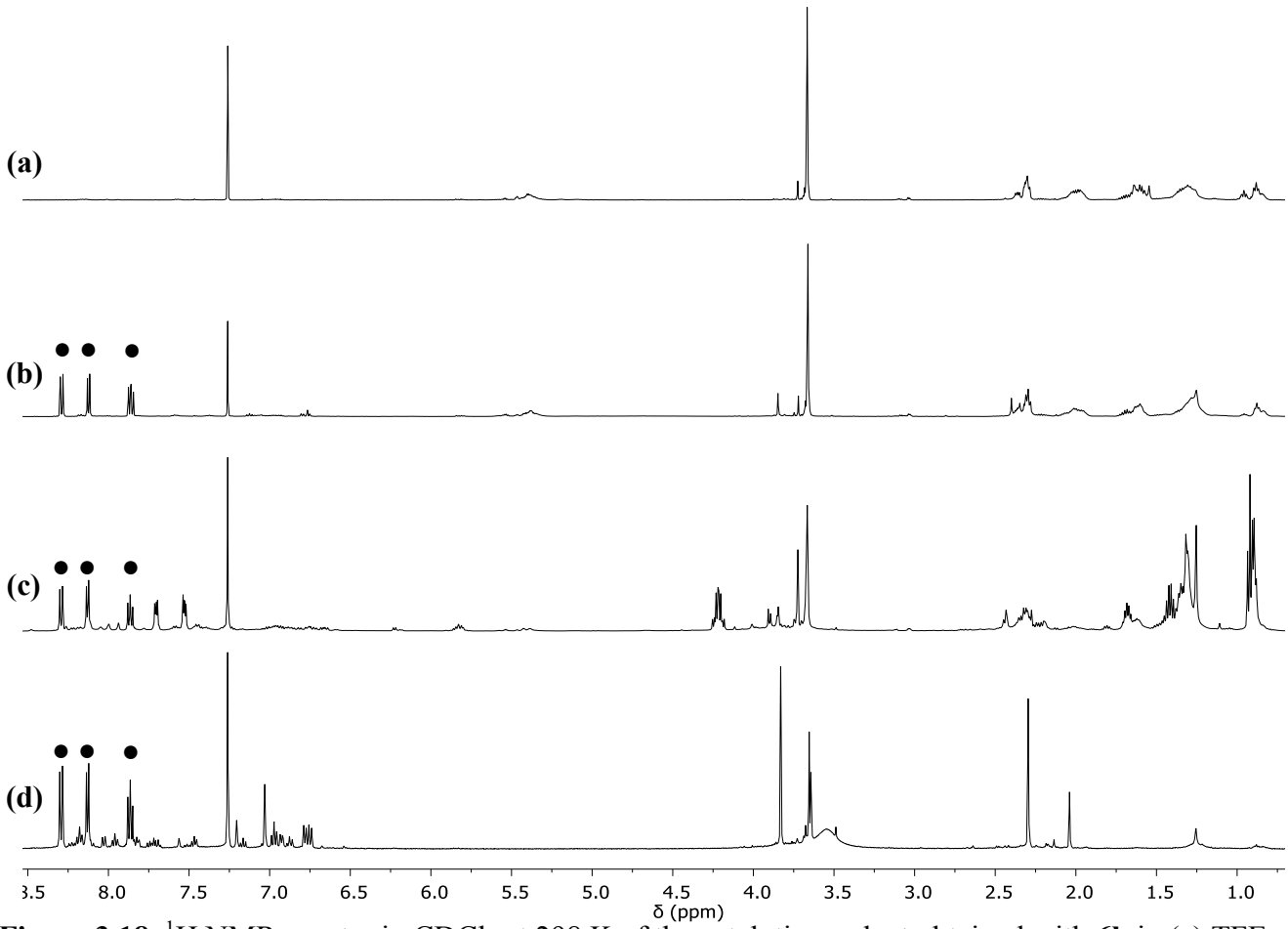

Figure 3.18. ^{1}H NMR spectra in $CDCl_3$ at 298 K of the catalytic product obtained with **6b** in (a) TFE, (b) CH_2Cl_2, (c) toluene, (d) methanol. ● acenaphthenequinone.

3.3. Conclusions

Two new nonsymmetric Ar,Ar'-BIAN ligands were synthesized (**5**, **6**) together with the corresponding symmetrical analogue **7**. These ligands were used to obtain the related palladium neutral and monocationic complexes; in particular, the series of the cationic complexes was extended to the dimethyl sulfoxide derivatives, which represent only the third example reported in literature of Pd-dmso complexes with α-diimines. The characterization in solution via NMR spectroscopy highlighted that complexes with ligands **5** and **6** are observed as both *cis* and *trans* isomers, in a ratio that depends on the ancillary ligand, while with **6** and **7** *syn* and *anti* conformers are possible, depending on the relative orientation of the substituents on the aryl rings with respect to the coordination plane.

The ^{19}F-^{1}H HOESY spectrum of complex **6b** indicated that in solution the hexafluorophosphate ion is preferentially located towards the Pd-$NCCH_3$ fragment, as reported in literature for other palladium complexes with BIAN ligands.

The characterization of the dmso derivatives showed that different species are present in solution depending on the nature of the ancillary ligand. For **5**, two species featured by S-bonded dmso and differing for the relative orientation of the Pd-CH_3 fragment with respect to the two nonequivalent halves of the ligand were observed, while with ligands **6** and **7** also traces of the complex having the dmso coordinated via the oxygen atom were present.

All the synthesized monocationic complexes were tested as precatalysts in the ethylene/methyl acrylate cooligomerization reaction under mild conditions of temperature and pressure. In contrast to our previous results obtained with catalysts having other nonsymmetric Ar,Ar'-BIANs, these complexes were found to be inactive in the studied reaction, and no effect was observed moving from the acetonitrile to the dmso derivatives.

Precatalyst **6b** was tested in different solvents, and the collected data showed that, in contrast with the expectations, moving from TFE to other solvents did not result in any catalytic activity. Moreover, the NMR characterization highlighted the presence of acenaphthenequinone, which indicates the dissociation and brake-down of the ligand into its reagents.

3.4. Experimental.

3.4.1. Materials and methods. All complex manipulations were performed using standard Schlenk techniques under argon. Anhydrous dichloromethane was obtained by distilling it over CaH_2 and under argon. $ZnCl_2$ and basic Al_2O_3 were stored in oven at 383 K overnight prior to use. [Pd(cod)(CH_3)Cl],[13b] neutral palladium complexes,[13b] acetonitrile[13b] and dimethyl sulfoxide derivatives[4] were synthesized according to literature procedures. [$Pd(OAc)_2$] was a donation from Engelhard Italia and used as received. Deuterated solvents (Cambridge Isotope Laboratories, Inc. (CIL)) were stored as recommended by CIL. Ethylene (purity ≥ 99.9 %) supplied by SIAD and methyl acrylate (99.9%, with 0.02% of hydroquinone monomethyl ether) supplied by Aldrich were used as received. TFE, and all the other reagents and solvents were purchased from Sigma-Aldrich and used without further purification for synthetic, spectroscopic and catalytic purposes.

NMR spectra of ligands, complexes and catalytic products were recorded on a Varian 500 spectrometer at the following frequencies: 500 MHz (^{1}H), 125.68 MHz (^{13}C) and 470 MHz (^{19}F). The resonances are reported in ppm (δ) and referenced to the residual solvent peak versus $Si(CH_3)_4$: $CDCl_3$ at δ 7.26 (^{1}H)

and δ 77.0 (^{13}C), CD_2Cl_2 at δ 5.32 (^{1}H) and δ 54.0 (^{13}C). NMR experiments were performed employing the automatic software parameters. In the case of NOESY experiments a mixing time of 500 ms was used. GC-MS analyses were performed with an Agilent GC 7890 instrument using a DB-225ms column (J&W, 60 m, 0.25 mm ID, 0.25 μm film) and He as carrier coupled with a 5975 MSD. Before analysis, samples were diluted with methanol and nonane was added as internal standard.

3.4.2. Synthesis of ligands 5-7

0.81 mmol of either (3,5-$(CF_3)_2$Ar)$_2$BIAN·$ZnCl_2$ for **5** or (2-CF_3Ar)$_2$BIAN·$ZnCl_2$ for **6** were dissolved in methanol at 298 K, then the 2-methoxy-6-methylaniline (3 equiv) were added dropwise to the stirred solution. After the established reaction time (24 h for **5**, 5 days for **6**, to be verified through TLC or NMR), the methanol was removed under vacuum, the resulting oil was dissolved in CH_2Cl_2 (50 mL), and a solution of $Na_2C_2O_4$ (3 equiv) in water (25 mL) was added. After 10 min of vigorous stirring, the organic phase was recovered, washed three times with distilled water, dried over anhydrous Na_2SO_4, then the solvent was removed under vacuum yielding a red oil. The mixture containing either **5** or **6** and **7** was purified by column chromatography (basic Al_2O_3, eluent : petroleum ether 40-60 : Et_2O = 4 : 1 for **5**, 3 : 1 for **6**): the nonsymmetric ligand (**5** or **6**) elutes second as a red-orange band, while the symmetric derivative **7** elutes last as a bright red band.

5: Red oil, yield 28 %. ^{1}H NMR (500 MHz, CD_2Cl_2, 298 K) (*E*,*E*) : (*E*,*Z*) = 5 : 1. (*E*,*E*) isomer δ = 7.96 – 7.92 (m, 2H, $H^{5,8}$), 7.82 – 7.80 (m, 1H, H^{18}), 7.68 – 7.63 (m, 1H, H^{16}), 7.42 – 7.37 (m, 3H, $H^{4,9,17}$), 7.19 – 7.13 (m, 2H, $H^{15,16'}$), 6.98 - 6.89 (m, 4H, $H^{3,10,15',17'}$), 3.73 (s, 3H, Ar-OCH_3), 2.12 (s, 3H, Ar-CH_3).

6: Red oil, yield 27 %. ^{1}H NMR (500 MHz, CD_2Cl_2, 298 K) (*E*,*E*) : (*E*,*Z*) = 2 : 1. (*E*,*E*) isomer δ = 8.01 – 7.94 (m, 2H, $H^{5,8}$), 7.88 – 7.78 (m, 1H, H^{16}), 7.70 (s, 2H, $H^{14,18}$), 7.49 – 7.37 (m, 2H, $H^{4,9}$), 7.19 (t, 1H, $H^{16'}$), 7.00 (d, 1H, $H^{17'}$), 6.98 – 6.92 (m, 2H, $H^{3,15'}$), 6.87 - 6.77 (m, 1H, H^{10}), 3.73 (s, 3H, Ar-OCH_3), 2.18 (s, 3H, Ar-CH_3).

7: Red oil, yield 62 %. ^{1}H NMR (500 MHz, CD_2Cl_2, 298 K) (*E*,*E*) : (*E*,*Z*) = 3 : 1. (*E*,*E*) isomer δ = 7.91 (d, 2H, H^5), 7.42 – 7.33 (m, 2H, H^4), 7.18 - 7.11 (m, 2H, H^{16}), 6.99 – 6.90 (m, 4H, $H^{15,17}$), 6.90 – 6.85 (m, 2H, H^3), 3.77 - 3.71 (2s, 6H, Ar-OCH_3), 3.71 – 3.58 (2s, 6H, Ar-CH_3).

3.4.3. Synthesis of neutral Pd-complexes [Pd(CH_3)Cl(Ar$_2$-DAB)] (5a-7a).

To a stirred solution of [Pd(cod)(CH_3)Cl] (0.51 mmol) in 2 mL of anhydrous CH_2Cl_2, a solution of 1.1 equiv of the desired ligand in 2 mL CH_2Cl_2 was added. After 1 h at room temperature, the reaction mixture was concentrated and the product precipitated upon addition of n-pentane at 277 K.

5a: red solid, yield 80 %. ^{1}H NMR (500 MHz, CD_2Cl_2, 298 K) *trans* : *cis* isomeric ratio = 3 : 1. *trans* isomer δ = 8.12 – 8.08 (m, 2H, $H^{5,8}$), 7.88 – 7.80 (m, 2H, $H^{15',17'}$), 7.56 (t, 1H, $H^{16'}$), 7.48 (t, 2H, $H^{4,9}$), 7.42 – 7.36 (m, 2H, $H^{16,18'}$), 7.07, 7.03 (m, 2H, $H^{15,17}$), 6.76 (d, 1H, H^{10}), 6.70 (d, 1H, H^3), 3.82 (s, 3H, Ar-OCH_3), 2.31 (s, 3H, Ar-CH_3), 0.63 (s, 3H, Pd-CH_3).

6a: orange solid, yield 63 %. ^{1}H NMR (500 MHz, CD_2Cl_2, 298 K) *trans* : *cis* isomeric ratio = 10 : 1. *trans* isomer δ = 8.15 (d, 2H, $H^{5,8}$), 7.97 (s, 3H, $H^{14,16,18}$), 7.61 – 7.46 (m, 3H, $H^{4,9}$), 7.39 (t, 1H, $H^{16'}$), 7.18 (d, 1H, H^3), 7.09 – 7.03 (m, 2H, $H^{15',17'}$), 6.75 (d, 1H, H^{10}), 3.81 (s, 3H, Ar-OCH_3), 2.31, (s, 3H, Ar-CH_3), 0.71 (s, 3H, Pd-CH_3).

7a: deep red solid, yield 60 %. ^{1}H NMR (500 MHz, CD_2Cl_2, 298 K) δ = 8.09 (d, 1H, H^8), 8.05 (d, 1H, H^5), 7.54 – 7.42 (m, 2H, $H^{4,9}$), 7.38 (t, 1H, $H^{16 \text{ or } 16'}$), 7.29 (td, 1H, $H^{16 \text{ or } 16'}$), 7.10 – 6.94 (m, 5H, $H^{3,15,15',17,17'}$), 6.73 (t, 1H, H^{10}), 3.86 – 3.82 (2s, 3H, Ar-OCH_3'), 3.82 – 3.78 (2s, 3H, Ar-OCH_3), 2.46 – 2.44 (2s, 3H, Ar-CH_3), 2.33 – 2.31 (2s, 3H, Ar-CH_3'), 0.58 (2s, 3H, Pd-CH_3).

3.4.4. Synthesis of monocationic Pd-complexes

[Pd(CH_3)($NCCH_3$)(Ar,Ar'-BIAN)][PF_6^-] (5b-7b). To a stirred solution of the neutral complex [Pd(CH_3)Cl(Ar,Ar'-BIAN)] (**5a-7a**) (0.20 mmol) in 3 mL CH_2Cl_2, a solution of 1.15 equivalents of $AgPF_6$ in 2 mL of anhydrous acetonitrile was added. The reaction mixture was protected from light and stirred at room temperature for 45 min, then it was filtered over Celite®, concentrated and precipitated upon addition of cold diethyl ether at 277 K.

5b: bright red solid, yield 72 %. ^{1}H NMR (500 MHz, CD_2Cl_2, 298 K) *trans* : *cis* isomeric ratio = 4 : 1. *trans* isomer δ = 8.19 (dt, 2H, $H^{5,8}$), 7.98 (d, 1H, $H^{15'}$), 7.94 – 7.89 (m, 1H, $H^{17'}$), 7.69 (t, 1H, $H^{16'}$), 7.58 – 7.54 (m, 2H, $H^{4,9}$), 7.48 – 7.43 (m, 2H, $H^{16,18'}$), 7.08 (t, 2H, $H^{15,17}$), 6.83 – 6.79 (2d, 1H, H^3), 6.76 – 6.72 (m, 1H, H^{10}), 3.82 (m, 3H, Ar-OCH_3), 2.27 (2s, 3H, Ar-CH_3), 2.03 (s, 3H, Pd-$NCCH_3$), 0.77 (s, 3H, Pd-CH_3).

6b: orange solid, yield 92 %. ^{1}H NMR (500 MHz, CD_2Cl_2, 298 K) *trans* : *cis* isomeric ratio = 7 : 1. *trans* isomer δ = 8.30 – 8.19 (m, 2H, $H^{5,8}$), 8.10 (s, 1H, H^{16}), 8.02 (s, 2H, $H^{14,18}$), 7.68 – 7.61 (m, 1H, H^4), 7.61 – 7.54 (m, 1H, H^9), 7.46 (t, 1H, $H^{16'}$), 7.31 (d, 1H, H^3), 7.14 – 7.04 (m, 2H, $H^{15',17'}$), 6.73 (d, 1H, H^{10}), 3.81 (s, 3H, Ar-OCH_3), 2.28 (s, 3H, Ar-CH_3), 2.18 (s, 3H, Pd-$NCCH_3$), 0.85 (s, 3H, Pd-CH_3).

7b: red-orange solid, yield 65 %. ^{1}H NMR (500 MHz, CD_2Cl_2, 298 K) δ = 8.17 (m, 2H, $H^{5,8}$), 7.62 – 7.58 (m, 1H, H^4), 7.53 (t, 1H, H^9), 7.44 – 7.38 (2t, 2H, $H^{16,16'}$), 7.19 – 7.15 (m, 1H, H^3), 7.09 – 7.04 (m, 4H, $H^{15,15'17,17'}$), 6.75 – 6.2 (m, 1H, H^{10}), 3.84 – 3.81 (4s, 6H, Ar-OCH_3), 2.46 - 2.28 (4s, 6H, Ar-CH_3), 2.00 (s, 3H, Pd-$NCCH_3$), 0.68 (2s, 3H, Pd-CH_3).

[Pd(CH_3)(dmso)(Ar,Ar'-BIAN)][PF_6^-] (5c-7c). To a stirred solution of the neutral complex [Pd(CH_3)Cl(Ar,Ar'-BIAN)] (**5a-7a**) (0.12 mmol) in 3 mL CH_2Cl_2, 2.0 equivalents of dmso and then a solution of 1.15 equivalents of $AgPF_6$ in 1 mL of anhydrous CH_2Cl_2 were added. The reaction mixture was protected from light and stirred at room temperature for 30 min, then it was filtered over Celite®, concentrated and precipitated upon addition of cold diethyl ether at 277 K.

5c: yellow-orange solid, yield 60 %. ^{1}H NMR (500 MHz, CD_2Cl_2, 298 K) *trans* S-dmso isomer δ = 8.22 – 8.17 (m, 2H, $H^{5,8}$), 7.90 (d, 1H, $H^{15'}$), 7.83 (d, 1H, $H^{17'}$), 7.55 (t, 1H, $H^{16'}$), 7.59 – 7.52 (m, 2H, $H^{4,9}$), 7.47 – 7.43 (m, 2H, $H^{16,18'}$), 7.11 – 7.04 (m, 2H, $H^{15,17}$), 6.74 (2d, 1H, H^3), 6.56 (2d, 1H, H^{10}), 3.83 – 3.79 (2s, 3H, Ar-OCH_3), 3.02 (m, 6H, Pd-S(O)(CH_3)$_2$), 2.30 – 2.21 (2s, 3H, Ar-CH_3), 0.52 (2s, 3H, Pd-CH_3).

6c: orange solid, yield 66 %. ^{1}H NMR (500 MHz, CD_2Cl_2, 298 K) *trans* S-dmso : *cis* S-dmso : *trans* O-dmso isomeric ratio = 12.5 : 3 : 1. *trans* S-dmso isomer δ = 8.22 (d, 2H, $H^{5,8}$), 8.04 (s, 1H, H^{16}), 7.90 (s, 1H, $H^{14 \text{ or } 18}$), 7.86 (s, 1H, $H^{14 \text{ or } 18}$), 7.58 (td, 1H, $H^{4,9}$), 7.45 (t, 1H, $H^{16'}$), 7.08 (d, 1H, $H^{17'}$), 7.05 (d, 1H, $H^{15'}$), 6.72 (d, 2H, $H^{3,10}$), 3.77 (s, 3H, Ar-OCH_3), 3.07 (s, 6H, Pd-S(O)(CH_3)$_2$), 2.24 (s, 3H, Ar-CH_3), 0.52 (s, 3H, Pd-CH_3).

7c: orange solid, yield 52 %. ^{1}H NMR (500 MHz, CD_2Cl_2, 298 K) S-dmso isomer δ = 8.21 – 8.14 (m, 2H, $H^{5,8}$), 7.60 – 7.50 (m, 2H, $H^{4,9}$), 7.50 – 7.42 (m, 1H, $H^{16 \text{ or } 16'}$), 7.42 – 7.34 (m, 1H, $H^{16 \text{ or } 16'}$), 7.15 – 6.84 (m, 4H, $H^{15,15',17,17'}$), 6.82 – 6.74 (m, 1H, H^3), 6.74 – 6.66 (m, 1H, H^{10}), 3.83 – 3.77 (m, 6H, Ar-OCH_3), 2.93 – 2.80 (m, 6H, Pd-S(O)(CH_3)$_2$), 2.28 – 2.17 (m, 6H, Ar-CH_3), 0.70 (b, 3H, Pd-CH_3).

3.4.5. Ethylene/methyl acrylate Cooligomerization Reactions. All catalytic experiments were carried out in a Büchi "tinyclave" reactor equipped with an interchangeable 50 mL glass vessel. The vessel was loaded with the desired complex (21 μmol), solvent (TFE, 21 mL; CH_2Cl_2, toluene, methanol, 22 mL) and methyl acrylate (1.13 mL). The reactor was then placed in a preheated oil bath, connected to the ethylene tank, ethylene was bubbled for 10 min then the reactor was pressurized. The reaction mixture was stirred at constant temperature and pressure. After the proper time, the reactor was cooled to room temperature and vented. An aliquot (200 μL) of the reaction mixture was withdrawn and diluted in CH_3OH (1 mL) for GC-MS analyses. The reaction mixture was poured in a 50 mL round flask, together with the dichloromethane (3 x 2 mL) used to wash the glass vessel. No separation of Pd black was observed. Volatiles were removed under reduced pressure and the residual gum or oil was dried at constant weight and analyzed by NMR spectroscopy.

3.5. Bibliography

[1] Johnson, L.K.; Killian, C.M.; Brookhart, M. *J. Am. Chem. Soc.* **1995**, *117*, 6414.

[2] Johnson, L. K.; Mecking, S.; Brookhart, M. *J. Am. Chem. Soc.* **1996**, *118*, 267.

[3] Tempel, D.J.; Johnson, L.K.; Huff, R.L.; White, P.S., Brookhart, M. *J. Am. Chem. Soc.* **2000**, *122*, 6686.

[4] Meduri, A.; Montini, T.; Ragaini, F.; Fornasiero, P.; Zangrando, E.; Milani, B. *ChemCatChem* **2013**, *5*, 1170.

[5] (a) Guironnet, D.; Roesle, P.; Runzi, T.; Gottker-Schnetmann, I.; Mecking, S. *J. Am. Chem. Soc.* **2009**, *131*, 422. (b) Runzi, T.; Guironnet, D.; Gottker-Schnetmann, I.; Mecking, S. *J. Am. Chem. Soc.* **2010**, *132*, 16623. (c) Neuwald, B.; Olscher, F.; Gçttker-Schnetmann, I.; Mecking, S. *Organometallics* **2012**, *31*, 3128.

[6] Koichi, T.; Yoshimura, K.; Nozaki, K. *Dalton Trans.* **2006**, 25.

[7] Meduri, A. PhD thesis "Development of palladium catalysts with nitrogen-donor ligands for controlled copolymerization reactions", A.A. 2010-2012.

[8] Rosar, V.; Meduri, A.; Montini, T.; Fini, F.; Carfagna, C.; Fornasiero, P.; Balducci, G.; Zangrando, E.; Milani, B. *ChemCatChem* **2014**, *6*, 2403.

[9] Gasperini, M.; Ragaini, F.; Gazzola, E.; Caselli, A.; Macchi, P. *Dalton Trans.* **2004**, 3376.

[10] Scarel, A.; Axet, M.R.; Amoroso, F.; Ragaini, F.; Elsevier, J.C.; Holuigue, A.; Carfagna, C.; Mosca, L.; Milani, B. *Organometallics* **2008**, *27*, 1486.

[11] Amoroso, F.; Zangrando, E.; Carfagna, C.; Müller, C.; Vogt, D.; Hagar, M.; Ragaini, F.; Milani, B. *Dalton Trans.* **2013**, *42*, 14583.

[12] (a) van Asselt, R.; Elsevier, C.J.; Smeets, W.J.J.; Spek, A.L.; Benedix, R. *Recl. Trav. Chim. Pays-Bas* **1994**, *113*, 88; (b) Gasperini, M.; Ragaini, F.; Cenini, S. *Organometallics* **2002**, *21*, 2950.

[13] (a) R. E. Rulke, J. M. Ernsting, A. L. Spek, C. J. Elsevier, P. W. N. M. Van Leeuwen, K. Vrieze, *Inorg. Chem.* **1993**, *32*, 5769; (b) Durand, J.; Zangrando, E.; Stener, M.; Fronzoni, G.; Carfagna, C.; Binotti, B.; Kamer, P. C. J.; Müller, C.; Caporali, M.; van Leeuwen, P. W. N. M.; Vogt, D.; Milani, B. *Chem. Eur. J.* **2006**, *12*, 7639.

[14] Binotti, B.; Bellachioma, G.; Cardaci, G.; Carfagna, C.; Zuccaccia, C.; Macchioni, A. *Chem. Eur. J.* **2007**, *13*, 1570.

[15] Fotheringham, J.D.; Heath, G.A.; Lindsay, A.J.; Stephenson, T.A. *J. Chem. Res. (S)* **1986**, 82.

[16] (a) Bastero, A.; Ruiz, A.; Claver, C.; Milani, B.; Zangrando, E. *Organometallics* **2002**, *21*, 5820; (b) Bastero, A.; Claver, C.; Ruiz, A.; Castillon, S.; Daura, E.; Bo, C.; Zangrando, E. *Chem. Eur. J.* **2004**, *10*, 3747; (c) Scarel, A; Durand, D.; Franhi, E.; Mestroni, G.; Milani, B.; Gladiali, S.; Carfagna, C.; Binotti,

B.; Bronco, S.; Gragnoli, T. *J. Organomet. Chem.* **2005**, *690*, 2106; (d) Axet, M. R.; Amoroso, F.; Bottari, G.; D'Amora, A.; Zangrando, E.; Faraone, F.; Drommi, D.; Saporita, M.; Carfagna, C.; Natanti, P.; Seraglia, R.; Milani, B. *Organometallics* **2009**, *28*, 4464.

[17] Bianchini, C.; Meli, A.; Oberhauser, W.; Segarra, A.M.; Claver, C.; Suarez, E.J.G. *J. Mol. Cat. A: Chem.* **2007**, *265*, 292.

[18] Milani, B.; Anzilutti, A.; Vicentini, L.; Sessanta o Santi, A.; Zangrando, E.; Geremia, S.; Mestroni, G. *Organometallics* **1997,** *16,* 5064.

CHAPTER 4

Pd-catalyzed ethylene/methyl acrylate copolymerization: effect of a new nonsymmetric α-diimine with a DAB skeleton

Overview

A new nonsymmetric Ar,Ar'-DAB ligand having one aryl ring substituted in *meta* positions with electron withdrawing CF_3 groups and the other aryl ring substituted in *ortho* positions with electron donating methyl groups was studied. A new protocol for the synthesis of the relevant Pd(II) complexes was developed using [Pd(cod)(CH_3)Cl] as templating agent and purifying the resulting mixture through column chromatography.

Neutral complexes with the new nonsymmetric ligand and its symmetrical analogues were synthesized, and used to obtain the desired monocationic derivatives [Pd(CH_3)(L)(Ar,Ar'-DAB)][X]. Both acetonitrile and dimethyl sulfoxide complexes were prepared (L = CH_3CN, dmso), and the series of cationic derivatives was extended to the use of hexafluoroantimonate as counterion (X^- = PF_6^-, SbF_6^-).

The monocationic complexes were tested as precatalysts in the ethylene/methyl acrylate cooligomerization under mild reaction conditions of temperature and pressure. The catalytic product was characterized as a mixture of ethylene/acrylate cooligomers and higher alkenes.

Part of this chapter will be published in a feature work:

Rosar, V.; Balducci, G.; Montini, T.; Fornasiero, P.; Milani B.

4.1. Introduction.

As previously discussed (Chapter 3), in 2013 in our group the palladium complex [Pd(CH_3)(CH_3CN)(Ar,Ar'-BIAN)][PF_6] with a new nonsymmetric Ar,Ar'-BIAN ligand (**L12**, Figure 1.9) was tested as catalyst for the ethylene/MA cooligomerization reaction. The collected data showed that the productivity of the nonsymmetric catalyst was higher than that of both corresponding symmetric derivatives, and it also led to a higher amount of incorporated acrylate in the catalytic product (Table 3.1).[1] These evidences suggested that a subtle steric and electronic unbalance on the N-donor atoms of the ancillary ligand had a positive effect on both productivity and polar monomer insertion.

The effect of the labile ligand was also investigated by comparing the catalytic activity of the acetonitrile derivatives and of the new dimethyl sulfoxide complexes [Pd(CH_3)(dmso)(Ar,Ar'-BIAN)][PF_6] in the target reaction (Table 3.1). The results showed that the Pd-dmso derivative was more productive than the corresponding Pd-$NCCH_3$ one, and it also displayed a longer catalyst lifetime, probably because the dmso competes with the last inserted acrylate unit, thus favoring the propagation of the chain (Scheme 1.4).[1]

Brookhart and coworkers reported that the α-diimines skeleton affected the productivity of the palladium catalysts, and, in particular, moving from the BIAN to the DAB skeleton an increase of one order of magnitude in productivity was achieved, without a significant loss in terms of polar monomer incorporation (0.11 kg CP/g Pd, 4.7 % MA for **L3** *vs* 1.05 kg CP/g Pd, 4.0 % MA for **L1**, Figure 1.6).[2] We later confirmed this trend by comparing the catalytic behavior of palladium complexes with naphthyl-substituted α-diimine ligands, as described in Chapter 2 (71.0 g P/g Pd with 37 % of MA for **1** *vs* 423.8 g P/g Pd with 20 % of MA for **3**; Table 2.3).[3]

On the basis of these considerations, with the aim to obtain better performing catalysts and to validate the ligand skeleton effect, we have studied a new nonsymmetric DAB α-diimine analogous to the nonsymmetric BIAN **L12** (Figure 1.9) we introduced.[1] Therefore, the new nonsymmetric Ar,Ar'-DAB is featured by one aryl ring substituted in *meta* positions with CF_3 groups and the other aryl ring substituted in *ortho* positions with CH_3 groups. For comparison purposes, we also studied the related symmetrical analogues (Figure 4.1).

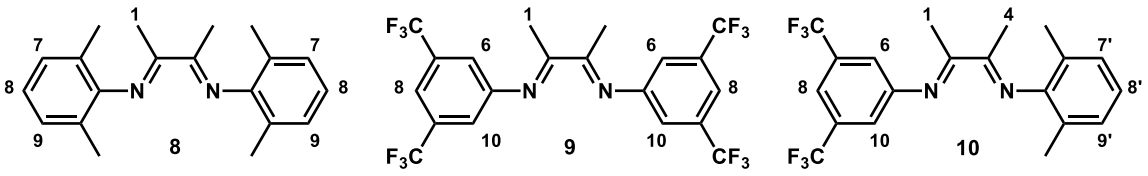

Figure 4.1. The studied α-diimines **1-3** and their numbering scheme.

Ligands **8**, **9** are known from literature,[4] while ligand **10** is reported here for the first time. To the best of our knowledge, only three examples of nonsymmetric Ar,Ar'-DAB molecules were reported up to now, and all of them shared the feature of having one 2,6-diisopropyl substituted aryl ring (Figure 4.2).[5]

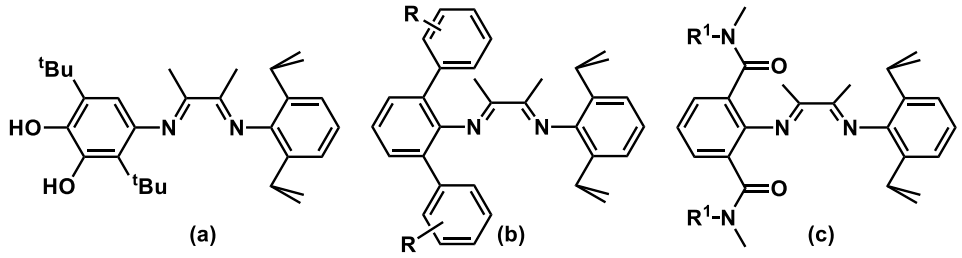

Figure 4.2. The reported nonsymmetric DAB molecules.[5]

All the reported synthetic procedures were based on the isolation of the monoketoimine deriving from the condensation of 2,3-butanedione and 2,6-diisopropylaniline and its further reaction with the proper substituted aniline. While compound (a) was not applied as ancillary ligand in metal complexes,[5a] ligands of group (b) (Figure 4.2) were used for the synthesis of nickel complexes of general formula [$NiBr_2$(Ar,Ar'-DAB)] that were applied as precatalysts in the ethylene homopolymerization. They were found to generate very active catalysts (1200 kg PE/mol Ni · h), leading to a product with high molecular weight (> 4000 g/mol), melting point between 378 and 393 K, and a low degree of branches (22 - 38 CH_3 branchings/1000 C atoms).[5b] Ligands of type (c) (Figure 4.2) were used for the synthesis of palladium complexes, both neutral [$Pd(CH_3)(X)$(Ar,Ar'-DAB)] (X^- = Cl^-, CH_3COO^-) and monocationic [$Pd(CH_3)(L)$(Ar,Ar'-DAB)][SbF_6] (L = CH_3CN, pyrazole). Due to the peculiar substitution of the aryl ring with the amide group, hydrogen bonding interactions involving the oxygen atom of the latter were found to be particularly important in determining the structure, isomer distribution, and ligand coordinating behavior of these compounds.[5c]

Considering the few known examples of nonsymmetric DAB molecules, it was necessary to develop a synthetic strategy to obtain the desired ligand **10**, and the protocol was based on the procedure reported up to now.[5]

Ligand **10** and its symmetrical analogues **8**, **9** were used to obtain the corresponding palladium(II) neutral [$Pd(CH_3)Cl$(Ar,Ar'-DAB)] and monocationic complexes [$Pd(CH_3)(L)$(Ar,Ar'-DAB)][X] (L = CH_3CN, dmso; X^- = PF_6^-, SbF_6^-), and the catalytic behavior of the latter in the ethylene/methyl acrylate copolymerization reaction was studied in detail.

4.2. Results and Discussion.

4.2.1. Synthesis and characterization of Pd-complexes with ligands 8 and 9.

Ligands **8**, **9** were synthesized according to literature procedures,[4] by reacting 2,3-butanedione with the proper substituted aniline in methanol, in the presence of catalytic amounts of formic acid (Scheme 4.1). Due to the different reactivity of the anilines, depending on the nature and number of substituents, the reaction time varied from 5 hours (ligand **8**) to 5 days (ligand **9**), and the products were isolated as white-yellow solids. The NMR spectra of **8** and **9** were in agreement with the reported characterization.[4]

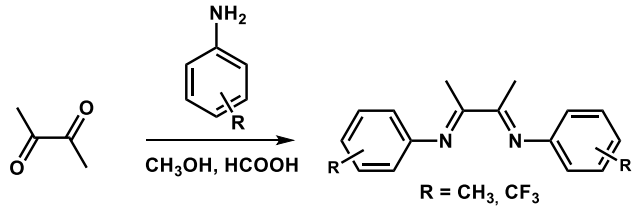

Scheme 4.1. Synthesis of ligands **8**, **9**.

Ligands **8**, **9** were reacted with [Pd(cod)(CH_3)Cl] to yield the corresponding neutral derivatives [Pd(CH_3)Cl(ArDAB)] (ArDAB = **8**, **8a**; **9**, **9a**) following the well-established procedure (Scheme 4.2).[6]

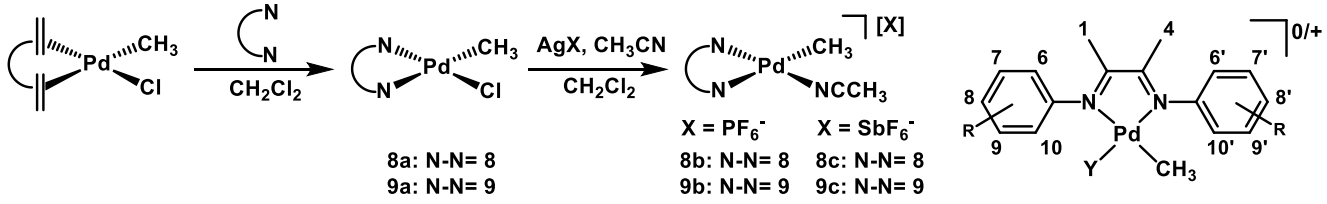

Scheme 4.2. Synthesis of neutral and monocationic complexes **8a-c**, **9a-c**, with the corresponding numbering scheme.

All the synthesized complexes were fully characterized by homo- and heteronuclear, mono- and bidimensional, NMR experiments in CD_2Cl_2 solution.

The NMR characterization of **8a** was in agreement with the literature,[7] while complex **9a** is reported here for the first time. (Figure 4.3). In both cases, upon coordination to palladium the two halves of the ligand are no longer magnetically equivalent; as well known from the literature,[3,8,9] the protons of the half of the ligand in *cis* to the Pd-Cl bond resonate at higher frequencies than the same protons on the other half of the ligand. The difference in chemical shift is more pronounced for the signals of the methyl groups of the ligand skeleton than for the protons of the aryl rings, for both **8a** and **9a**.

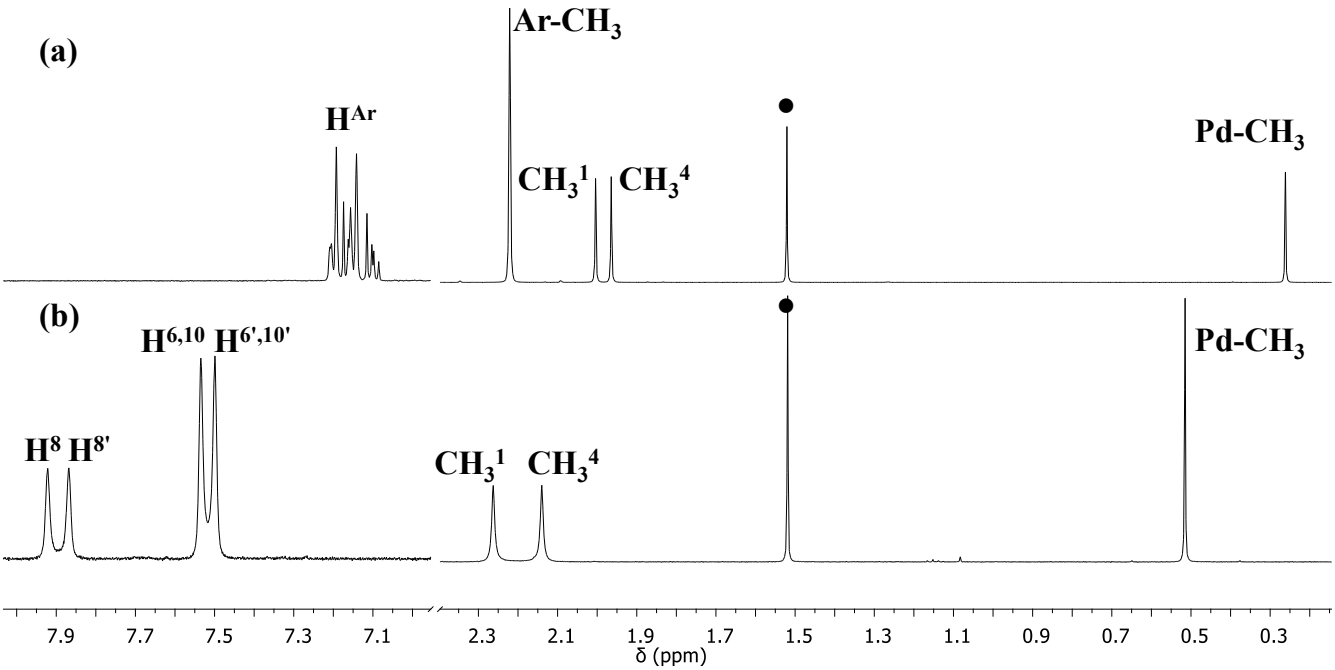

Figure 4.3. ^{1}H NMR spectra in CD_2Cl_2 at 298 K of: (a) **8a**, (b) **9a**. ●: water signal. The aliphatic and aromatic regions are not on scale.

When moving from the complex with the ligand having the electron repulsing groups (**8a**) to that with electron withdrawing groups (**9a**), the signal of the Pd-CH_3 fragment shifted to higher frequencies (0.26 ppm **8a** *vs* 0.51 ppm **9a**, Figure 4.3), suggesting a lower electron density on the palladium center for **9a**. This is in agreement with the expected lower basicity of ligand **9** with respect to that of ligand **8**, that might be reflected in a lower coordination capability of the former with respect to the latter. The same trend is also observed for the methyl groups of the DAB skeleton (2.00-1.96 ppm **8a** *vs* 2.26-2.14 ppm **9a**, Figure 4.3), thus indicating that the electronic properties of the substituents on the aryl rings are reflected the ligand skeleton, too.

The monocationic complexes with hexafluorophosphate anion were obtained from the neutral complexes following the well-established procedure (Scheme 4.2)[6] and the same protocol was followed for the hexafluoroantimonate derivatives.

Comparing the NMR spectra of **8b-c** and **9b-c**, the same signals are observed, confirming that the nature of the counterion does not affect them; therefore, only the characterization of the PF_6^- derivatives is discussed (Figure 4.4).

The ^{1}H NMR spectra of **8b** and **9b** show sharp signals at room temperature, as usually observed for Pd-acetonitrile derivatives with α-diimine ligands.[1,3,9]

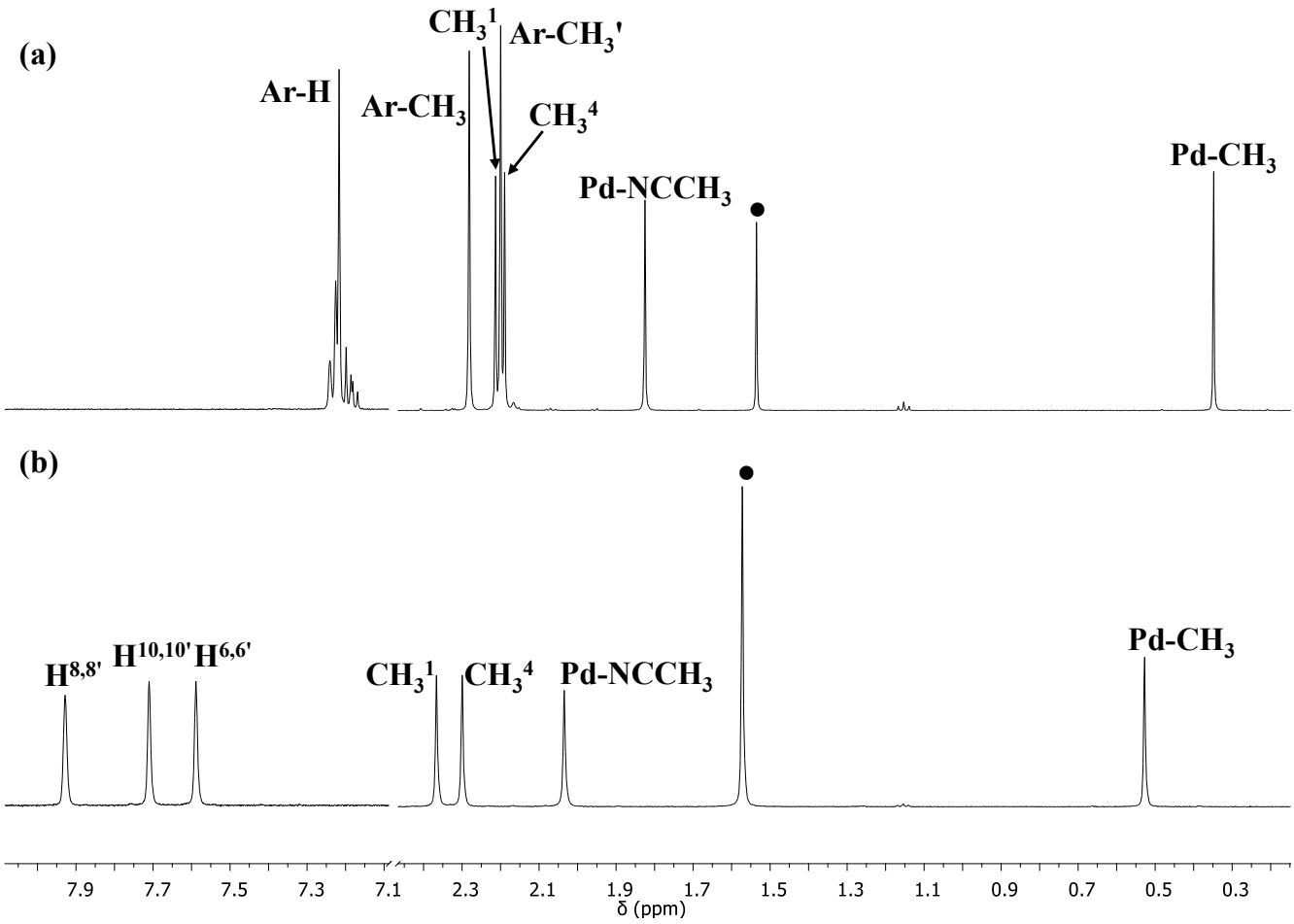

Figure 4.4. ^{1}H NMR spectra in CD_2Cl_2 at 298 K of: (a) **8b**, (b) **9b**. ●: water signal. Aliphatic and aromatic regions are not on scale.

The distinction of the two halves of the coordinated ligand is based on the previously reported trends[1,3,9] and on the comparison with the corresponding neutral derivatives (Figure 4.4).

As already observed for the neutral complexes, moving from the complex with ligand **8** to that with ligand **9**, the Pd-CH_3 singlet shifts to higher frequency, thus confirming that it is a sensitive probe for the electron density on palladium.

4.2.2. Synthesis and characterization of Pd-complexes with ligand 10.

As afore mentioned, the only examples of nonsymmetric DAB molecules were obtained by first isolating the monoketoimine deriving from the 2,6-diisopropylaniline and its further reaction with the proper aniline.[5] Therefore, in order to obtain the desired nonsymmetric ligand **10**, a similar approach was applied (Scheme 4.3).

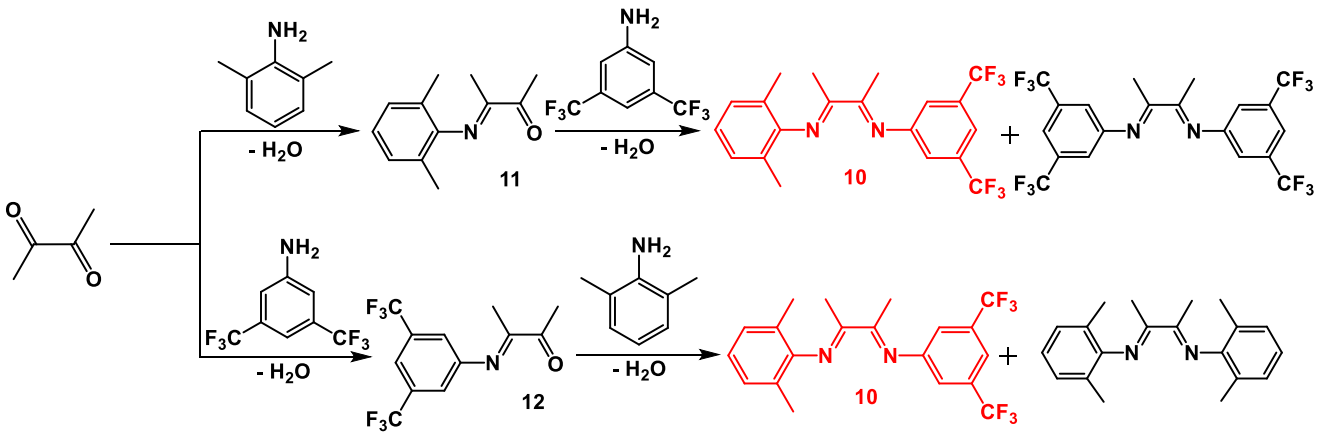

Scheme 4.3. Synthetic approaches to obtain the nonsymmetric ligand **10**.

The first attempt was based on the synthesis of the monoketoimine **11** deriving from the 2,6-dimethylaniline and its further reaction with the 3,5-bis(trifluoromethyl)aniline, which is deactivated towards the nucleophilic substitution and therefore should disfavour the transimination reaction that would lead to the symmetric ligand **9**. In the ^{1}H NMR spectrum of the crude yellow oil, the signals of **8** and starting aniline are observed, together with a new set of signals that is attributed to the desired compound **11** (Figure 4.6a). The yield in **11**, calculated from the integrations of the ^{1}H NMR signals, was 37 %. By varying the reaction conditions, such as solvent, temperature and reaction time, it was possible to increase the yield up to 45 %, but, since **11** was always obtained in a mixture with the corresponding symmetric disubstituted derivative **8** (best composition **11** : **8** : aniline = 1: 2.97: 0.44), and it was not possible to purify it, it was not suitable for the synthesis of the desired ligand **10**.

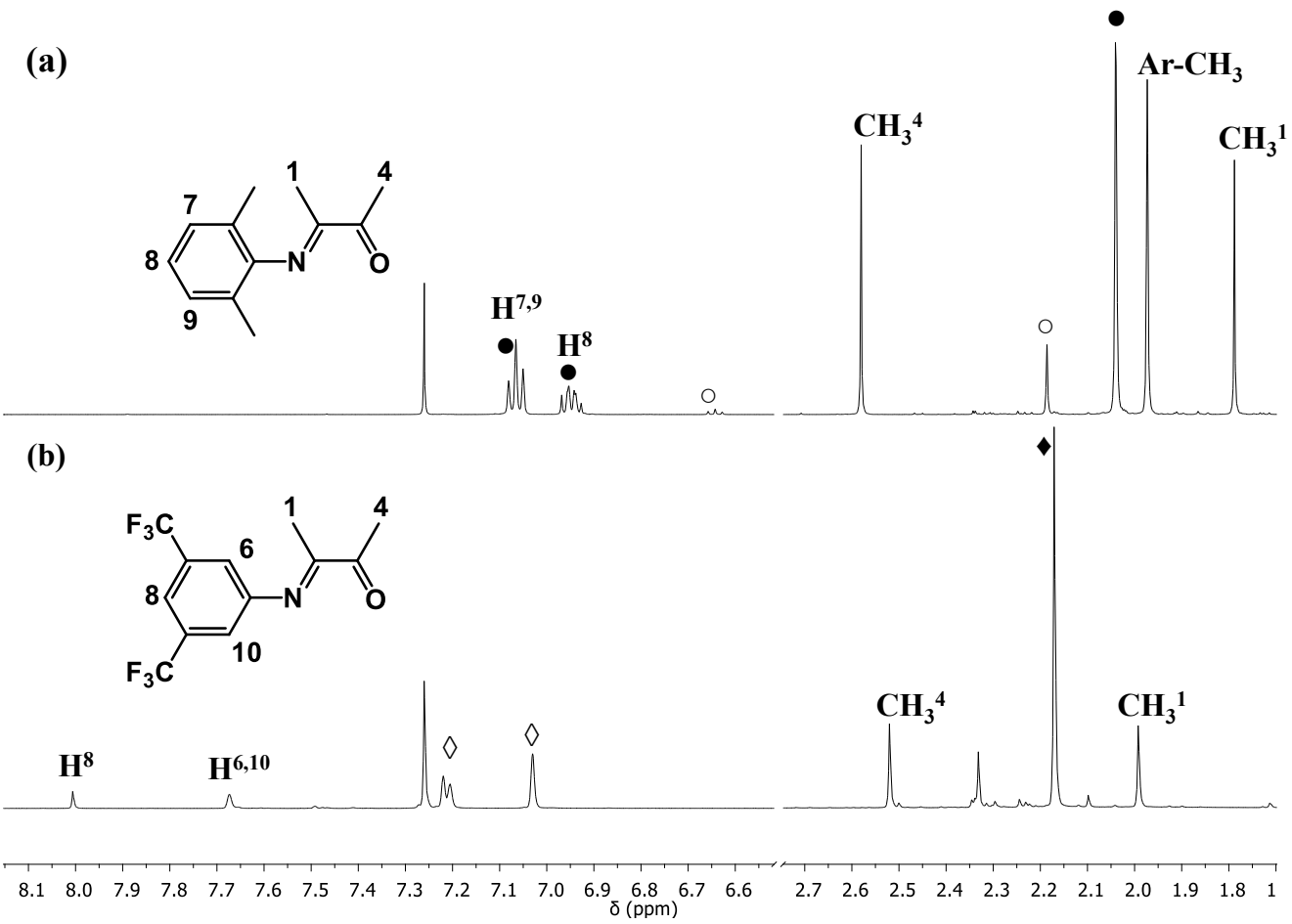

Figure 4.5. ^{1}H NMR spectra in $CDCl_3$ at 298 K of the crude reaction products of (a) **11**, (b) **12**.
● ligand **8**; ○ 2,6-dimethylaniline; ◊ 3,5-bis(trifluoromethyl)aniline; ♦ 2,3-butanedione.

For this reason, a different approach was tried by synthesizing first the monoketoimine **12** deriving from the 3,5-bis(trifluoromethyl)aniline and then reacting it with the 2,6-dimethylaniline. The ^{1}H NMR spectrum of the crude reaction mixture shows the presence of both reagents together with a new set of signals attributed to the desired monoketoimine **12**, and no traces of the symmetric ligand **9** is observed (Figure 4.5b). Several attempts to purify the monoketoimine via crystallization and column chromatography resulted either in the conversion to the symmetric ligand **9** or in the decomposition to the reactants.

Since the aim was to obtain the palladium derivatives with ligand **10**, we decided to perform a template reaction consisting in the condensation of **12** with the 2,6-dimethylaniline in the presence of [Pd(cod)(CH_3)Cl] as templating agent. To do so, the synthesis of **12** was interrupted after 1 h to have the highest conversion into the desired monoketoimine (30 %) and no trace of the symmetric derivative **9**.

To the crude reaction mixture, a suspension of the 2,6-dimethylaniline and the palladium precursor in methanol was added dropwise, and the reaction mixture was allowed to stir at 303 K for 2 h. The NMR characterization of the isolated solid indicated that this is a mixture of products comprising mainly the symmetric neutral derivative **8a** and the desired complex **10a** in a 1 : 0.7 ratio (Figure 4.6).

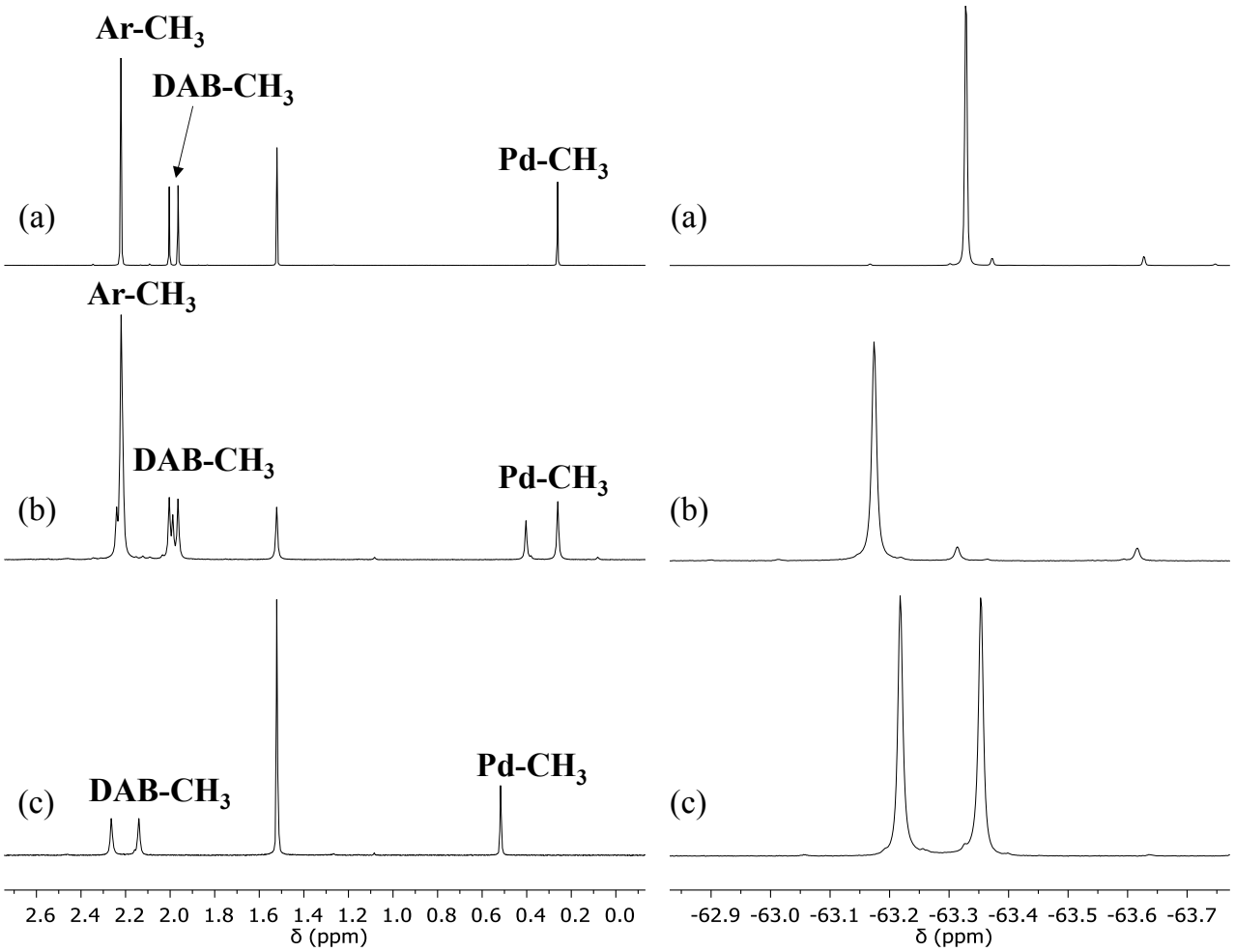

Figure 4.6. (*left*) ^{1}H NMR spectra (aliphatic region) in $CDCl_3$ at 298 K of: (a) **8a**, (b) crude reaction mixture, (c) **9a**. (*right*) ^{19}F NMR spectra of: (a) ligand **8**, (b) crude reaction mixture, (c) **9a**.

Indeed, in the aliphatic region of the spectrum two singlets are observed for the Pd-CH_3 fragment, one corresponding to that of **8a** and the other that does not corresponds to that of **9a**, therefore it indicates the formation of **10a**. From the integration of these peaks, the ratio between the two complexes was determined. This is also in agreement with its chemical shift value (0.40 ppm) that is intermediate with respect to those of **8a** (0.26 ppm) and **9a** (0.52 ppm) (Figure 4.6 left), and this trend is in agreement with that reported for the related BIAN analogues.[1] In the ^{19}F NMR spectrum of the crude reaction mixture, a

single major peak at -63.15 ppm is observed, and since its chemical shift cannot be related either to that of ligand **9** (-66.2 ppm) or to those of complex **9a** (-63.22, -63.35 ppm), is reasonably assigned to the CF_3 groups of complex **10a** (Figure 4.6 right).

After several attempts of purification and with a fine tuning of the reaction conditions, it was possible to obtain **10a** pure from column chromatography (Figure 4.7).

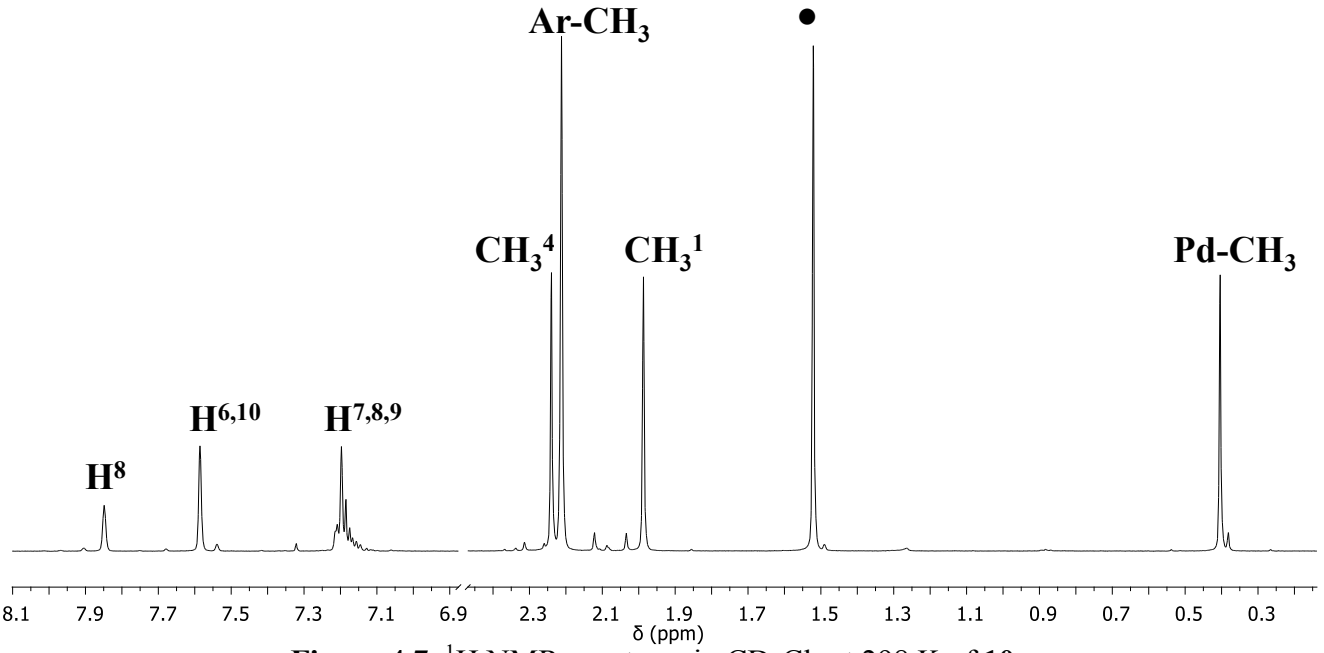

Figure 4.7. ^{1}H NMR spectrum in CD_2Cl_2 at 298 K of **10a**.

As already discussed for complexes **5a**-**6a**, even for the neutral derivative with ligand **10**, *trans* and *cis* isomers are possible. In the ^{1}H NMR spectrum of the pure solid the signals of almost only one species is observed that, thanks to the cross peak between the singlet of Pd-CH_3 fragment and that of the methyl groups on the aryl ring present in the NOESY spectrum, has been identified as the *trans* isomer (Figures 4.8 - 4.9). Only traces of the *cis* isomer are observed. However, the presence of an exchange cross peak between the singlet of $CH_3{}^4$ in the major species and the very weak peak at 2.12 ppm indicates that the two isomers are in equilibrium at slow rate with respect to the NMR time scale, at room temperature. The same strong preference for the *trans* species was also reported in the case of the palladium neutral complex with the nonsymmetric BIAN ligand **L12**,[1] suggesting that the peculiar steric and electronic properties of the N-donor atoms, deriving from the aryl substituents, determine the preference for one isomer over the other, and is not affected by the ligand skeleton.

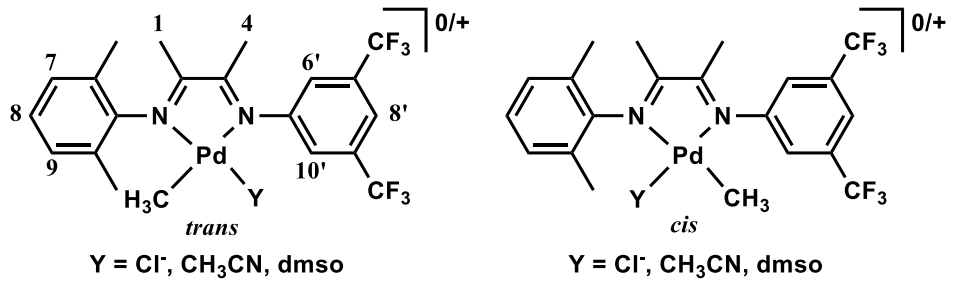

Figure 4.8. Possible isomers of complexes with the nonsymmetric ligand **10** and the corresponding numbering scheme.

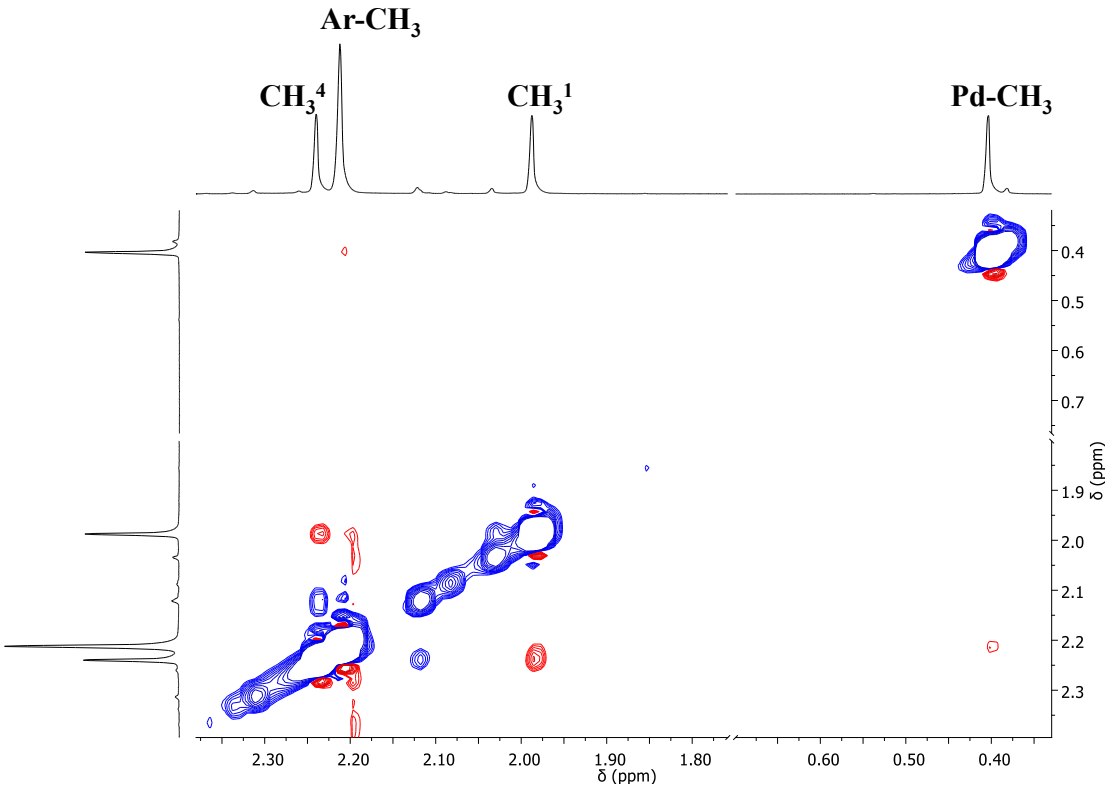

Figure 4.9. NOESY spectrum of **10a** in CD_2Cl_2 at 298 K. Red cross peaks are due to NOE; blue cross peaks are due to exchange.

Single crystals of **10a** suitable for X-ray diffraction were obtained by slow diffusion of n-hexane into a dichloromethane solution of the complex at 277 K. The solid state characterization shows the presence, in the unit cell, of the *trans* isomer only (Figure 4.10), that corresponds to almost the only species observed in solution. The palladium center had the expected square planar geometry with a relatively small bite angle (N(1)-Pd-N(2) of 77.18(8)°). The Pd-N bond distance *trans* to the Pd-CH_3 fragment was

longer than the other one (Pd-N(2) of 2.138(2) *vs* Pd-N(1) of 2.042(2) Å), in agreement with the stronger *trans* influence of the methyl group with respect to the chlorido, It is noteworthy that the Pd-N distances in **10a** were shorter than those observed in the BIAN analogue **L12** (Pd-N(1) 2.201(4) Å; Pd-N(2) 2.063(4) Å),[1] thus suggesting a stronger coordination of the DAB ligand with respect to the BIAN one.

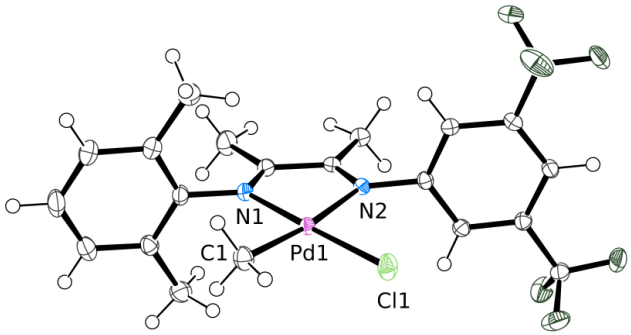

Figure 4.10. ORTEP representation of complex **10a**. Selected bond lengths (Å) and angles (°): Pd-C(1) 2.014(2), Pd-Cl(1) 2.2989(6), Pd-N(1) 2.042(2), Pd-N(2) 2.138(2); C(1)-Pd-Cl(1) 89.94(8), C(1)-Pd-N(1) 95.06(9), C(1)-Pd-N(2) 171.97(9), N(1)-Pd-Cl(1) 174.54(6), N(1)-Pd-N(2) 77.18(8), N(2)-Pd-Cl(1) 97.89(5); dihedral angles: $Ph(CH_3)_2$/square plane 89.8(0.1), $Ph(CF_3)_2$/square plane 82.8(0.1).

We reported that in the Pd(II) complexes with naphthyl substituted α-diimines and either BIAN or DAB skeleton, **1a-4a**, the Pd-N bond distances are longer for **1a** (Pd-N(1) 2.109(6)/2.139(6) Å, Pd-N(2) 2.062(6)/2.047(6) Å for the *anti* and *syn* isomers, respectively) than for the DAB analogue **3a** (Pd-N(1) 2.125(8) Å, Pd-N(2) 2.043(9) Å).

The same trend was found for palladium dichlorido complexes with α-diimine ligands having the aryl rings substituted in *ortho* positions with isopropyl groups and either the BIAN **L3** or the DAB, **L1**, skeleton: also in this case, the Pd-N bond distance is longer for the former complex (2.041(8) Å)[10] than for the latter (2.009(2) – 2.017(2) Å).[11] Therefore, despite the limited number of comparable complexes known it appears that, regardless to the nature of the substituents on the N-donor atoms, DAB ligands bind more strongly to palladium than the corresponding BIAN analogues.

In complex **10a** the aryl rings are nearly orthogonal to the square plane, with the CF_3-substituted one being slightly bent towards the Pd-Cl fragment, with a dihedral angle of 82.8(1)°, while the CH_3-substituted one shows a dihedral angle of 89.8(1)°. If these values are compared to those reported for the BIAN analogue, it is noteworthy that for **10a** the dihedral angles are significantly larger than those reported for the complex with **L12** ($Ph(CF_3)_2$: 82.8(1) *vs* 64.5(1); $Ph(CH_3)_2$: 89.8(1) *vs* 80.1(1) respectively)[1]. The same trend was found by comparing the corresponding palladium complexes with the naphthyl-substituted BIAN and DAB analogoues **1a** and **3a**; in **1a** the naphthyl group *cis* to the Pd-CH_3

fragment is more bent towards the coordination plane (69.3(1)° *vs* 86.9(1)°), while in **3a** both dihedral angles are closer to 90° (83.4(4)° *vs* 80.9(4)°).[3] This trend is reasonably due to the enhanced out-of-plane steric hindrance of the DAB skeleton with respect to the BIAN one.

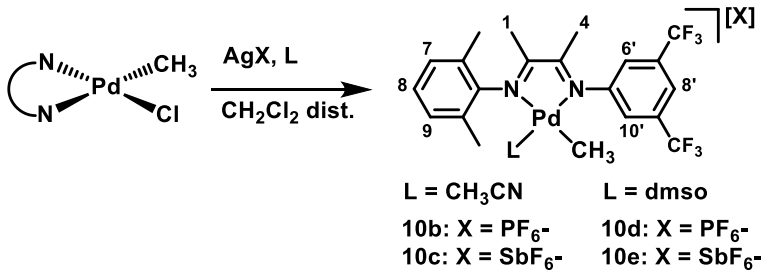

Scheme 4.4. Monocationic complexes **10b-e** and related numbering scheme of the *trans* isomer.

From complex **10a**, the monocationic complexes **10b** and **10c** were synthesized according to the reported procedure,[6] and the series was extended to the dimethyl sulfoxide derivatives **10d** and **10e**, obtained by following the procedure developed in our group for the analogues with the nonsymmetric BIAN **L12** (Scheme 4.4).[1] Both series of complexes were characterized through NMR spectroscopy in CD_2Cl_2 and, for complexes **10d-e**, also in dmso-d_6.

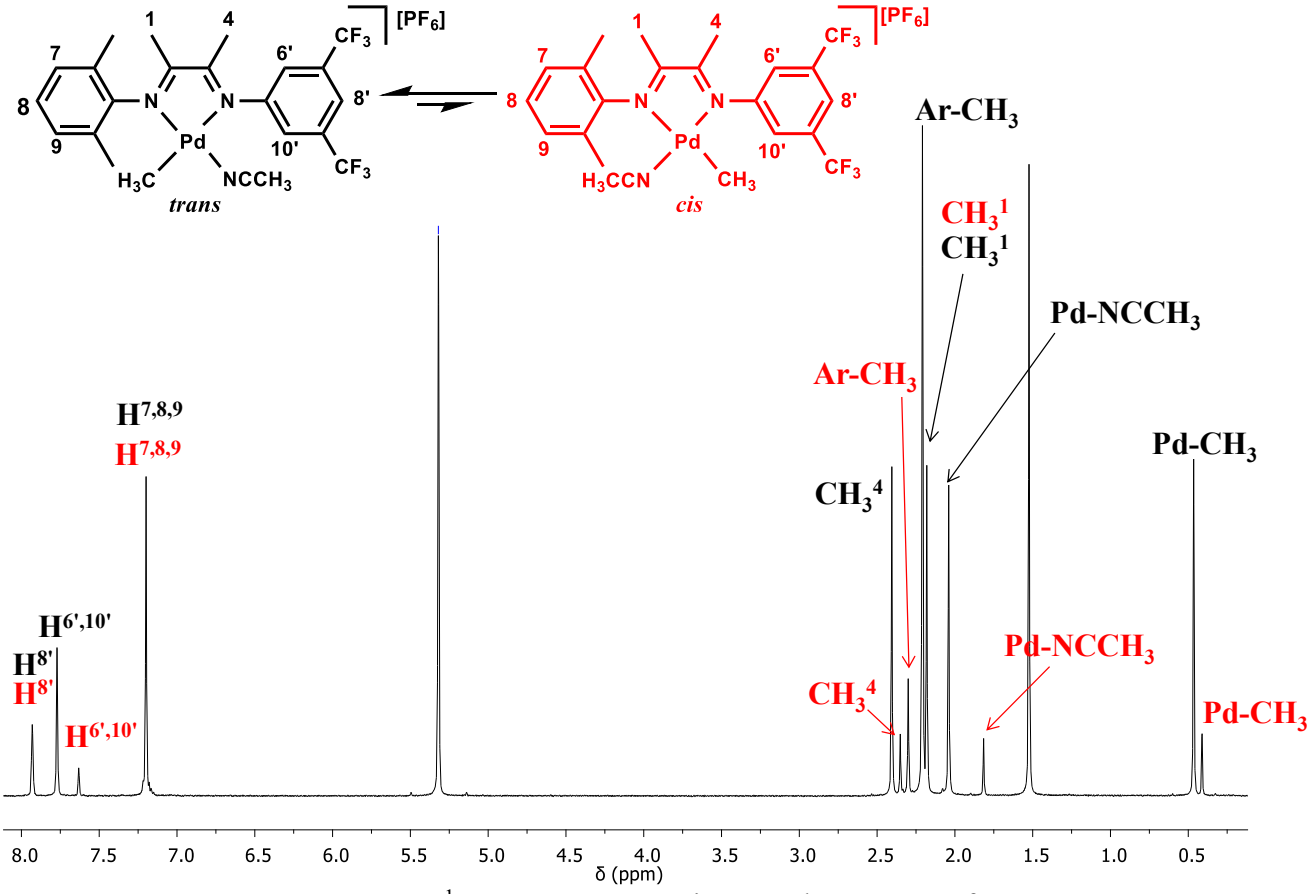

Figure 4.11. ^{1}H NMR spectrum in CD_2Cl_2 at 298 K of **10b**.

As observed for complexes **8b-c** and **9b-c**, even for **10b-c** the NMR spectra are identical, therefore the characterization is discussed only for complex **10b**. As generally observed for the Pd-acetonitrile derivatives,[1,3,8] in the ^{1}H NMR spectrum sharp signals are present at room temperature (Figure 4.11). The number of signals and their integration indicate the presence of the two *cis* and *trans* isomers in a 6 to 1 ratio. In the NOESY spectrum, the NOE peak between the signal of Pd-CH_3 fragment and that of the methyl groups of the aryl rings indicates that the major species in solution is always the *trans* isomer, and the presence of exchange peaks for both the Pd-CH_3 and Pd-$NCCH_3$ resonances in the two species indicated that they are in equilibrium at slow rate on the NMR time scale at room temperature (Figure 4.12).

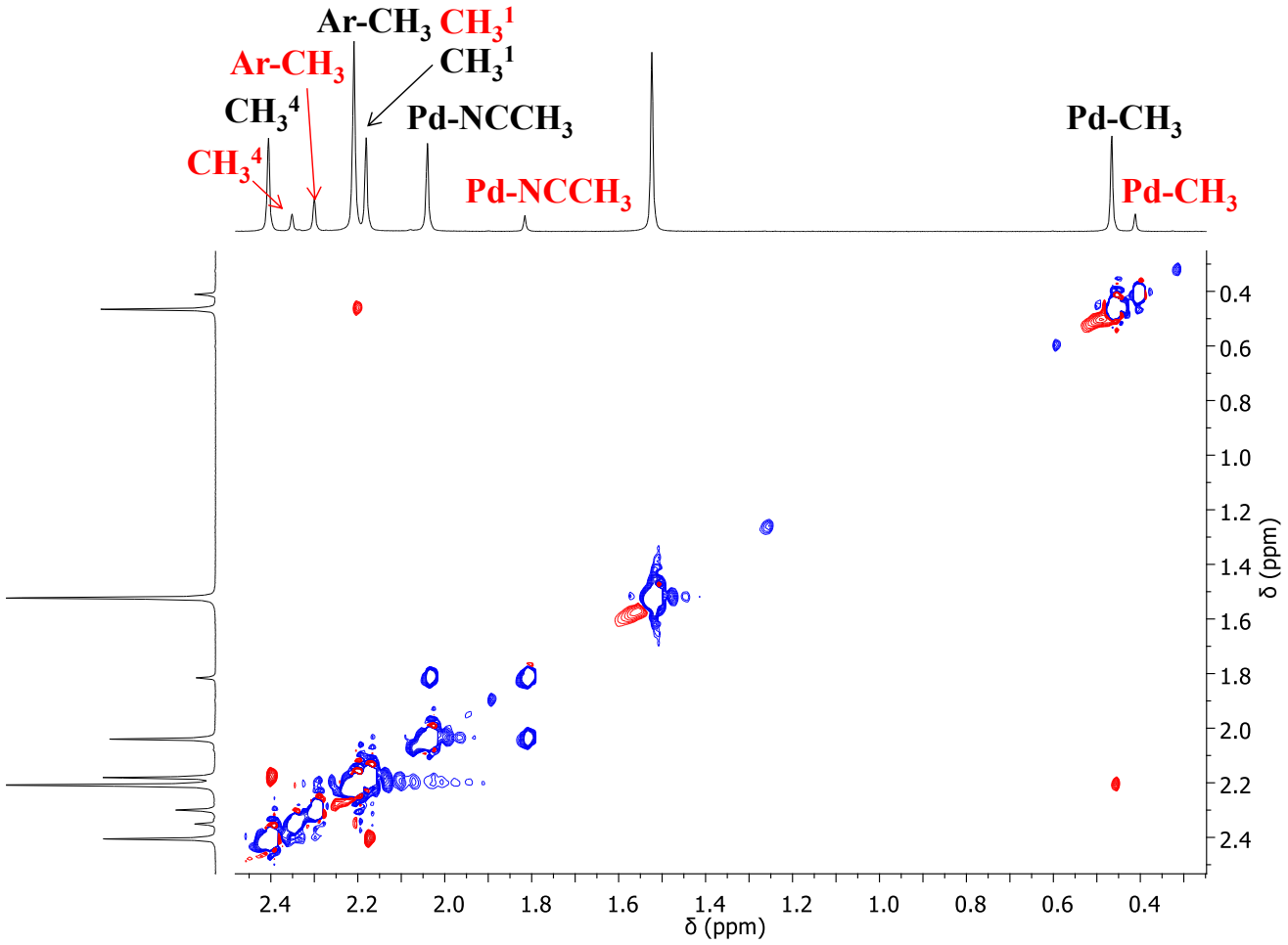

Figure 4.12. NOESY of **10b** in CD_2Cl_2 at 298 K. Red cross peaks are due to NOE; blue cross peaks are due to exchange.

For the corresponding Pd-acetonitrile complex with the nonsymmetric BIAN ligand **L12**,[1] the *trans* to *cis* ratio is 10 : 1, suggesting that it might be affected by the ligand skeleton.

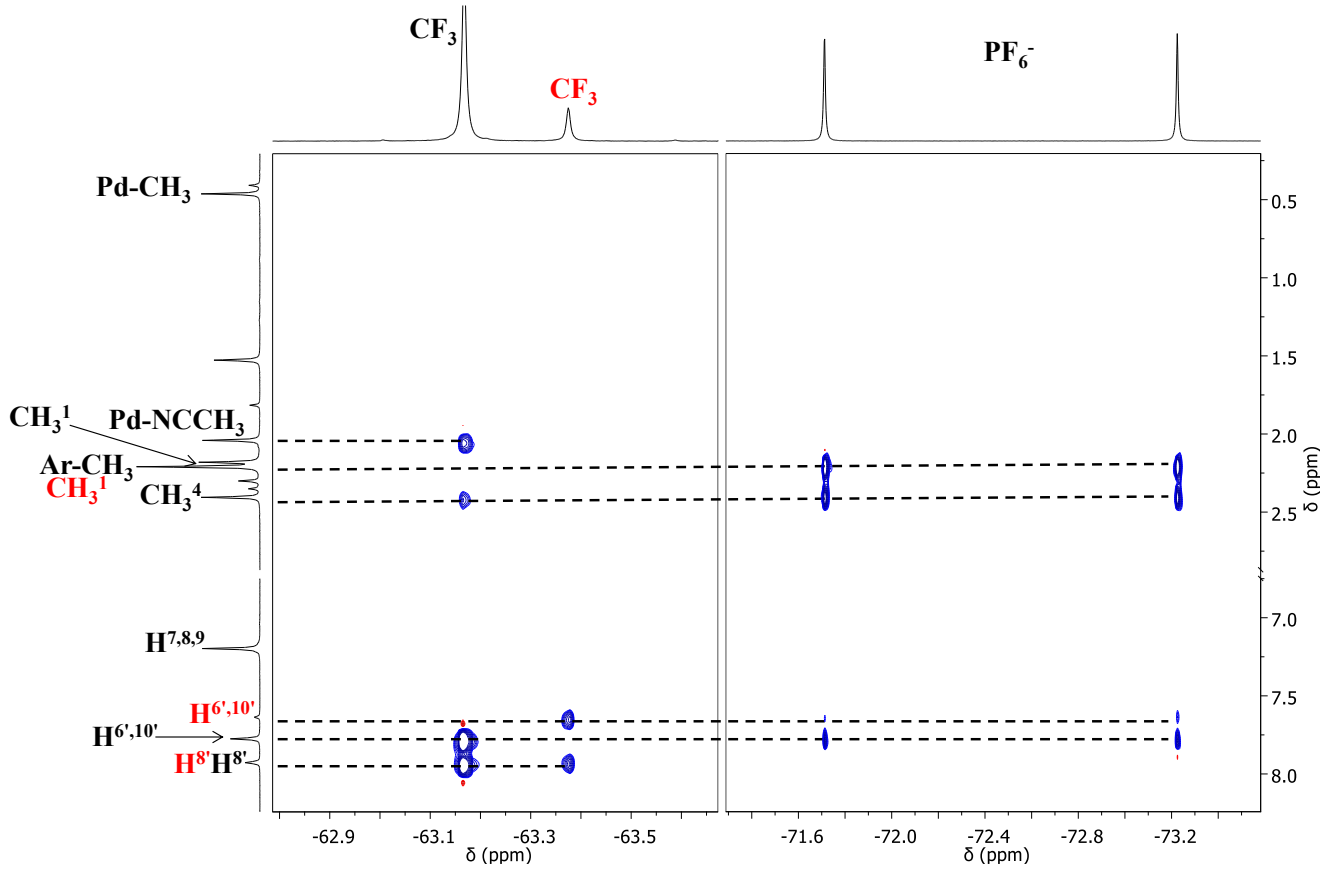

Figure 4.13. ^{19}F-^{1}H HOESY spectrum of **10b** in CD_2Cl_2 at 298 K.

The interionic structure in solution of complex **10b** was investigated by ^{19}F-^{1}H HOESY spectrum: the cross peaks of the CF_3 group of the major species with both the Pd-$NCCH_3$ fragment and one of the methyl groups of the DAB skeleton confirmed that this is the *trans* isomer, while the cross peaks of the PF_6^- anion with the methyl groups of the skeleton, those on the aryl ring and with the protons of the CF_3-substituted phenyl located the counterion on top of the complex, shifted towards the ligand skeleton (Figure 4.13). This is in agreement with the study reported for analogous palladium complexes with DAB ligands [Pd(η_1,η_2-$C_8H_{12}OMe$)(Ar_2DAB)][PF_6] (η_1,η_2-$C_8H_{12}OMe$ = methoxy-cyclooctenyl), that located the counterion always close to the N-donor atom and the ligand backbone.[12]

As far as the Pd-dmso complexes, **10d-e**, is concerned, for **10d** single crystals suitable for X-ray diffraction were obtained by slow diffusion of n-hexane in a dichloromethane solution of the complex at 277 K (Figure 4.14, Table 4.1). This is the first example of a solid state structure of a palladium(II) complex with dimethyl sulfoxide and an α-diimine.

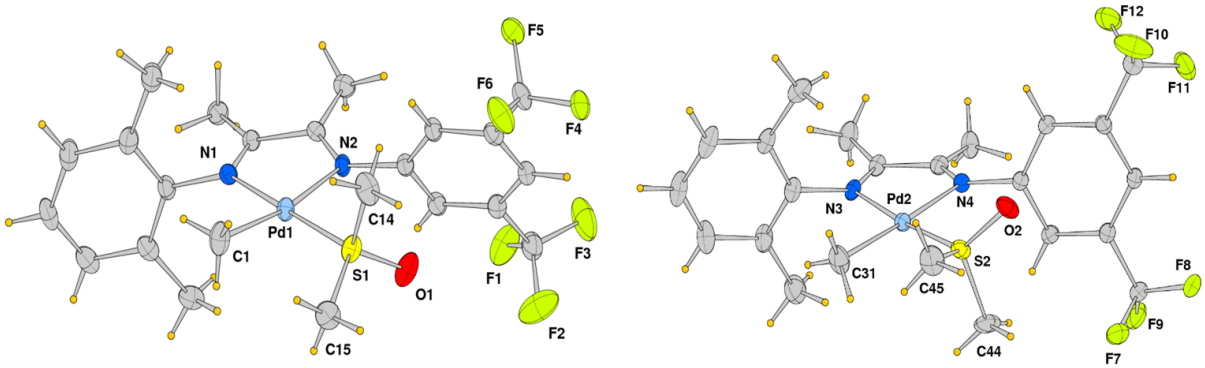

(a) (b)

Figure 4.14. ORTEP representation of complex **10d**.

In the unit cell two independent molecules are present, both featured by the expected square planar geometry around the palladium center, the Pd-CH_3 fragment *trans* to the N-atom bearing the CF_3-substituted aryl ring, the dmso S-bonded to the metal ion, and differing for the orientation of the oxygen atom of the coordinated dmso. In both molecules the Pd-N bond distances are significantly different, with that *trans* to the Pd-CH_3 fragment being longer than the other one, in agreement with the stronger *trans* influence of the coordinated methyl group with respect to that of dmso,.

Table 4.1. Selected bond lengths (Å) and angles (°) for complex **10d**.

(a)		**(b)**	
Pd(1)-N(1)	2.076(4)	Pd(2)-N(3)	2.068(4)
Pd(1)-N(2)	2.152(4)	Pd(2)-N(4)	2.172(4)
Pd(1)-C(1)	2.041(5)	Pd(2)-C(31)	2.020(5)
Pd(1)-S(1)	2.2422(13)	Pd(1)-S(2)	2.2303(13)
N(1)-Pd(1)-N(2)	76.33(15)	N(3)-Pd(2)-N(4)	76.65(14)
N(2)-Pd(1)-S(1)-O(1)	-31.5	N(4)-Pd(2)-S(2)-O(2)	+34.0
$Ph(CH_3)_2$/square plane	82.8	$Ph(CH_3)_2$/square plane	85.7
$Ph(CF_3)_2$/square plane	72.2	$Ph(CF_3)_2$/square plane	71.8

The bite angle N(1)-Pd(1)-N(2) in the two molecules is relatively small for an ideal square planar geometry, but, as in the case of **10a**, it is in the range of the bite angles usually observed for Pd(II)

complexes with bidentate nitrogen ligands that form five-membered metallacycles. The dihedral angles are similar to those calculated for the corresponding neutral complex, although the CF_3-substituted aryl ring is slightly more bent towards the plane in **10d**, probably due to the presence of the Pd-dmso fragment. As generally observed by us for Pd-dmso complexes[1,3] and as already discussed in the previous chapters (Chapters 2, 3), in the ^{1}H NMR spectra of **10d-e** in CD_2Cl_2 broad signals were present at room temperature, and they became sharper by decreasing temperature; the decoalescence of the methyl group signals was reached at 233 K (Figures 4.15, 4.16).

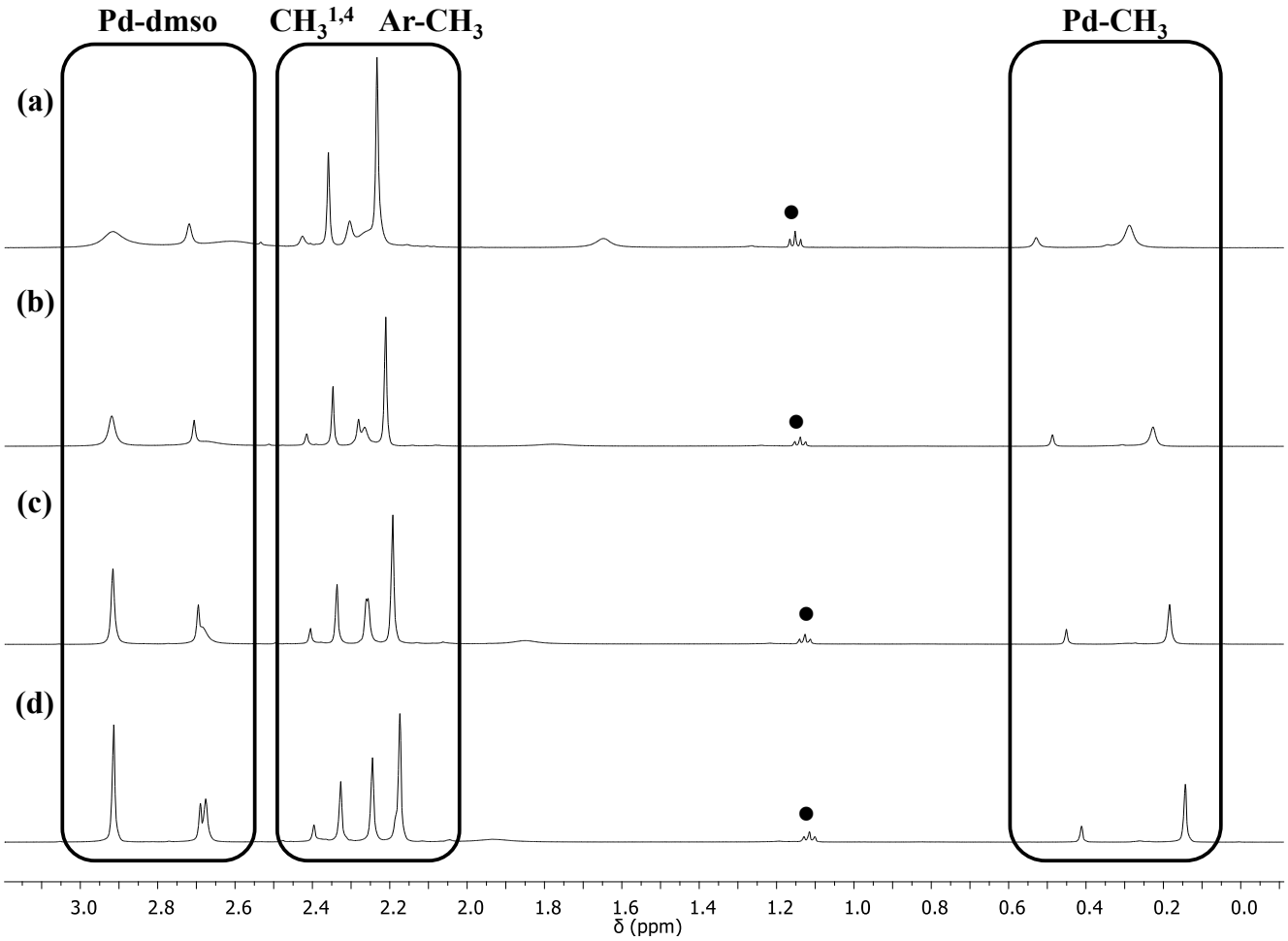

Figure 4.15. ^{1}H NMR spectra of **10d** in CD_2Cl_2 at (a) 298 K; (b) 273 K; (c) 253 K; (d) 233 K. Aliphatic region. ● diethyl ether.

In contrast with the observed presence of *trans* isomer as the only species in the solid state, in the ^{1}H NMR spectrum at the decoalescence temperature both *cis* and *trans* isomers were observed, in a 1 to 4 ratio. Comparing the chemical shift of the Pd-CH_3 fragment in the two species with the values reported

for the BIAN analogue[1] and with that observed for the acetonitrile derivatives (Figure 4.12), the major species is reasonably identified as the *trans* isomer.

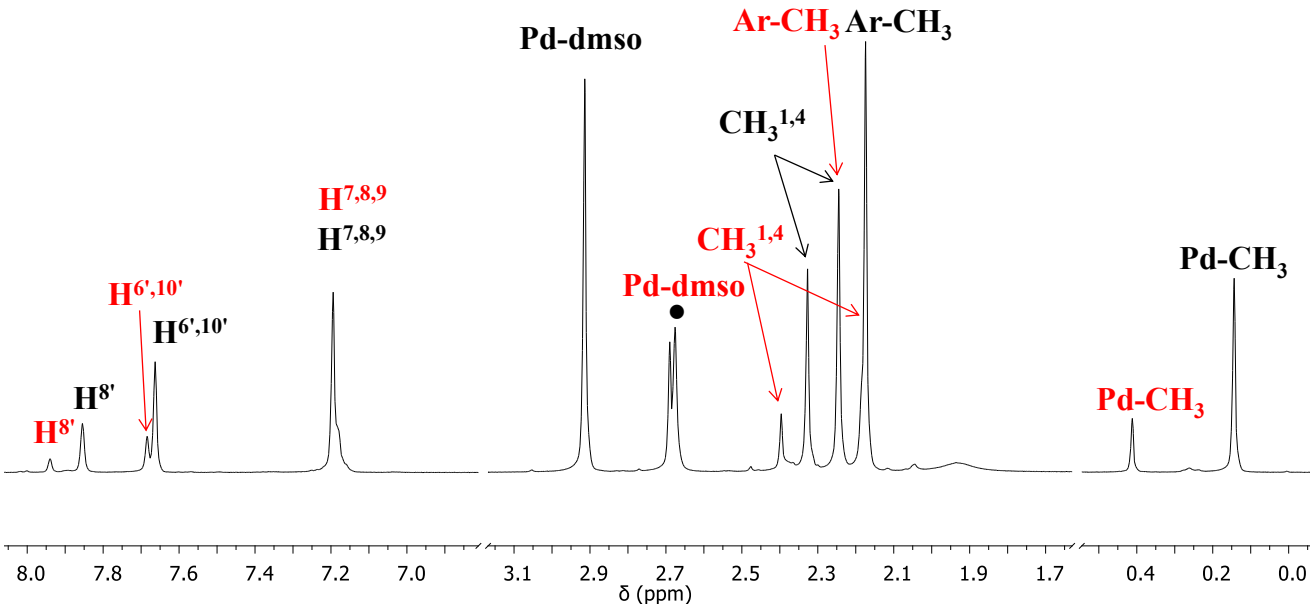

Figure 4.16. ^{1}H NMR spectrum of **10d** in CD_2Cl_2 at 233 K, *trans* (black) and *cis* (red) isomers. ● free dmso.

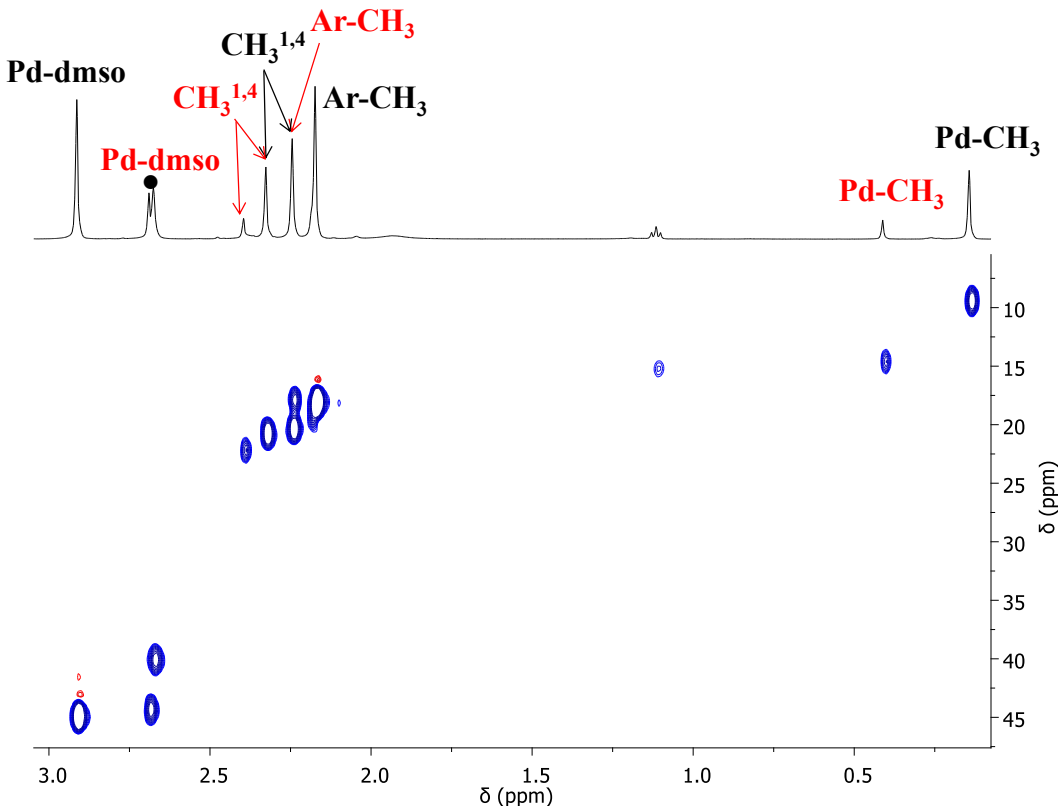

Figure 4.17. ^{1}H-^{13}C HSQC spectrum of **3d** in CD_2Cl_2 at 233 K, *trans* (black) and *cis* (red) isomers. Aliphatic region. ● free dmso.

As discussed in the previous chapters (Chapters 2, 3), the ^{13}C chemical shift of the methyl groups of the dimethyl sulfoxide are particularly significant to unravel the coordination of the dmso; in particular, the ^{1}H-^{13}C HSQC spectrum recorded at 233 K highlighted that in both isomers the dmso is coordinated to the palladium center via the sulfur atom (Figure 4.17), as also confirmed by the IR spectrum in solid state, that shows the presence of a single band at 1128 cm^{-1}, typical for S-bonded dmso. This is in agreement with the solid state structure.

In the ^{1}H NMR spectrum of **10d** recorded in dmso-d_6 sharp signals were observed already at room temperature, and indicated the presence of *trans* and *cis* isomers in a 3 to 2 ratio (Figure 4.18), and the major isomer was identified as the *trans* one by an NOE experiment performed upon irradiation of the signal of the Pd-CH_3 fragment at 0.16 ppm and observing the Overhauser effect with the peak of the methyl group bonded to the aryl ring. In addition, in the NOE spectrum the resonance of the Pd-CH_3 moiety of the *cis* isomer appears as a negative peak, thus indicating that the two species are in exchange at slow rate on the NMR time scale at room temperature (Figure 4.19).

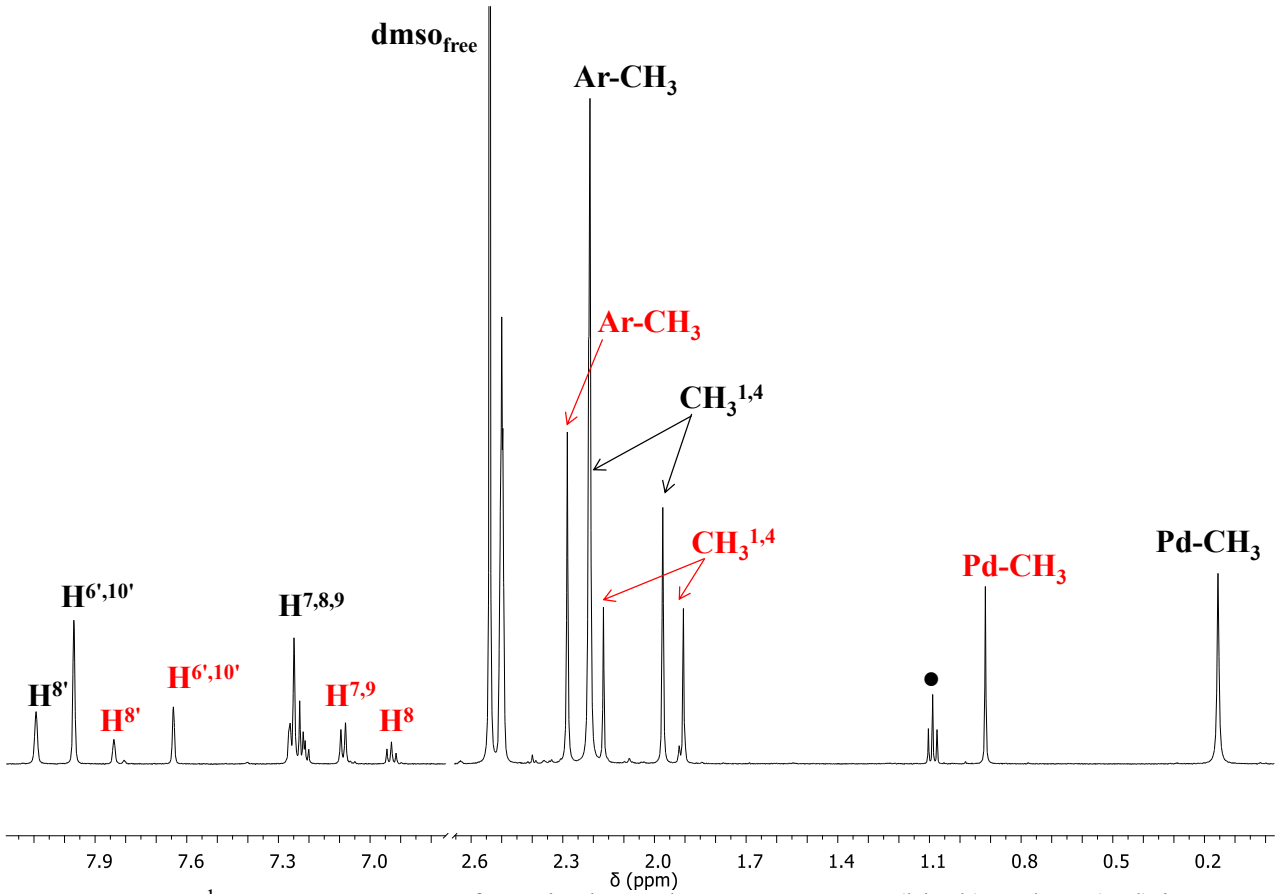

Figure 4.18. ^{1}H NMR spectrum of **10d** in dmso-d_6 at 298 K, *trans* (black) and *cis* (red) isomers. ● diethyl ether.

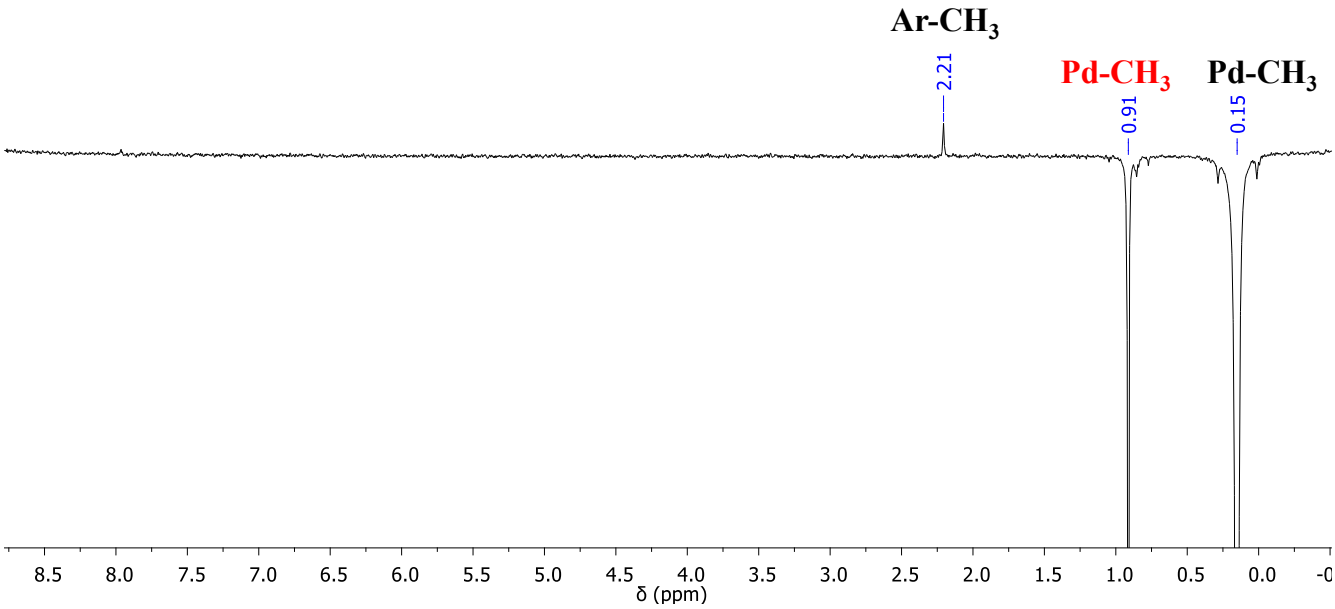

Figure 4.19. NOE spectrum of **10d** in dmso-d_6 at 298 K obtained upon irradiation of the Pd-CH_3 signal at 0.16 ppm.

4.2.3. Ethylene/methyl acrylate cooligomerization reaction.

The synthesized monocationic complexes **8b-c**, **9b-c**, **10b-e** were tested as precatalysts in the ethylene/methyl acrylate (MA) cooligomerization reaction (Scheme 1.3a) in 2,2,2-trifluoroethanol (TFE) as solvent, at T = 308 K and $P_{ethylene}$ = 2.5 bar, for 18h. The isolated products were characterized by NMR spectroscopy after the removal of the volatile fraction at reduced pressure, while the presence of higher alkenes was determined by GC-MS spectrometry on the crude reaction mixture (Table 4.2).

A remarkable effect of the nitrogen-donor ligand on both productivity and polar monomer incorporation was observed. Precatalyst **9b** with the symmetrically substituted ligand was found inactive, yielding an oil that contained mainly palladium derivatives and higher alkenes (Table 4.2). This inactivity can be related to the fast decomposition of the catalyst to inactive palladium black, which was observed already within the first 30 min of reaction. On the other hand, the most productive catalyst was generated from complex **8b**, achieving a productivity as high as 1.3 kg P/g Pd, that was two times as high as the productivity of precatalyst **10b** (0.5 kg P/g Pd).

Table 4.2. Ethylene/methyl acrylate cooligomerization reaction: effect of the Ar,Ar'-DAB ligand and of the counterion X. Precatalyst: $[Pd(CH_3)(NCCH_3)(Ar,Ar'\text{-DAB})][PF_6]$, **8b-10b** [a]

Run	Ar,Ar'-DAB	yield (g)	productivity (g P/g Pd) [b]	mol % MA[c]	Alkenes/ Esters[d]
1	**8**	2.90	1298.8	2.8	none
2	**9**	0.01	-	-	C^{4-8} C^{5-7}
3	**10**	1.28	544.6	4.5	C^{4-16}
4	**L13**[e]	0.171	79.4	10.4	-
5	**L14**[e]	0.019	/	/	C^{4-6}
6	**L12**[e]	0.297	133.2	14.7	C^{4-16}

[a] Reaction conditions: $n_{Pd} = 2.1 \cdot 10^{-5}$ mol, $V_{TFE} = 21$ mL, $V_{MA} = 1.130$ mL, [MA]/[Pd] = 594, T = 308 K, $P_{ethylene} = 2.5$ bar, t = 18 h; [b] isolated yield, productivity as g P/g Pd = grams of product per gram of Pd; [c] calculated by ^{1}H NMR spectroscopy on isolated product; [d] calculated by GC-MS; [e] ref. 1, t = 24 h.

Comparing these data with those reported for the corresponding BIAN catalysts **L12** (Figure 1.9),[1] in agreement with literature, moving from the BIAN catalysts to the DAB derivatives (Table 4.2, runs 4 *vs* 1, 6 *vs* 3), a remarkable increase in the productivity was observed. However, in the case of the catalysts containing the nonsymmetric ligands (runs 6 *vs* 3) the increase in productivity was not as pronounced as that found for the symmetric methyl-substituted derivatives (runs 4 *vs* 1). Interestingly, for both precatalyst **8b** and **10b** negligible decomposition to inactive palladium black was observed at the end of the reaction time, in contrast with the reported decomposition of **L13** and **L12** in 24 h.[1]

In agreement with Brookhart's system,[13,14] in the case of catalysts with the symmetrically *ortho*-substituted ligands, **8** and **L13**, no higher alkenes were formed, while in the case of those with the nonsymmetric **10** and **L12** a remarkable amount of alkenes from C^4 to C^{16} was detected, especially with the former. Moreover, it was experimentally observed that the catalyst with ligand **10** absorbed a higher amount of ethylene within the first 2 h of reaction with respect to catalysts with both **8** and **L12**, and at the end of the reaction time a remarkable evolution of volatile products was observed as well. Therefore, it is reasonable to assume that a considerable amount of ethylene is actually converted to higher alkenes that are lost with the removal of the volatile fraction, and, therefore, with the current set up of the reactor their amount cannot be quantified.

From this analysis, it is clear that, in order to have a consistent comparison of these catalytic systems, the productivity values, that up to now are calculated on the isolated yield, should be corrected by considering all the products of the reaction and therefore the overall consumption of ethylene.

In all cases, the formed alkenes are a complex mixture of isomers, as a result of the chain walking mechanism;[13] the observed chain length distribution, expressed in terms of molar fraction of each alkene, can be reasonably fitted by the Poisson distribution.

In analogy with the trends found for the catalysts containing the BIAN analogues **L12-14** (see Table 4.2)[1] and for those with the naphthyl-substituted α-diimines **1-4** (see Chapter 2),[3] the formation of higher alkenes with the catalysts containing the symmetrically *meta*-substituted ligand **9** was due to the lack of steric hindrance on the *ortho* positions of the aryl rings of the ancillary ligand, which did not prevent the β-hydride elimination.[2,14] In the case of the catalyst with ligand **10**, having only one aryl ring substituted on both *ortho* positions, longer alkenes were produced, suggesting that the β-hydrogen elimination was slightly slowed down.

As far as the content of the polar monomer inserted, the NMR analysis of the catalytic products pointed out that precatalysts **8b** and **10b** led to cooligomers with a similar percentage of methyl acrylate, slightly higher for those obtained with **10b**, and in both case the acrylate incorporation was remarkably lower than that obtained with the corresponding BIAN analogues **L13** and **L12** (Table 4.2).[1] This trend is in agreement with that found for the naphthyl-substituted α-diimine derivatives: when moving from the BIAN to the DAB catalysts, a decrease in the polar monomer content was observed together with the increase in productivity (see Chapter 2).[3] The decrease in the MA incorporation might be due not only to the different catalyst nature, BIAN *vs* DAB, but also for the more productive catalysts to the consumption of the polar monomer, whose concentration in solution decreases with the proceeding of the catalytic reaction, whereas the ethylene pressure is kept constant, in agreement with our previously findings.[1]

It is interesting to note that using precatalyst **10b** the reaction mixture became turbid in less than 10 min, while with complex **8b** it remained clear for at least the first 6 h, suggesting that the lower productivity of the system with the nonsymmetric ligand might be at least partially related to a diffusion problem. With the purpose to evaluate this hypothesis, the effects of reaction time, and [MA]/[Pd] ratio were evaluated for these two precatalysts.

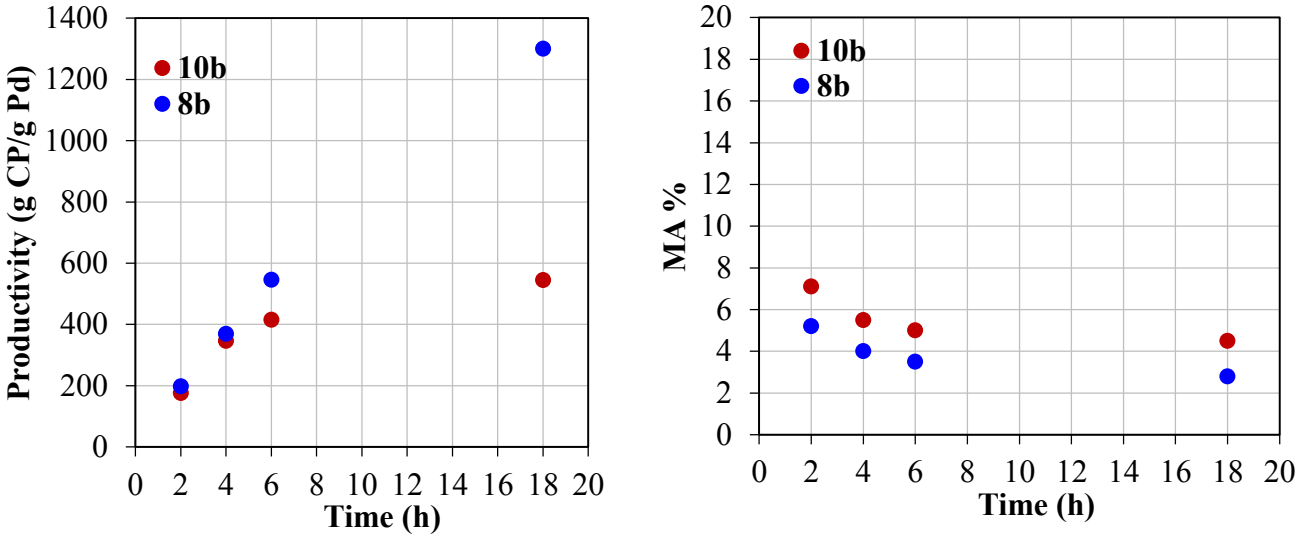

(a) (b)

Figure 4.20. Ethylene/MA cooligomerization: effect of reaction time. (a) Productivity *vs* time; (b) MA content (mol %) *vs* time. Reaction conditions: see Table 4.2.

The effect of reaction time was investigated in the range from 2 to 18 h. For **8b** the increase in productivity with time followed an almost linear relationship; whereas, the productivity of **10b** increased in the first 6 h, afterward an asymptotic behavior was observed (Figure 4.20a). Also the Poisson distribution of the higher alkenes produced with precatalyst **10b** changed with time, becoming sharper and moving towards shorter alkenes for longer reaction times. At the moment it is difficult to provide an explanation for this behavior, that, as already mentioned for the productivity values, in our opinion, requires the evaluation of the amount of ethylene consumed during the catalysis.

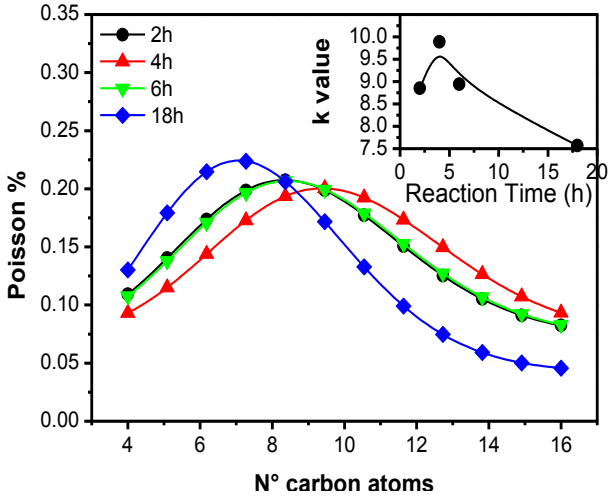

Figure 4.21. Effect of time on the Poisson distribution of higher alkenes produced with precatalyst **10b**. Reaction conditions: see Table 4.2.

The polar monomer incorporation decreased with time following an almost identical trend for both **8b** and **10b**, and the MA content in the product was always slightly higher for the latter with respect to that obtained with its symmetrical analogue (Figure 4.20b). As already discussed, this trend is due to the decrease in the MA concentration in solution as the catalytic reaction proceeds, while the ethylene pressure is kept constant.

The effect of [MA]/[Pd] ratio was studied by decreasing the amount of precatalyst and keeping constant all other parameters. Both complexes showed the same behavior, that is a slight increase in the productivity by doubling the [MA]/[Pd] ratio, followed by an almost negligible decrease for a further increase up to [MA]/[Pd] = 2400 (Figure 4.22a). As expected, the effect on the MA content reflected the variation of the productivity (Figure 4.22b). It should be noted that the reaction mixture of **10b** became turbid within the first 10-30 minutes also at lower catalyst concentrations, while with **8b** the reaction mixture remained clear at least for the first 6 h, regardless to the concentration of precatalyst.

Neither decreasing the reaction time nor decreasing the precatalyst concentration resulted in an increase in productivity for **10b**, thus suggesting that its lower productivity with respect to that of **8b** is not related to diffusion problem. Thus, the possibility to evaluate the total consumption of ethylene with both precatalysts represents a key issue to clarify the observed behavior, which is opposite to that reported for the BIAN analogues **L12-L13**.[1]

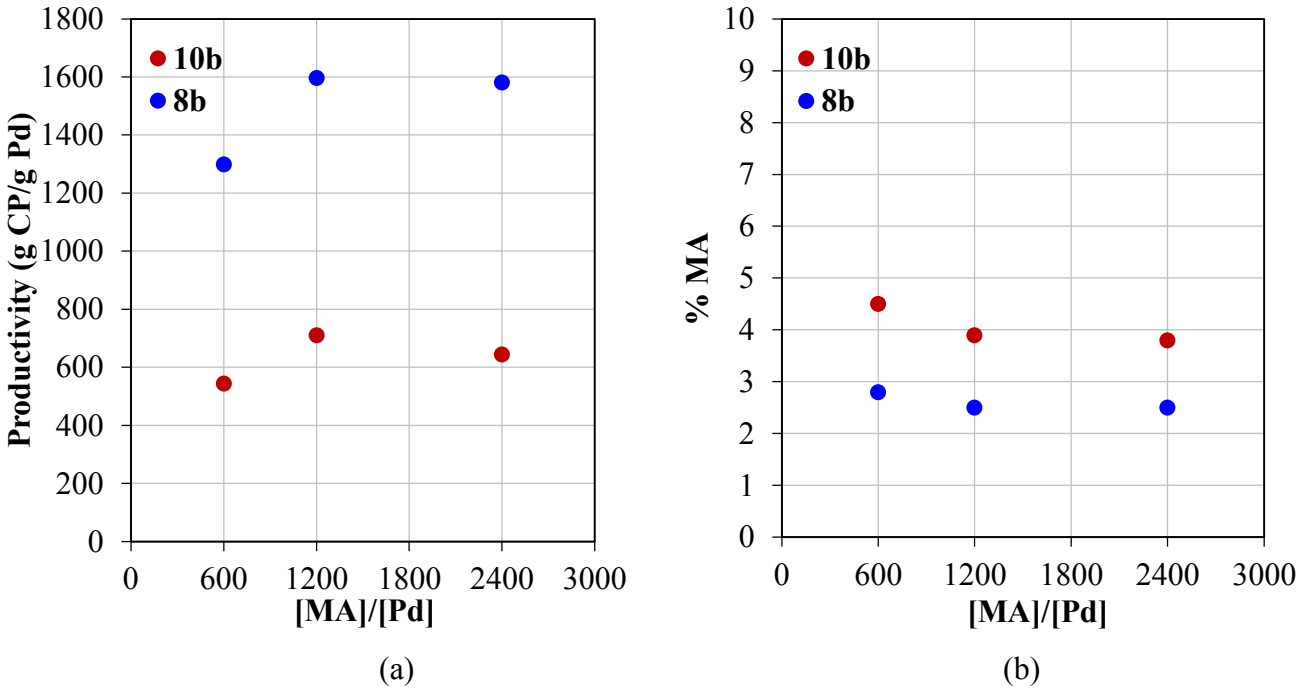

Figure 4.22. Ethylene/MA cooligomerization: effect of MA to palladium ratio. (a) Productivity *vs* MA to palladium ratio; (b) MA content (mol %) *vs* ratio. Reaction conditions: see Table 4.2.

In contrast to what we reported for the precatalyst with the nonsymmetric BIAN **L12** (see Chapter 3, Table 3.1),[1] in the case of complexes with ligand **10b**, moving from the acetonitrile to the dimethyl sulfoxide derivatives a slight decrease in the productivity was observed, while the MA insertion was unchanged, even at longer reaction time, up to 48 h (Table 4.3). The highest value of productivity, corresponding to 570.1 g P/g Pd, was achieved with precatalyst **10b**, having the acetonitrile as labile ligand, at 48 h (Table 4.3, run 2).

Table 4.3. Ethylene/methyl acrylate cooligomerization reaction: effect of the labile ligand and reaction time. Precatalyst: $[Pd(CH_3)(L)(\mathbf{10})][PF_6]$ [a]

Run	Precatalyst	L	time (h)	yield (g)	productivity (g P/g Pd) [b]	mol % MA[c]	Alkenes/ Esters[d]
1	**10b**	CH_3CN	18	1.28	544.6	4.5	C^{4-16}
2	**10b**	CH_3CN	48	1.27	570.1	5.2	C^{4-14}
3	**10d**	dmso	18	1.14	511.6	5.5	C^{4-8}
4	**10d**	dmso	48	1.22	549.0	5.4	C^{4-16}

[a] Reaction conditions: $n_{Pd} = 2.1 \cdot 10^{-5}$ mol, $V_{TFE} = 21$ mL, $V_{MA} = 1.130$ mL, [MA]/[Pd] = 594, T = 308 K, $P_{ethylene} = 2.5$ bar; [b] isolated yield, productivity as g P/g Pd = grams of product per gram of Pd; [c] calculated by ^{1}H NMR spectroscopy on isolated product; [d] calculated by GC-MS.

No influence of the labile ligand, acetonitrile *vs* dimethyl sulfoxide, was observed by us for the precatalysts with the naphthyl-substituted α-diimines **1-4** (Chapter 2),[3] together with no catalyst decomposition to inactive palladium metal.[3] In that context, the lack of the positive effect of dmso was ascribed to the fact that the difference between dmso and acetonitrile precatalysts became evident only if catalyst decomposition was relevant. In the case of precatalysts with ligand **10**, the productivity data obtained by varying the labile ligand are difficult to be explained. In conclusion the current absence of a clear general trend about the effect of the labile ligand with precatalysts belonging to same family suggests that number of collected are too limited and additional catalysts have to be investigated.

The effect of the counterion present in the precatalyst, hexafluorophosphate *vs* hexafluoroantimonate, was investigated in two different solvents, 2,2,2-trifluoroethanol (TFE) and dichloromethane (Table 4.4). When the reaction medium was the fluorinated alcohol a slight increase in the productivity was observed moving from the hexafluorophosphate to the hexafluoroantimonate precatalysts, regardless to the nature

of the ancillary ligand (Table 4.4, runs 1 *vs* 2, and 3 *vs* 4). These data are in agreement with the high dielectric constant of the solvent that disfavors the formation of the ion pair and therefore hampers the role of the counterion.

Table 4.4. Ethylene/methyl acrylate cooligomerization reaction: effect of the ArDAB ligand and of the counterion X in TFE and CH_2Cl_2. Precatalyst: $[Pd(CH_3)(L)(N\text{-}N')][X]$[a]

Run	Precat.	X	L	solvent	yield (g)	productivity (g P/g Pd) [b]	mol % MA[c]	Alkenes/ Esters[d]
1	**8b**	PF_6^-	CH_3CN	TFE	2.90	1298.8	2.8	none
2	**8c**	SbF_6^-	CH_3CN	TFE	2.92	1310.1	2.6	none
3	**10b**	PF_6^-	CH_3CN	TFE	1.28	544.6	4.5	$C^{4\text{-}16}$
4	**10c**	SbF_6^-	CH_3CN	TFE	1.31	588.0	5.3	$C^{4\text{-}12}$ C^5
5	**8b**	PF_6^-	CH_3CN	CH_2Cl_2	1.26	566.7	3.7	none
6	**8c**	SbF_6^-	CH_3CN	CH_2Cl_2	3.89	1744.7	3.5	none
7	**10b**	PF_6^-	CH_3CN	CH_2Cl_2	0.140	62.5	8.9	$C^{4\text{-}16}$
8	**10c**	SbF_6^-	CH_3CN	CH_2Cl_2	0.500	224.4	9.3	$C^{4\text{-}16}$
9	**10d**	PF_6^-	dmso	CH_2Cl_2	0.070	31.3	5.7	$C^{4\text{-}14}$
10	**10e**	SbF_6^-	dmso	CH_2Cl_2	0.185	82.7	5.2	$C^{4\text{-}14}$

[a] Reaction conditions: $n_{Pd} = 2.1 \cdot 10^{-5}$ mol, $V_{solvent} = 21$ mL, $V_{MA} = 1.130$ mL, [MA]/[Pd] = 594, t = 18 h, T = 308 K, $P_{ethylene} = 2.5$ bar; [b] isolated yield, productivity as g P/g Pd = grams of product per gram of Pd; [c] calculated by ^{1}H NMR spectroscopy on isolated product; [d] calculated by GC-MS.

When the cooligomerization reaction was carried out in dichloromethane, the productivity was found to be remarkably lower than in TFE in all the cases but one that with precatalyst **8c**, that requires to be reconsidered. These data confirmed the positive effect, highlighted by us,[15] of the fluorinated alcohol as reaction medium for the copolymerization reactions based on palladium catalysts with nitrogen-donor ligands. The nature of the solvent slightly affected the content of the polar monomer inserted that was a little bit higher in CH_2Cl_2 than in TFE; whereas it did not influence the formation of higher alkenes that was similar in both solvents.

As observed in TFE (Table 4.3), the catalytic behavior strongly depends on the nature of the ancillary ligand: regardless to the nature of the counterion, in dichloromethane, unexpectedly catalysts with the

nonsymmetric ligand **10** were found to be almost one order of magnitude less productive than those having the corresponding symmetric ligand **8**. In addition, with precatalyst **8b**, at the end of the reaction time, no palladium black was observed, while remarkable decomposition to inactive palladium metal was detected for complexes with ligand **10**. Thus, the low stability of the catalyst with the nonsymmetric ligand might be at the origin of its low productivity in CH_2Cl_2, suggesting that, since in TFE the catalyst is stable, the positive effect observed on the productivity might be due to its higher intrinsic activity.

Nevertheless, dichloromethane was the right solvent to evaluate the effect of the counterion. Indeed, regardless to the nature of the ancillary ligand, moving for PF_6^- to SbF_6^-, an increase of roughly three times in productivity was observed, while the amount of inserted polar monomer was not affected. This trend was in agreement with the lower coordinating ability of the hexafluoroantimonate with respect to hexafluorophosphate, and it confirmed the formation of the ion pair in dichloromethane.

Conversely to what observed in TFE, in CH_2Cl_2 the Pd-$NCCH_3$ derivatives **10b-10c** were found to be more productive than the corresponding dmso precatalysts **10d-10e**, regardless to the nature of the counterion, thus pointing out once more that the labile ligand is non so innocent as it might be expected.

In conclusion, this study highlighted that in the catalytic reaction under investigation, as already observed for the CO/vinyl arene copolymerization, the reaction medium plays a fundamental role in determining the catalytic behaviour of the complexes and thus, each comparison, even with the data reported in the literature, must be carefully made by taking the latter observation in mind.

4.3 Conclusions.

A new protocol for the synthesis of palladium complexes with a novel nonsymmetric DAB ligand **10** was developed using [Pd(cod)(CH_3)Cl] as templating agent, the mixture of neutral palladium complexes was purified through column chromatography and the desired complex was fully characterized.

The neutral complex was used for the synthesis of the monocationic acetonitrile complexes, and the ^{19}F-^{1}H HOESY spectrum of the hexafluorophosphate derivative indicated that in solution the counterion is preferentially located on top of the complexes and shifted towards the DAB skeleton, in contrast with the observation that in BIAN derivatives it is located mainly towards the Pd-$NCCH_3$ fragment.

The series of monocationic complexes was extended to the dimethyl sulfoxide derivatives following the procedure recently developed in our group, confirming its general validity. The NMR characterization of the Pd-dmso derivatives highlighted that with this nonsymmetric Ar,Ar'-DAB ligand the dmso is always coordinated via the sulfur atom, in contrast with the observation of both S-bonded and O-bonded species reported for the related Pd-dmso derivatives with the nonsymmetric BIAN ligand.

The corresponding symmetric ligands **8-9** were synthesized according to literature procedures, and employed to obtain the relevant palladium neutral and monocationic acetonitrile derivatives.

All the monocationic complexes were tested as precatalysts for the ethylene/MA cooligomerization reaction under mild conditions in TFE as solvent. Complexes with the *meta*-substituted symmetric ligand were found inactive, while the other derivatives led to a mixture of ethylene/MA cooligomers and ethylene oligomers. Comparing the catalytic behavior of the DAB precatalysts with that reported for the corresponding BIAN derivatives, moving from the BIAN to the DAB skeleton an increase in productivity was observed, in agreement with literature, but for the catalysts with the nonsymmetric ligand the increase was not as pronounced as that found for the symmetric methyl-substituted derivative.

With the catalysts having ligand **10** a remarkable formation of higher alkenes was observed, suggesting that for a homogeneous comparison with the derivatives containing ligand **8**, that does not produce higher alkenes, the overall consumption of ethylene should be considered rather than the isolated yield.

The effect of some reaction parameters was tested with complexes **8b** and **10b**. A linear increase of productivity with time was observed for **8b** while for **10b** it increased only within the first 4 hours and then reached a maximum; the polar monomer content decreased on increasing time for both precatalysts and was always higher for **10b**. For the latter the formation of higher alkenes increased for longer reaction time, and it was higher than that reported for the analogous BIAN derivative. When the MA to palladium ratio was increased, the productivity followed a Bell-like trend for both catalysts, while the MA content decreased, thus confirming the inhibiting effect of the polar monomer on the cooligomerization reaction. No effect of the labile ligand nor of the counterion was observed on the catalytic behavior of the tested complexes, the latter being related to the high dielectric constant of TFE.

Moving to a less polar solvent such as dichloromethane, a general decrease in productivity was observed, with the exception of precatalyst **8c**; complexes with ligand **8** generated catalysts that were nearly one order of magnitude more productive than the precatalysts with ligand **10**, while the difference was much less pronounced in TFE. The nature of the counterion affected the productivity, being SbF_6^- derivatives roughly three times more productive than the corresponding PF_6^- derivatives, in agreement with the formation of the ion pair in dichloromethane.

Interestingly, acetonitrile derivatives were found more productive than the dmso analogues, leading to a product with a higher content of polar monomer.

4.4. Experimental.

4.4.1. Materials and methods. All complex manipulations were performed using standard Schlenk techniques under argon. Anhydrous dichloromethane was obtained by distilling it over CaH_2 and under argon. Deuterated solvents (Cambridge Isotope Laboratories, Inc. (CIL)) were stored as recommended by CIL. Ethylene (purity ≥ 99.9 %) supplied by SIAD and methyl acrylate (99.9%, with 0.02% of hydroquinone monomethyl ether) supplied by Aldrich were used as received. TFE, and all the other reagents and solvents were purchased from Sigma-Aldrich and used without further purification for synthetic, spectroscopic and catalytic purposes. Ligands **8**, **9** were synthesized according to literature procedures.[4] $[Pd(OAc)_2]$ was a donation from Engelhard Italia and used as received. $[Pd(cod)Cl_2]$, $[Pd(cod)(CH_3)Cl]$ were synthesized according to literature procedures.

NMR spectra of ligands, complexes and catalytic products were recorded on a Varian 500 spectrometer at the following frequencies: 500 MHz (^1H), 125.68 MHz (^{13}C) and 470 MHz (^{19}F). The resonances are reported in ppm (δ) and referenced to the residual solvent peak versus $Si(CH_3)_4$: $CDCl_3$ at δ 7.26 (^1H) and δ 77.0 (^{13}C), CD_2Cl_2 at δ 5.32 (^1H) and δ 54.0 (^{13}C), dmso-d_6 at δ 2.50 (^1H) and δ 39.51 (^{13}C). NMR experiments were performed employing the automatic software parameters. In the case of NOESY experiments a mixing time of 500 ms was used. IR spectra were recorded in Nujol on a Perkin Elmer System 2000 FT-IR. Elemental analyses were performed in the analytical laboratories of Department of Chemistry of Universities of Udine and of Bologna. GC-MS analyses were performed with an Agilent GC 7890 instrument using a DB-225ms column (J&W, 60 m, 0.25 mm ID, 0.25 μm film) and He as carrier coupled with a 5975 MSD. Before analysis, samples were diluted with methanol and nonane was added as internal standard.

4.4.2. Synthesis of neutral Pd-complexes.

$[Pd(CH_3)Cl(Ar_2\text{-DAB})]$ (8a, 9a). To a stirred solution of $[Pd(cod)(CH_3)Cl]$ (0.38 mmol) in 1 mL of CH_2Cl_2, a solution of 1.1 equiv of the desired ligand in CH_2Cl_2 (2 mL for **8**, 6 mL for **9**) was added. After the established reaction time (2.5 h for **8a** synthesis, 5 h for **9a**) at room temperature, the reaction mixture was concentrated and the product precipitated upon addition of cold diethyl ether.

8a. Yield 91 %. Found C = 56.70, H = 6.16, N = 6.34. Calc. % for $C_{21}H_{24}N_2ClPd$: C = 56.14, H = 6.06, N = 6.23.

^1H NMR (500 MHz, CD_2Cl_2, 298 K) δ = 7.21 – 7.08 (m, 6H, Ar-H), 2.22 (s, 12H, Ar-CH_3), 2.00 (s, 3H, CH_3^1), 1.96 (s, 3H, CH_3^4), 0.26 (s, 3H, Pd-CH_3). ^1H NMR (500 MHz, $CDCl_3$, 298 K) δ = 7.18 – 7.08 (m, 6H, Ar-H), 2.25 (s, 6H, Ar-CH_3), 2.22 (s, 6H, Ar'-CH_3), 2.03 (s, 3H, CH_3^1), 1.97 (s, 3H, CH_3^4), 0.43 (s,

3H, Pd-CH_3). ^{13}C NMR (125.68 MHz, CD_2Cl_2, 298 K) δ = 128.23 - 125.90 (C_{Ar}), 17.48 (Ar-CH_3), 18.26 (C^1), 19.09 (C^4), 0.03 (Pd-CH_3).

9a. Yield 51 %. Found C = 39.16, H = 2.28, N = 4.23. Calc. % for $C_{21}H_{15}N_2ClF_{12}Pd$: C = 37.92, H = 2.27, N = 4.21.

^{1}H NMR (500 MHz, CD_2Cl_2, 298 K) δ = 7.92 (s, 1H, H^8), 7.87 (s, 1H, $H^{8'}$), 7.54 (s, 2H, $H^{6,10}$), 7.50 (s, 2H, $H^{6',10'}$), 2.26 (s, 3H, CH_3^1), 2.14 (s, 3H, CH_3^4), 0.52 (s, 3H, Pd-CH_3). ^{13}C NMR (125.68 MHz, CD_2Cl_2, 298 K) δ = 121.07 (C^8), 120.94 ($C^{8'}$), 122.29 ($C^{6,10}$), 122.09 ($C^{6',10'}$), 21.10 (CH_3^4), 19.75 (CH_3^1), 2.46 (Pd-CH_3).

^{19}F NMR (470 MHz, CD_2Cl_2, 25°C) δ = -63.22, -63.35 (CF_3).

[Pd(CH_3)Cl(10)] 10a. To a stirred solution of 2,3-butanedione (3.0 mmol) in 5 mL of methanol with a catalytic amount of formic acid at 303 K, 1 equivalent of 3,5-bis(trifluoromethyl)aniline (3.0 mmol) was added dropwise. The solution was stirred at 303 K for 1 h, than a 1H NMR spectrum of the reaction mixture was recorded to determine the amount of monoketoimine **5** formed. 0.8 equivalent of [Pd(cod)(CH_3)Cl] and 1.2 equivalent of 2,6-dimethylaniline were suspended in 2 mL of methanol and added to the reaction mixture. After 2 h at 303 K, the solvent was removed and the resulting oil was treated with diethyl ether (0.5 mL) and cold n-hexane (1 mL), with the precipitation of a little yellow solid. After 56 h at room temperature, the formed solid was filtered and washed thoroughly with n-hexane. The solid, containing complexes **8a** and **10a**, was purified through flash chromatography on silica with chloroform/n-hexane 1 : 1, and the polarity was gradually varied by increasing the amount of chloroform. The desired complex was eluted second as a bright orange band, and was recovered after removing the solvent by precipitation with diethyl ether (yield 23 %).

10a. Found C = 44.96, H = 3.63, N = 4.96. Calc. % for $C_{21}H_{21}N_2Pd_1F_6Cl_1$: C = 45.26, H = 3.80, N = 5.03.

^{1}H-NMR (500 MHz, CD_2Cl_2, 298 K) δ = 7.81 (s, 1H, $H^{8'}$), 7.57 (s, 2H, $H^{6',10'}$), 7.17 (m, 3H, $H^{7,8,9}$), 2.28 (s, 3H, CH_3^4), 2.21 (s, 3H, Ar-CH_3), 2.01 (s, 3H, CH_3^1), 0.57 (s, 3H, Pd-CH_3). ^{13}C-NMR (125.68 MHz, CD_2Cl_2, 25 °C) δ = 128.85 ($C^{7,8,9}$), 123.24 ($C^{6',10'}$), 121.04 ($C^{8'}$), 20.11 (CH_3^4), 19.84 (CH_3^1), 18.09 (Ar-CH_3), 1.27 (Pd-CH_3).

4.4.3. Synthesis of monocationic Pd-complexes.

[Pd(CH_3)($NCCH_3$)(Ar,Ar'-DAB)][X] (X = PF_6^-, 8b-10b; X = SbF_6^-, 8c-10c). To a stirred solution of the neutral complex [Pd(CH_3)Cl(Ar,Ar'-DAB)] (**8a-10a**) (0.10 mmol) in 5 mL CH_2Cl_2, a solution of 1.15 equivalents of AgX ($AgPF_6$ for **8b-10b**, $AgSbF_6$ for **8c-10c**) in 1 mL of anhydrous acetonitrile was added.

The reaction mixture was protected from light and stirred at room temperature for 45 min, then it was filtered over Celite®, concentrated and precipitated upon addition of cold diethyl ether.

8b. Yield 92 %. Found C = 32.76, H = 2.46, N = 4.98. Calc. % for $C_{23}H_{30}N_3F_6PdP$: C = 33.86, H = 2.22, N = 5.15. IR: υ_{max} = 842.44 (PF_6^-). **8c.** Yield 79 %. Found C = 40.66, H = 4.51, N = 6.07. Calc. % for $C_{23}H_{30}N_3F_6PdSb$: C = 40.00, H = 4.38, N = 6.08. IR : υ_{max} = 657.38 cm^{-1} (SbF_6^-).

^{1}H NMR (500 MHz, CD_2Cl_2, 298 K) δ = 7.24 – 7.17 (m, 6H, Ar-H), 2.28 (s, 6H, $CH_3^{6,10}$), 2.21 (s, 3H, CH_3^1), 2.20 (s, 6H, $CH_3^{6',10'}$), 2.19 (s, 12H, CH_3^4), 1.83 (s, 3H, Pd-NCCH_3), 0.35 (Pd-CH_3). ^{13}C NMR (125.68 MHz, CD_2Cl_2, 298 K) δ = 128.76 (C^8) , 127.59 (C^{Ar}), 17.76 (Ar-CH_3), 18.65 (CH_3^1), 17.71 (Ar'-CH_3), 19.97 (CH_3^4), 2.11 (Pd-NCCH_3), 4.31 (Pd-CH_3).

9b. Yield 82 %. Found C = 45.48, H = 5.42, N = 6.86. Calc. % for $C_{23}H_{30}N_3F_6PdP$: C = 46.05, H = 5.04, N = 7.00. IR: υ_{max} = 837.82 (PF_6^-). **9c.** Yield 37 %. Found C = 32.76, H = 1.78, N = 4.72. Calc. % for $C_{23}H_{30}N_3F_6PdSb$: C = 30.47, H = 2.00, N = 4.64. IR: υ_{max} = 658.72 cm^{-1} (SbF_6^-).

^{1}H NMR (500 MHz, CD_2Cl_2, 298 K) δ = 7.93 (s, 2H, $H^{7,7'}$), 7.71 (s, 2H, $H^{5,9}$), 7.59 (s, 2H, $H^{5',9'}$), 2,37 (s, 3H, CH_3^1), 2.30 (s, 3H, CH_3^4), 2.03 (s, 3H, Pd-NCCH_3), 0.53 (s, 3H, Pd-CH_3). ^{13}C NMR (125.68 MHz, CD_2Cl_2, 298 K) δ = 121.82 ($C^{7,7'}$), 122.33 ($C^{5,9}$), 122.52 ($C^{5',9'}$), 20.01 (CH_3^1), 21.89 (CH_3^4), 2.87 (Pd-NCCH_3), 6.40 (Pd-CH_3). ^{19}F NMR (470 MHz, CD_2Cl_2, 298 K) δ = -63.21, -63.42 (CF_3).

10b. Yield 82 %. Found C = 37.80, H = 3.40, N = 5.61. Calc. % for $C_{23}H_{24}N_3Pd_1P_1F_{12}$: C = 39.03, H = 3.42, N = 5.94. **10c.** Yield 91 %. Found C = 34.71, H = 3.29, N = 5.01. Calc. % for $C_{23}H_{24}N_3Pd_1Sb_1F_{12}$: C = 34.59, H = 3.03, N = 5.26. IR: υ = 663 cm^{-1} (SbF_6^-).

^{1}H NMR (500 MHz, CD_2Cl_2, 298 K), *cis : trans* = 1 : 6. *trans* isomer δ = 7.93 (s, 1H, $H^{8'}$), 7.77 (s, 2H, $H^{6',10'}$), 7.20 (s, 3H, $H^{7,8,9}$), 2.41 (s, 3H, CH_3^4), 2.21 (s, 6H, Ar-CH_3), 2.18 (s, 3H, CH_3^1), 2.04 (s, 3H, Pd-NCCH_3), 0.47 (s, 3H, Pd-CH_3); isomer *cis* δ = 7.93 (s, 1H, $H^{8'}$), 7.61 (s, 2H, $H^{6',10'}$), 7.20 (s, 3H, $H^{7,8,9}$), 2.35 (s, 3H, CH_3^4), 2.30 (s, 6H, Ar-CH_3), 2.22 (s, 3H, CH_3^1), 1.89 (s, 3H, Pd-NCCH_3), 0.43 (s, 3H, Pd-CH_3). ^{13}C-NMR (125.68 MHz, CD_2Cl_2, 298 K), *trans* isomer δ = 129.00 ($C^{7,8,9}$), 122.91 ($C^{6',10'}$), 121.77 ($C^{8'}$), 20.31 (CH_3^1), 20.26 (CH_3^4), 18.04 (Ar-CH_3), 5.85 (Pd-CH_3), 3.00 (Pd-NCCH_3).

[Pd(CH_3)(dmso)(10)][X] (X = PF_6^-, 10d; X = SbF_6^-, 10e). To a stirred solution of the neutral complex [Pd(CH_3)Cl(**10**)] (**10a**) (0.13 mmol) in 7 mL CH_2Cl_2, 2 equivalent of anhydrous dimethyl sulfoxide (18.5 µL) and a suspension of 1.15 equivalents of AgX (0.15 mmol; $AgPF_6$ for **10d**, $AgSbF_6$ for **10e**) in 1 mL of CH_2Cl_2 was added. The reaction mixture was protected from light and stirred at room temperature for 30 min, then it was filtered over Celite®, concentrated and precipitated upon addition of cold n-hexane for **10d** and diethyl ether for **10e** after 2-3 h at 277 K.

10d. Yield 88 %. Found C = 36.00, H = 3.91, N = 3.61. Calc. % for $C_{23}H_{27}N_2Pd_1P_1F_{12}O_1S_1$: C = 37.09, H = 3.65, N = 3.76. IR: υ= 843 cm^{-1} (PF_6^-), υ= 1128 cm^{-1} (S=O, S-bonded dmso). **10e.** Found C = 32.43, H = 3.30, N = 3.39. Calc. % for $C_{23}H_{27}N_2Pd_1Sb_1F_{12}O_1S_1$: C = 33.06, H = 3.26, N = 3.52.

^{1}H NMR (500 MHz, CD_2Cl_2, 298 K) *trans* : *cis* = 4 : 1. *trans* isomer δ = 7.85 (s, 1H, $H^{8'}$), 7.66 (s, 2H, $H^{6',10'}$), 7.19 (s allargato, 3H, $H^{7,8,9}$), 2.91 (s, 6H, Pd-$SO(CH_3)_2$), 2.33 (s, 3H, $CH_3^{4 \text{ or } 1}$), 2.24 (s, 3H, $CH_3^{1 \text{ or } 4}$), 2.17 (s, 6H, Ar-CH_3), 0.14 (s, 3H, Pd-CH_3); *cis* isomer δ = 7.94 (s, 1H, $H^{8'}$), 7.68 (s, 2H, $H^{6',10'}$), 7.19 (s broad, 3H, $H^{7,8,9}$), 2.69 (s, 6H, Pd-$SO(CH_3)_2$), 2.40 (s, 3H, $CH_3^{4 \text{ or } 1}$), 2.24 (s, 6H, Ar-CH_3), 2.17 (s, 3H, $CH_3^{1 \text{ or } 4}$), 0.41 (s, 3H, Pd-CH_3).

^{13}C-NMR (125.68 MHz, CD_2Cl_2, -40 °C) *trans* isomer δ = 128.52 ($C^{7,8,9}$), 122.08 ($C^{6',10'}$), 121.11 ($C^{8'}$), 44.85 (Pd-$SO(CH_3)_2$), 20.71 (CH_3^4), 20.29 – 17.86 (CH_3^1), 17.99 (Ar-CH_3), 9.37 (Pd-CH_3); *cis* isomer δ = 128.52 ($C^{7,8,9}$), 122.08 ($C^{6',10'}$), 121.88 ($C^{8'}$), 44.27 (Pd-$SO(CH_3)_2$), 22.13 ($CH_3^{4,1}$), 20.29 – 17.86 (Ar-CH_3), 14.56 (Pd-CH_3).

^{1}H NMR (500 MHz, dmso-d_6, 298 K) *trans* : *cis* = 3 : 2. *trans* isomer δ = 8.09 (s, 1H, $H^{8'}$), 7.97 (s, 2H, $H^{6',10'}$), 7.25 (m, 3H, $H^{7,8,9}$), 2,21 (s broad, 9H, Ar-CH_3, $CH_3^{4 \text{ or } 1}$), 1.97 (s, 3H, $CH_3^{1 \text{ or } 4}$), 0.16 (s, 3H, Pd-CH_3); *cis* isomer δ = 7.84 (s, 1H, $H^{8'}$), 7.64 (s, 2H, $H^{6',10'}$), 7.08 (d, 2H, $H^{7,9}$), 6,93 (t, 1H, H^8), 2.29 (s, 6H, Ar-CH_3), 2,17 – 1.91 (2s, 6H, $CH_3^{1,4}$), 0.92 (s, 3H, Pd-CH_3).

^{13}C NMR (125.68 MHz, dmso-d_6, 298 K) *trans* isomer δ = 128.72 ($C^{7,8,9}$), 123.42 ($C^{6',10'}$), 121.00 ($C^{8'}$), 20.56 (Ar-CH_3), 18.11 - 17.92 ($CH_3^{1,4}$), 8.30 (Pd-CH_3), *cis* isomer δ = 128.24 ($C^{7,9}$), 123.70 (C^8), 120.32 ($C^{6',10'}$), 117.44 ($C^{8'}$), 21.39 (Ar-CH_3), 16.16 - 15.96 ($CH_3^{1,4}$), 5.83 (Pd-CH_3).

4.4.4. Ethylene/methyl acrylate cooligomerization reactions. All catalytic experiments were carried out in a Büchi "tinyclave" reactor equipped with an interchangeable 50 mL glass vessel. The vessel was loaded with the desired complex (21 μmol), TFE (21 mL) or distilled CH_2Cl_2 (22 mL) and methyl acrylate (1.13 mL). The reactor was then placed in a preheated oil bath, connected to the ethylene tank, ethylene was bubbled for 10 min then the reactor was pressurized. The reaction mixture was stirred at constant temperature and pressure. After the proper time, the reactor was cooled to room temperature and vented. An aliquot (200 μL) of the reaction mixture was withdrawn and diluted in CH_3OH (1 mL) for GC-MS analyses. The reaction mixture was poured in a 50 mL round flask, together with the dichloromethane (3 x 2 mL) used to wash the glass vessel. No separation of Pd black was observed. Volatiles were removed under reduced pressure and the residual gum or oil was dried at constant weight and analyzed by NMR spectroscopy.

4.5. Bibliography.

[1] Meduri, A.; Montini, T.; Ragaini, F.; Fornasiero, P.; Zangrando, E.; Milani, B. *ChemCatChem* **2013**, *5*, 1170.

[2] Johnson, L. K.; Mecking, S.; Brookhart, M. *J. Am. Chem. Soc.* **1996**, *118*, 267.

[3] Rosar, V.; Meduri, A.; Montini, T.; Fini, F.; Carfagna, C.; Fornasiero, P.; Balducci, G.; Zangrando, E.; Milani, B. *ChemCatChem* **2014**, *6*, 2403.

[4] a) tom Dieck, H.; Svobada, M.; Greiser, T. *Z. Naturfosch.* **1981**, *86b*, 823; b) Johansson, L.; Ryan, O.B.; Tilset, M. *J. Am. Chem. Soc.* **1999**, *121,* 1974.

[5] a) Abakumov, G.A.; Cherkasov, V.K.; Druzhkov; N.O.; Kocherova, T.N.; Shavyrin, A.S. *Russ. Chem. Bull. Int. Ed.* **2011**, *60*, 112; b) Schmid, A.; Eberhardt, R.; Kukral, J.; Rieger, B. *Z. Naturforsch.* **2002**, *57b*, 1141; c) Zhai, F.; Jordan, R.F. *Organometallics.* **2014**, *33*, 7176.

[6] Durand, J.; Zangrando, E.; Stener, M.; Fronzoni, G.; Carfagna, C.; Binotti, B.; Kamer, P. C. J.; Müller, C.; Caporali, M.; van Leeuwen, P. W. N. M.; Vogt, D.; Milani, B. *Chem. Eur. J.* **2006**, *12*, 7639.

[7] Hinderling, C.; Chen, P. *Int. J. Mass Spec.* **2000**, *195/196*, 377.

[8] a) Rülke, R. E.; Ernsting, J. M.; Spek, A. L.; Elsevier, C. J.; van Leeuwen, P. W. N. M.; Vrieze, K. *Inorg. Chem.* **1993**, *32*, 5769; b) Abraham, R.J.; Mobli, M.; Smith, R.J. *Magn. Reson. Chem.* **2004**, *42*, 436.

[9] Scarel, A.; Axet, M. R.; Amoroso, F.; Ragaini, F.; Elsevier, J. C.; Holuigue, A.; Carfagna, C.; Mosca, L.; Milani, B. *Organometallics* **2008**, *27*, 1486.

[10] Conventry, D.N.; Batsanov,A.S.; Goeta, A.E.; Howard, J.A.K.; Marder, T.B. *Polyhedron* **2004**, *23*, 2789.

[11] Cope-Eatough, E.K.; Mair, F.S.; Pitchard R.G.; Warren, J.E.; Woods, R.J. *Polyhedron* **2003**, *22*, 1447.

[12] Binotti, B.; Bellachioma, G.; Cardaci, G.; Carfagna, C.; Zuccaccia, C.; Macchioni, A. *Chem. Eur. J.* **2007**, *13*, 1570.

[13] Johnson, L.K.; Killian, C.M.; Brookhart, M. *J. Am. Chem. Soc.* **1995**, *117*, 6414.

[14] Tempel, D.J.; Johnson, L.K.; Huff, R.L.; White, P.S., Brookhart, M. *J. Am. Chem. Soc.* **2000**, *122*, 6686.

[15] Milani, B.; Anzilutti, A.; Vicentini, L.; Sessanta o Santi, A.; Zangrando, E.; Geremia, S.; Mestroni, G. *Organometallics* **1997,** *16,* 5064

CHAPTER 5

Pyridylimines: versatile ligands for Pd-catalyzed copolymerization reactions

Overview

Pyridylimine ligands (**13-16**) featured by an aryl ring on the imino nitrogen atom and differing for the presence of a hydrogen atom or a methyl group on the imino carbon atom and/or on the *ortho* positions of the aryl ring were synthesized and used to obtain the corresponding neutral, [Pd(CH_3)Cl(N-N')], and monocationic, [Pd(CH_3)($NCCH_3$)(N-N')][PF_6], (N-N' = **13-16**) palladium(II) complexes. The NMR characterization pointed out the influence of the number and position of the methyl groups on the chemical shift of the signals of some protons, especially that related to the Pd-CH_3 fragment, indicating that it might be a sensitive probe for the electron density on the palladium center. Moreover, while for the neutral complexes only one isomer was observed in solution, featured by the Pd-CH_3 group *trans* to the pyridine nitrogen, in the monocationic derivatives a loss in stereoselectivity was observed, having both *cis* and *trans* isomers present in solution in a ratio depending on the nature of the ancillary ligand. The monocationic complexes were tested as precatalysts for the CO/vinyl arene copolymerization reaction, using either styrene or 4-methy-styrene as comonomers, under mild reaction conditions of temperature and pressure.

Part of this chapter will be published in a feature work:

Rosar, V., Dedeic, D.; Nobile, T.; Carfagna, C.; Balducci, G.; Milani, B.

5.1. Introduction.

Thanks to their cheap and relatively easy and modular synthesis, pyridylimines (N-N') are widely used as ancillary ligands in coordination chemistry. Many of the synthesized coordination compounds have found application as homogeneous catalysts in different processes,[1] and a few examples are reported below. Iridium(I) complexes of general formula [Ir(cod)(N-N')][X] (cod = 1,5-*cis*,*cis*-cyclooctadiene, X = Cl^-, PF_6^-) were applied as catalysts for the dehydrogenation reaction of cyclooctane to cyclooctene, showing that catalyst activity and selectivity depended on the nature of the ancillary ligand (Figure 5.1a).[2]

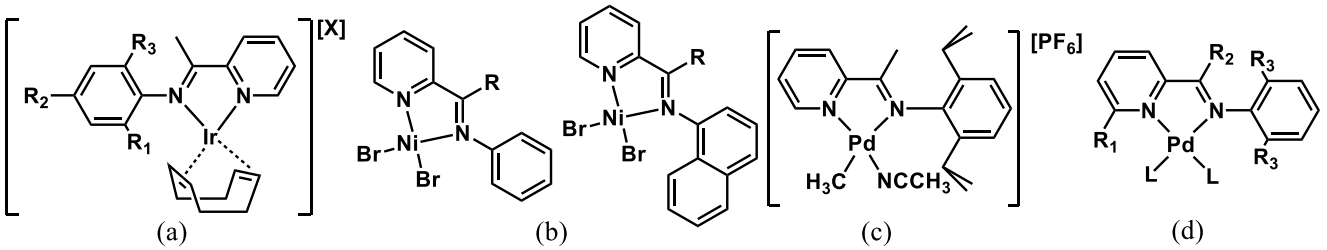

(a) (b) (c) (d)

Figure 5.1. A few examples of complexes with pyridylimines.

Ni(II) complexes with pyridylimine ligands having general formula [$NiBr_2$(N-N')] (Figure 5.1b) were reported to catalyze the homopolymerization of ethylene, leading to highly branched oligomers with low molecular weight,[3] while a similar palladium complex [Pd(CH_3)($NCCH_3$)(N-N')][BAr^F_4] (BAr^F_4 = 3,5-$(CF_3)_2C_6H_3$) (Figure 5.1c) was applied as long-lived catalyst for the ethylene oligomerization.[4]

Focusing on the synthesis of CO/vinyl arene polyketones, *in situ* generated Pd catalysts containing pyridylimines derived by the condensation of 2-pyridinecarboxaldehyde with aliphatic amines led to syndiotactic or isotactic CO/styrene copolymers depending on the aliphatic group on the imino nitrogen atom.[5] The pyridylimine functionality was also exploited to obtain dendritic palladium catalysts applied in the CO/vinyl arene copolymerization to yield the corresponding polyketones with different stereochemistry depending on the ligand itself.[6]

Pyridylimines were also used as ancillary ligands for palladium complexes [Pd(N-N')$(L)_2$] (L = acetate, trifluoroacetate; Figure 5.1d) that catalyzed the methoxycarbonylation of styrene to give dimethyl phenylsuccinate as major product.[7]

Pyridyliminic fragments were also employed as bidentate domains in polydentate ligands able to coordinate two metal centers leading to dinuclear complexes.[8]

More recently, in our group, monocationic palladium complexes [Pd(CH_3)($NCCH_3$)(N-N')][PF_6] with two new pyridylimines (N-N' = **L15**, **L16**) deriving from the condensation reaction of aminopyrene and

either 2-pyridinecarboxaldehyde or 2-acetylpyridine were used as precatalysts for the CO/vinyl arene copolymerization reaction (Figure 5.2).[9]

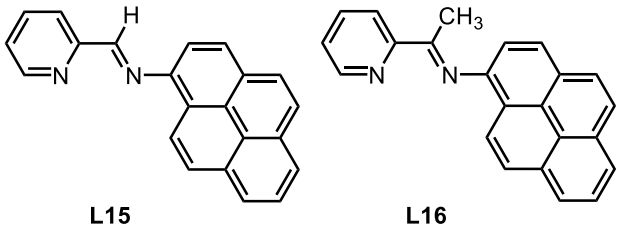

Figure 5.2. Pyrene-tagged pyridylimine ligands **L1**, **L2**.[8]

Both monocationic complexes were found to be active for the CO/vinyl arene copolymerization, showing a strong effect of the nature of the ancillary ligand on productivity. In fact, regardless of the nature of the vinyl arene comonomer, styrene (S), 4-methyl-styrene (MS) or 4-*tert*-butil-styrene (TBS), by changing on the imino carbon atom the hydrogen atom with the methyl group an increase of more than five times in productivity was achieved, together with an increase in the molecular weight of the produced copolymer (Table 5.1). The catalyst containing **L16** led to productivities as high as 5.38 kg CP/g Pd and to molecular weights up to 471 000 g/mol without evident formation of inactive palladium black.[8]

Table 5.1. CO/vinyl arene copolymerization reaction: effect of the N-N' ligand and of the vinyl arene. Precatalyst: $[Pd(CH_3)(NCCH_3)(\mathbf{N\text{-}N'})][PF_6]$[a]

RUN	**N-N'**	Vinyl arene	Yield (g)	Productivity (kg CP/g Pd) [b]	Mw (Mw/Mn)	TON[c]
1	**L15**	S	0.86	0.64	31 000 (2.0)	2.18
2	**L15**	MS	0.57	0.42	8 000 (1.5)	5.61
3	**L15**	TBS	0.39	0.29	8 000 (1.7)	3.84
4	**L16**	S	5.10	3.78	256 000 (2.2)	1.57
5	**L16**	MS	7.27	5.38	302 000 (2.6)	1.89
6	**L16**	TBS	6.26	4.64	471 000 (2.1)	1.05

[a] Reaction conditions: $n_{Pd} = 1.27 \cdot 10^{-5}$ mol, V_{TFE} = 20 mL, V_{arene} = 10 mL, [S]/[Pd] = 6800, [MS]/[Pd] = 6000, [TBS]/[Pd] = 4300, T = 303 K, P_{CO} = 1 bar, [BQ]/[Pd] = 5, t = 24 h. [b] kg CP/g Pd = kilograms of copolymer per gram of palladium. [c] TON = moles of copolymer per mole of Pd.[9]

As far as the stereochemistry of the obtained polyketones was concerned, syndiotactic copolymers were produced with the **L16**-containing catalyst (Table 5.2, runs 4-6), whereas for the polyketones obtained with the **L15**-containing catalyst, the stereochemistry was strongly dependent on the vinyl arene comonomer. Indeed, whereas the CO/styrene copolymer was prevailingly syndiotactic (Table 5.2, run 1), the CO/MS polyketone was prevailingly isotactic (Table 5.2, run 2), and the CO/TBS macromolecule was atactic (Table 5.2, run 3). To the best of our knowledge, this is the first report concerning the influence of a substituent in the *para* position of the vinyl arene on the stereochemistry of the produced polyketones.[9]

Table 5.2. Triads distribution in the polyketones. Precatalyst: $[Pd(CH_3)(NCCH_3)(\mathbf{N\text{-}N})][PF_6]$[a]

RUN	N-N'	Vinyl arene	Stereochemistry			
			ll (%)	*lu* (%)	*ul* (%)	*uu* (%)
1	**L15**	S	16	16	16	52
2	**L15**	MS	47	17	18	18
3	**L15**	TBS	30	37		33
4	**L16**	S	-	13	16	71
5	**L16**	MS	-	21	19	60
6	**L16**	TBS	-	15	10	75

[a] Determined by ^{13}C NMR spectra recorded in HFIP/$CDCl_3$, T = 298 K, integration of C_{ipso} signals.[9]

With the aim to investigate in more detail the effect on the nature of the ligand on the stereochemistry of the obtained macromolecules, the simplest possible pyridylimines, featured by a phenyl ring on the imino carbon atom, ligands **13-16** (Figure 5.3), were synthesized and used to obtain the corresponding palladium(II) neutral $[Pd(CH_3)Cl(N\text{-}N')]$ and monocationic complexes $[Pd(CH_3)(NCCH_3)(N\text{-}N')][PF_6]$ to be applied as precatalysts for the CO/vinyl arene copolymerization reaction.

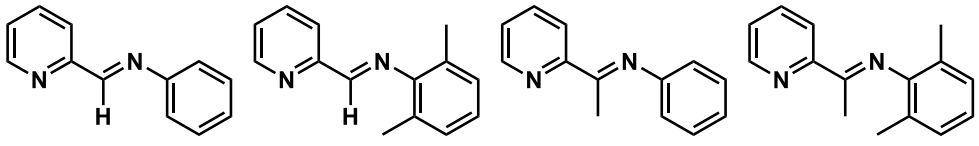

Figure 5.3. The studied pyridylimine ligands **13-16**.

5.2. Results and Discussion.

5.2.1. Synthesis and characterization of ligands 13-16.

Ligands **13**, **14** and **16** were synthesized following slightly modified literature procedures,[3] consisting in the condensation reaction of the carbonyl derivative of pyridine with the proper aniline, optimizing the reaction time and the ratio between the reagents (Scheme 5.1).

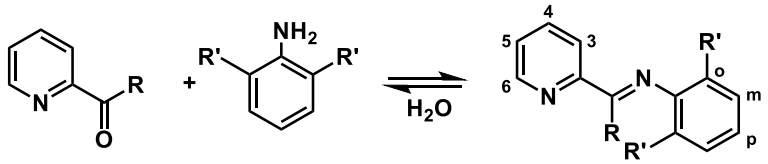

13: R = R' =H
14: R = H, R' = CH_3
16: R = R' = CH_3

Scheme 5.1. Synthesis of ligands **13**, **14**, **16** and their numbering scheme.

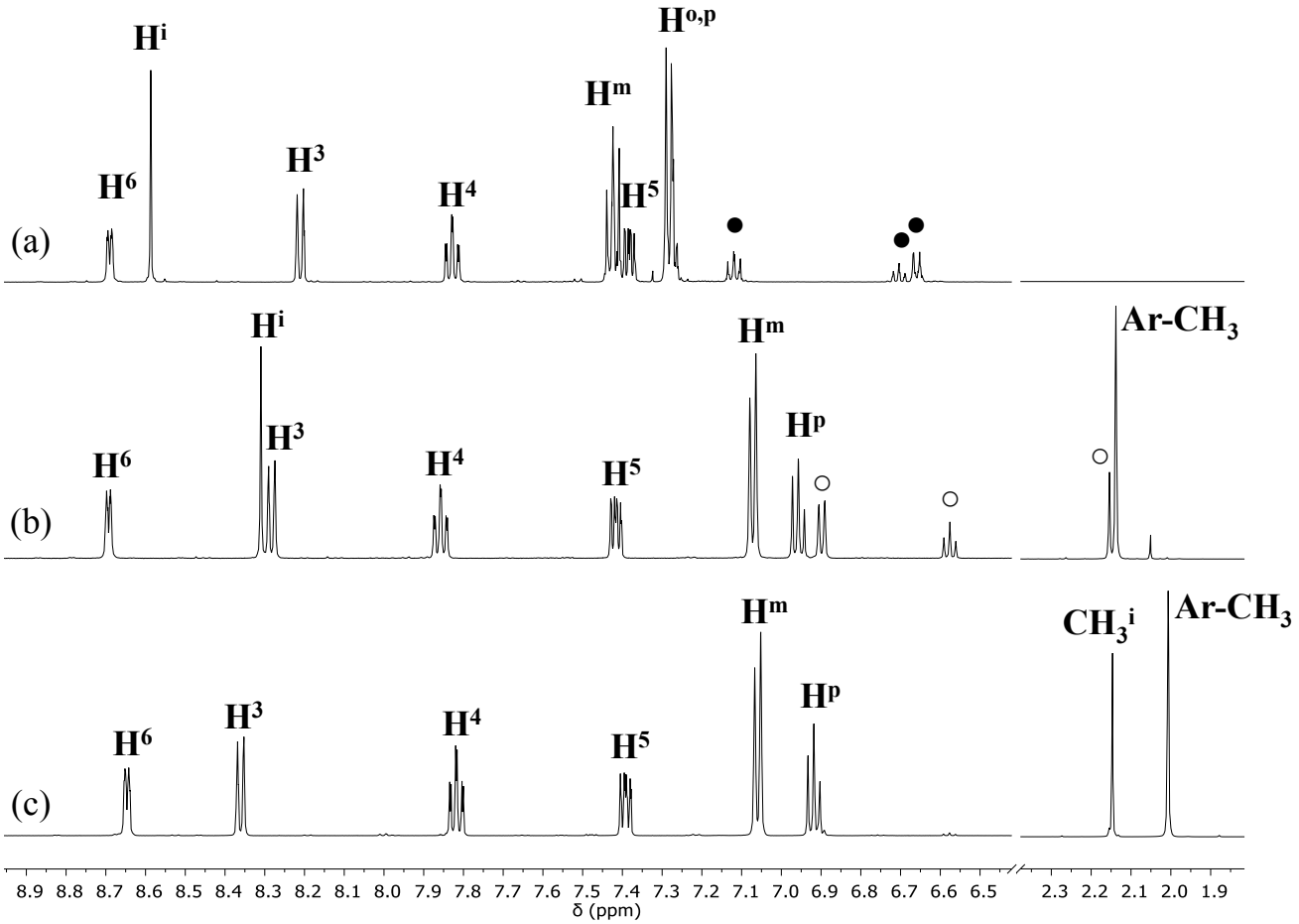

Figure 5.4. ^1H NMR spectra in CD_2Cl_2 at 298 K of (a) **13**; (b) **14**; (c) **16**; ● aniline; ○ 2,6-dimethylaniline. Aliphatic and aromatic regions are not on scale.

The yields were in the range 40 - 80 %, and the NMR characterization in solution was in agreement with that reported in the literature.[3,10] In some cases, traces of unreacted anilines were still present, but they did not affect the subsequent reaction with the palladium precursor to obtain the corresponding neutral derivatives (Figure 5.4).

The NMR spectra highlighted that moving from **13** to **14**, the singlet of the proton on the imino carbon atom moved to lower frequency (8.59 ppm *vs* 8.31 ppm, respectively), as well as moving from **14** to **16**, the singlet of the methyl groups on the aryl ring shifted in the same direction (2.14 ppm *vs* 2.01 ppm, respectively), indicating that these signals are mutually affected by the introduction of the methyl groups either on the *ortho* positions of the aryl ring (going from **13** to **14**) or on the imino carbon atom (going from **14** to **16**) and suggesting that these positions are crucial in determining the electron density on the imino fragment of the ligand and therefore, they might have a key role in the catalytic behavior of the relevant complexes

When the same synthetic procedure was applied to obtain ligand **15**, the desired product was obtained in a 15 % yield after 72 h, and a longer reaction time resulted in the formation of unidentified byproducts, only. A different approach was tested, using a Dean-Stark apparatus, and running the reaction in toluene at reflux for 6.5 h; the crude reaction mixture, after removing the solvent, contained the desired ligand in 30 % yield together with the reagents, and it was not possible to purify it through column chromatography. Since the aim was to obtain the palladium derivatives, we decided to synthesize directly the neutral complex [Pd(CH_3)Cl(**15**)] by performing a template reaction, as discussed afterwards.

5.2.2. Synthesis and characterization of neutral Pd-complexes 13a-16a.

Ligands **13**, **14**, **16** were reacted with [Pd(cod)(CH_3)Cl] to yield the corresponding neutral derivatives [Pd(CH_3)Cl(N-N')] (N-N' = **13**, **13a**; **14**, **14a**; **16**, **16a**) following the well-established procedure,[11] and they were isolated as yellow solids in high yields (87 – 94 %). All the synthesized complexes were fully characterized by homo- and heteronuclear, mono- and bidimensional, NMR experiments in CD_2Cl_2 solution, and in solid state via X-ray diffraction.

Complex **15a** was obtained by reacting 2-acetyl pyridine with a slight excess of aniline in the presence of [Pd(cod)(CH_3)Cl] as templating agent (Scheme 5.2); the product was obtained pure in a 67 % yield.

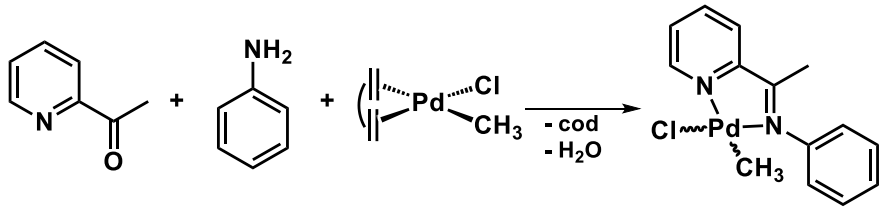

Scheme 5.2. Template synthesis of complex **15a**.

As reported for the palladium complexes with pyridylimine ligands **L15**, **L16**,[9] and for those with the nonsymmetric BIAN (**L12**, **5**, **6**) and DAB (**10**) ligands (Chapters 3, 4), even for ligands **13-16**, upon coordination to palladium in a nonsymmetric environment, two isomers are possible, differing for the relative position of the Pd-CH_3 fragment with respect to the two inequivalent moieties of the ligand. As described in literature,[8] we have defined as the *cis* isomer the species featured by the Pd-CH_3 fragment *cis* to the Pd-N bond of the imino nitrogen atom (Figure 5.5).

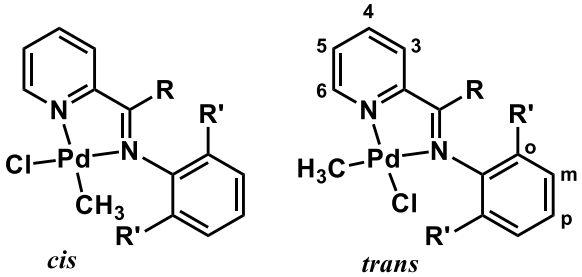

Figure 5.5. Possible isomers of complexes **13a-16a** with the related numbering scheme.

In the ^{1}H NMR spectra of the neutral derivatives, sharp signals were observed at room temperature, in agreement with the characterization reported for similar complexes (Figure 5.6).[9] In all cases, two sets of signals were present, with different intensities, indicating the presence of both *cis* and *trans* isomers in solution, although for complexes **14a** and **16a**, both sharing the presence of methyl groups on the aryl ring, only traces of the minor species were observed.

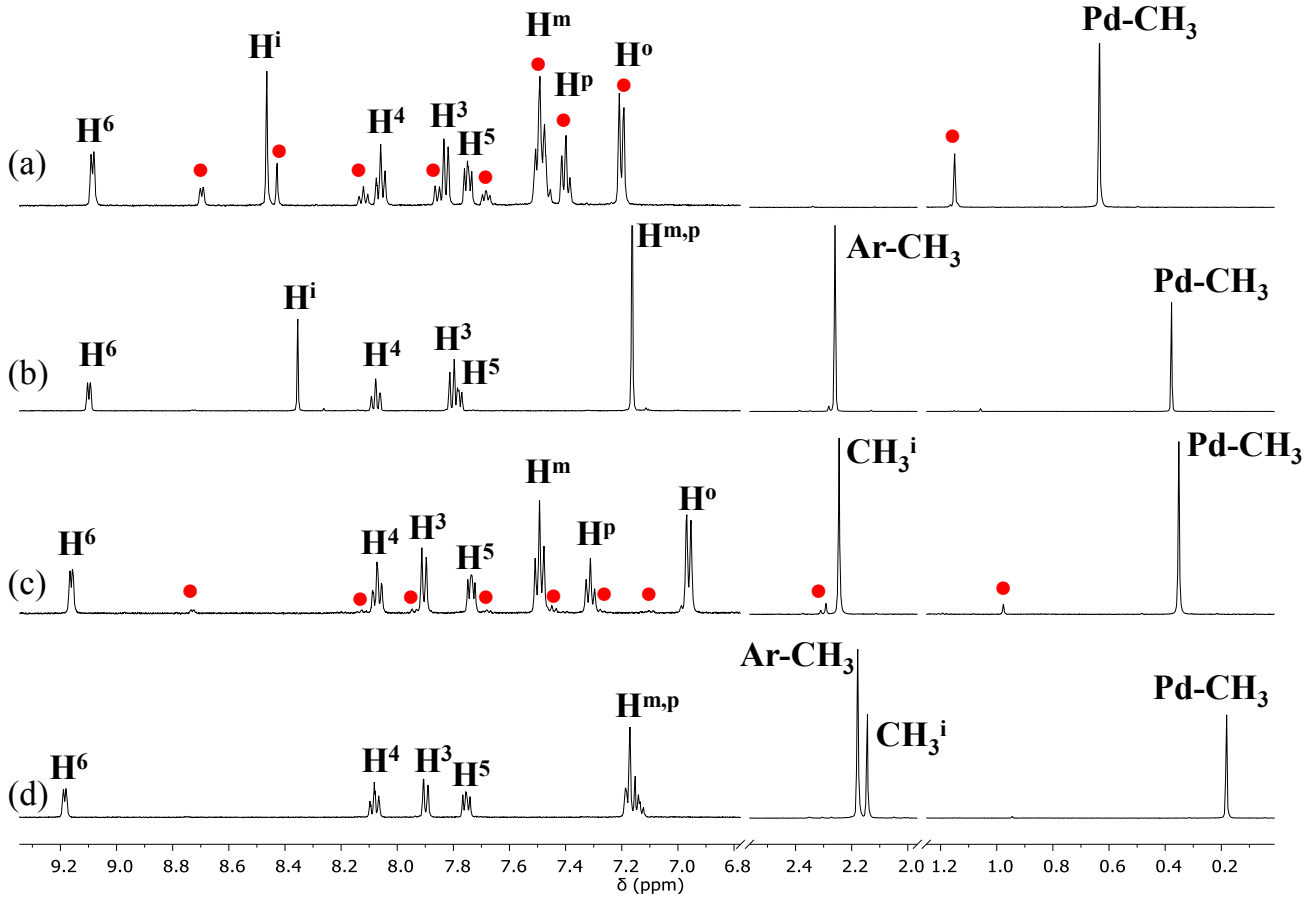

Figure 5.6. ^{1}H NMR spectra in CD_2Cl_2 at 298 K of (a) **13a**; (b) **14a**; (c) **15a**; (d) **16a**: *cis* (black) and *trans* (red) isomers. Aliphatic and aromatic regions are not on scale.

For all complexes, the major species was identified as the *cis* isomer from NOE experiments performed upon irradiation of the Pd-CH_3 singlet of the major species: for **13a** and **15a** an NOE peak with the singlet of the protons in *ortho* positions on the aryl ring was observed (Figure 5.7a), while for **14a** and **16a** the NOE peak with the singlet of the methyl groups of the aryl ring was present. To demonstrate the validity of these assignments for complex **13a** an NOE experiment was performed by irradiating the singlet the Pd-CH_3 moiety of the minor species and observing the NOE effect with the doublet due to H^6 of the pyridine ring, confirming that the minor species is the *trans* isomer (Figure 5.7b).

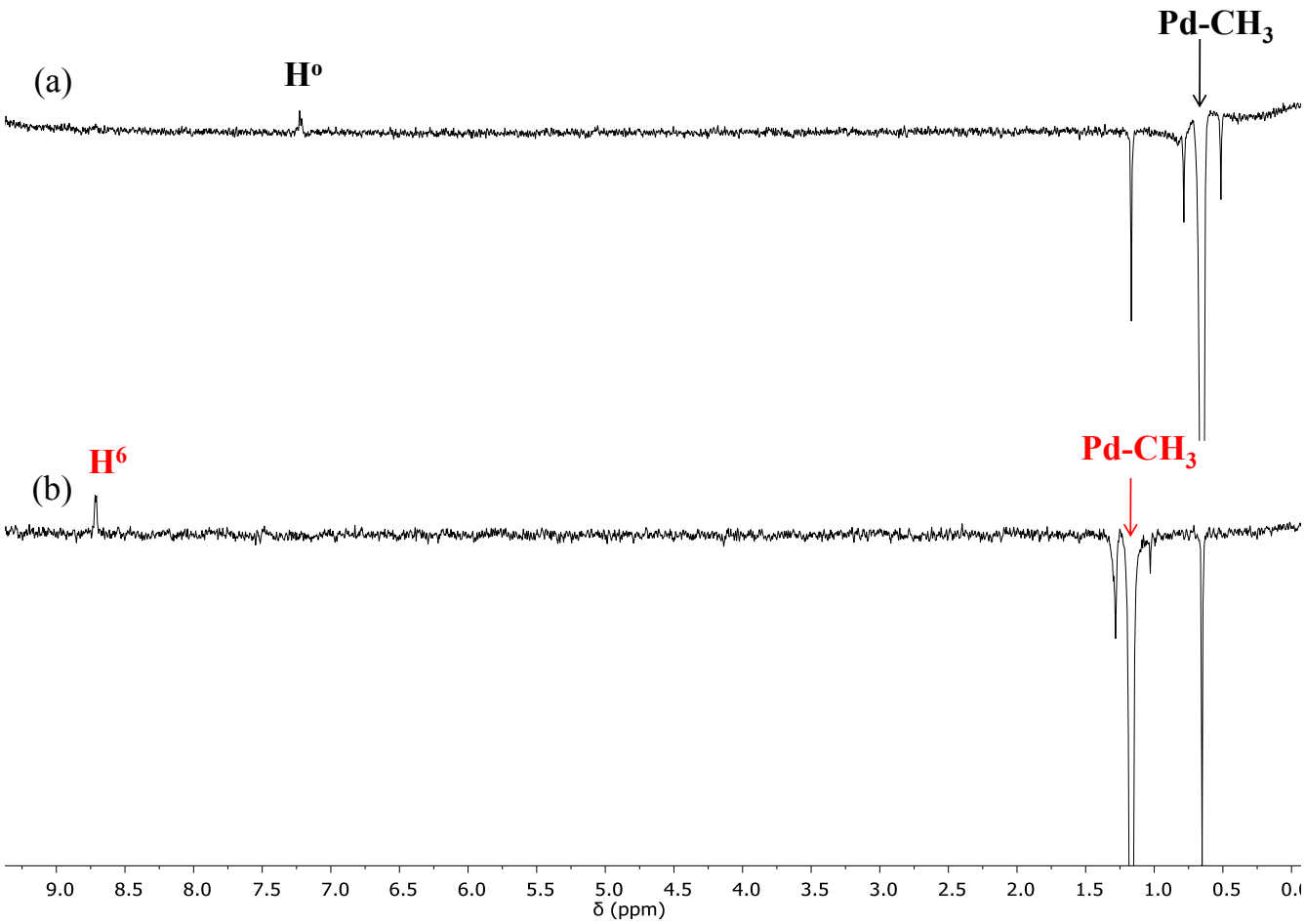

Figure 5.7. NOE spectra in CD_2Cl_2 at 298 K of **13a** obtained by irradiating the Pd-CH_3 signal of (a) *cis* and (b) *trans* isomer.

In addition, in the NOE spectra of complexes **13a** and **15a**, when the Pd-CH_3 singlet of the *cis* isomer was irradiated, a negative peak for the Pd-CH_3 peak of the other species was observed, thus indicating that the two isomers are in exchange at slow rate on the NMR timescale, at room temperature. The preference for the *cis* isomer observed for all the studied complexes is in agreement with the strong *trans* influence of the methyl group that prefers to coordinate *trans* to the nitrogen atom with the lower Lewis basicity, which, in the case of pyridylimino ligands, is the pyridine nitrogen. This is in agreement with the behavior reported for the neutral palladium complexes with ligands **L15**, **L16**,[9] as well as for other similar palladium complexes with pyridylimines **L17-19**[6] and **L20**[4] (Figure 5.8).

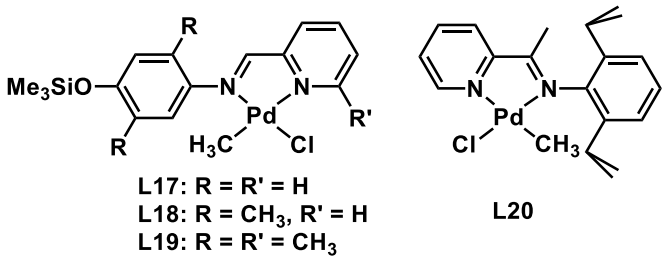

Figure 5.8. Palladium(II) neutral complexes with pyridylimine ligands reported in the literature.[4,6]

The *cis* : *trans* ratio, determined from the ^{1}H NMR spectra, depends on the nature of the ligand coordinated on the palladium center: the selectivity in the *cis* isomer increased moving from **13a** to **16a**, in the order **13a** < **15a** < **14a** < **16a** (Table 5.3). Since in the same direction the number of electronic repulsing methyl groups on the ligand increased, thus enhancing the electronic differentiation of the two nitrogen-donor atoms, this trend suggests that the distribution of the two isomers is mainly driven by the electronic properties of the ancillary ligand, assuming that the methyl group and the chlorido coordinated to palladium are assimilated to spheres having similar steric hindrance.

Table 5.3. Isomer composition for complexes **13a-16a**.[a]

%	**13a**	**14a**	**15a**	**16a**
cis	75	97	94	98
trans	25	3	6	2

[a] determined from ^{1}H NMR spectra.

Comparing the chemical shift of the signals of the neutral complexes with those reported for the corresponding free ligands, protons H^6 and H^3 were the most sensitive for the coordination to palladium, and their signals moved in opposite directions: proton H^6 shifted to higher frequency, while H^3 moved to lower frequency, due to the change from the *E,anti* conformation of the free ligand to the *E,syn* required for the coordination to the metal center (Table 5.4).

Table 5.4. Effect of the coordination to palladium on selected chemical shift values of the *cis* isomer.

Ligand/complex	H^6	H^i	H^3	$CH_3{}^i$	Ar-CH_3	Pd-CH_3 (^1H)	Pd-CH_3 (^{13}C)
13	8.69	8.59	8.21	-	-	-	-
14	8.69	8.31	8.28	-	2.14	-	-
16	8.65	-	8.36	2.15	2.01	-	-
13a	9.09	8.46	7.83	-	-	0.63	0.2
14a	9.10	8.35	7.84	-	2.26	0.38	-1.5
15a	9.16	-	7.91	2.24	-	0.35	-0.1
16a	9.19	-	7.90	2.14	2.18	0.18	-1.8

Chemical shifts are reported in ppm.

Focusing on the substituent on the imino carbon atom, either a proton or a methyl group, the coordination led to a sensible shift towards lower frequency only in the case of ligand **13**, while for the other ligands the effect of coordination was negligible.

The increase in the number of methyl groups on the ligand resulted in a progressive shift to lower frequency of the Pd-CH_3 singlet both in the ^1H and in the ^{13}C NMR spectra; in particular, in the latter the difference is less pronounced when the proton on the imino carbon atom is replaced with the methyl group (**13a** *vs* **15a**, $|\Delta\delta|$ = 0.3 ppm; **14a** *vs* **16a**, $|\Delta\delta|$ = 0.3 ppm), while it is more pronounced for the introduction of the methyl groups on the aryl rings (**13a** *vs* **14a**, $|\Delta\delta|$ = 1.7 ppm; **15a** *vs* **16a**, $|\Delta\delta|$ = 1.7 ppm). These trends highlighted that the Pd-CH_3 signal is a sensitive probe for the electron density on the palladium center, as already observed for complexes with ligands **L15** and **L16**[9] and with α-diimines (Chapters 3, 4).

Single crystals suitable for X-ray diffraction were obtained by slow diffusion of n-hexane in a CH_2Cl_2 solution of complexes **13a**, **15a** and **16a** at 277 K (Figures 5.9 and 5.10).

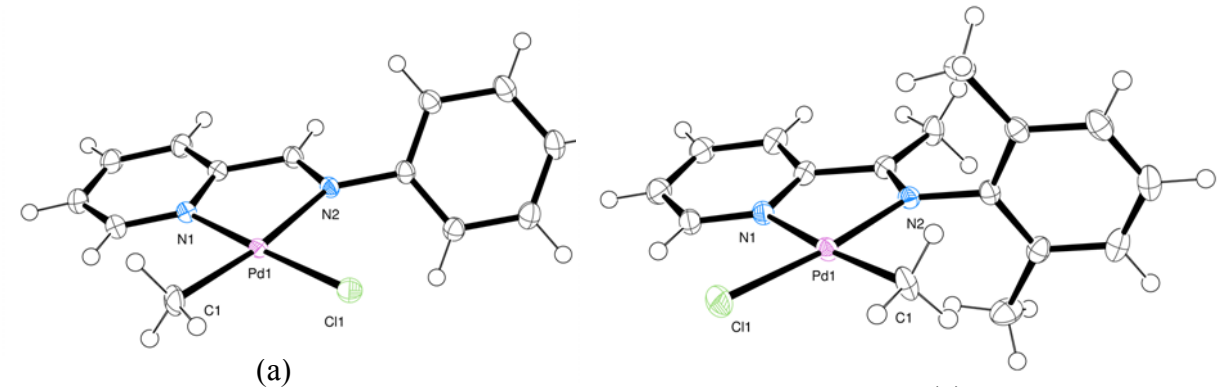

(a)

Figure 5.10. ORTEP representation of (a) **13a**, (b) **16a**.

Table 5.5. Selected bond lengths (Å) and angles (°) for complexes **13a** and **16a**.

	13a	**16a**
Pd(1)-N(1)	2.0359(16)	2.1687(14)
Pd(1)-N(2)	2.1305(18)	2.0527(16)
Pd(1)-C(1)	2.0401(18)	2.0484(18)
Pd(1)-C(l1)	2.3020(8)	2.3055(7)
N(1)-Pd(1)-N(2)	79.04(6)	78.27(7)
C(1)-Pd(1)-Cl(1)	88.64(6)	89.13(5)
C(1)-Pd(1)- N(1)	93.89(7)	173.10(7)
N(2)-Pd(1)-Cl(1)	98.46(4)	174.47(5)
Dihedral angle	53.42(5)	84.17(7)

For both **13a** and **16a** the palladium center was featured by the expected square planar geometry, and in both cases the unit cell contained a single molecule. For **13a** the complex was characterized by having the Pd-CH_3 fragment *trans* to the imino nitrogen atom, corresponding to the minor species observed in solution; on the other hand, for **16a** the only species present in the unit cell had the Pd-CH_3 fragment *cis* to the imino nitrogen atom, corresponding to the main isomer detected in solution.

In both complexes the Pd-N bond distances *trans* to the Pd-CH_3 fragment were significantly shorter than the corresponding Pd-N bond distances *trans* to the Pd-Cl bond, in agreement with the stronger *trans* influence of the methyl group with respect to that of the chlorido (Table 5.5). The dihedral angle between

the aryl ring and the square plane was 84.17° in **16a**, indicating that it is nearly orthogonal to the plane, while in **13a** the aryl ring was significantly more bent towards the Pd-Cl fragment, with an angle of 53.42°. This difference is in agreement with the values of the dihedral angles observed in the crystal structures of the palladium neutral complexes with the α-diimines, where the aryl ring *cis* to the Pd-CH_3 fragment was found to be more orthogonal to the square plane of the complex than the aryl ring *cis* to the Pd-Cl moiety (Figures 3.5, 4.10 and Table 3.2).

As far as **15a** was concerned, two independent molecules were observed in the unit cell, both featured by the expected square planar geometry around the palladium and by the Pd-CH_3 fragment *cis* to the imino nitrogen atom, which is the same isomer found as major species in solution (Figure 5.10). Little differences in the bond distances and angles were observed between the two independent molecules (Table 5.6).

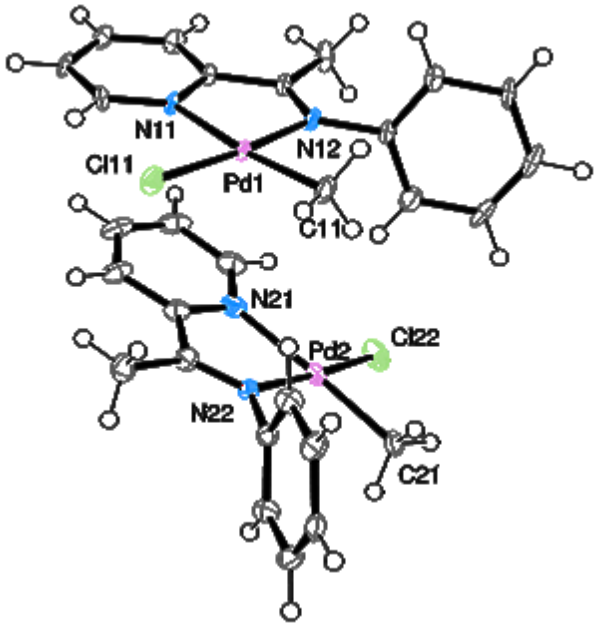

Figure 5.10. ORTEP representation of **15a**.

Table 5.6. Selected bond lengths (Å) and angles (°) for complex **15a**.

Pd(1)-N(12)	2.0416(16)	Pd(2)-N(22)	2.0501(17)
Pd(1)-N(11)	2.1293(16)	Pd(2)-N(21)	2.1161(19)
Pd(1)-C(11)	2.030(2)	Pd(2)-C(21)	2.044(2)
Pd(1)-Cl(11)	2.2934(5)	Pd(2)-C(21)	2.2972(5)
C(11)-Pd(1)-Cl(11)	90.41(7)	C(21)-Pd(2)-Cl(22)	88.37(6)
C(11)-Pd(1)-N(11)	172.73(8)	C(21)-Pd(2)-N(21)	175.59(8)
C(11)-Pd(1)-N(12)	94.44(8)	C(21)-Pd(2)-N(22)	97.30(7)
N(11)-Pd(1)-Cl(11)	96.24(5)	N(21)-Pd(2)-Cl(22)	96.04(5)
N(12)-Pd(1)-Cl(11)	174.81(4)	N(22)-Pd(2)-Cl(22)	173.65(5)
N(12)-Pd(1)-N(11)	78.83(6)	N(22)-Pd(2)-N(21)	78.29(7)
Dihedral angle	80.649(0.052)	Dihedral angle	77.922(0.54)

As expected, the Pd-N bond distance *trans* to the Pd-CH_3 fragment was significantly shorter than the corresponding Pd-N bond distance *trans* to the Pd-Cl in both independent molecules, in agreement with the stronger *trans* influence of the methyl group with respect to that of the chlorido (Table 5.6).

The dihedral angle between the plane of the aryl ring and the coordination plane was about 80° in both molecules.

Single crystals of **14a** suitable for X-ray diffraction were obtained by slow diffusion of n-hexane in a $CDCl_3$ solution at 277K; in the unit cell two independent molecules were observed, both featured by the expected square planar geometry around the palladium and the pyridylimine coordinated as a bidentate ligand, but, in contrast with the structures of **13a, 15a** and **16a**, the coordination sphere was completed by two chloride ions (Figure 5.11). It was already reported for organometallic Pd(II) complexes with nitrogen-donor ligands that during the crystallization process the methyl group can be replaced by a chlorido due to the presence of traces of HCl in the chloroform, that protonate the methyl group to methane, generating a coordinative vacancy that is occupied by the chlorido.[12]

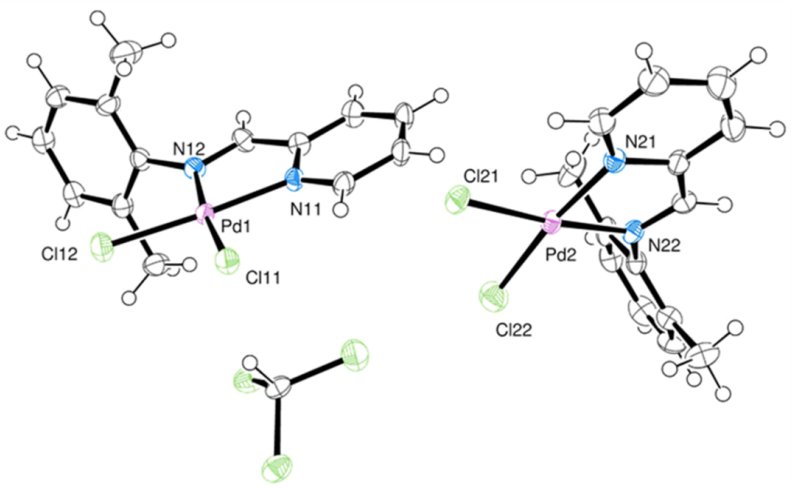

Figure 5.11. ORTEP representation of **14a**.

The Pd-N bond distance was shorter for the imino nitrogen with respect to that of the pyridine nitrogen, in confirming the stronger Lewis basicity of the former; in both molecules the aryl ring is nearly orthogonal to the coordination plane, with dihedral angles of 81.97° and 75.56° (Table 5.7).

Table 5.7. Selected bond lengths (Å) and angles (°) for complex **14a**.

Pd1-N12	2.025(2)	Pd2-N22	2.030(2)
Pd1-N11	2.044(2)	Pd2-N21	2.045(3)
Pd1-Cl12	2.2685(9)	Pd2-Cl22	2.2654(13)
Pd1-Cl11	2.2876(8)	Pd2-Cl21	2.2966(8)
N12-Pd1-N11	80.60(10)	N22-Pd2-N21	80.48(10)
N12-Pd1-Cl12	95.07(7)	N22-Pd2-Cl22	94.92(8)
N11-Pd1-Cl12	175.51(7)	N21-Pd2-Cl22	173.07(7)
N12-Pd1-Cl11	173.46(7)	N22-Pd2-Cl21	174.43(8)
N11-Pd1-Cl11	93.33(7)	N21-Pd2-Cl21	95.16(7)
Cl12-Pd1-Cl11	90.95(3)	Cl22-Pd2-Cl21	89.73(4)
Dihedral angle	81.97(9)	Dihedral angle	75.56(8)

The NMR characterization of the neutral complexes was completed by measuring the chemical shift of the N-atoms in order to evaluate the possible presence of an effect of the structure of the ligands. The nuclear properties of ^{15}N, such as its very low natural abundance and its rather low and negative

gyromagnetic ratio, render acquisition of ^{15}N data employing the $\{^{1}H,^{15}N\}$-HMBC experiment the method of choice, provided a suitable $^{n}J(^{15}N, ^{1}H)$ is present. The coupling constant was not available from literature, and it had to be determined through a trial-and-error approach, highlighting that for the studied ligands **13**, **14** and **16** a suitable value for ^{2}J was 3 Hz, while for the neutral complexes **13a-16a** the value had to be increased to 4 or 5 Hz. The ^{15}N chemical shifts were assigned on the basis of their cross peaks with the signal of the closest proton to each nitrogen atom in the molecule. As an example, the spectra of ligand **1** and the corresponding neutral derivative **13a** are discussed (Figures 5.12-5.13).

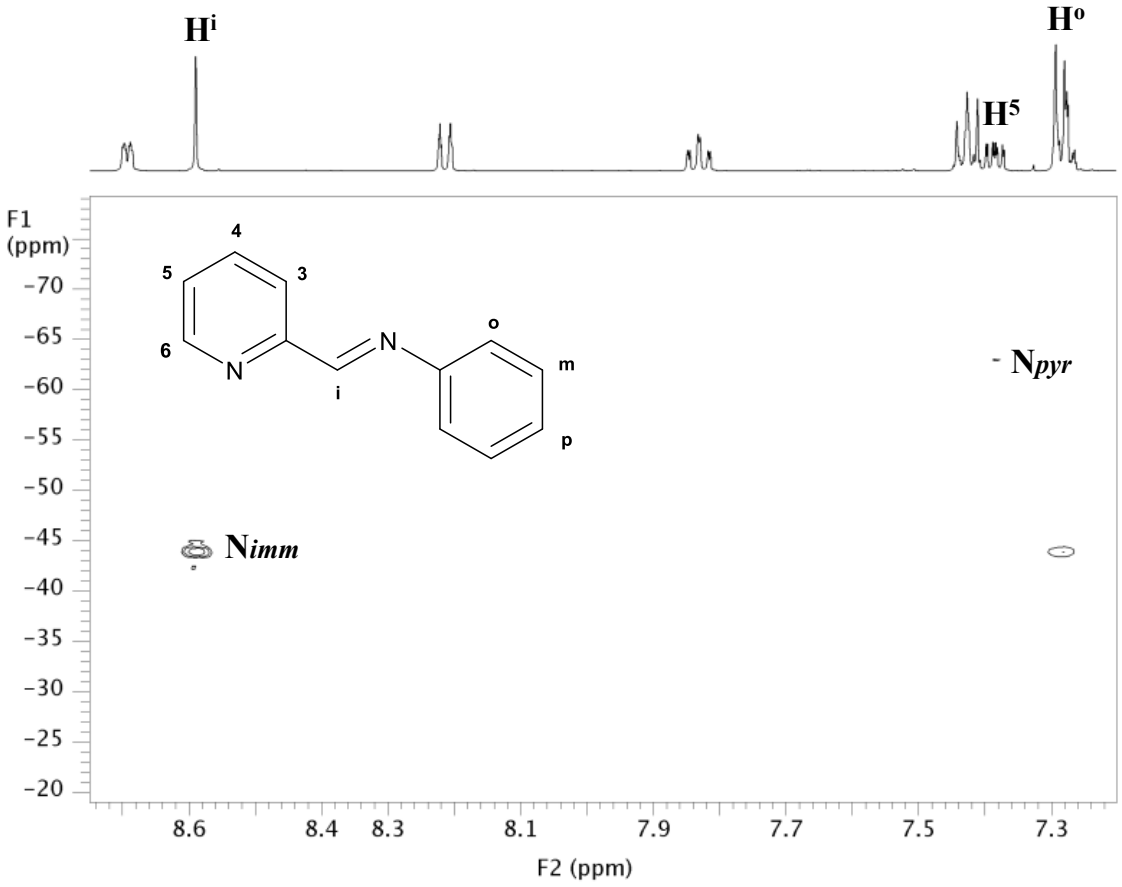

Figure 5.12. $\{^{1}H,^{15}N\}$-HMBC spectrum of ligand **13** in CD_2Cl_2 at 298 K.

In the spectrum of ligand **13** the cross peaks between the imino nitrongen (N*imm*) and both the proton on the imino carbon atom and that in the *ortho* position of the aryl ring were observed, as well as the cross peak between the pyridine nitrogen (N*pyr*) and H^5 (Figure 5.12).

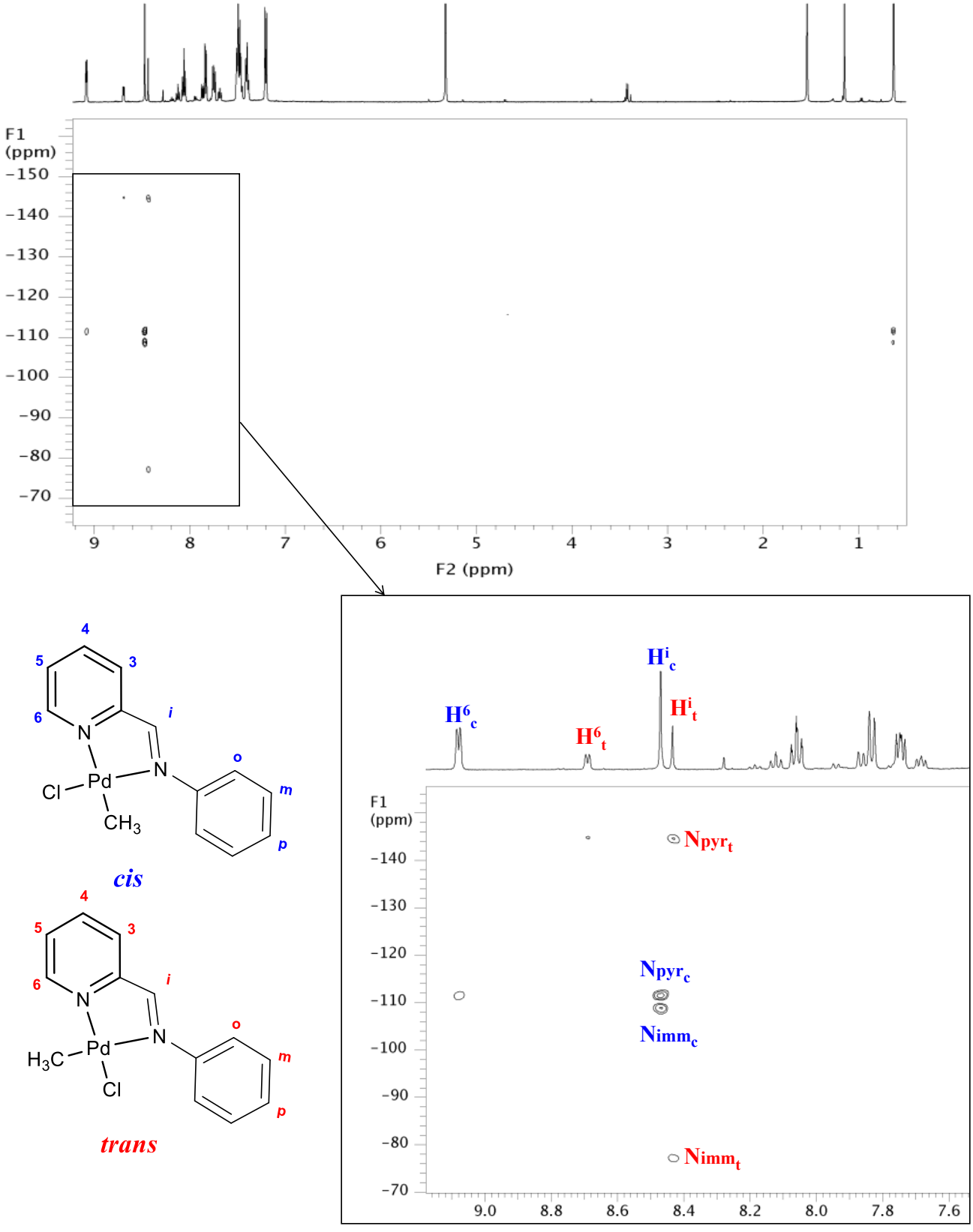

Figure 5.13. $\{^1H,^{15}N\}$-HMBC spectrum of **13a** in CD_2Cl_2 at 298 K.

As previously discussed, complex **13a** was observed in solution as a mixture of the *cis* and *trans* isomer in a 3 : 1 ratio in slow exchange on the NMR timescale at room temperature. In the corresponding $\{^1H,^{15}N\}$-HMBC, recorded using $^2J = 5$ Hz, the cross peaks of both nitrogen atoms in both isomers were observed, thus allowing to measure the related chemical shift. In fact, N*pyr* generated cross peaks with both H^6 and H^i in both species, as well as with the Pd-CH_3 fragment in the *cis* isomer. The latter was more intense than the cross peak between the N*imm* and the Pd-CH_3 in the same species, in agreement with the literature.[13] For N*imm* the cross peaks with the imino proton of both isomers were observed (Figure 5.14).

From this analysis the Coordination Induced Shift (CIS) was calculated for the nitrogen atoms of **13a**, observing that coordination to palladium resulted in a shift of 30-90 ppm in absolute value of the frequency of the ^{15}N (Table 5.8). In agreement with the literature data,[13] the CIS value for the nitrogen atom *trans* to the Pd-CH_3 fragment was lower with respect to that observed for the nitrogen atom *trans* to the chlorido (Table 5.8, 48.4 ppm *vs* 81.8 ppm e 33.3 ppm *vs* 65.1 ppm).

Table 5.8. Chemical shift values of ^{15}N for ligands **13**, **14**, **16** and complexes **13a**-**16a**.[a]

Ligand/complex	N*pyr* (CIS)	N*imm* (CIS)
1	-63.0	-43.9
1a	-111.4 (-48.4)$_{cis}$, -144.8 (-81.8)$_{trans}$	-109.0 (-65.1)$_{cis}$, -77.2 (-33.3)$_{trans}$
2	n.o.	-34.3
2a	-111.7$_{cis}$	-107.9 (-73.6) $_{cis}$
3a	-112.5$_{cis}$	-116.9$_{cis}$, -80.82$_{trans}$
4	n.o.	-44.2
4a	-112.3$_{cis}$	-118.6 (-74.4)$_{cis}$

[a] Measures at 50.64 MHz in CD_2Cl_2 at 298 K; chemical shifts are reported in ppm; CIS = Coordination Induced Shift, obtained as difference between the chemical shift of the complex and of the related ligand.

5.2.3. Synthesis and characterization of monocationic Pd-complexes 13b-16b

Complexes **13a-16a** were reacted with $AgPF_6$ in the presence of acetonitrile to yield the corresponding monocationic complexes, **13b-16b**, following the reported procedure,[11] and the desired complexes were obtained with average yields of 70 - 90 %.

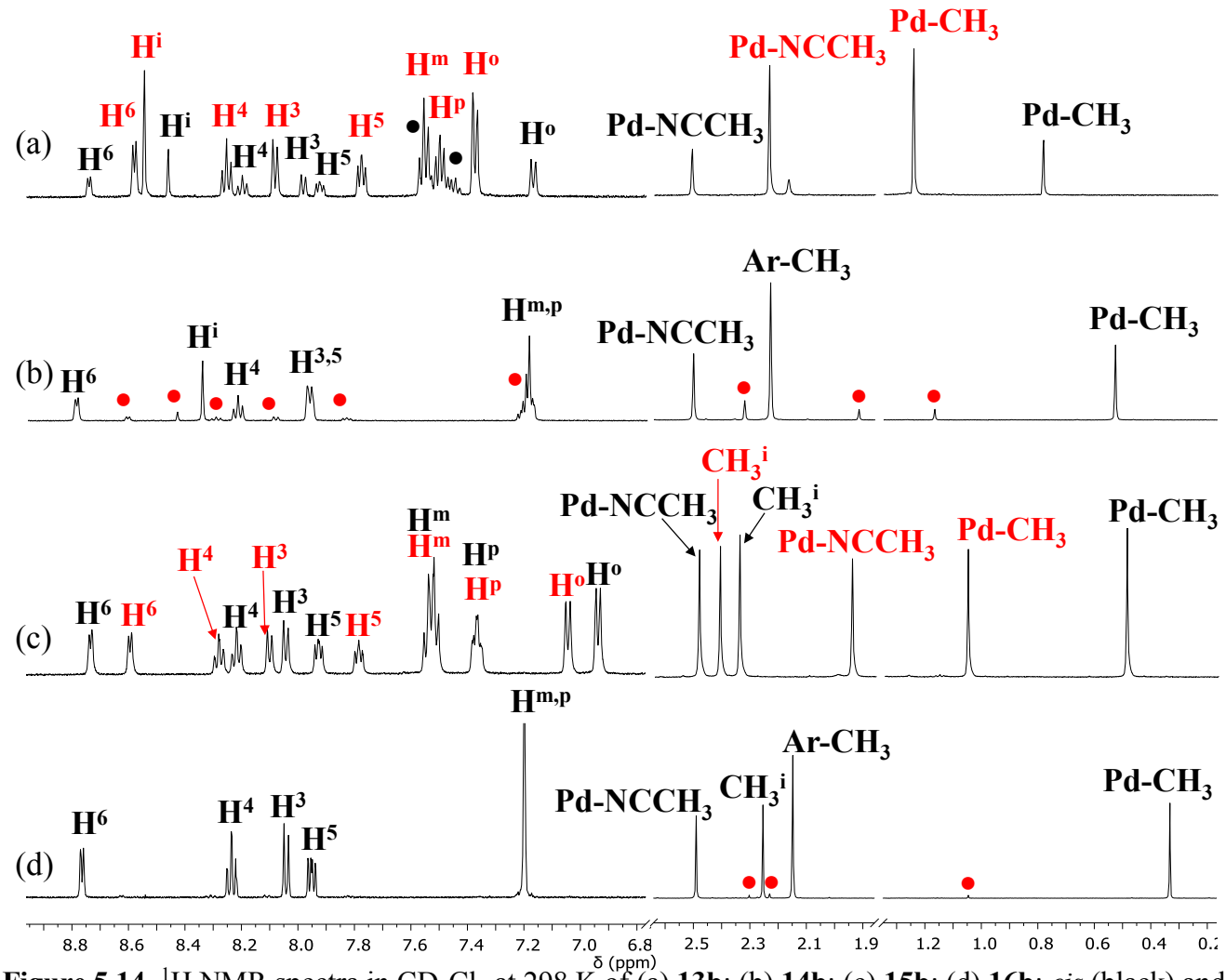

Figure 5.14. ^{1}H NMR spectra in CD_2Cl_2 at 298 K of (a) **13b**; (b) **14b**; (c) **15b**; (d) **16b**: *cis* (black) and *trans* (red) isomers. Aliphatic and aromatic regions are not on scale.

In the ^{1}H NMR spectra of all complexes sharp signals were observed at room temperature (Figure 5.14), in agreement with the behavior observed for Pd-$NCCH_3$ derivatives with ligands **L15** and **L16**.[8] As for the neutral complexes, two sets of peaks were observed, indicating that both *cis* and *trans* isomers were present in solution. They were identified on the basis of NOE experiments recorded at room temperature by irradiating a Pd-CH_3 singlet and observing positive signals for either H^o or Ar-CH_3 in the case of the *cis* isomers, or for H^6 in the case of the *trans* derivatives (Figure 5.15). The NOE experiments also highlighted, for the complexes in which the ratio between the two species was closer to one, that the two isomers were in exchange at slow rate on the NMR timescale, at room temperature.

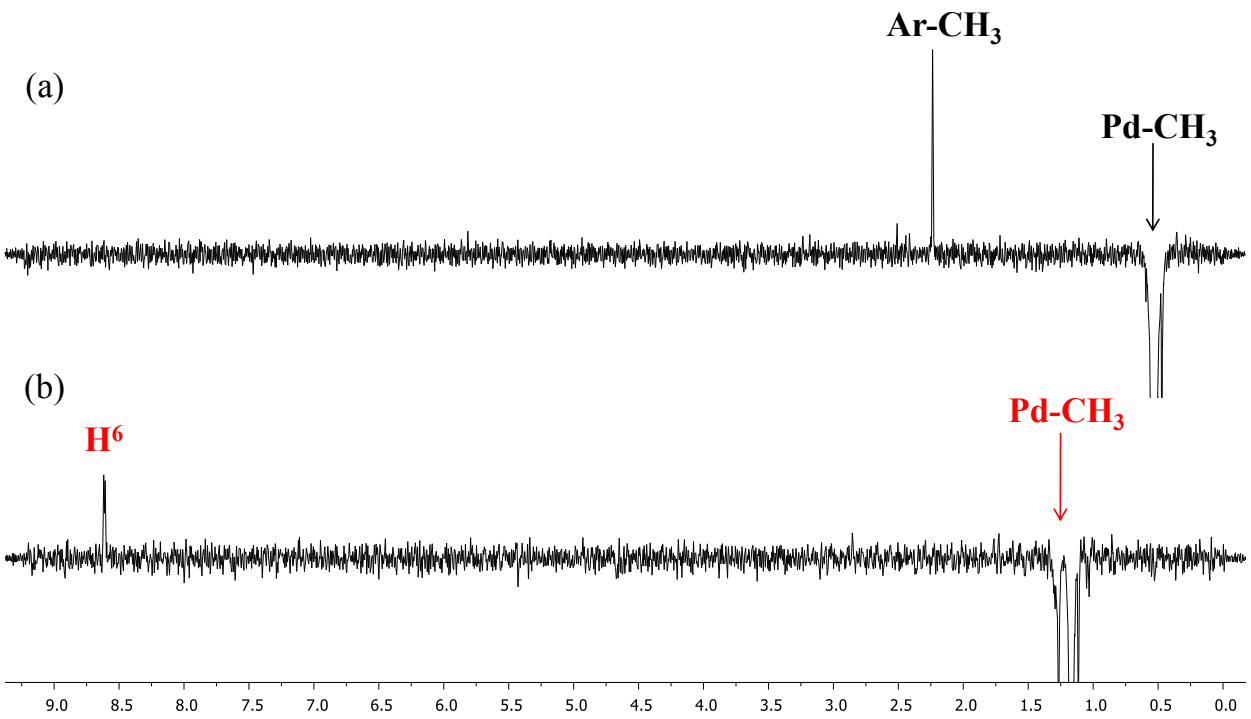

Figure 5.15. NOE spectra in CD2Cl2 at 298 K of **14b** obtained by irradiating the Pd-CH_3 signal of (a) *cis* and (b) *trans* isomer.

The comparison of the isomer composition between the neutral and the monocationic complexes pointed out that moving from the neutral to the corresponding monocationic complexes a loss in stereoselectivity was obtained. In fact, while for the neutral derivatives the *cis* isomer was always the prevailing species in solution (Table 5.3), for the Pd-$NCCH_3$ complexes the major isomer depended on the nature of the ligand (Table 5.9): the *cis* isomer was the major species for **14b** and **16b**, while it was the minor species for **1b** and a nearly 1 to 1 ratio between the two isomers was found for **15b**.

Table 5.9. Isomer composition for complexes **13b-16b** (values of the neutral derivatives in brackets).[a]

%	**13b (13a)**	**14b (14a)**	**15b (15a)**	**16b (16a)**
cis	26 (75)	87 (97)	46 (94)	97 (98)
trans	74 (25)	13 (3)	54 (6)	3 (2)

[a] determined from ^{1}H NMR spectra.

A possible explanation for the observed different isomeric composition might be related to the fact that when the chlorido ion was replaced by the linear acetonitrile, it might be envisaged that the difference in

steric hindrance of the two groups coordinated on palladium, methyl *vs* acetonitrile, was now increased with respect to the difference between methyl and chloride, thus suggesting that steric effects started to play a role in determining the stereoselectivity of the prevailing isomer. In fact, whereas the prevalence of the *cis* isomer for **14b** and **16b**, both featured by having methyl groups on the aryl ring of the ligand, indicated that the electronic effects are still dominating in determining the prevailing isomer, for complexes **13b** and **15b** the higher relative amount of the *trans* isomer suggested that the isomer distribution in solution was the result of both electronic and steric factors. However, it has to be pointed out that the difference in the ground state energy of the two isomers should not be that high and that DFT calculations would help in clarifying the discussed aspects.

fact, Focusing on the chemical shift of the most indicative signals for the coordination to palladium reported in Table 5.10, proton H^6 in the monocationic *cis* complexes resonated at lower frequency than in the neutral derivatives, in agreement with the substitution of the chlorido ion with the acetonitrile in the palladium coordination sphere.

Table 5.10. Effect of the coordination to palladium on selected chemical shift values (values of the neutral derivatives in brackets).

Ligand/complex	H^6	$H^i/CH_3{}^i$	Ar-CH_3	Pd-$CH_3{}^{cis}$	Pd-$CH_3{}^{trans}$
13b (13a)	8.74 (9.09)	8.46 (8.46)	-	0.78 (0.63)	1.24 (1.15)
14b (14a)	8.79 (9.10)	8.35 (8.35)	2.23 (2.26)	0.53 (0.38)	1.17
15b (15a)	8.74 (9.16)	2.34 (2.24)	-	0.49 (0.35)	1.05
16b (16a)	8.76 (9.19)	2.25 (2.14)	2.15 (2.18)	0.33 (0.18)	1.05

Chemical shifts are reported in ppm.

As already observed for the neutral complexes, the Pd-CH_3 singlet progressively shifted towards lower frequency moving from **13b** to **16b**, in both *cis* and *trans* isomers, thus further confirming that its resonance is a sensitive probe for the electron density on the palladium. However, the fact that the shift is much more pronounced for the *cis* than for the *trans* isomer, does not allow to rule out that this shift is originated by the combination of the increase in the electronic density on the metal center with the shielding effect of the aryl ring *cis* to Pd-CH_3 moiety. In fact, on increasing the number of the methyl groups on the ligand the aryl ring is more orthogonal to the square plane and the Pd-CH_3 fragment should be more affected by the its shielding cone.

5.2.4. CO/vinyl arene copolymerization reaction.

The synthesized monocationic complexes **13b-16b** were tested as precatalysts in the CO/vinyl arene copolymerization by performing the reaction under the same conditions reported for the complexes with pyrene-tagged pydirylimines,[8] that are 2,2,2-trifluoroethanol (TFE) as a solvent, at T = 303 K, under a CO pressure of 1 bar, for 24 h and with a slight excess of 1,4-benzoquinone (BQ) with respect to palladium (Scheme 2.1a). The vinyl arene could be either styrene (S) or 4-methyl-styrere (MS). The produced polyketones were isolated as white solids and characterized by ^{13}C NMR spectroscopy.

All complexes generated active catalysts for the target copolymerization reactions, showing a remarkable effect of the N-N' ligand on the productivity. Regardless to the vinyl arene used as comonomer, catalyst containing ligand **13** was the least productive, while the highest value of productivity was obtained with precatalyst **15b** (Table 5.11). It was interesting to note that for **13b** and **14b** moving from styrene to 4-methyl-styrene resulted in a decrease in productivity, while the opposite trend was observed for catalysts containing ligands **15** and **16**, both characterized by the presence of a methyl group on the imino carbon atom.

Table 5.11. CO/vinyl arene copolymerization reaction: effect of the N-N' ligand and of the vinyl arene. Precatalyst: $[Pd(CH_3)(NCCH_3)(\mathbf{N\text{-}N'})][PF_6]$[a]

RUN	N-N'	Vinyl arene	Yield (g)	Productivity (kg CP/g Pd) [b]	Mw (Mw/Mn)	TON[c]
1	**13**	S	1.54	1.14	9 000 (3.94)	13.47
2	**14**	S	4.82	3.57	102 000 (2.04)	3.72
3	**15**	S	5.86	4.34	217 000 (2.65)	2.13
4	**16**	S	3.56	2.64	402 000 (1.67)	0.70
5	**13**	MS	0.80	0.59	20 000 (2.07)	3.15
6	**14**	MS	3.61	2.67	174 000 (3.84)	1.63
7	**15**	MS	6.23	4.61	465 000 (8.08)	1.05
8	**16**	MS	4.24	3.14	1 775 000 (2.29)	0.19

[a] Reaction conditions: $n_{Pd} = 1.27 \cdot 10^{-5}$ mol, $V_{TFE} = 20$ mL, $V_{arene} = 10$ mL, [S]/[Pd] = 6800, [MS]/[Pd] = 6000, [BQ]/[Pd] = 5, T = 303 K, P_{CO} =1 bar, t = 24 h. [b] kg CP/g Pd = kilograms of copolymer per gram of palladium. [c] TON = moles of copolymer per mole of Pd.

As far as the CO/styrene copolymerization was concerned, negligible decomposition to inactive palladium black was observed for all the catalysts, while in the case of 4-methyl-styrene traces of palladium black were observed within the first 6 h of reaction, with the remarkable exception of **16b**. This suggested that the higher productivity found for **15b** was not related to a higher stability, but it might be ascribed to a higher intrinsic activity of the catalyst.

The molecular weight of the obtained polyketones increased in the order **13b** < **14b** < **15b** < **16b** regardless of the vinyl arene investigated, thus indicating that the ratio between the propagation and the termination rate increased in the same order. In addition, it also increased moving from styrene to 4-methyl-styrene, reaching values as high as 1 775 000 g mol^{-1}. Polydispersity values were rather high for homogeneous catalysts, in particular for the CO/4-methyl-styrene copolymer (Mw/Mn = 8.08) produced with precatalyst **15b**, suggesting that for these catalysts more than one species might be active in the copolymerization reaction, and this might be related to the presence of *cis* and *trans* isomers, as observed in solution for the monocationic complexes. The high value observed for **13b** with styrene should be ascribed to the low productivity and low molecular weight of the produced copolymer. To explain this behavior, a series of *in situ* NMR experiments will be performed by reacting the precatalysts with CO in the NMR tube.

The calculated turnover numbers (TON) followed the opposite trend, decreasing from **13b** to **16b** for both vinyl arenes, indicating that the increase in the productivity was due to an increase in the length of the polymer chains rather in their number.

The stereochemistry of the obtained polyketones was determined by ^{13}C NMR spectroscopy, recording the spectra in 1,1,1,3,3,3-hexafluoro-2-propanol (HFIP) at room temperature (Table 5.12).

All the isolated macromolecules had a prevailingly syndiotactic microstructure, with a content of *uu* triad around 70 %, which was in line with the values reported in the literature for copolymers produced with other pyridylimino ligands.[6] It was noteworthy that the catalyst with the highest productivity, **15b**, led also to the highest content of *uu* triad, as well as to the total absence of *ll* triad; this suggested that only the stereochemistry of the copolymer obtained with precatalyst **15b** was the result of a pure chain-end control, regardless to the nature of the vinyl arene.

Table 5.12. Triads distribution in the CO/vinyl arene polyketones.

Precatalyst: $[Pd(CH_3)(NCCH_3)(\mathbf{N\text{-}N'})][PF_6]$[a]

RUN	**N-N'**	Vinyl arene	Stereochemistry			
			ll (%)	*lu* (%)	*ul* (%)	*uu* (%)
1	**13**	S	1	12	11	76
2	**14**	S	3	17	16	64
3	**15**	S	-	7	8	85
4	**16**	S	5	16	17	62
5	**13**	MS	7	17	13	62
6	**14**	MS	3	15	16	66
7	**15**	MS	-	12	9	79
8	**16**	MS	5	18	17	61

[a] Determined by ^{13}C NMR spectra recorded in HFIP/$CDCl_3$, T = 298 K, integration of C_{ipso} signals.

The stereochemistry of the polyketones synthesized with pyridylimines **13-16** was completely different from that observed for the polyketones obtained with the catalysts having the pyrene-tagged pyridylimines (Table 5.2),[8] indicating a peculiar behavior of the catalysts with this class of nitrogen-donor ligands. In order to unravel the nature of this phenomenon, palladium complexes with other pyridylimine ligands featured by different aromatic groups on the imino nitrogen atom will be studied.

5.3. Conclusions

Four pyridylimine ligands **13-16** were used for the synthesis of new neutral $[Pd(CH_3)Cl(N\text{-}N')]$ and monocationic complexes $[Pd(CH_3)(NCCH_3)(N\text{-}N')][PF_6]$ (N-N' = **13-16**). The studied pyridylimines differ for the nature of the substituents on the iminic carbon atom and the *ortho* positions of the aryl ring, being it either hydrogens or methyl groups.

The synthesis of complexes **13a**, **14a** and **16a** and of all monocationc complexes was performed following literature procedures. Complex **15a** was obtained through a template synthesis using $[Pd(cod)(CH_3)Cl]$ as templating agent, and no purification was required.

All complexes were fully characterized both in solution by NMR and IR spectroscopy and, when possible, in solid state through X-ray diffraction on single crystals. The NMR spectra of the neutral

complexes highlighted a strong preference for the *cis* isomer, with a selectivity ranging from 75 % for **13a** to 98 % for **16a**, indicating a remarkable effect of the ligand on directing the selectivity towards the *cis* isomer. The analysis of {^{1}H,^{15}N}-HMBC spectra of both ligands and neutral complexes highlighted that coordination to Pd(II) led to significant effects on the chemical shift of both N-donor atoms.

The NMR characterization in solution of the monocationc complexes showed the presence of both *cis* and *trans* isomers, with a sensible loss in terms of stereoselectivity: the amount of *trans* isomer varied from as low as 2 % for **16b** to up to 74 % for **13b**, confirming again a remarkable effect of the ancillary ligand on determining the major species in solution.

All these data indicated that the difference in stability between the two isomers is relatively low, and the selectivity might be finely tuned by changing the steric and electronic properties of the ligand.

The monocationic complexes generated very efficient catalysts for the copolymerization of carbon monoxide with vinyl arenes such as styrene and 4-methyl-styrene, leading to the corresponding alternated polyketones. In particular, catalyst with ligand **15** led to productivities as high as 4.61 kg CP/g Pd, and molecular weights up to 1 775 000 g/mol were achieved with precatalyst **16b**. The relatively high values of polydispersity suggested the presence of more than one active species, and future in situ experiments will help to understand this phenomenon.

All synthesized polyketones were syndiotactic, with a *uu* triad content depending on the ancillary ligand nature; surprisingly enough, the strongest stereoselectivity (*uu* triad 85 %) was observed for the most productive catalyst deriving from **15b**.

In contrast with the previously reported data, no effect of the vinyl arene on the stereoselectivity was observed, and to get deeper insights into the nature of the peculiar stereocontrol, Pd(II) catalysts with pyridylimines having different polyaromatic groups on the imino nitrogen will be studied.

5.4. Experimental.

5.4.1. Materials and methods. All complex manipulations were performed using standard Schlenk techniques under argon. Anhydrous dichloromethane was obtained by distilling it over CaH_2 and under argon. Deuterated solvents (Cambridge Isotope Laboratories, Inc. (CIL)) were stored as recommended by CIL. Carbon monoxide (SIAD, CP grade 99.9%), 2-pyridinecarboxyaldehyde, 2-acetylpyridine, aniline, 2,6-dimethylaniline, the vinyl arenes, TFE, and all the other reagents and solvents were purchased from Sigma-Aldrich and used without further purification for synthetic, spectroscopic and catalytic purposes. Ligands **13**, **14** and **16** were synthesized according to literature procedures.[3] Palladium(II) neutral complexes were synthesized from [Pd(cod)(CH_3)Cl], obtained from [Pd($OAc)_2$],

HCl 37% Fluka and [*cis*,*cis*-cyclooctadiene] Fluka without further purification. [$Pd(OAc)_2$] was a donation from Engelhard Italia and used as received.

NMR spectra of ligands, complexes and catalytic products were recorded on a Varian 500 spectrometer at the following frequencies: 500 MHz (^1H), 125.68 MHz (^{13}C) and 50.64 MHz (^{15}N). The resonances are reported in ppm (δ) and referenced to the residual solvent peak versus $Si(CH_3)_4$: $CDCl_3$ at δ 7.26 (^1H) and δ 77.0 (^{13}C), CD_2Cl_2 at δ 5.32 (^1H) and δ 54.0 (^{13}C). NMR experiments were performed employing the automatic software parameters. ^{13}C NMR spectra of polyketones were recorded in 1,1,1,3,3,3-hexafluoro-2-propanol (HFIP) with addition of $CDCl_3$ for locking purposes. Caution: HFIP is a very volatile and highly toxic solvent, so proper protection should be used when is handled. IR spectra were recorded in Nujol on a Perkin Elmer System 2000 FT-IR.

Average molecular weight (Mw) and polydispersity (Mw/Mn) values of CO/styrene copolymers were measured in the laboratories of Dr. Carla Carfagna at the University of Urbino through gel permeation chromatography using polystyrene standards. Analyses were determined by a Knauer HPLC (K-501 pump, K-2501 UV detector) with a PLgel 5 mm 10^4 Å column. Chloroform was used as the eluent, with a flow rate of 0.6 mL min^{-1}. Samples were prepared by dissolving copolymer (2 mg) in chloroform (10 mL). Calculations were performed with the Bruker Chromstar software.

5.4.2 Synthesis of Pd-complexes.

[$Pd(CH_3)Cl(N\text{-}N')$] (13a, 14a, 16a)

General synthesis. To a stirred solution of [$Pd(cod)(CH_3)Cl$] (0.35 mmol) in CH_2Cl_2 (1.5 mL) a solution of the ligand (1.1 equiv) in CH_2Cl_2 (1.5 mL) was added. After 1.5 h at room temperature the reaction mixture was concentrated and the product precipitated upon addition of diethyl ether at 277 K. Average yield: 90 %.

13a. ^1H NMR (500 MHz, CD_2Cl_2, 298 K) *cis* : *trans* = 3 : 1. *cis* isomer: δ = 9.09 (d, 1H, H^6), 8.46 (s, 1H, H^i), 8.06 (t, 1H, H^4), 7.83 (d, 1H, H^3), 7.75 (t, 1H, H^5), 7.54 - 7.36 (m, 3H, $H^{m,p}$), 7.20 (d, 2H, H^o), 0.63 (s, 3H, Pd-CH_3); *trans* isomer: δ = 8.70 (d, 1H, H^6), 8.43 (s, 1H, H^i), 8.12 (t, 1H, H^4), 7.86 (d, 1H, H^3), 7.68 (t, 1H, H^5), 7.54 - 7.36 (m, 5H, $H^{m,p,o}$), 1.15 (s, 3H, Pd-CH_3). ^{13}C NMR *cis* isomer: δ = 167.30 (C^i), 149.37 (C^6), 138.81 (C^4), 128.98 (C^m), 128.78 (C^3), 128.06 (C^p), 126.77 (C^5), 122.38 (C^o), -0.02 (Pd-CH_3).

14a.- ^1H NMR (500 MHz, CD_2Cl_2, 25°C) δ = 9.10 (d, 1H, H^6), 8.35 (s, 1H, H^i), 8.08 (t, 1H, H^4), 7.84-7.74 (m, 2H, $H^{3,5}$), 7.19 - 7.14 (m, 3H, $H^{m,p}$), 2.26 (s, 6H, Ar-CH_3), 0.38 (s, 3H, Pd-CH_3). ^{13}C NMR δ =

168.33 (C^i), 149.47 (C^6), 138.71 (C^4), 128.91 (C^3), 127.84 ($C^{m,p}$), 126.67 (C^5), 17.91 (Ar-CH_3), -1.88 (Pd-CH_3).

16a.- ^{1}H NMR (500 MHz, CD_2Cl_2, 25°C) δ = 9.19 (d, 1H, H^6), 8.08 (t, 1H, H^4), 7.90 (d, 1H, H^3), 7.75 (t, 1H, H^5), 7.21 - 7.10 (m, 3H, $H^{m,p}$), 2.18 (s, 6H, Ar-CH_3), 2.14 (s, 3H, CH_3^i), 0.18 (s, 3H, Pd-CH_3). ^{13}C NMR δ = 149.04 (C^6), 138.82 (C^4), 128.62 (C^3), 128.21 – 126.53 ($C^{m,p}$), 17.76 (Ar-CH_3), 17.32 (CH_3^i), -1.92 (Pd-CH_3).

[Pd(CH_3)Cl(15)] (15a). To a solution of 0.377 mmol (0.042 mL) of 2-acetylpyridine in 4 mL of ethanol, 1.2 equiv of aniline (0.452 mmol, 0.041 mL) were added, and the reaction mixture was stirred for 2.5 h at 298 K. 1 equiv of [Pd(cod)(CH_3)Cl] (0.377 mmol, 100.5 mg) was suspended in 3 mL of ethanol and added to the reaction mixture. The solution was stirred at 298 K for 1.5 h, then it was concentrated to half the volume, cooled in an ice bath and the product was precipitated upon addition of diethyl ether cooling for one night at 277 K. The solid was filtered and washed thoroughly with diethyl ether, and it was isolated in a 67 % yield.

15a.- ^{1}H NMR (500 MHz, CD_2Cl_2, 25°C) δ = 9.16 (d, 1H, H^6), 8.07 (t, 1H, H^4), 7.91 (d, 1H, H^3), 7.74 (t, 1H, H^5), 7.50 (t, 2H, H^m), 7.31 (t, 1H, H^p), 6.96 (d, 2H, H^o), 2.24 (s, 3H, CH_3^i), 0.35 (s, 3H, Pd-CH_3). ^{13}C NMR δ = 149.04 (C^6), 138.71 (C^4), 129.13 (C^m), 128.50 (C^5), 126.50 (C^p), 125.00 (C^3), 121.68 (C^o), 18.46 (CH_3^i), -0.47 (Pd-CH_3).

[Pd(CH_3)($NCCH_3$)(N-N')][PF_6] (13b-16b)

General synthesis. To a solution of neutral precursor (0.205 mmol) in 10 mL of CH_2Cl_2 a solution of 1.3 equivalents of $AgPF_6$ (0.267 mmol) in 1.5 mL of anhydrous acetonitrile was added. The reaction mixture was protected from light and stirred at room temperature for 2.5 h, then it was filtered over Celite®, concentrated and the product was precipitated upon addition of cold diethyl ether. Average yield 70 – 90 %.

13b.- IR: ν_{max} = 842.18 cm^{-1} (PF_6^-). ^{1}H NMR (500 MHz, CD_2Cl_2, 298 K) *cis* : *trans* = 1 : 3. *cis* isomer δ = 8.74 (d, 1H, H^6), 8.46 (s, 1H, H^i), 8.20 (t, 1H, H^4), 7.98 (d, 1H, H^3), 7.92 (t, 1H, H^5), 7.60 - 7.41 (m, 3H, $H^{m,p}$), 7.17 (d, 2H, H^o), 2.51 (s, 3H, Pd-$NCCH_3$), 0.78 (s, 3H, Pd-CH_3); *trans* isomer δ = 8.58 (d, 1H, H^6), 8.55 (s, 1H, H^i), 8.25 (t, 1H, H^4), 8.08 (d, 1H, H^3), 7.78 (t, 1H, H^5), 7.60 - 7.41 (m, 3H, $H^{m,p}$), 7.37 (d, 2H, H^o), 2.23 (s, 3H, Pd-$NCCH_3$), 1.24 (s, 3H, Pd-CH_3). ^{13}C NMR *cis* isomer δ = 171.20 (C^i), 150.15 (C^6), 140.29 (C^4), 130.76 (C^5), 129.62 (C^m), 128.86 (C^p), 128.38 (C^3), 122.20 (C^o), 4.76 (Pd-CH_3), 3.38 (Pd-$NCCH_3$); *trans* isomer δ = 162.79 (C^i), 149.40 (C^6), 141.09 (C^4), 129.76 (C^3), 129.58 (C^m), 129.46 (C^p), 128.95 (C^5), 121.80 (C^o), 3.78 (Pd-CH_3), 3.28 (Pd-$NCCH_3$).

14b.- IR: ν_{max} = 847.91 cm^{-1} (PF_6^-). ^1H NMR (500 MHz, CD_2Cl_2, 25°C) *cis* : *trans* = 7 : 1. *cis* isomer δ = 8.79 (d, 1H, H^6), 8.35 (s, 1H, H^i), 8.22 (t, 1H, H^4), 7.97 (m, 2H, $H^{3,5}$), 7.25 - 7.15 (m, 3H, $H^{m,p}$), 2.50 (s, 3H, Pd-$NCCH_3$), 2.23 (s, 3H, Ar-CH_3), 0.53 (s, 3H, Pd-CH_3); *trans* isomer δ = 8.61 (d, 1H, H^6), 8.44 (s, 1H, H^i), 8.30 (t, 1H, H^4), 8.09 (d, 1H, H^3), 7.84 (t, 1H, H^5), 7.25 - 7.15 (m, 3H, $H^{m,p}$), 2.32 (s, 3H, Ar-CH_3), 1.92 (s, 3H, Pd-$NCCH_3$), 1.17 (s, 3H, Pd-CH_3). ^{13}C NMR *cis* isomer δ = 172.41 (C^i), 150.77 (C^6), 140.54 (C^4), 128.51 ($C^{3,5}$), 128.73 ($C^{m,p}$), 17.95 (Ar-CH_3), 3.32 (Pd-$NCCH_3$), 3.21 (Pd-CH_3); *trans* isomer δ = 165.77 (C^i), 150.08 (C^6), 141.01 (C^4), 129.88 (C^3), 128.37 ($C^{m,p}$), 18.31 (Ar-CH_3), 3.39 (Pd-CH_3), 2.32 (Pd-$NCCH_3$).

15b.- IR: ν_{max} = 842.80 cm^{-1} (PF_6^-). ^1H NMR (500 MHz, CD_2Cl_2, 25°C) *cis* : *trans* = 5 : 6. *cis* isomer δ = 8.74 (d, 1H, H^6), 8.22 (t, 1H, H^4), 8.04 (d, 1H, H^3), 7.93 (t, 1H, H^5), 7.59 - 7.47 (m, 2H, H^m), 7.43 - 7.32 (m, 1H, H^p), 6.94 (d, 2H, H^o), 2.49 (s, 3H, Pd-$NCCH_3$), 2.34 (s, 3H, $CH_3{}^i$), 0.49 (s, 3H, Pd-CH_3); *trans* isomer δ = 8.60 (d, 1H, H^6), 8.28 (t, 1H, H^4), 8.10 (d, 1H, H^3), 7.79 (t, 1H, H^5), 7.59 - 7.47 (m, 2H, H^m), 7.43 - 7.32 (m, 1H, H^p), 7.05 (d, 2H, H^o), 2.41 (s, 3H, $CH_3{}^i$), 1.94 (s, 3H, Pd-$NCCH_3$), 1.05 (s, 3H, Pd-CH_3). ^{13}C NMR *cis* isomer δ = 149.87 (C^6), 141.15 (C^4), 129.69 (C^m), 129.00 (C^5), 127.78 (C^3), 127.41 (C^p), 121.70 (C^o), 17.65 ($CH_3{}^i$), 2.74 (Pd-CH_3), 2.63 (Pd-$NCCH_3$); *trans* isomer δ = 149.74 (C^6), 140.56 (C^4), 130.53 (C^5), 129.69 (C^m), 127.41 (C^p), 121.09 (C^o), 19.06 ($CH_3{}^i$), 4.49 (Pd-CH_3), 3.48 (Pd-$NCCH_3$).

16b.- IR: ν_{max} = 841.16 cm^{-1} (PF_6^-). ^1H NMR (500 MHz, CD_2Cl_2, 25°C) δ = 8.76 (d, 1H, H^6), 8.23 (t, 1H, H^4), 8.04 (d, 1H, H^3), 7.95 (t, 1H, H^5), 7.20 (s, 3H, $H^{m,p}$), 2.49 (s, 3H, Pd-$NCCH_3$), 2.25 (s, 3H, $CH_3{}^i$), 2.15 (s, 6H, Ar-CH_3), 0.33 (s, 3H, Pd-CH_3). ^{13}C NMR δ = 149.80 (C^6), 140.36 (C^4), 130.52 (C^5), 128.42 ($C^{m,p}$), 126.35 (C^3), 17.72 ($CH_3{}^i$), 17.64 (Ar-CH_3), 3.27 (Pd-$NCCH_3$), 2.72 (Pd-CH_3).

5.4.3. CO/Styrene copolymerization reactions. All experiments were carried out at atmospheric CO pressure in a three-necked, thermostated, 75 mL glass reactor equipped with a magnetic stirrer. After establishment of the reaction temperature, the precatalyst ($1.27 \cdot 10^{-5}$ mol), 1,4-benzoquinone ([BQ]/[Pd] = 5), styrene (10 mL) and TFE (20 mL) were added. CO was bubbled through the solution for 10 min; afterwards two 4 L balloons previously filled with CO were connected to the reactor. After the desired time, the reaction mixture was poured into 100 mL of methanol and stirred for 1.5 h at room temperature. The solid was filtered and washed thoroughly with methanol, then dried under vacuum to constant weight.

5.5. Bibliography.

[1] Sadimenko, A.P. in *Advances in Heterocyclic Chemistry* **2012**, ed. Elsevier, chap. 4, vol. 107, p. 133.

[2] Taubmann, S.; Alt, H.G. *J. Mol. Cat. A: Chem.,* **2008**, *284*, 134.

[3] Köppl, A,; Alt, H.G. *J. Mol. Cat. A: Chem.,* **2000**, *154*, 45.

[4] Meneghetti, S.P.; Lutz, P.J.; Kress, J. *Organometallics*, **1999**, *18*, 2734.

[5] Jiang, Z.; Adams, S.E.; Sen, A. *Macromolecules* **1994**, *27*, 2694.

[6] Benito, J.M.; de Jesús, E.; de la Mata, F.J.; Flores, J.C.; Gómez, R. *Organometallics*, **2006**, *25*, 3045.

[7] Bianchini, C.; Lee, H.M.; Mantovani, G.; Meli A.; Oberhauser, W. *New J. Chem*., **2002**, *26*, 387.

[8] Pelletier, J.D.A.; Fawcett, J.; Singh, K.; Solan, G.A. *J. Organomet. Chem.* **2008**, *693*, 2723.

[9] Canil, G.; Rosar, V.; Dalla Marta, S.; Bronco, S.; Fini, F.; Carfagna, C.; Durand, J.; Milani, B. *ChemCatChem* **2015**, *7*, 2255.

[10] Miller, K.J.; Kitagawa, T.T.; Abu-Omar, M.M. *Organometallics*, **2001**, *20*, 4403.

[11] Durand, J.; Zangrando, E.; Stener, M.; Fronzoni, G.; Carfagna, C.; Binotti, B.; Kramer, P.C.J.; Müller, C.; Caporali, M.; van Leeuwen, P.W.M.N.; Vogt, D.; Milani, B. *Chem. Eur. J*., **2006**, *12*, 7639.

[12] Rosar, V.; Meduri, A.; Montini, T.; Fini, F.; Carfagna, C.; Fornasiero, P.; Balducci, G.; Zangrando, E.; Milani, B.; *ChemCatChem*, **2014**, *6*, 2403.

[13] a) Meduri, A.; Cozzula, D.; D'Amora, A.; Zangrando, E.; Gladiali, S.; Milani, B., *Dalton Trans*., **2012**, *41*, 7474; b) Rülke, R.E.; Ernsting, J.M.; Spek, A.L.; Elsevier, C.J.; Van Leeuwen, P.W.N.M.; Vrieze.K.; *Inorg. Chem.*, **1993**, *32*, 5769; c) Milani, B.; Marson, A.; Zangrando, E.; Mestroni, G.; Ernsting, J.M.; Elsevier, C.J.; *Inorg. Chim. Acta*, **2002**, *327*, 188.

CHAPTER 6

Bis-alkoxycarbonylation of alkenes catalyzed by Pd(II) complexes with pyridylimine ligands

Overview

A series of palladium(II) complexes of general formula $[Pd(N\text{-}N')(L)_2]$, with N-N' being a pyridylimine ligand and L either acetate or trifluoroacetate, was tested in the alkoxycarbonylation conversion of alkenes under reaction conditions analogous to those applied for the isomerizing alkoxycarbonylation of methyl oleate.

1-octene was not converted into the expected methyl nonanoate: the main product obtained was dimethyl 2-hexylsuccinate, which is the result of the double methoxycarbonylation of the double bond.

The same reaction performed on 4-octene led to the corresponding diester derivative, dimethyl 2,3-dipropylsuccinate, which is the result of the bis-methoxycarbonylation of the internal double bond; surprisingly enough, no isomerization of the double bond towards the terminal position was observed in the main product, although the minor products were not characterized.

The effect of reaction parameters such as temperature and pressure was investigated.

The work reported in this chapter related to the catalytic reactions was carried out by V. Rosar in the group of Prof. Stefan Mecking at the Univerisity of Konstanz thanks to a DAAD B1 fellowship.

Part of this chapter will be published in a feature work:

Rosar, V.; Mecking, S.; Milani, B.

6.1. Introduction.

The catalytic alkoxycarbonylation of C-C double bonds is a powerful tool to transform cheap feedstocks, like CO, alkenes and alcohols, into more valuable molecules, like esters, diesters, ketones and other derivatives (Figure 6.1).[1] This reaction has long been known, but the first example reported required the use of a palladium salt as a reagent, making the reaction very expensive.[2] Just one year later a palladium-catalyzed process able to convert simple terminal alkenes into succinates was developed, but it required high amount of copper(II) chloride or iron(III) chloride, together with small quantities of sodium acetate, and led to low yields, in particular when the substrate was 1-octene (<10 % yield) instead of propylene.[3]

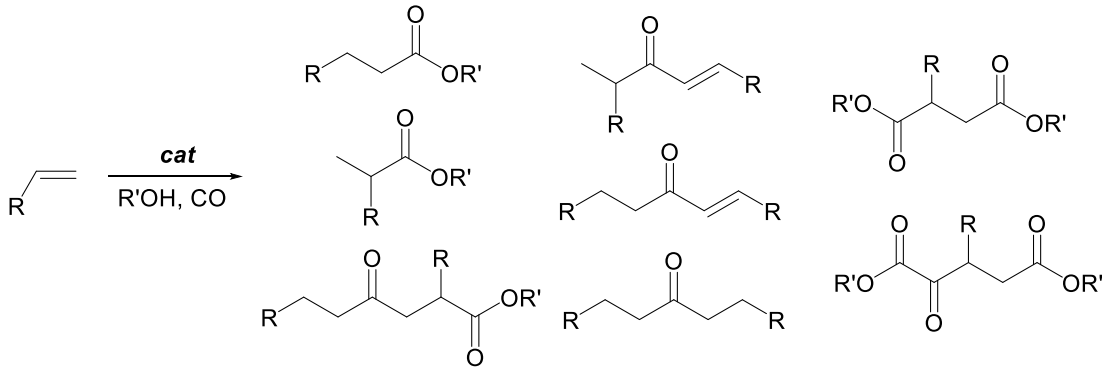

Figure 6.1. Various carbonylation products of terminal alkenes.

For many years the reaction was studied focusing either on model substrates such as styrene,[4,5] or on the development of palladium catalysts for the asymmetric mono- and bis-alkoxycarbonylation of vinyl arenes,[6] since the obtained 2-arylpropionic acids are precursors for non-steroidal anti-inflammatory drugs such as Ibuprofen and Naproxen.[7] On the other hand, data about the possible application of this process to aliphatic alkenes and especially to internal ones are very rare. Pd(II) complexes of general formula $[Pd(L\text{-}L')X_2]$ (X = weakly coordinating anion), with L-L' being an enantiomerically pure diphosphine ligand with C_2 symmetry were reported to catalyze the enantioselective bis-alkoxycarbonylation of 1-olefins such as 3-phenyl-1-propene, 4-methyl-1-pentene and propene to optically active 2-substituted butanedioates.[8]

The mechanism of the double alkoxycarbonylation of aliphatic alkenes, in particular propylene, catalyzed by a Pd(II) complex with a chiral diphosphine ligand $[Pd\{(S)\text{-MeO-Biphep}\}(H_2O)_2](OTf)_2$ (OTf = triflate, MeO-Biphep = (6,6'-dimethoxy biphenyl-2,2'-diyl)bis(diphenylphosphine)) in the presence of 1,4-benzoquinone (BQ) was reported in 1997 (Scheme 6.1).[1b]

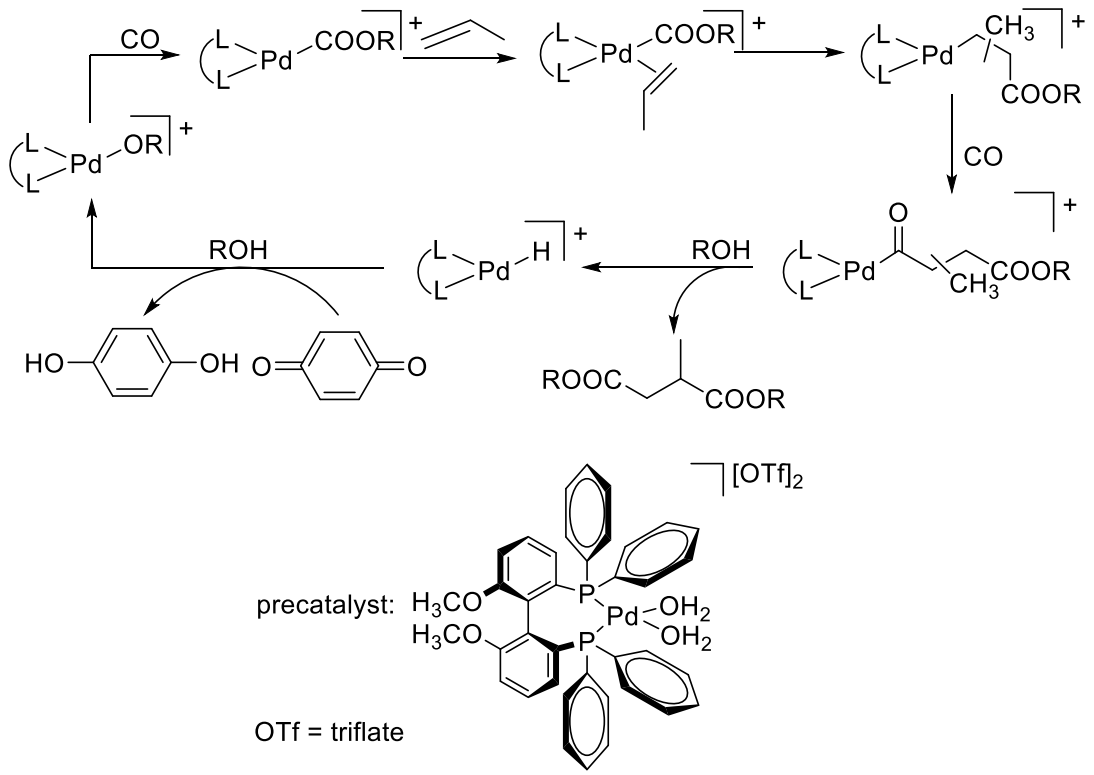

Scheme 6.1. Proposed mechanism for the bis-methoxycarbonylation of propylene and the studied precatalyst.

The first step consisted in the coordination insertion of carbon monoxide into the palladium-alkoxy species to generate the –COOR group, which was then transferred to the incoming alkene; the regiochemistry of this insertion step was not taken into account, since the nature of the product was not affected by it. The formed Pd-alkyl species further reacted with CO leading to the Pd-acyl intermediate, which underwent the nucleophilic attack of an alcohol molecule to give the free diester and the Pd-H species. To close the catalytic cycle, this intermediate has to be transformed into the Pd-alkoxy by reacting with an alcohol molecule and the 1,4-benzoquinone, leading to the Pd-OR species and 1,4-hydroquinone.

Another application of the methoxycarbonylation is the conversion of ethylene into methyl propionate, that was recently implemented as a part of the industrial process for the production of methyl methacrylate, developed by Lucite International.[9] This reaction is catalysed with high rates by palladium(II) complexes with 1,2-$(tBu_2PCH_2)_2C_6H_4$ (dtbpx; "Lucite ligand", Figure 6.2).[10]

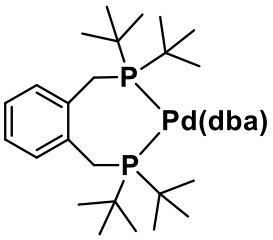

dba = *trans*,*trans*-dibenzylideneacetone

Figure 6.2. Palladium catalyst with Lucite ligand.[10]

More recently, the alkoxycarbonylation reaction coupled with the isomerization of internal double bonds to the terminal position was applied to unsaturated fatty acids, such as methyl oleate (MO), one of the major components of plant oils, to obtain the corresponding α,ω-diesters.[11] The latter, thanks to the long aliphatic chain that links the two functional groups, which make them suitable for thermoplastic applications, represent valuable building blocks for the synthesis of semicrystalline aliphatic polyesters and hydrophobic polyamides from renewable resources, (Scheme 6.2).[12]

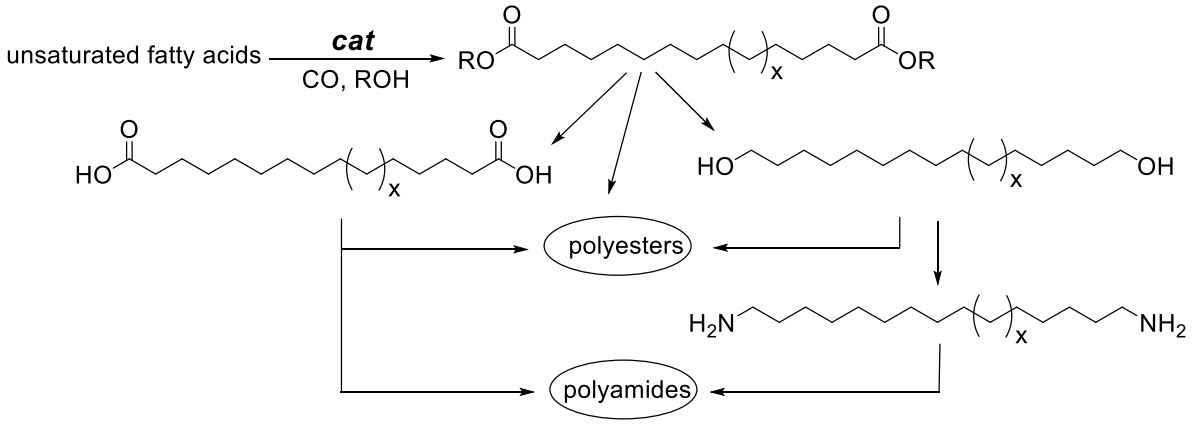

Scheme 6.2. Long-chain α,ω-difunctionalized compounds from unsaturated fatty acids.[11]

Unsaturated fatty acids possess two functional groups, one terminal carboxylic group and one double bond, the latter being in the center of the molecule. For a fully linear incorporation of the entire fatty acid chain into crystallizable linear polymers, the functionalization at both chain ends is required, thus a synthetic route to transform the internal double bond into a terminal ester functionality had to be developed. Mecking's approach was based on exploiting the capability of Pd(II) complexes with sterically demanding diphosphines of acting as catalysts for the tandem isomerization carbonylation of internal alkenes to terminal, linear esters.[13] The applied precatalyst was the palladium-triflate (OTf) complex with the Lucite ligand dtbpx, [Pd(dtbpx)(OTf)][OTf] (Scheme 6.3).

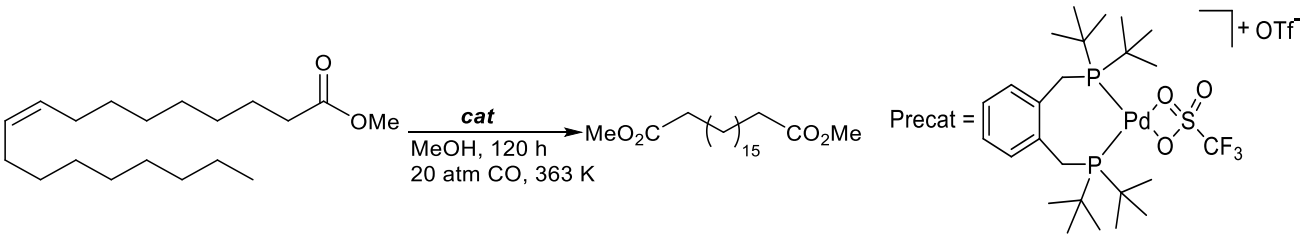

Scheme 6.3. The catalytic reaction and the Pd-dtbpx complex.

In the presence of carbon monoxide (20 bar) and methanol at T = 363 K, the [Pd(dtbpx)(OTf)][OTf] complex catalyzes the isomerizing methoxycarbonylation of methyl oleate to dimethyl-1,19-nonadecanedioate (Scheme 6.3). The desired product was obtained with a conversion of 80 % and a selectivity higher than 99 % in 22 h of reaction.[11,14] Afterward the diester was reduced to the corresponding diol, nonadecane-1,19-diol. The diol and the diester led, through a polycondensation reaction, to a novel polyester, whose thermal properties were similar to those of thermoplastic low-density polyethylene.

With the aim to develop a Pd catalyst better performing and different from the Lucite one, a series of complexes with diphosphine ligands featured by an α-tolyl skeleton and differing for the substituents on the P-atoms was investigated in the target reaction (Figure 6.3).[15]

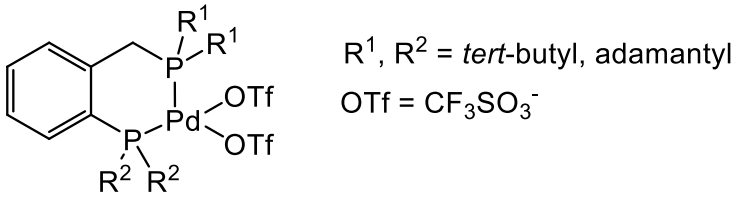

Figure 6.3. Palladium precatalysts with diphosphine ligands having α-tolyl skeleton.[15]

The catalytic data highlighted a significant influence of the steric hindrance around the palladium center on both conversion of the substrate and selectivity in the linear diester, with the best results obtained with the catalyst having all adamantyl residues. Anyhow, these results were still lower than those obtained with the Lucite catalyst on longer reaction time (120 h), that led to a conversion of 95.8 % with more than 90 % selectivity in the desired product.[15]

To confirm the general validity of this reaction, the Lucite catalyst was applied to a series of unsaturated substrates, ranging from ethylene to sunflower oil, which is a mixture of fatty acids comprising more than 90 % of MO. The collected data showed that the reaction grew faster as the alkyl chain got shorter; in particular, 1- and 4-octene, the terminal and the corresponding internal alkenes with the same chain

length, were converted into methyl nonanoate at the same rate, thus indicating that the isomerization of the double bond to the terminal position was not the rate determining step of the overall process.[16] In fact, DFT calculations highlighted that the isomerization of the double bond along the substrate hydrocarbon chain was associated with relatively low activation barriers, therefore all isomers were in equilibrium and readily accessible. On the other hand, the rate determining step was identified in the methanolysis of the acyl intermediate deriving from the CO insertion on the alkyl species, and its barrier was lowest for the linear acyl for sterically encumbered catalysts, explaining the influence of steric hindrance on selectivity. In this case, the Pd-H generated after the methanolysis did not require further transformation to close the catalytic cycle, as reported for the bis-alkoxycarbonylation,[1b] since it represented the active species of the overall process.[16]

Always with the aim to develop better performing catalysts, we focused our attention on nitrogen-donor ligands belonging to the family of pyridylimines. Indeed, the corresponding palladium(II) complexes having general formula [Pd(N-N')$(L)_2$] (N-N' = **14**, **17**, **18**; L = acetate, trifluoroacetate; Figure 6.4) were reported to catalyze the methoxycarbonylation of styrene to dimethyl phenylsuccinate, using a CO pressure between 400 psi (ca. 28 bar) and 1500 psi (ca. 100 bar), at 353 K, in the presence of 1,4-benzoquinone (BQ) as oxidant in one to one ratio with the vinyl arene.[5] The best results in terms of both conversion of the substrate (57 %) and selectivity in the dimethyl phenylsuccinate (47 %) were obtained with precatalyst **1b** under a CO pressure of 800 psi (55 bar).

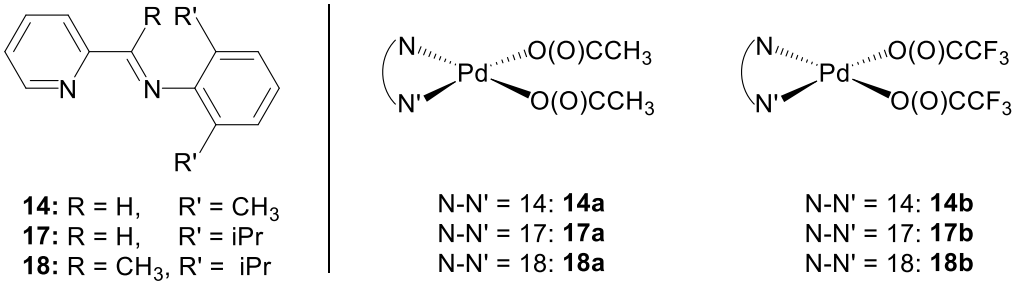

Figure 6.4. The studied pyridylimine ligands and related Pd(II) complexes.[5]

It was interesting to note that, beside the major product, a mixture of carbonylated compounds was formed. In addition, these complexes did not catalyze the copolymerization of styrene with CO, as reported for other palladium catalysts with pyridylimine ligands (Chapter 5) (Scheme 6.4).[17]

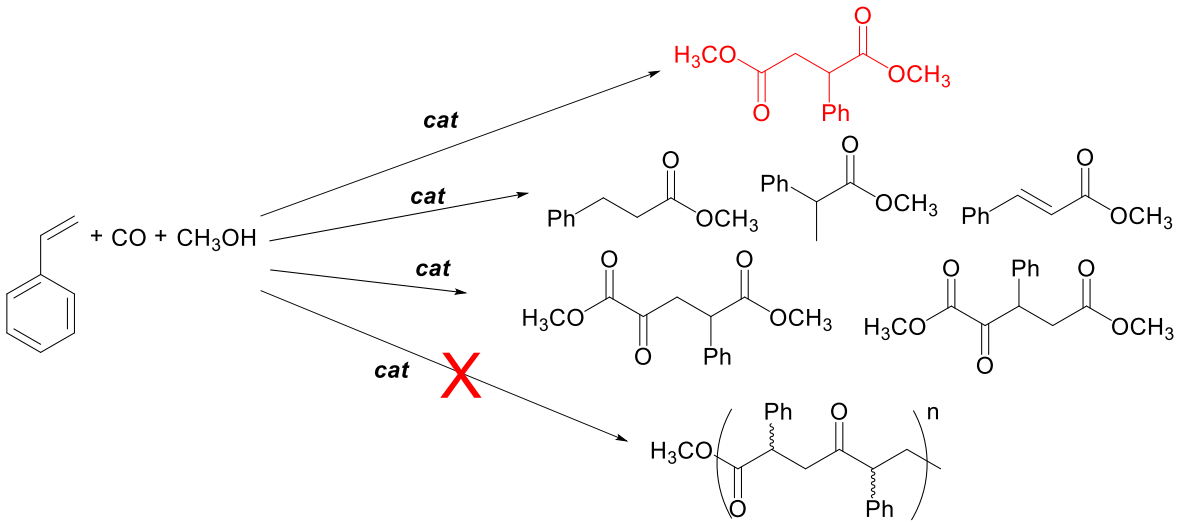

Scheme 6.4. Examples of products obtained from the catalytic carbonylation of styrene.[5]

Considering the characteristics of these palladium complexes with pyridylimine ligands and taking into account the lack of examples of alkoxycarbonylation of internal alkenes, we decided to study the catalytic activity of complexes **14a**, **17a**, **18a**, **14b**, **17b**, **18b** in the methoxycarbonylation of octenes.

6.2. Results and Discussion.

Complexes **14a, 17a, 18a**, **14b, 17b, 18b** were synthesized following the literature procedures, and the NMR characterization was in agreement with the spectra reported.[5]

Complex **18b** was tested as precatalyst in the methoxycarbonylation of 1-octene under the slightly modified reaction conditions with respect to those reported for methyl oleate, that are 20 bar of CO pressure and 363 K for 18 h in methanol,[16] adding 1,4-benzoquinone in a 20 : 1 ratio with respect to palladium to enhance catalyst stability (Scheme 6.5).

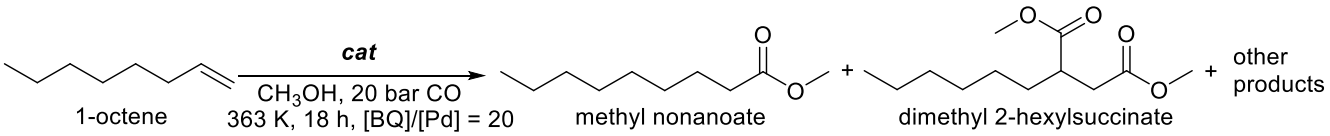

Scheme 6.5. Methoxycarbonylation reaction of 1-octene.

The catalytic product was an oil that, after removing the solvent, resulted to be formed by a complex mixture of products. The conversion of the starting material was as low as 11 %, with the formation of considerable amounts of palladium black, suggesting that the low conversion might be related to the low stability of the catalyst. Conversely to the data reported for the Pd-catalysts based on P-donor ligands,[16]

in this case the main product, obtained with a 44 % selectivity, was not the methyl nonanoate, deriving from the methoxycarbonylation of the double bond.

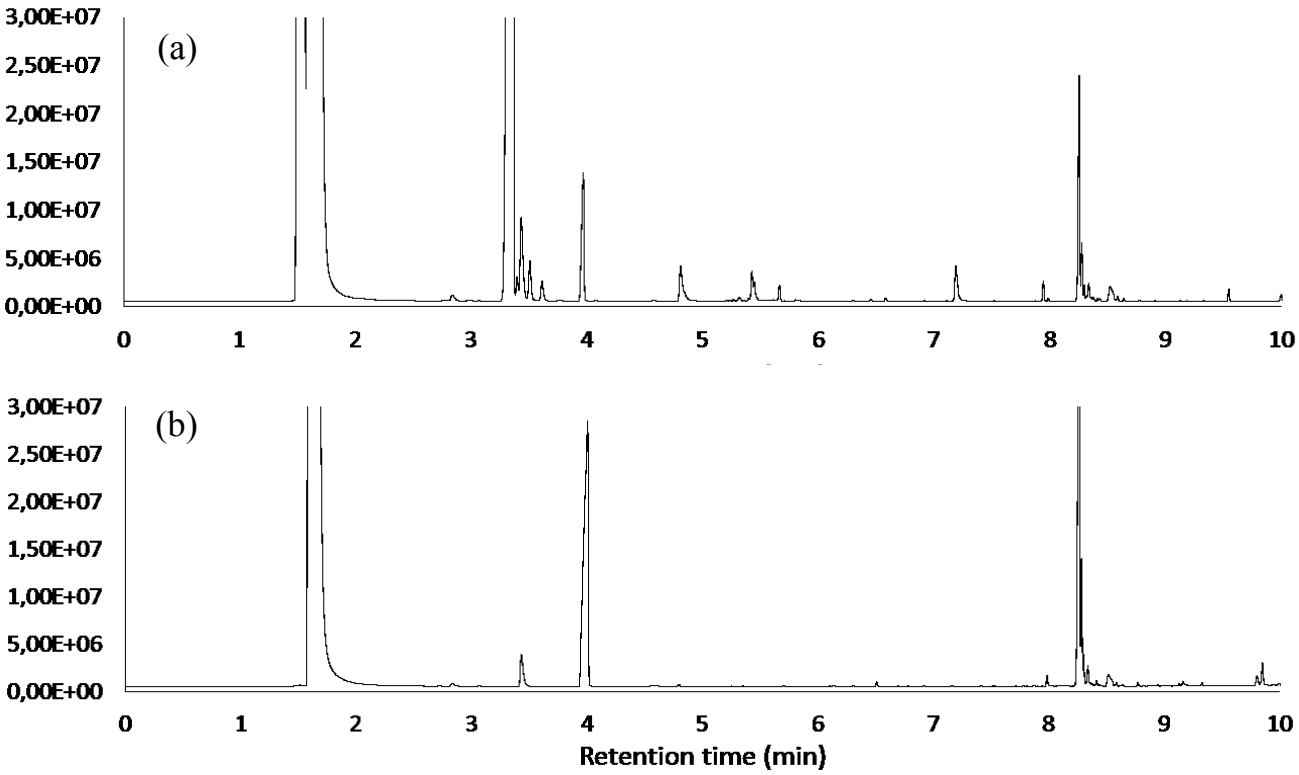

Figure 6.5. Gas chromatograms of: (a) crude reaction mixture; (b) purified product.

The crude mixture was purified through column chromatography (Figure 6.5), and the main product was characterized via NMR spectroscopy as the methyl 2-hexylsuccinate (Figure 6.6), this being the result of the double methoxycarbonylation of the terminal double bond. The other components of the crude reaction mixture were observed in much lower amount, thus they were not characterized.

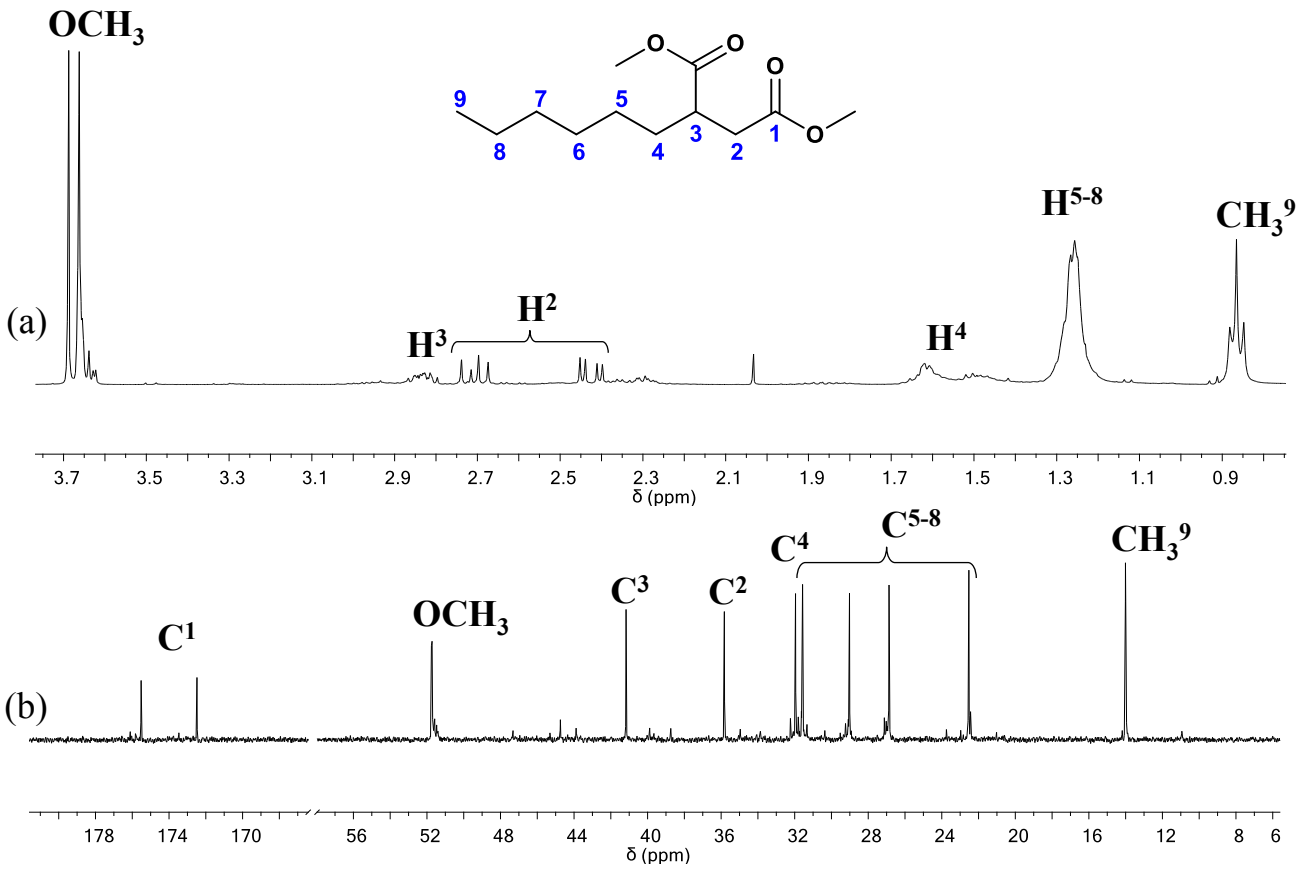

Figure 6.6. (a) ^{1}H NMR and (b) ^{13}C NMR spectra ($CDCl_3$, 298 K) of dimethyl 2-hexylsuccinate.

The observed catalytic behavior of **18b** suggested that the nature of the ancillary ligand on the palladium center deeply affected the selectivity of the catalyst, since with sterically hindered P-donor ligands alkenes were converted to terminal esters, whereas with pyridylimines the selectivity switched towards the formation of vicinal diesters, as it was observed in the case of styrene carbonylation.[5]

When precatalyst **18b** was tested in the same reaction using 4-octene as substrate instead of the corresponding terminal alkene 1-octene, under the same reaction conditions, again a complex mixture of products was obtained, observing a low conversion (10 %) of the substrate and remarkable formation of inactive palladium black (Figure 6.7).

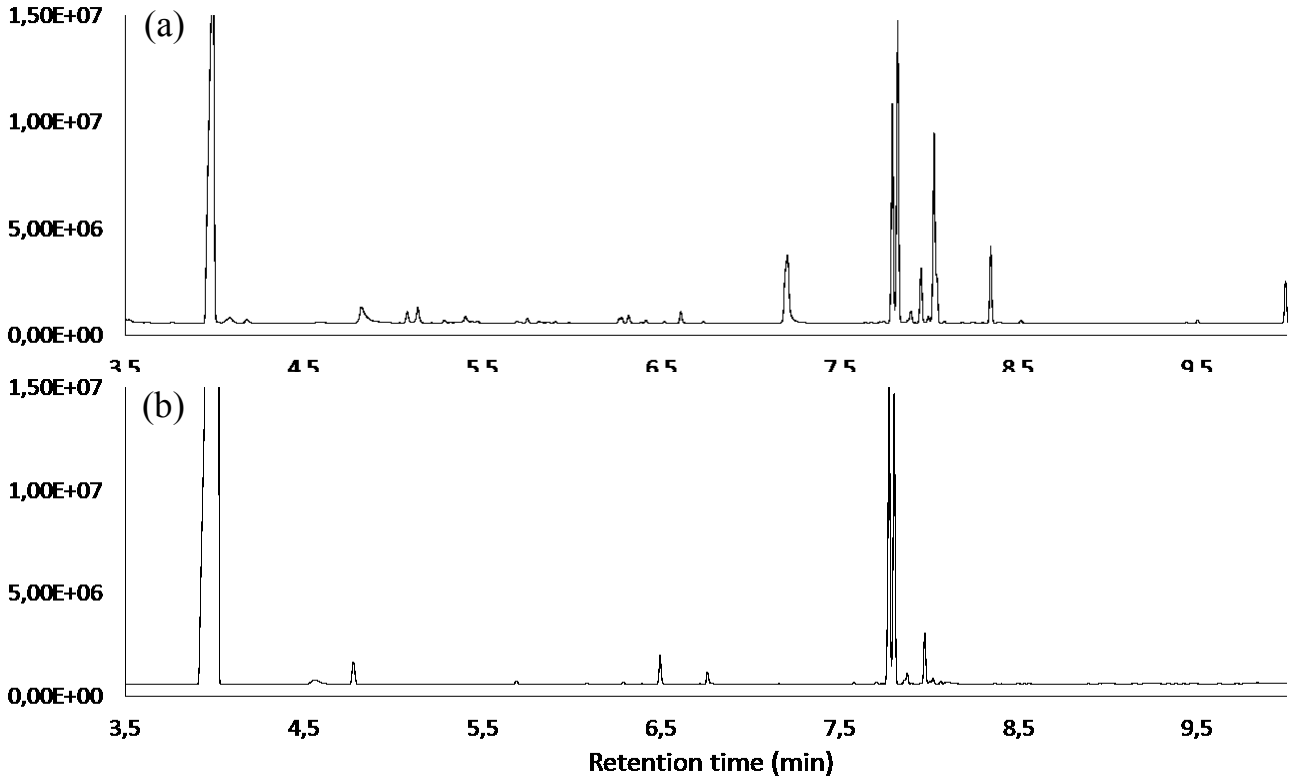

Figure 6.7. Gas chromatograms of: (a) crude reaction mixture; (b) purified product.

The oil isolated after removing the solvent was purified through column chromatography, and the main product, formed with 23 % selectivity, was characterized via NMR spectroscopy as dimethyl 2,3-dipropylsuccinate, which is the result of the double methoxycarbonylation of the internal double bond (Figure 6.8).

Therefore, in contrast with the catalytic behavior of the palladium derivatives with the hindered diphosphines when palladium complexes with pyridylimine ligands were applied as catalysts no isomerization of the double bond was observed, and the internal double bond was converted into the bis-alkoxycarbonylated adduct.

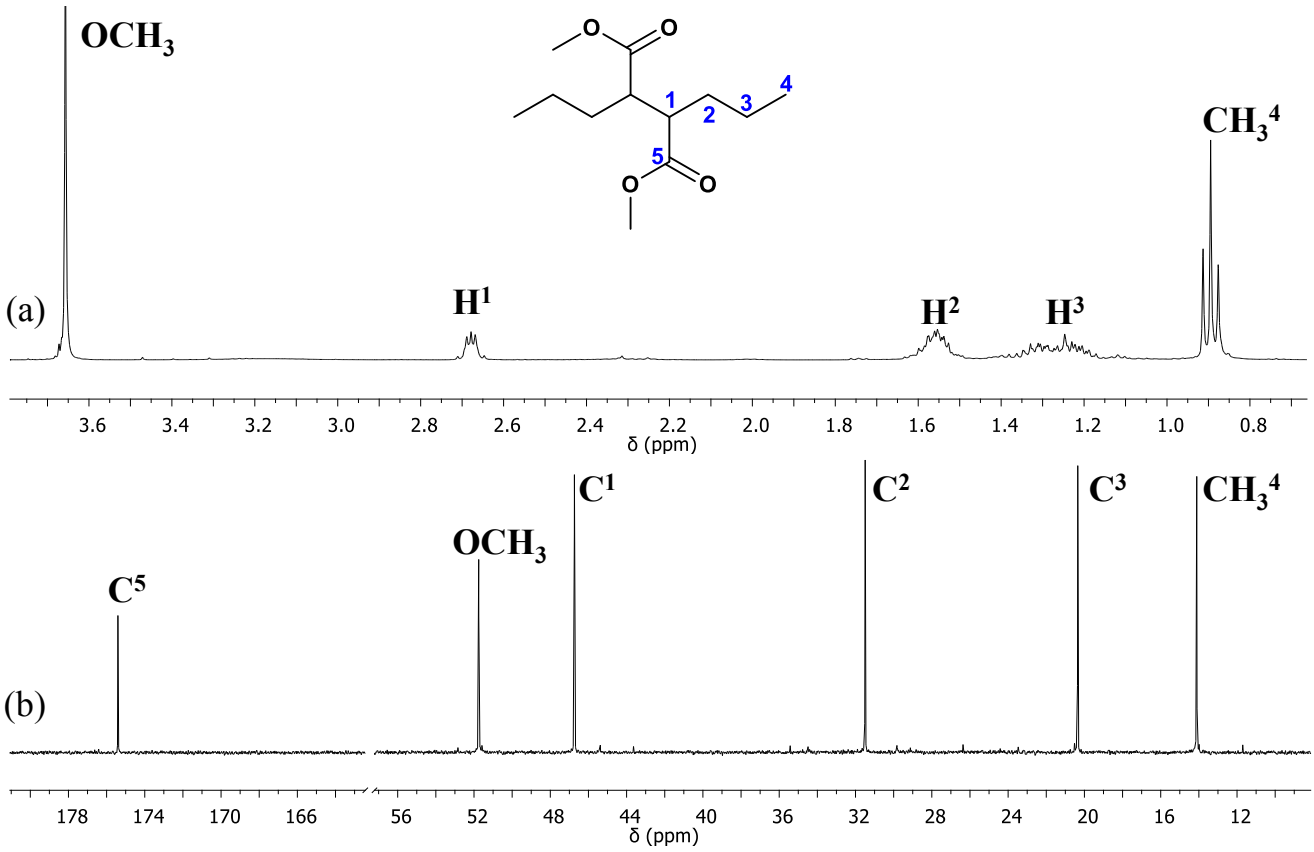

Figure 6.8. (a) ^{1}H NMR and (b) ^{13}C NMR spectra ($CDCl_3$, 298 K) of dimethyl 2,3-dipropylsuccinate.

All complexes **14a, 17a, 18a**, **14b, 17b, 18b** were tested as catalysts for the methoxycarbonylation of 4-octene under the same conditions, leading to the formation of the expected vicinal diester, as observed for **18b**. A remarkable effect of the anion L was observed on both conversion and selectivity, being catalysts with trifluoroacetate more active than the acetate derivatives, but leading to a lower selectivity in the target diester (Table 6.1). On the other hand, regardless the nature of the anion L, precatalysts having ligand **14** led to the highest conversion values and the lowest selectivity, while complexes with ligand **18** generated the most selective catalysts, although with low conversions.

Table 6.1. Methoxycarbonylation of 4-octene: effect of the N-N' ligand and of the anion L. Precatalyst: $[Pd(N\text{-}N')(L)_2]$.[a]

Run	N-N'	L	Conversion (%)[b]	Selectivity (%)[b]
1	**14**	CH_3COO^-	46	43
2	**17**	CH_3COO^-	41	56
3	**18**	CH_3COO^-	29	61
4	**14**	CF_3COO^-	86	18
5	**17**	CF_3COO^-	40	5
6	**18**	CF_3COO^-	51	38

[a] Reaction conditions: n_{Pd} = 24 μmol; $n_{4\text{-octene}}$ = 6.37 mmol; [4-octene]/[Pd] = 265; n_{BQ} = 6.37 mmol; [4-octene]/[BQ] = 1; V_{MeOH} = 10 mL; T = 363 K; P_{CO} = 20 bar; t = 18 h; [b] determined from GC analysis.

In general it can be highlighted that the higher was the conversion, the lower was the selectivity in the dimethyl 2,3-dipropylsuccinate, and the best compromise between conversion and selectivity was represented by the palladium complexes with ligand **18**, that were therefore chosen as catalysts to investigate the effect of reaction parameters.

The benzoquinone to palladium ratio was investigated, and using a higher amount of oxidant a higher conversion was achieved together with less decomposition to inactive palladium black. In particular, the best results were obtained with a benzoquinone to palladium ratio of 265, which means a one to one ratio between the oxidant and the substrate (Table 6.2), suggesting that BQ was necessary to close the catalytic cycle.

As already observed, the nature of the anion affects the catalytic behavior of the complexes, being trifluoroacetate derivatives more active than the acetate ones in the conversion of the alkene, although the increase in conversion was always accompanied by a decrease in selectivity.

Table 6.2. Methoxycarbonylation of 4-octene: effect of the anion L and of [BQ]/[Pd]. Precatalyst: [Pd(**18**)(L)$_2$].[a]

Run	L	[BQ]/[Pd]	Conversion (%)[b]	Selectivity (%)[b]
1	CH_3COO^-	20	5	77
2	CH_3COO^-	130	22	41
3	CH_3COO^-	265	29	61
4	CF_3COO^-	20	11	44
5	CF_3COO^-	130	45	17
6	CF_3COO^-	265	51	38

[a] Reaction conditions: see Table 6.1.

When the effect of the reaction temperature was investigated in the range 303 - 393 K using precatalyst **18b**, an increase in conversion with increasing temperature was observed up to 363 K, while a further increase in temperature resulted in a lower conversion, and the major product was not the expected one (Figure 6.9).

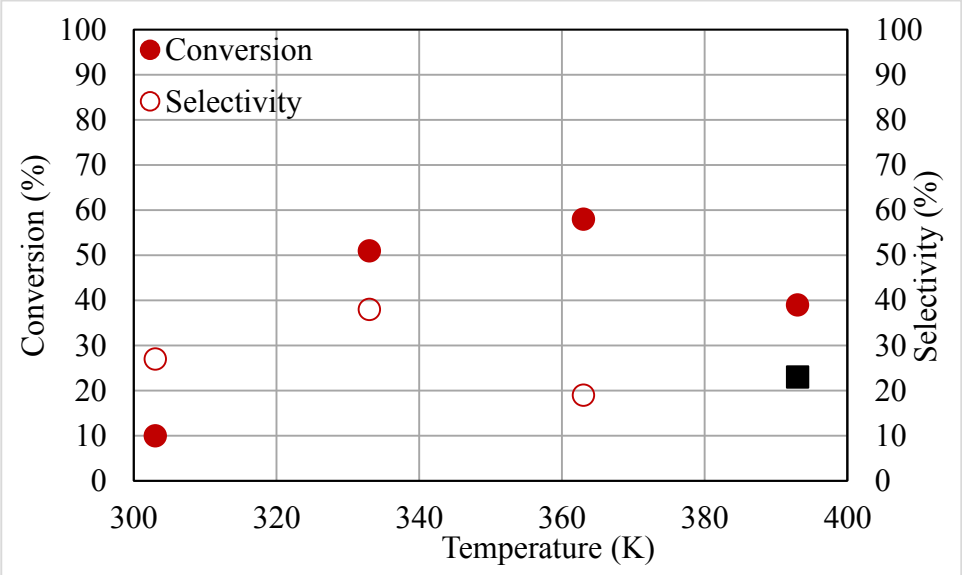

Figure 6.9. Methoxycarbonylation of 4-octene: effect of temperature. Precatalyst: **18b**. Reaction conditions: see Table 6.1. ■ main product was not the expected one.

Similarly, the selectivity increased with the increasing temperature, reaching the highest value of 38 % at 333 K, whereas a remarkable loss and change in selectivity was observed when the temperature was

further increased, thus indicating that the best compromise in order to have good conversion and selectivity was to run the reaction at 333 K.

The effect of CO pressure on the catalytic behavior of **18b** was investigated in the range 5 - 40 bar: the highest conversion of 67 % was obtained at 10 bar, while a further increase in the CO pressure resulted in a decrease in the conversion. On the other hand, the selectivity increased on increasing pressure, with the highest value of 63 % obtained at 40 bar (Figure 6.10). These trends highlighted that the best compromise was to run the reaction at 20 bar of CO.

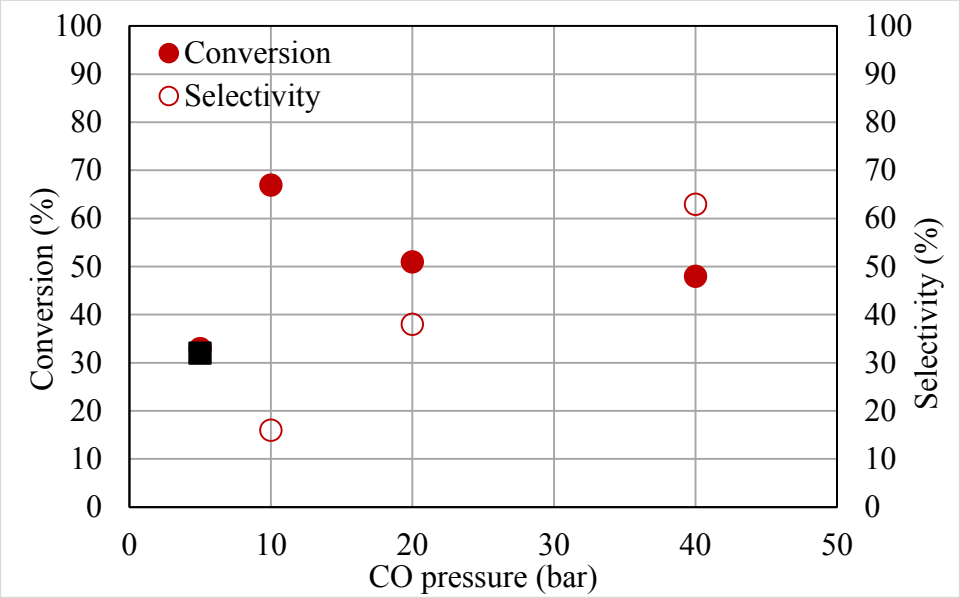

Figure 6.10. Methoxycarbonylation of 4-octene: effect of CO pressure. Precatalyst: **18b**. Reaction conditions: see Table 6.1. ■ main product was not the expected one.

On the basis of the collected data, it is possible to propose a catalytic cycle for the methoxycarbonylation of internal alkenes (Scheme 6.6). The palladium precatalyst, either an acetate or trifluoroacetate derivative, is activated by the dissociation of both anions, that are replaced by a methoxy group and carbon monoxide. The migratory insertion of CO into the Pd-methoxy bond takes place leading to the Pd-acetyl species; on the latter the coordination of the alkene followed by its migratory insertion into the Pd-acyl bond occurs yielding the Pd-alkyl species (Scheme 6.6).

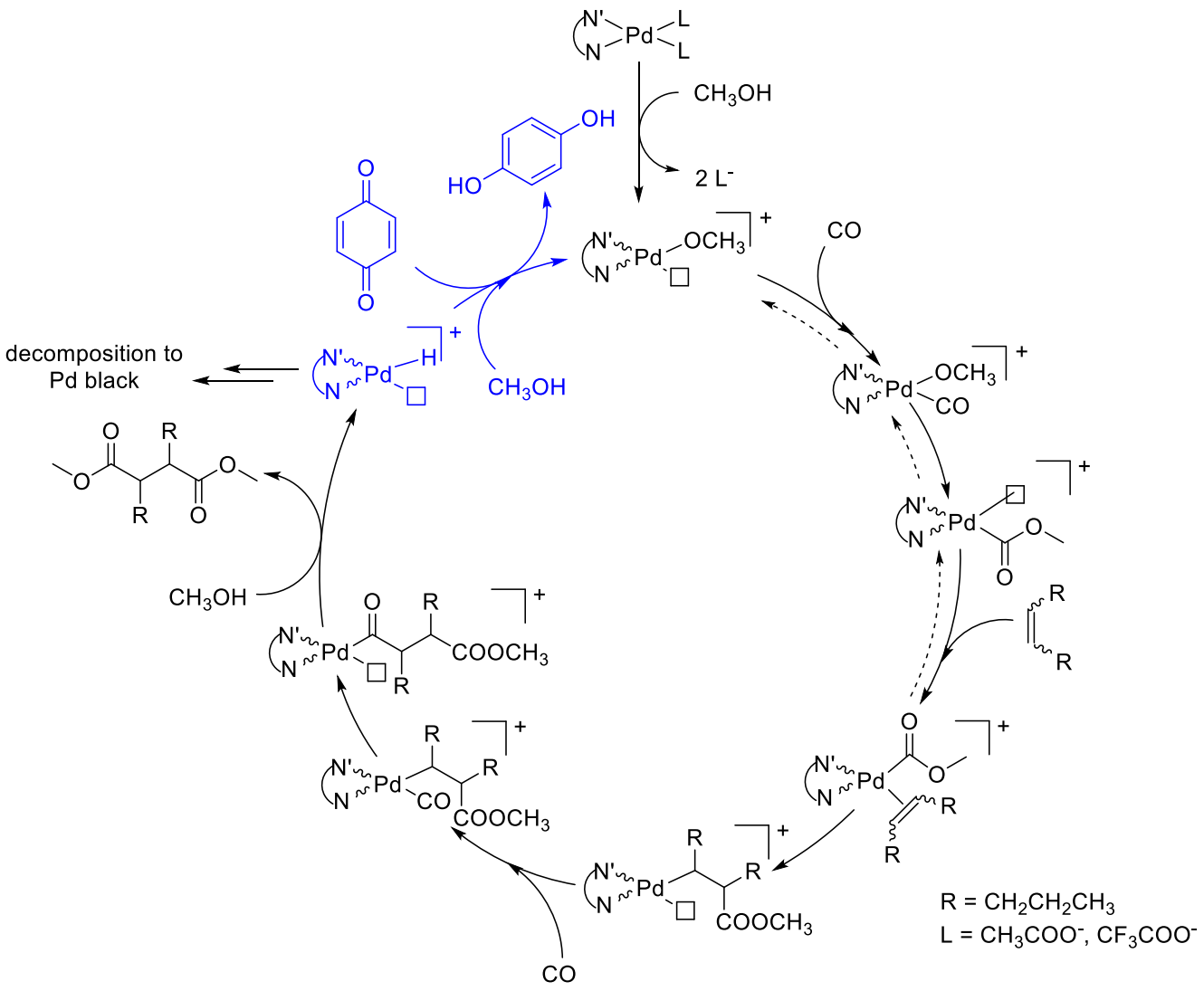

Scheme 6.6. Proposed catalytic cycle for the methoxycarbonylation of 4-octene.

The reaction proceeds through the carbonylation of the alkyl fragment and subsequent nucleophilic attack of a methanol molecule on the Pd-acyl bond, which generates the succinic ester and the Pd-H species. The latter can either undergo decomposition to palladium black or react with benzoquinone and methanol to restore the active species.

The effect of CO pressure and nature of the anion on the selectivity, which increased on increasing CO pressure and was higher for precatalysts containing the acetate anion, suggested that the species responsible for the selectivity might be the Pd-alkyl intermediate. In fact, to increase the selectivity the fourth coordination site on palladium should be temporarily occupied, either by CO or by the anion, suggesting that the use of terdentate hemilabile ligands might have a beneficial effect for this reaction.

Preliminary tests on different substrates suggested that these catalytic systems are active on other internal alkenes, even if bearing functional groups. For *cis*-cyclooctene, conversion of 13 % was observed, with a selectivity of 47 % in the bis-methoxycarbonylated product. For methyl oleate a conversion of 29 % was obtained, with 60 % selectivity, but the nature of the product is still under investigation, although it is reasonable to suppose that two ester groups have been added to the double bond. These results, although still incomplete, suggested that the reaction could be further optimized and its scope explored for the synthesis of valuable succinic derivatives.

6.3 Conclusions.

In this study palladium complexes with pyridylimine ligands $[Pd(N\text{-}N')(L)_2]$ have been investigated as catalysts for the methoxycarbonylation of aliphatic alkenes.

It was found that they generated moderately active catalysts for the bis-methoxycarbonylation of 1-octene leading to dimethyl 2-hexylsuccinate and of 4-octene yielding dimethyl 2,3-dipropylsuccinate, indicating that no isomerization of the internal double bond to the terminal position occurs before the carbonylation process takes place.

Both the anion and the ligand affected catalyst activity and selectivity, pointing out that the best combination is represented by ligand **18** and trifluoroacetate.

The detailed investigation of the catalytic behavior allowed to identify the best reaction parameters, that are the alkene to 1,4-benzoquinone ratio of 1, the reaction temperature of 333 K and the CO pressure of 20 bar.

The collected data allowed to depict a possible mechanism for the catalytic cycle to explain the conversion of an alkene to the corresponding vicinal diester.

6.4 Experimental

6.4.1. Materials and methods. Methanol was distilled from activated (iodine) magnesium and stored under argon prior to use, all other solvents were commercial grade. 1-octene and 4-octene were degassed prior to use. All reagents were used as received. $[Pd(OAc)_2]$ was a donation from Engelhard Italia and used as received. Palladium complexes **14a, 17a, 18a**, **14b, 17b, 18b** were synthesized according to literature procedure.[5] Deuterated solvents supplied by Deutero and Eurisotop were stored as recommended. NMR spectra were recorded on a Varian Unity Inova 400 equipped with a 4NUC/switchable mode - 5 mm "direct detection" probe, a Bruker Avance III 400 equipped with a BBFO

plus probe at 298 K. The resonances are reported in ppm (δ) and were referenced to the residual protiated solvent signals. NMR experiments were performed employing the automatic software parameters. Gas chromatography was carried out on a PerkinElmer (PE) Clarus 500 instrument with autosampler and FID detection on a PerkinElmer Elite-5 (5% Diphenyl- 95% Dimethylpolysiloxane) Series Capillary Columns (Length: 30m, Inner Diameter: 0.25mm, Film Thickness: 0.25mm), using Helium as carrier gas at a flow rate of 1.5 mL min-1. The injector temperature was 300 °C. After injection the oven was kept isothermal at 90 °C for 1 min, heated with 30 K min-1 to 280 °C, and kept isothermal at 280 °C for 8 min.

6.4.2. Carbonylation reaction. All experiments were carried out in a 20 mL stainless steel pressure reactor equipped with heating jacket and a glass inlay. Mixing was provided by a magnetic stirring bar. Prior to a carbonylation experiment the reactor was purged several times with argon. The catalyst precursor was weighed into a Schlenk tube, then all other reactants (1,4-benzoquinone, 1- or 4-octene and MeOH) were added using standard Schlenk techniques. Vigorous stirring afforded a homogenous reaction mixture, which was cannula-transferred into the reactor in an argon counter stream. The reactor was closed, pressurized with carbon monoxide and then heated to the desired temperature. After the desired reaction time, the reactor was cooled to room temperature and vented. The reaction mixture was diluted with methylene chloride and filtered to remove Pd-black. Conversion and selectivity were determined by GC analysis. Volatiles were removed under reduced pressure; the residual oil was separated through column chromatography on Silica gel using dichloromethane/ethyl acetate 95 : 5 for the product from 1-octene or petroleum ether (40-60)/ethyl acetate 95 : 5 as eluent for the product from 4-octene and the polarity was gradually increased by increasing the amount of ethyl acetate.

Dimethyl 2-hexylsuccinate. ^{1}H NMR (400 MHz, $CDCl_3$, 298 K) δ = 3.69 (s, 3H, OCH_3), 3.66 (s, 3H, OCH_3), 2.88 - 2.80 (m, 1H, H^3), 2.75 – 2.67 (m, 1H, H^2), 2.42 (dd, 1H, H^2), 1.68 – 1.42 (m, 2H, H^4), 1.26 (broad, 8H, H^{5-8}), 0.87 (t, 3H, H^9). ^{13}C NMR (100.54 MHz; CD_2Cl_2) δ = 175.7 (C^1), 172.6 (C^1), 51.9 (OCH_3), 41.3 (C^3), 36.0 (C^2), 32.1 (C^4), 31.7 - 22.7 (C^{5-8}), 14.2 (C^9).

Dimethyl 2,3-dipropylsuccinate. ^{1}H NMR (400 MHz, $CDCl_3$, 298 K) δ = 3.60 (s, 6H, OCH_3), 2.63 – 2.60 (m, 2H, H^1), 1.55 – 1.46 (m, 4H, H^2), 1.35 – 1.10 (m, 4H, H^3), 0.83 (t, 6H, H^4). ^{13}C NMR (100.54 MHz; CD_2Cl_2) δ = 175.4 (C^5), 51.8 (OCH_3), 46.7 (C^1), 31.5 (C^2), 20.4 (C^3), 14.1 (C^4).

6.5. Bibliography.

[1] (a) Sperrle, M.; Consiglio, G. *J. Am. Chem. Soc.* **1995**, *117*, 12130; (b) Sperrle, M.; Consiglio, G. *Chem. Ber./Recueil* **1997**, *130*, 1557; (c) Sperrle, M.; Consiglio, G. *Inorg. Chim. Acta* **2000**, *300-302*, 264.

[2] Heck, R.F. *J. Am. Chem. Soc.* **1972**, *94*, 2712.

[3] Fenton, D.M.; Steinwand, P.J. *J. Org. Chem.* **1972**, *37*, 2034.

[4] del Rio, I.; Claver, C.; van Leeuwen, P.W.N.M. *Eur. J. Inorg. Chem.* **2001**, 2719.

[5] Bianchini, C.; Lee, H.M.; Mantovani, G.; Meli, A.; Oberhauser, W. *New J. Chem.* **2002**, *26*, 387.

[6] Godard, C.; Munoz, B.K.; Ruiz, A.; Claver, C. *Dalton Trans.* **2008**, 853.

[7] Beller, M.; Seayad, J.; Tillack, A.; Jiao, H. *Angew. Chem. Int. Ed.* **2004**, *43*, 3368.

[8] Sperrle, M.; Consiglio, G. *J. Mol. Cat.: A-Chem.* **1999**, *143*, 263.

[9] (a) McCoy, M.; Tremblay, J.-F. *Chem. Eng. News* **2009**, *87(33)*, 9; (b) Harris, B. *Ingenia* **2010**, *45*, 19; (c) Now: Mitsubishi Rayon.

[10] Clegg, W.; Eastham, G.R.; Elsegood, M.R.J.; Tooze, R.P.; Wang, X.L.; Whiston, K. *Chem. Commun.* **1999**, 1877.

[11] Quinzler, D.; Mecking, S. *Angew. Chem. Int. Ed.* **2010**, *49*, 4306.

[12] a) Biermann, U.; Bornscheuer, U.; Meier, M. A. R.; Metzeger, J. O.; Schäfer, H. J.M *Angew. Chem. Int. Ed.* **2011**, *50*, 3854; b) Chikkali, S.; Mecking, S. *Angew. Chem. Int. Ed.* **2012**, *51*, 5802.

[13] a) Pugh, R. I.; Drent, E.; Pringle, P. G. *Chem. Commun.* **2001**, 1476; b) Rodriguez, C. J.; Fotser, D. F.; Eastham, G. R.; Cole-Hamilton, D. J. *Chem. Commun.* **2004**, 1720.

[14] Stempfle, F.; Quinzler, D.; Heckler, I.; Mecking, S. *Macromolecules* **2011**, *44*, 4159.

[15] Christl, J.T.; Roesle, P.; Stempfle, F.; Wucher, P.; Göttker-Schnetmann, I.; Müller, G.; Mecking, S.; *Chem. Eur. J.* **2013**, *19*, 17131.

[16] Roesle, P.; Caporaso, L.; Schnitte, M.; Goldbach, V.; Cavallo, L.; Mecking, S.; *J. Am. Chem. Soc.* **2014**, *136*, 16871.

[17] Canil, G.; Rosar, V.; Dalla Marta, S.; Bronco, S.; Fini, F.; Carfagna, C.; Durand, J.; Milani, B. *ChemCatChem* **2015**, *7*, 2255.

ACKNOWLEDGEMENTS

The first and most special thanks goes to my supervisor, Prof. Barbara Milani, who never failed in encouraging me to give the best of myself and never give up, who always gladly shared her deep knowledge, and who gave me the most amazing opportunity to learn and to grow into a better researcher as well as a better person.

I would like to thank Prof. Stuart Macgregor and his group, particularly Dr. Tobias Krämer and Dr. Claire McMullin, of the Heriot-Watt University of Edinburgh, not only for hosting me in the group and teaching me the bases of DFT calculations (Chapter 2), but most of all for making me feel really part of the group. The COST Action CM1205-CARISMA in gratefully acknowledge for the STSM fellowship I was awarded for the period spent in the UK, and for the fellowships for the participation to many conferences and PhD schools.

I would also like to thank Prof. Stefan Mecking of the University of Konstanz for hosting me in his group, and the DAAD for awarding me a B1 fellowship for the period I spent in Germany (Chapter 6).

I would like to thank Prof. Gabriele Balducci and Prof. Ennio Zangrando for the X-ray analysis (Chapters 3 - 5) Dr. Tiziano Montini and Prof. Paolo Fornasiero for the GC-MS analysis and Poisson analysis (Chapters 3, 4); Dr. Carla Carfagna for the GPC analysis (Chapter 5).

I would like to thank all the Alessio-Milani-Iengo's group, with which I shared much more than three years of hard work.

List of publications

1. *"Unprecedented comonomer dependence of the stereochemistry control in Pd-catalyzed CO/vinyl arene polyketone synthesis"*
Canil, G.; Rosar, V.; Dalla Marta, S.; Bronco, S.; Fini, F.; Carfagna, C.; Durand, J.; Milani, B. *ChemCatChem* **2015**, *7*, 2255-2264.

2. *"Pd-catalyzed z-selective semihydrogenation of alkynes: determining the type of active species"*
Drost, R.M.; Rosar, R.; Dalla Marta, S.; Lutz, M.; Demitri, N.; Milani, B.; de Bruin, B.; Elsevier, C.J. *ChemCatChem* **2015**, *7*, 2095-2107.

3. *"Coordination chemistry to palladium(II) of pyridylbenzamidine ligands and the related reactivity with ethylene"*
Tognon, A.; Rosar, V.; Demitri, N.; Montini, T.; Felluga, F.; Milani, B. *Inorg. Chim. Acta* **2015**, *431*, 206-218.

4. *"Analogies and differences in palladium-catalyzed CO/styrene and ethylene/methyl acrylate copolymerization reactions"*
Rosar, V.; Meduri, A.; Montini, T.; Fini, F.; Carfagna, C.; Fornasiero, P.; Balducci, G.; Zangrando, E.; Milani, B. *ChemCatChem* **2014**, *6*, 2403-2418.

Conference participation

1. Rosar, V.; Kraemer, T.; Milani, B.; Macgregor, S.
"Comparing BIAN and DAB Pd-catalysts in CO/styrene and ethylene/methyl acrylate copolymerization: a DFT study" – Poster, presented by Rosar, V., assegnee of a grant to attend the **Carisma 2016 Annual meeting**, Ljubljana (Slovenia), March 21st – 23rd 2016.

2. Tognon, A.; Rosar, V.; Demitri, N.; Montini, T.; Felluga, F.; Milani, B.
"Pyridylbenzamidines: versatile ligands for palladium(II)" - Poster 42, presented by Rosar, V., accepted for an oral presentation, assegnee of a grant from Carisma COST Action CM1205 to attend the **XL International Summer School on Organic Synthesis "A. Corbella"**, Gargnano (BS, Italy), June 14th-18th 2015.

3. Rosar, V.; Milani, B.; Mecking, S.
"Palladium-catalyzed bis-alkoxycarbonylation to produce valuable succinic esters from internal alkenes and CO" - Poster P26, presented by Rosar, V., assegnee of a grant to attend the **Carisma 2015 Annual meeting**, Tarragona (Spain), March 18th – 20th 2015.

4. Rosar, V.; Meduri, A.; Montini, T.; Fini, F.; Carfagna, C.; Fornasiero, P.; Balducci, G.; Zangrando, E.; Milani, B.
"Analogies and differences in palladium-catalyzed CO/vinyl arene and ethylene/methyl acrylate copolymerization reactions" - Oral communication, presented by Rosar V., assegnee of a grant to attend the **Carisma 2014 Annual meeting**, Venice (Italy), May 5th – 7th 2014.

5. Rosar, V.; Meduri, A.; Montini, T.; Fornasiero, P.; Zangrando, E.; Milani, B.
"Nonsymmetric a-diimines in Pd-catalyzed ethylene/polar monomer copolymerization" - Poster 27, presented by Rosar V., assignee of grant to attend the **9th International School of Organometallic Chemistry**, Camerino (Italy) August 30th –September 3rd 2013.

6. Rosar, V.; Meduri, A.; Zangrando, E.; Montini, T.; Fornasiero, P.; Carfagna, C.; Milani, B.
"Comparing Pd-catalyzed CO/vinyl arene and ethylene/acrylate copolymerization" - Poster P136A, presented by Rosar V., accepted for a short oral preview presentation of the poster (flash presentation), **20th EuCheMS Conference on Organometallic Chemistry**, St. Andrews (Scotland, UK), June 30th – July 4th 2013. Assignee of S.H.A.R.M. (FSE – European Social Fund) fellowship to attend the conference.

7. Rosar, V.; Meduri, A.; Zangrando, E.; Grassi, A.; Milani, B.
"Pd complexes with naphthalene a-diimines as catalysts for copolymerization: from atactic to stereoblock copolymers?" - Poster P31, presented by Rosar V., **X Congresso del Gruppo Interdivisionale di Chimica Organometallica (Co.G.I.C.O)**, Padova (Italy), June, 5-8th 2012.